Cellular and molecular mechanisms by which specific GSK3 inhibition affects the processing of the Amyloid Precursor Protein

Callum John Christopher Parr

Centre for Neuroscience
Division of Brain Science
Department of Medicine
Faculty of Medicine
Imperial College London

Submitted for the Diploma of Imperial College (DIC), PhD degree of Imperial College London // Clinical Medicine Research (A3Z1DM)

DECLARATION

In submitting this thesis I declare that the work presented henceforth is purely that of my own unless disclosed otherwise, in which case it is fully referenced or acknowledged.

ACKNOWLEDGEMENTS

A three-year divisional PhD studentship was awarded from Imperial College London and allowed me to conduct full-time research that has led to the submission of the generated data.

My initial gratitude goes to my first supervisor Dr Magdalena Sastre as during my time at Imperial College, she has always been readily available for guidance, critical appraisal of my work and technical assistance. Secondly I would like to thank my second supervisor, Professor Steve Gentleman for his periodical assessment of my project and also corrections of this manuscript.

To the many members of the Centre for Neuroscience both past and current, I have greatly appreciated the enjoyment you brought to the quite lonely experience of doctoral research not to mention the great advice and support. Many of whom I feel privileged to call a friend and not just a colleague. This is especially true of my immediate neighbours, Dr Loukia Katsouri, Enrico Cristante and Dr. Simon McArthur and I should also apologise for my sometimes, or I should say often, eccentric behaviour. I am truly indebted to Loukia who gave me just as much emotional support as she did technical and when not sharing her expertise would simply listen and provide a soundboard for my frustrations.

As a manner of disclosure I wish to thank Dr Michael Willem who provided the data required to demonstrate the specificity of the BACE1 antibody. The same must also be said for Dr Cristina Perez for help given in the sub-cloning work for the Wnt3a construct. I would also like to extend my thanks to her for discussing the many queries I had and it was a joy to be able to discuss our similar research interests.

Although detailed within the methods chapter, I would like to thank the many that have kindly donated cell-lines, constructs and antibodies without which this work would have not been possible. In particular, Professor Fred Van Leuven at the Katholieke Universiteit Leuven has been a fantastic source of knowledge and tools to understand the biology of GSK3 in reference to Alzheimer's disease. I am extremely

grateful to Professor Leuven and his group members for hosting me for a month and making me feel so welcome. This was a great opportunity that allowed me to gain invaluable knowledge for investigating Alzheimer's disease in mouse models.

My last words of acknowledgement are lovingly given to my family, friends and the random set of circumstances that have brought me here.

ABSTRACT

Alzheimer's disease (AD) has long been associated with altered activity of the serine/threonine kinases, Glycogen Synthase Kinase-3 (GSK3) isozymes, which are proposed to contribute to both neurofibrillary tangles and amyloid plaque formation. While the molecular links between GS3K and tau pathology are well established, the molecular basis by which GSK3 affects the formation of amyloid-β (Aβ) remains unknown. The aim of this investigation was to identify the underlying mechanisms by which inhibition of GSK3 affects the processing of the amyloid precursor protein (APP).

To this end various methods were employed to alter the basal activity of the GSK3 enzyme in N2a cells, a mouse neuroblastoma cell-line, overexpressing the Swedish variant of APP. Specific perturbation of GSK3 activity leads to an alteration in APP processing and Aβ production, something that until now, was seen as controversial. Specific pharmacological inhibition of GSK3 resulted in a decrease in activity, expression and transcription of BACE1, which is the main enzyme responsible for Aβ generation. Activation of the canonical Wnt pathway, which is associated with negative regulation of GSK3, reproduced the previous findings and led to reduction in transcription and expression of BACE1.

Furthermore, specific pharmacological GSK3 inhibition and GSK3α/β knockdown enhanced full-length APP degradation via an increase in the number of lysosomes. This induction of the lysosomal/autophagy pathway was associated with the effect of specific GSK3 inhibition on the nuclear translocation of transcription factor EB (TFEB), which is a master regulator of lysosomal biogenesis.

All together, GSK3, in addition to being associated with hyper-phosphorylation of tau, can also influence Aβ generation through regulating BACE1 expression and the homeostatic turnover of APP. This data reinforces the hypothesis that GSK3 could be a therapeutic target for AD as it is shown to be a central signalling node in the pathogenesis of the disease.

DECLARATION 2

ACKNOWLEDGEMENTS 2

ABSTRACT 4

LIST OF ABBREVIATIONS 11

CHAPTER 1 : SUMMARY 18

1.1 Background 18

1.2 Aims 19

CHAPTER 2 : GENERAL INTRODUCTION 20

2.1 A coming of age story 20
2.1.1 Alois Alzheimer 20
2.1.2 A ticking time bomb 20

2.2 Diagnosis of dementia and AD 22

2.3 Neuropathology and hallmarks of AD 24

2.4 Progression of AD 26

2.5 Aβ pathology and APP processing 29
2.5.1 Aβ deposition 29
2.5.2 APP metabolism 29
2.5.2.1 APP trafficking and processing 31
2.5.2.2 α-secretase processing 32
2.5.2.3 β-secretase processing 33
2.5.2.4 γ-secretase processing 36
2.5.2.5 Aβ clearance and degradation 41
2.5.2.6 Physiological functions of APP 43
2.5.3 Amyloid cascade hypothesis 44
2.5.4 Aβ oligomerisation and toxicity 48

2.6 Variations on a theme: LOAD versus FAD 49

2.7 Tau protein and Braak staging of NFT pathology 51

2.8 Glycogen synthase kinase-3 53
2.8.1 GSK3 as the tau kinase 54
2.8.2 Regulation of GSK3 54
2.8.2.1 Regulation by phosphorylation 54
2.8.2.2 Primed substrate prerequisite 55
2.8.2.3 Subcellular pooling 55
2.8.2.4 Differential isoform expression and substrate specificity 55
2.8.3 GSK3 hypothesis of AD 56
2.8.3.1 GSK3 activity and aging 56
2.8.3.2 GSK3 and APP processing 58

2.8.3.3 Aβ toxicity, apoptosis and GSK3 58
2.8.3.4 GSK3 and memory impairment 59
2.8.3.5 GSK3 and inflammation 60
2.8.4 GSK3 and the canonical Wnt signalling 63

2.9 The canonical Wnt cascade and AD 66
2.9.1 Receptor-level alterations in the Wnt cascade with sporadic AD 67
2.9.2 *PSEN1* mutations and regulation of cytoplasmic β-catenin 68

CHAPTER 3 : MATERIALS AND METHODS 70

3.1 Antibodies and reagents 70

3.2 Human post-mortem brain samples 73

3.3 Mouse tissue homogenisation 75

3.4 Cell culture 75

3.5 Cell treatments 76

3.6 Cell transfection of plasmid constructs and siRNA 77

3.7 Western blotting 78
3.7.1 Cell lysis and eletrophoresis of SDS-PAGE gels 78
3.7.2 Determination of secreted Aβ and sAPPα ectodomain 79
3.7.3 Subcellular fractionation 80
3.7.4 Analysis of APP C-terminal fragments 81

3.8 Pulse-chase analysis 82

3.9 Autophagy assessment/LC3-II production 82

3.10 Enzymatic activity of the β- and α-secretases 83

3.11 Microscopy 84
3.11.1 Lysotracker®-Red DN-99 staining 84
3.11.2 Immunocytochemistry 84
3.11.3 Image capture and analysis 85
3.11.4 Transmission electron microscopy 86

3.12 mRNA extraction and RT-PCR 87

3.13 Luciferase dual reporter assays 92

3.14 Statistical analysis 93

Buffers 95

CHAPTER 4 : ROLE OF GSK3 ON APP PROCESSING 96

4.1 Introduction 96

4.2 Results 98
4.2.1 GSK3 expression and activity increases with age 98
4.2.2 Changes in GSK3 activity lead to alterations in the amyloidogenic processing of APP 99
4.2.2 Altered GSK3 activity does not result in changes in the activities of the α-secretase and the γ-secretase 102
4.2.3 GSK3 regulation of the β-secretase 104
4.2.3.1 Specific GSK3 inhibition results in a decrease in β-secretase activity, transcription and expression of BACE1 104
4.2.3.2 Transient overexpression of GSK3 led to an increase in BACE1 expression 106
4.2.4 GSK3 regulation of full-length APP 109
4.2.4.1 Steady-state levels of FL-APP are reduced when GSK3 is inhibited specifically 109
4.2.4.2 Specific GSK3 inhibition does not result in reduced APP transcription 112
4.2.4.3 Specific Inhibition of GSK3 results in increased degradation of FL-APP 113
4.2.5 Destabilisation and degradation events of FL-APP 115
4.2.5.1 Inhibition of the 26S proteasome partially attenuates the effect of specific GSK3 inhibition on FL-APP stability 115
4.2.5.2 Inhibition of autophagy induction reverses the effects of specific GSK3 inhibition on FL-APP 117
4.2.6 Bif-1 silencing does not prevent degradation of FL-APP by specific GSK3 inhibition 118

4.3 Discussion 120
4.3.1 GSK3 can regulate the processing of APP 120
4.3.2 Changes in GSK3 activity can alter the expression and activity of the β-secretase 123
4.3.3 Specific GSK3 inhibition led to increased degradation of FL-APP 124
4.3.3 Proteasomal and autophagy targeting of FL-APP upon specific GSK3 inhibition 125

CHAPTER 5 : SPECIFIC GSK3 INHIBITION ALTERS AUTOPHAGY-LYSOSOMAL DEGRADATION OF FL-APP 128
5.1 Introduction 128
5.1.1 Autophagy and metabolic sensing 128
5.1.3 Autophagosome formation 129

5.2 Results 133
5.2.1 Specific inhibition of GSK3 activity can induce autophagy vesicle formation as shown by LC3-GFP puncta and LC3-II production 133
5.2.3 Ultrastructure observation reveals no change in the AV formation but a dramatic increase in primary lysosome formation 138
5.2.4 Specific inhibition of GSK3 led to an increase in the biogenesis of lysosomes 142
5.2.5 Blockade of lysosomal degradation rescues FL-APP protein level reduced by specific GSK3 inhibition 150

5.3 Discussion 151
5.3.1 Specific GSK3 inhibition induces autophagy and increases autophagy flux 152
5.3.2 Specific GSK3 inhibition does not lead to a significant increase in autophagy vesicles 153
5.3.3 Specific GSK3 inhibition led to an increase in lysosome vesicles 155
5.3.4 Specific GSK3 inhibition results in an increase of TFEB nuclear localisation 155
5.3.5 FL-APP degradation induced by specific GSK3 inhibition is dependent on lysosomal degradation 156

CHAPTER 6 : THE ROLE OF CANONICAL WNT SIGNALLING IN THE REGULATION OF APP PROCESSING 158

6.1 Introduction 158

6.2 Results 160
6.2.1 Alterations in the activity of the canonical Wnt cascade affect APP processing 160
6.2.2 Canonical Wnt stimulation affects mouse *Bace1* transcription 165
6.2.3 b-catenin protein levels are reduced in the brains of sporadic AD patients 167

6.3 Discussion 170
6.3.1 Canonical Wnt induction influences APP processing via its negative regulation of GSK3 171
6.3.2 Canonical Wnt induction affects BACE1 transcription 172

CHAPTER 7 : DISCUSSION 174

7.1 Introduction 174

7.2 GSK3 hypothesis of AD 174

7.3 LiCl versus specific GSK3 inhibition 176

7.4 GSK3 activity and FL-APP stability 178
7.4.1 TFEB and lysosomal biogenesis 178
7.4.2 Further investigation on TFEB 180

7.5 Decreased GSK3 activity reduces BACE1 transcription 181
7.5.1 Decreased GSK3 activity reduces BACE1 transcription through β-catenin regulation 181
7.5.2 Decreased GSK3 activity reduces BACE1 transcription through β-catenin-transactivation independent mechanisms 187
7.5.3 Further investigation 190

7.5 Canonical Wnt cascade and sporadic AD 191

7.6 General limitations and future directions 192

7.7 Developments of current AD therapies and GSK3 as a promising therapeutic target 194

CONCLUSION 197

Figure 2.1: Inside of the AD brain. 25
Figure 2.2: The staging and major biomarkers of AD progression. 28
Figure 2.3: APP metabolism. 30
Figure 2.4: Trafficking of APP through the cell. 31
Figure 2.5: The putative topology of PSEN1/2 and the stepwise model for generation of major Aβ metabolites from β-CTF by the γ-secretase complex. 38
Figure 2.6: Amyloid cascade hypothesis. 47
Figure 2.7: Staging of NFT pathology in AD human brains from the BrainNet human consortium. 52
Figure 2.8: Increased GSK3 activity links several aspects of AD pathogenesis. 62
Figure 2.9: Schematic of canonical Wnt signalling in metazoa. 64
Figure 2.10: Schematic of signalling sequestrome upon canonical Wnt stimulation. 65
Figure 2.11: Signalling events connecting Aβ neurotoxicity to Wnt cascade disruption. 67
Figure 3.1: Schematic of APP metabolism and antibody epitopes. 71
Figure 3.2: Efficiency and post melt-curve analysis of primer sets. 91
Figure 4.1: GSK3 expression and activity increase with age. 98
Figure 4.2: GSK3 inhibition with various inhibitors leads to stabilisation of b-catenin. 99
Figure 4.3: Changes in the activity of GSK3 led to alteration in the amyloidogenic processing of APP. 101
Figure 4.4: Changes in GSK3 activity do not affect the α-secretase or the γ-secretase activity. 103
Figure 4.5: Changes in the GSK3 activity led to reduced β-secretase activity and BACE1 expression. 108
Figure 4.6: Specificity of the Millipore rabbit polyclonal anti-BACE1 antibody. 109
Figure 4.7: Steady-state protein level of FL-APP is reduced in N2aSw cells by specific GSK3 inhibition. 111
Figure 4.8: Specific GSK3 inhibition does not affect transcription of APP. 112
Figure 4.9: Specific inhibition of GSK3 results in increased degradation of FL-APP. 114
Figure 4.10: The reduction of FL-APP with specific GSK3 inhibition was partially rescued by proteasome blockade. 116
Figure 4.11: Blockade of autophagy reverses the effect of specific GSK3 inhibition on FL-APP. 119
Figure 5.1: Formation and regulation of autophagy. 131
Figure 5.2: Autophagosome formation as visualised with LC3-GFP formation. 135
Figure 5.3: VIII treatment in HEK293 LC3-GFP cells leads to GFP puncta formation 135
Figure 5.4: Specific GSK3 inhibition increases both endogenous LC3-II production and autophagy flux. 137
Figure 5.5: Characterisation of intracellular autophagy-lysosomal compartments for cell vesicle counts. 139
Figure 5.6: Ultrastructure analysis of N2aSw cells incubated with or without GSK3 inhibitor VIII. 141
Figure 5.7: Specific GSK3 inhibition increases Lysotracker®-red retention. 143
Figure 5.8: Specific GSK3 inhibition increases the number of lysosomes and the subcellular localisation of APP in lysosomes. 146
Figure 5.9: Specific GSK3 inhibition promotes the translocation of TFEB in N2aSw cells. 149
Figure 5.10: Increased nuclear localisation of TFEB by specific GSK3 inhibition. 149
Figure 5.11: FL-APP degradation induced by specific GSK3 inhibition is dependent on lysosomal proteolysis. 150
Figure 6.1: Confirmation of transfection with Wnt3a, β-catenin and β-catenin shRNA and the effect on β-catenin levels. 161
Figure 6.2: Wnt3a and b-catenin overexpression led to induction of the canonical Wnt cascade. 163
Figure 6.3: Changes in the canonical Wnt cascade activity affect APP processing. 165

Figure 6.4: Altering the activity of the canonical Wnt cascade affects the expression of BACE1. 167
Figure 6.5: Nuclear b-catenin levels are reduced in post-mortem sporadic AD brains. 169
Figure 7.1: Schematics of the hypothetical effects of specific GSK3 inhibition on FL-APP degradation. 179
Figure 7.2: Hypothetical mechanism for BACE1 transcriptional regulation 1. 182
Figure 7.3: Putative consensus LEF/TCF binding sites within the rat BACE1 promoter. 184
Figure 7.4: Hypothetical mechanism for BACE1 transcriptional regulation 2. 185
Figure 7.5: Hypothetical mechanism for BACE1 transcriptional regulation 3. 186
Figure 7.6: Hypothetical mechanism for BACE1 transcription regulation 4 and 5. 188

Table 2.1: Familial linkage to AD. 50
Table 3.1: List of antibodies. 72
Table 3.2: Case histories of the different sporadic AD patients. 74
Table 3.3: Beclin-1 and GSK3α/β siRNA transfection with Lipofectamine™ 2000. 78
Table 3.4: Step 1a. 87
Table 3.5: Step 1b. 87
Table 3.6: Cycling conditions and reaction mastermix. 89
Table 3.7: List of drugs and concentrations 94
Table 7.1: Putative binding sites for LEF/TCF family of transcription factors in the rat BACE1 promoter. 183
Table 7.2: List of selected putative GSK3 kinase targets. 189

LIST OF ABBREVIATIONS

3-MA- 3-methyladenine

Aβ- Amyloid-β

AChE- Acetylcholinesterase

AD- Alzheimer's disease

ADAM-10- α-Secretase activity of the disintegrin metalloprotease-10

ADP- Adenosine diphosphate

AICD- APP intracellular domain

AMPK- Adenosine monophosphate activated kinase

ANOVA- Analysis of variance

APC- Adenomatous polyposis coli

Aph- Anterior pharynx-defective-1

APLP- APP like protein

Apoε4-Apolipoprotein ε4

APP- Amyloid precursor protein

ATP- Adenosine triphosphate

AV- Autophagy vesicle

AVL- AV lysosome

BACE1- β-site APP cleaving enzyme-1

BEC1- Beclin-1

BSA- Bovine seurm albumin

CANTLAB-PAL- Cambridge neuropsychology test automated battery-paired associate learning

CDK- Cycline-dependent kinase

cDNA- Copy DNA

ChIP- Chromatin immunoprecipitation

CHO- Chinese hamster ovary

CK1α- Casein kinase-1

CMA- Chaperone mediated ovary

CNS- Central nervous system

Cntrl- Control

CRD- Cysteine-rich domain

Ct- Cycle threshold

CTD- C-terminal domain

CTFα/β/γ-C- terminal fragment α/β/γ

CSF- Cerebrospinal fluid

DAPT- N- [N-(3,5-difluorophenacetyl)-L-alanyl]-S-phenylglycine t-butyl ester

DAPI- 4',6-diamidino-2-phenylindole

DISC1- Disrupted In schizophrenia-1

DFCP1- Double FYVE-containing protein-1

DKK- Dikkopf

DMEM- Dulbecco's modified Eagle's medium

DMSO- Dimethyl sulfoxide

DNA- Deoxynucleic acid

dNTP- Deoxyribonucleic triphosphate

D-PBS- Dulbecco's PBS

DS- Down's syndrome

DTT- Dithiothreitol

Dsh- Dishevelled

E- Efficiency

ECL- Enhanced chemiluminescence

eIF4- Eukaryotic initiation factor-4

EOAD- Early-onset AD

ER- Endoplasmic reticulum

ERAD- ER-associated degradation

ERK- Extracellular signal-regulated kinase

ESCRT- Endosomal sorting complex required for transport

FAD- Familial AD

FBS-Foetal bovine serum

FCS- Foetal calf serum

FDA- Federal drug administration

FL-APP- Full length APP

FRET- Fluorescence resonance emission transfer

G-418- Geneticin

GAPDH- Glyceraldehyde 3-phosphate dehydrogenase

GBP- GSK3 binding protein

GFP- Green fluorescent protein

GGA- Golgi-localized γ-ear-containing ARF-binding

GSKIP- GSK3 interaction protein

GSK3- Glycogen synthase kinase-3

GWAS- Genome-wide associated study

HCl- Hydrochloric

HEK- Human embryonic kidney

hiN- Human induced neurons

HRD1- Human othologue of Hrd1p/Der3p

HRP- Horseradish peroxidase protein

ICAT- Inhibitor of β–catenin and Tcf

ICC- Immunocytochemistry

IHC- Immunohistochemistry

IMPase- Inositol monophosphatase

IP- Immunoprecipitation

JNK- c-Jun N-terminal kinase

JIP- JNK interacting protein

kDa- kilodalton

KPI- Kunitz protease inhibitor

LB- Luria Bertani

LC3- Light chain-3

LOAD- Late-onset AD

LRP- Low-density lipoprotein receptor-related protein

LTD- Long-term depression

LTP- Long-term potentiation

M1 and 2- Mander's coefficient 1 and 2

MAPK- Mitogen-activated protein kinase

MCI- Mild cognitive impairment

MEF- Mouse embryonic fibroblast

MES- 2-(*N*-morpholino) ethanesulfonic acid

Mint- Munc-interacting protein

miRNA- micro RNA

NMDA- N-methyl-D-aspartic-acid

NMDAR- NMDA receptor

MMSE- Mini-mental state-examination

MRI- Magnetic resonance imaging

mRNA- messenger RNA

MTA- Medial temporal atrophy

mTOR- Mammalian target of rapamycin

mTORC- mTOR complex

MVB- Multivesicular body

N2a- Neuroblastoma 2a

N2aSw- N2a-Swedish

NAD- Nicotinamide adenine dinucleotide

NFDM- Non-fat dried milk

NFκB- Nulear factor κB

NFT- Neurofibrillary tangles

PBS- Phosphate-buffered saline

PCC- Pearson's correlation coefficient

PCR- Polymerase chain reaction

PDB- Phosphotyrosine-binding domain

PDZ- Postsynaptic density-95, Discs large, Zona occludens

PE- Phosphatidylethanolamine

PEN2- Presenilin enhancer-2

PFA- Paraformaldehyde

PH- Pleckstrin homology

PI3K- Phosphoinositide-3-kinase

PI3P- PhosphatidylInositol-3-phosphate

PPARγ- Peroxisome proliferator-activated receptor-γ

PPRRE- PPARγ repression element

PrP^{C}- Prion protein

PSEN1- Presenilin-1

PVDF- Polyvinylidene fluoride

Opti-MEM- Optimum modified Eagle's medium

RE- Repression element

RIPA- Radioimmunoprecipitation

ROI- Region of interest

RPM- Revolutions per minute

RNA- Ribonucleic acid

RNAi- RNA interference

RT- Reverse transcription

RT-qPCR- RT quantitative PCR

SAD- Sporadic AD

sAPPα/β- Soluble APPα/β

Scr- Scramble

SDS- Sodium dodecyl sulfate

SDS-PAGE- SDS polyacrylamide gel electrophoresis

SEM- Standard error of mean

sFRP1- Secreted Frizzled receptor protein-1

shRNA- small-hairpin RNA

siRNA- small-interfering RNA

STAT- Signal transducers and activators of transcription protein

SVG- Subventricular granule

SVZ- Subventricular zone

TBST-Tris-buffered saline tween

TCA- Trichloroacetic acid

LEF/TCF- Lymphoid enhancer factor/T-cell factor

TE- Tris-EDTA

TEM- Transmission electron microscopy

TFEB- Transcription factor EB

TGN- Trans golgi network

Tm- Melting temperature

TPK1- Tau protein kinase-1

TSC2- Tumour sclerosis- 2

ULK- UNC-51 like kinase

UPS- Ubiquitin-proteasome system

UTR- Untranslated region

WB- Western blotting

WIP12- WD-repeat domain interacting protein-12

YY1- Ying yang

CHAPTER 1 : SUMMARY

1.1 Background

The Ser/Thr kinase Glycogen Synthase Kinase-3 (GSK3), originally identified for its role in glucose metabolism, has been shown to be a key regulator in molecular pathogenesis of Alzheimer's disease (AD). The two isozymes of GSK3, α and β, share a high sequence identity within their respective kinase domains; however their functional redundancy is still debated (Jope and Johnson, 2004). The GSK3β isoform has particular relevance in AD because it is highly expressed in neuronal tissue (Bhat et al., 2004). It has been postulated that deregulation of GSK3 activity occurs with aging, although it remains unclear whether such effects may occur in nervous tissue. GSK3 activity might be increased in AD, through changes in its phosphorylation state as well as expression levels, although direct evidence for this is still limited at present (Pei et al., 1997; Blalock et al., 2004). GSK3 has been proposed to contribute to both neurofibrillary tangles and amyloid plaque formation. This is based on evidence that GSK3 phosphorylates protein tau and also APP, thereby promoting Aβ production (Bhat et al., 2004). GSK3β transgenic mice have impaired LTP in CA1, while conversely induction of LTP appears to decrease kinase activity as indicated indirectly by phosphorylation of Ser9 (Hooper et al., 2007). In addition, tyrosine phosphorylation of GSK3 (associated with increased activity) is increased in AD transgenic mice early in life by the soluble amyloid species (Terwel et al., 2008). Interestingly, exposure of hippocampal neurons to Aβ has been shown to increase GSK3β activity (Takashima et al., 1996). As active GSK3β triggers not only phosphorylation of tau but other events that could contribute to cell death, a major part of AD pathology could result from increased GSK3 activity.

On the other hand, treatment with LiCl, a well-known, and widely used, but non-specific GSK3 inhibitor in cultured neuronal cells and Tg2576 mice resulted in different outcomes, from reduced Aβ40 and Aβ42 load (Phiel et al, 2003; Su et al., 2004; Sun et al, 2002) to increased Aβ generation (Feyt et al., 2005; Caccamo et al., 2007). A recent study treating double transgenic *APP/Tau* mouse model with a novel specific GSK3 inhibitor resulted in lower levels of tau phosphorylation, decreased Aβ

deposition and plaque-associated astrocytic proliferation, neuronal protection, and prevention of memory deficits (Sereno et al., 2009).

1.2 Aims

The effects of aging on GSK3 in the CNS have not still been clarified. Yet this could have consequences in the development of aging-related disorders, such as AD. Combined data point to a damaging cycle of amyloid generation and GSK3 activation, but the molecular mechanisms by which GSK3 affects the formation of Aβ remain unknown. Due to the highly relevant role of GSK3 in AD and in order to clarify and identify the molecular mechanisms by which GSK3 affects APP processing, this thesis is centred on the following aims:

1. *To determine the potential changes of GSK3 with aging and to ascertain if the processing of the APP is affected by GSK3 and, if so, what are the potential mechanism(s).*

2. *To determine whether specific GSK3 inhibition could induce autophagy and account for the increased degradation rate of FL-APP.*

3. *To investigate whether activation of the canonical Wnt signalling cascade can affect APP processing and if so, to determine what mechanism(s) are involved. As activation of the canonical Wnt pathway results in inhibition of GSK3, some of the outcomes should be similar to those found by GSK3 pharmacological inhibition. In addition, the specific role of β-catenin transactivation on the processing of APP will be evaluated.*

CHAPTER 2 : GENERAL INTRODUCTION

2.1 A coming of age story

2.1.1 Alois Alzheimer

Alzheimer's disease (AD) is currently the most prevalent neurodegenerative disease and is characterised by the symptoms of cognitive decline and memory impairment as a result of progressive neuronal loss from cortical and hippocampal areas (Frolich, 2002).

Alois Alzheimer originally described the disease in 1906 in which he was the first to observe the neuropathological hallmarks of AD by post-mortem examination (Alzheimer, 1907). Thus the vague umbrella term, dementia, has been stratified to include approximately 50-70 disorders through a century of research based on slight variations in clinical symptoms and/ or specific histopathological hallmarks (Squire, 2008). Alzheimer's original case was the description of a 51 year-old woman who presented the classical symptoms of dementia in addition to having delusions and hallucinations. Upon autopsy the German pathologist astutely observed that besides the obvious brain atrophy, the neurones were laden with tightly bundled neurofibrillary tangles (NFT) and the parenchyma was dotted with plaques (see figure 2.1). For whatever reason, neurones in key areas such as the hippocampus and cortical regions degenerate leading to atrophy of the brain. AD is therefore described as a neurodegenerative disease that leads to a general demented state.

2.1.2 A ticking time bomb

Since humble beginnings at the turn of the 20th century, the breadth and depth of our knowledge of this disease is vast and ever increasing. This accelerating expansion of research is driven by an epidemiological and a demographic ticking time bomb. Approximately 50% of the diagnosed dementia cases are attributed to be AD. In the United Kingdom alone there are 820, 000 people suffering from the disease with a new case being diagnosed every 3.2 minutes. On average, 60, 000 deaths are a direct result of the disease (Matthews et al., 2005). However this is merely a drop in the ocean if one compares the statistics to the United States of America where

approximately 5.4 million people are currently diagnosed with AD from the last census data (Hebert et al., 2003)[1].

Age is the greatest risk factor for developing the disease. AD cases are found in 13% of individuals aged between 65yrs and 85yrs and 43% of those who are older (Plassman et al., 2007). Unlike a pathogen that can be immunised against and eradicated, people will always grow old and therefore a large proportion of any population will go to develop some form of dementia. But why this current position is untenable, is that with an aging population, which characterises so many developed countries, the proportion of individuals developing dementia will explode exponentially. It is predicted in the USA that individuals who are aged 65 and over with AD will increase by 50% to 7.7 million sufferers by 2030, again taken from statistics compiled by the Alzheimer's association (Plassman et al., 2007). Similar devastation has been predicted for the UK, which would surely crush a national healthcare system and squeeze its economy.

The simplistic view is that the disease is a greater burden on the developed nations, with higher life expectancies, however this is not the case if one considers that 60% of the 35 million global cases of dementia are from developing countries. In this case, the emphasis is not so much on the aging population but rather the exponential rate at which the population size is growing in all age-brackets. For this reason the dementia rate is set to climb in India and China by more than 300% by 2040 when compared with a 2001 baseline (Ferri et al., 2005). Owing to the fact that these nations have weaker economies, there are simply neither public nor private healthcare systems put in place to deal with this situation. Current drug therapies are relatively expensive and apart from the immediate family there simply is no caring profession to speak of.

Smart economies have realised that the problem of AD is growing in magnitude rapidly. This has resulted in a recent shift to increase publicity of dementia. The goal of this publicity is to raise awareness and increase the percentage of funding from governments to research AD and other dementias. While efforts have succeeded in many ways, the current funding is still well below that of what is given to other research areas such as cancer and heart disease. To realise how

---

[1] Statistics taken from recent report from the Alzheimer's association: **Facts and Figures 2011**. http://www.alz.org/downloads/Facts_Figures_2011.pdf [Accessed on 1st of August 2011].

nonsensical this is, one has to consider that each AD patient has an economic impact of £27, 647pa while that from a cancer or a heart disease patient is only £5, 999pa and £3, 455pa respectively. The UK alone spends £23 billion every year on ineffective drug therapies and patient care needed for someone who has this debilitating disease [2]. The US spends an untenable $183 billion a year from a recent review from 2011 by the Alzheimer's Association. Merely delaying the onset by five years would dramatically decrease the proportion of individuals requiring permanent care and with it the economic burden. And thus the gauntlet has been set for Science to delay, if not cure AD and the related dementias.

It is important however to see as scientists, politicians and activists that the economic crisis is indirect and secondary to the tragedy that befalls any family that has to deal with a loved one suffering from AD. It has the power to take away the pride and independence of a person and most of all it can corrupt their mind and the very faculties that make them human. It is for this reason alone that more needs to be done in terms of funding innovative research that can rectify this.

2.2 Diagnosis of dementia and AD

The Diagnostic and Statistical Manual of Mental Conditions defines and sets out criteria required to be met in order to be diagnosed as having dementia, these state that the patient must have:

- Memory impairment along with a failure in at least one of the following cognitive abilities that is so severe that it interferes with daily life.

1. The ability of coherent speech or to understand others or written language.
2. The ability to recognise everyday objects provided that this is not due to loss of some sensory input such as sight or touch.
3. The ability to carry out complex motor tasks.
4. The ability to think in abstract ways and comprehend, make rational decisions and plan out complex tasks.

[2] Statistics taken from recent report from the Alzheimer's Research Trust UK: **Statistics data 2011**. http://www.alzheimersresearchuk.org/siteFiles/resources/documents/ARUK_Dementia_statistics.pdf [Accessed on 1st of August 2011].

In rare cases, there is a rapid onset of symptoms that are acute in nature and maybe brought on by treatable conditions such as depression, which can be controlled with mood stabilisers such as LiCl, and reverses the symptoms (Ladika and Gurevitz, 2011).

However, in most cases the dementia is a result of an underlying molecular pathogenesis that has played out over many years and resulted in large neurodegenerative damage leading to substantial atrophy and morphological changes in the brain machinery. From this point forward, the physician is tasked with teasing out the disease that leads to the current state of the patient. It is thought that AD determines 60-80% of dementia cases, 10-20% by vascular dementia, frontotemporal dementia (FTD) and dementia with Lewy bodies but may vary slightly depending on the country (Holtzman et al., 2011) (Barker et al., 2002).

While a demented state is clear from the *norm*, on clinical inspection, AD can present itself in a very similar fashion to many of the other forms of dementia in addition to the normal cognitive decline that correlates with age. This is especially true in the later stages of the disease where so many of the brain regions are affected and the presentation may resemble a variety of dementias. This leads to a conundrum where patients will most likely seek advice from a physician once it is obvious something is wrong and by then, already in the later stages of the disease. So in this respect a specific diagnosis can be very problematic and requires testing by specialists trained to decipher the myriad of nuances that specify a particular form of dementia. To aid the diagnosis, physicians follow a list of criteria such as the NINCDS ARDA that was set out in 1984 (McKhann et al., 1984). A physician can make use of neuropsychiatric testing and imaging studies to provide a diagnosis. For example in AD, an early impairment hallmark is believed to be in the episodic memory and thus distinguishes it from any other form of dementia. This latter function can be tested by the Cambridge Neuropsychology Test Automated Battery-Paired Associate Learning (CANTLAB-PAL) task (Fowler et al., 1997)

2.3 Neuropathology and hallmarks of AD

Alois Alzheimer's first description of the extracellular amyloid-β (Aβ) plaques and intracellular neurofibrillary tangles (NFT) has paved the way for great descriptive analysis of the neuropathology of this disease. Further biochemical examination (discussed later), identified the Aβ peptide and the hyperphosphorylated tau to be the main constituents of the plaques and NFT respectively (see below) (Golde et al., 2000, Wischik et al., 1988, Allsop et al., 1988). Surrounding the plaques, are dystrophic neurites (dendrites or axons) that indicate some form of toxic event is occurring. Surveying microglia and resident astrocytes are activated leading to the release of inflammatory mediators that generate an inflammatory response. These CNS immune cells are also capable of secreting molecules to degrade and clear Aβ, as well as phagocytosing amyloid plaques. A phagocytic response is also required to clear the debris from apoptotic cells (Lucin and Wyss-Coray, 2009). The immediate toxicity will lead to synaptic dysfunction and pruning of the neuronal processes in a series of events leading to apoptosis and massive neuronal loss. As such, one common observation upon post-mortem is the general atrophy of the brain compared to an aged-match control. However this kind of general observation is present in many brains suffering from neurodegenerative diseases at post-mortem and therefore is not particularly helpful in a diagnosis. What is better is the combinatorial use of structural and functional magnetic resonance imaging (MRI) that can be used to reveal, in living patients, the atrophy, hypometabolism and reduced blood flow in the medial temporal lobes, which is characteristic for AD progression (Jack et al., 1998, Scheltens et al., 2002, Wahlund et al., 2000, Patwardhan et al., 2004).

Like other neurodegenerative diseases, in AD there is a peculiar over-excitation of the N-methyl-D-aspartate receptor (NMDAR), which is detrimental and leads to excitotoxicity. In response to the NMDAR-excitoxicity, memantine, as a partial NMDAR antagonist, was approved for symptomatic-treatment of AD (Osborn and Saunders, 2010). These drugs, while doing some good in alleviating some of the symptoms, are incapable of modifying the disease progression.

While the focus of research has been on the formation of the neuritic plaques, the Aβ peptide can also be deposited in the vessel walls of the brain, which can lead to blockages and cerebral amyloid angiopathy (CAA). This is in itself can be very detrimental and lead to ischemic injury as the result of the poor blood flow (Soontornniyomkij et al., 2010) (see 2.5.2.5 Aβ degradation and clearance).

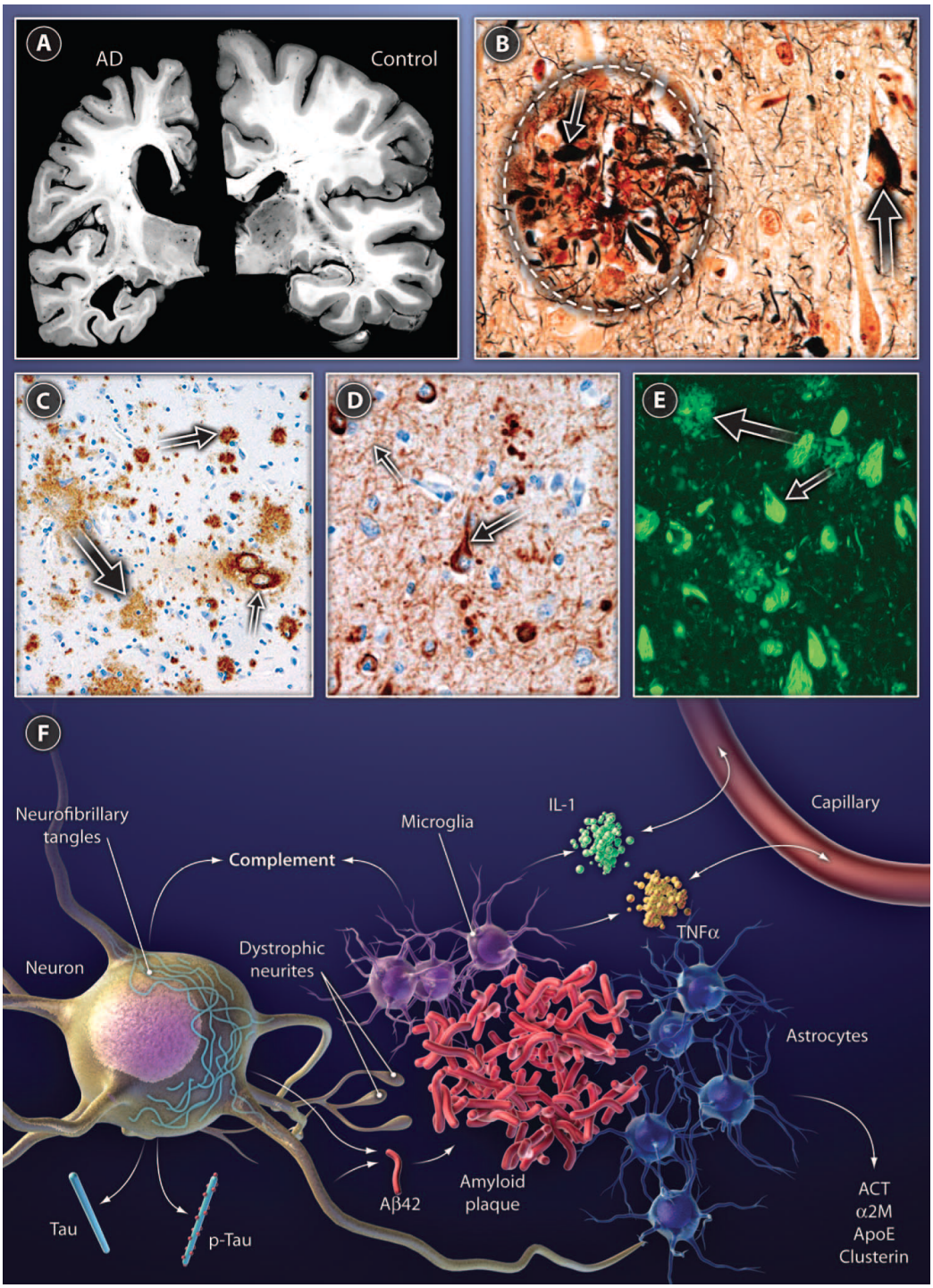


Figure 2.1: Inside of the AD brain.

Images shown above were taken from the Holtzman et al., 2011 review. Images show the atrophy (A), neuritic plaques (B), cerebral amyloid angiopathy (C, small arrow) and NFTs (D) associated with AD. (E) Plaques as visualised with Thioflavin staining under fluorescent light. (F) Shown is a putative scheme of molecular players and pathologies through the matrix of the brain. Illustrated is the influence inflammation may play with the activation of microglia and astrocytes and the release of complement molecules and pro-inflammatory mediators TNFα and IL-1.

2.4 Progression of AD

The period between the initial diagnosis and death, usually from pneumonia, is on average approximately ten years (Swerdlow, 2007). A cognitive dementia rating (CDR) can be ascribed to patients to assess their progression where "0" marks cognitively normal, "0.5" as very mildly impaired or mild-cognitive impairment (MCI), "1" as mildly impaired, "2" as moderately impaired, and "3" as severely impaired at which the sort of brain atrophy and neuropathology illustrated in figure 2.1 would be present (Morris, 1993). In the UK, scores on the mini-mental state examination is used as a means to rate disease progression.

Ultimately, synaptic dysfunction will lead to neuronal loss from firstly the limbic areas such as the entorhinal cortex and the hippocampus, an area critical for short-term memory formation and conversion to long-term memory (Holtzman et al., 2011). This will lead to the symptom of memory impairment in the patient. As the disease progresses, so the atrophy will spread to wider areas through the cortex leading to cognitive decline and often behavioural alterations (Holtzman et al., 2011). In addition, cholinergic neuronal types of the basal forebrain, which again are involved in memory formation, are afflicted by tau and Aβ pathology preferentially (Davies and Maloney, 1976). And as such the first drug therapies introduced for AD were for the treatment of symptoms with acetylcholinesterase inhibitors. The acetylcholinesterase enzyme functions within the synaptic cleft to degrade the neurotransmitter, acetylcholine, in order to prevent sustained synaptic transmission. However with the depletion of these signalling events in AD, preventing the breakdown of this neurotransmitter is believed to have some beneficial, if slight, effect clinically (Ballard et al., 2011). It still remains controversial as to whether there are real benefits to patients on such therapies when carrying out meta-analyses (Birks et al., 2009, Waldemar et al., 2011).

Recent developments using tracer compounds such as [C^{11}]-Pittsburgh compound now allow for the direct visualisation of Aβ species and to measure the clearance of these species from the CNS in patients before and during cognitive decline (Mosconi et al., 2010). What is clear is that Aβ deposition can occur years and even decades before the onset of noticeable symptoms and can be extensive at these early stages (Jack et al., 2010). While a patient may be ranked as CDR=0, it is evident that a multitude of molecular events are playing out unseen in the brain as shown from figure 2.2 (Perrin et al., 2009).

Using the developments in neuropyschometric testing and imaging, a subset of patients could be identified as having MCI (Kidd, 2008, Ringman et al., 2009). Of interest is that these patients had a high prevalence in converting to a full blown demented state, more often than not of the AD type, when followed up longitudinally (Tierney et al., 1996). This amnestic MCI (aMCI) state was therefore seen as a transitional state between normal cognitive aging and AD (Kidd, 2008).

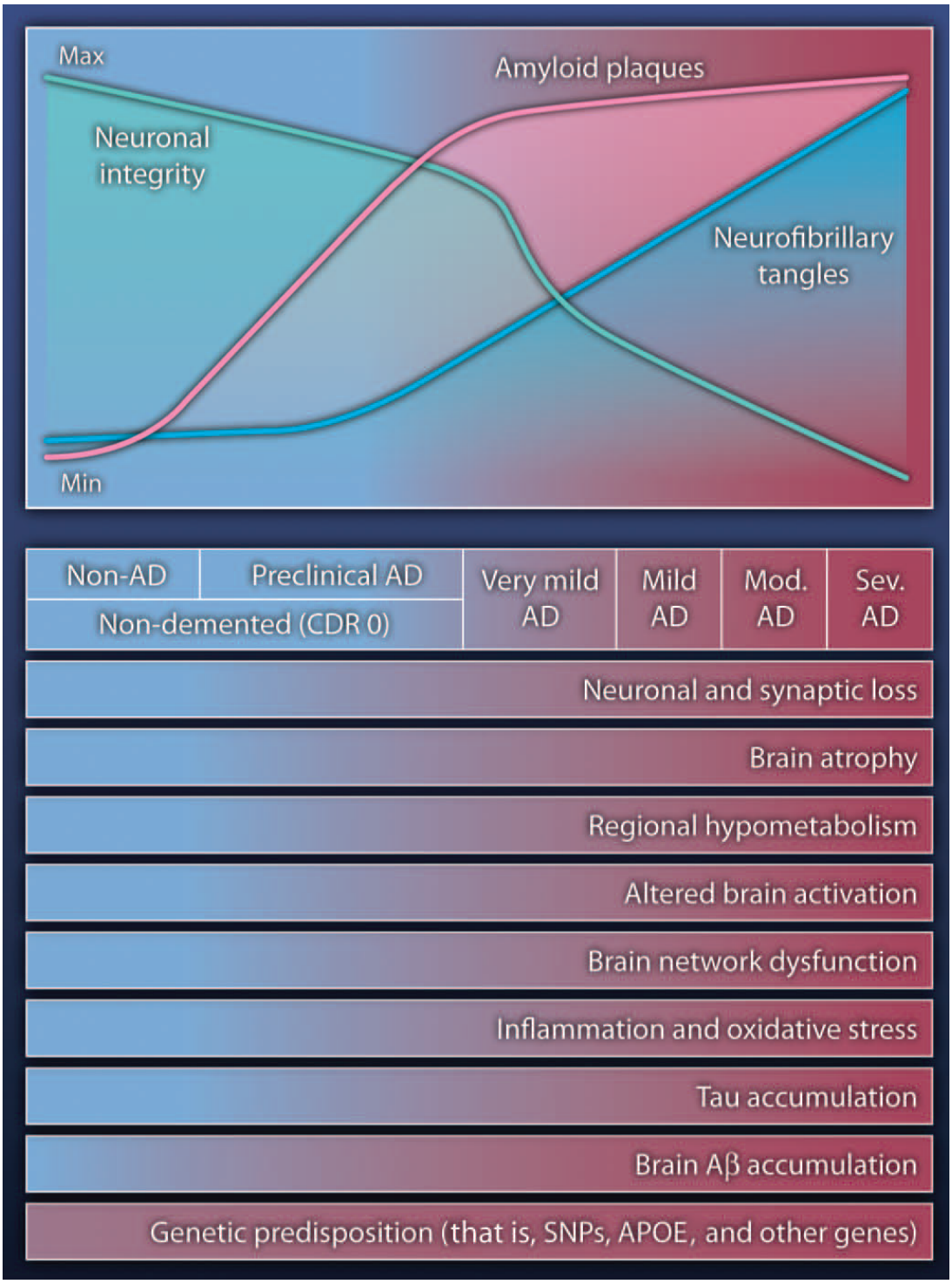


Figure 2.2: The staging and major biomarkers of AD progression.

Schematic taken from (Holtzman et al., 2011). The CDR, used in the USA, rates the progression of AD in the inflicted individual from asymptomatic (CDR=0) to symptomatic 0.5 to 3. The genetic factors unfold from birth while environmental factors build up over life. What is evident is that major molecular dysregulation occurs many years before symptoms are noticeable whereby the amyloid pathology precedes the NFT formation, which in turn leads to neuronal degeneration.

2.5 Aβ pathology and APP processing

2.5.1 Aβ deposition

AD has come to be dominated and defined by the amyloid plaque first witnessed by Alois Alzheimer (1907) and Fischer (1907) independently (Goedert, 2009). These *pathogenic* plaques have been found encroached by dystrophic neurites and gliosis and an activation of surrounding glia that infers an inflammatory response has been provoked. Whether the inflammatory response is a result of tissue damage or is a concomitant and/ or causative phenomenon is under debate (Sastre et al., 2011).

The main constituent of the plaques found in AD and trisomy of chromosome (Chr) 21 Down's Syndrome (DS) patients, was later identified to be the Aβ peptide (Masters et al., 1985). The initial reasoning that lead to the identification of Aβ was that every case of trisomy of Chr21 went onto to develop AD-like symptoms with dramatic Aβ pathology upon post-mortem examination at ages as early as 35yrs (Wisniewski et al., 1985). Three major papers from separate groups in 1987 established the Aβ peptide was a small sub-region of a much larger holo-protein encoded on Chr21 and subsequently entitled the amyloid precursor protein (APP) (Goldgaber et al., 1987, Kang et al., 1987, Tanzi et al., 1987). This key genetic piece of evidence in combination with linkage analysis from family pedigrees of autosomal dominant AD (FAD) fed the amyloid cascade hypothesis of AD (see 2.5.3 Amyloid cascade hypothesis).

2.5.2 APP metabolism

APP is a type-1 integral membrane protein (Kang et al., 1987) that resembles a signal-transduction receptor and belongs to a larger family including APLP1 and APLP2. Single knockout mice show subtle phenotypes suggesting some redundancy between the three. Of interest, a triple *App/Aplp1/Aplp2* KO show decreased life expectancy (Heber et al., 2000). Three isoforms of 695, 751 and 770 amino acids in length are alternatively spliced from one gene encoded on Chr21 (Levy-Lahad et al., 1995). While the 751 and 770 isoform are expressed throughout the body, the 695 variant is predominantly expressed in neurones and lacks the Kunitz Protease Inhibitor (KPI) domain in the extracellular portion (Kang and Müller-Hill, 1990, Anderson et al., 1989). Interestingly, there is evidence that the alternative splicing and expression of the variants can alter with age resulting in a shift to KPI containing splice forms in neurones and an increase in Aβ production (Menéndez-González et al., 2005). This

phenomenon has also been observed in neurones undergoing prolonged NMDA receptor activity, which underlies the excitotoxicity observed in AD (Bordji et al., 2010).

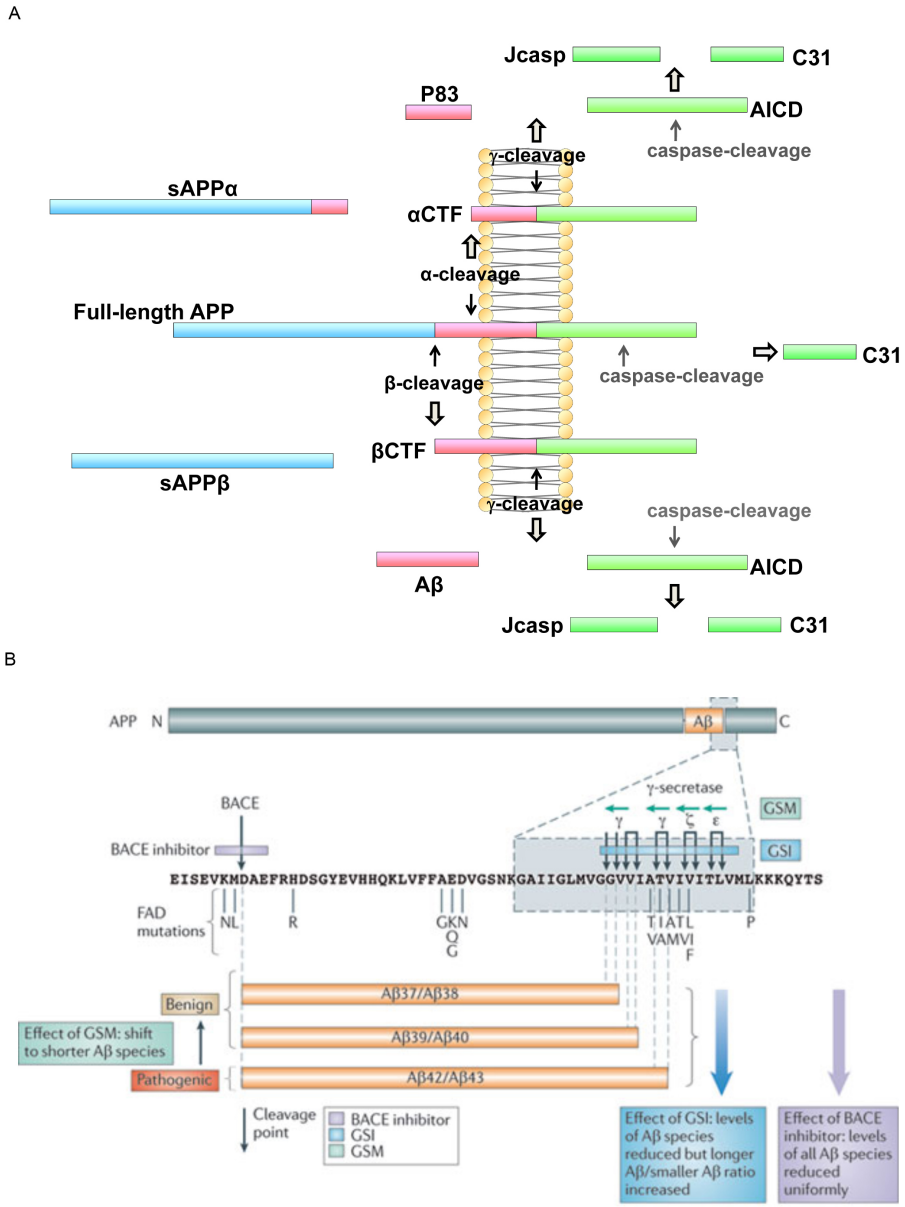


Figure 2.3: APP metabolism.

(A) Approximately 90% of APP is cleaved in what is termed the non-amyloidogenic pathway whereby α-secretase (ADAM10) cleaves first to produce a neuroprotective soluble fragment termed the sAPPα and the p83 of unknown function. However, less often, β-secretase (BACE1) acts before ADAM-10 resulting in a C-terminal stub that will inevitably be cleaved by the γ-secretase (complex of PSEN1/2, Aph-1 and Nicastrin) to form secreted Aβ in the amyloidogenic pathway. (B) Shown is the generation of Aβ of varying lengths with varying propensities for aggregation and toxicity. Indicated are current therapies under development to intervene in amyloid generation (Karran et al., 2011).

2.5.2.1 APP trafficking and processing

The APP molecule is synthesised in the ER and post-translational modified with glycosylation, sulfation and phosphorylation events. Trafficking within the cell moves the APP through the classic secretory pathway where its maturation through the trans Golgi network (TGN) results in vesicular budding and delivery to the plasma membrane (Bossy-Wetzel et al., 2004, King and Scott Turner, 2004, Kang et al., 1987). The full-length protein or its catabolites are then re-internalised and follow the endocytic pathway through the early to late endosomes and finally degraded within the lysosomes (Caporaso et al., 1994). At varying points within this cycle, several secretase cleavages occur which produce Aβ and other catabolites mentioned in the following sections (see α/β/γ-secretase-processing). The trafficking and processing of APP are an interwoven continuum, which is regulated by various molecular interactions of the C-terminal domain of APP and several key adaptor molecules (Suzuki and Nakaya, 2008). The various secretase cleavage events that occur with the trafficking of APP can only happen after the full O-linked glycosylation of the C-terminus (Tomita et al., 1998).

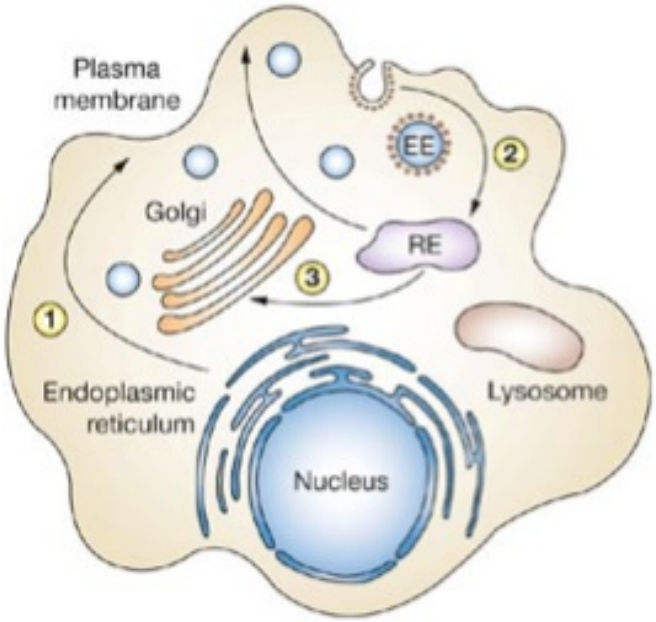


Figure 2.4: Trafficking of APP through the cell.

Trafficking of APP within the cell matures through the secretory pathway where it is internalised and recycled through endocytic compartments or degraded by lysosomes. This illustration was taken from Cheng et al., 2007.

2.5.2.2 α-secretase processing

The initial secretase cleavage event of APP is the α-secretase, which can occur from the TGN to the plasma membrane in the secretory pathway (De Strooper et al., 1993, Kuentzel et al., 1993). This cleavage event leads to the production of a secreted neuroprotective fragment, sAPPα (96kDa), and a membranous α-CTF (10kDa) (Mattson, 1997) (see 2.5.2.6 Physiological functions of APP). As this cleavage site between Lys16-Leu17, lies within the amyloid domain, any such activity precludes Aβ production and as a result forms the non-amyloidogenic pathway (Sisodia, 1992). This activity is believed to be constitutive and the majority of APP molecules undergo this typical non-amyloidogenic processing (Hardy and Higgins, 1992).

The use of a pharmacological inhibition screen discovered the α-cleavage to be encoded by a metalloproteinase (Roberts et al., 1994), with *ADAM* (a disintegrin and metalloproteinase) *9, 10* and *17* being the likely candidate genes. There are several studies that prove α-secretase cleavage for each of these ADAM isoforms and there may be some functional redundancy but with this being said, ADAM-10 is believed to be the constitutive α-secretase (Kuhn et al., 2010) while ADAM-9 and 17 are regulated forms (Buxbaum et al., 1998, Koike et al., 1999, Merlos-Suárez et al., 2001). In addition to identifying ADAM-10 as the α-secretase, transgenic mice studies have illustrated that the sAPPα fragment is neurotropic (Mattson et al., 1993, Mattson et al., 1999) and promotes synaptogenesis within the cortex of the major neurotransmitter presynaptic terminals (Bell et al., 2008, Postina et al., 2004). A similar increase in synapse formation is believed to occur in AD as a compensatory mechanism to counter the loss in neuronal mass, specifically cholinergic neurones. Furthermore ADAM-10 overexpression in a bigenic model crossed with APP.V717I is associated with neuroprotection against excitotoxicity, another hallmark of AD (Clement et al., 2008). The overall majority of studies have therefore shown α-secretase and the non-amyloidogenic processing of APP to be associated with positive neuroprotection.

2.5.2.3 β-secretase processing

Full-length APP (FL-APP) can alternatively be cleaved by the initial amyloidogenic cleavage of the β-secretase (Selkoe and Schenk, 2003). The β-site lies immediately N-terminal of the Aβ domain and when cleaved releases an analogous sAPPα fragment, the soluble APPβ (94kDa), although it is thought to be neurotoxic rather than protective. The remaining membrane bound β-CTF (12kDa) is cleaved by the γ-secretase to release the varying Aβ species. The α- and β-cleavage of APP is generally described as ectodomain shedding, a phenomenon that is very important in regulating the physiological functions of membrane proteins (Reiss and Saftig, 2009).

Several simultaneous studies identified the β-secretase as the β-site APP-cleaving enzyme 1 (BACE1) (Sinha et al., 1999, Vassar et al., 1999, Yan et al., 1999, Hussain et al., 2000). The BACE1 protein is synthesised as a larger pro-BACE1 protein, which is subsequently cleaved by a furin-like endoprotease, which produces the mature and active form as a membrane-bound aspartyl protease (Bennett et al., 2000, Creemers et al., 2001). Like APP, pro-BACE1 is secondary modified after synthesis in the ER, which largely regulates its concomitant trafficking within the cell. In addition to these modifications, there is also an endoproteolytic cleavage event that occurs in the Golgi apparatus to generate mature BACE1. BACE1 is preferentially active in the TGN and early endosomal compartments owing to the more acidic nature of the lumen they enclose. This mirrors previous reports of β–secretase mediated cleavage of APP in the same cellular locations (Haass et al., 1995, Koo and Squazzo, 1994). Populations of BACE1 molecules recycle between these acidic intracellular compartments and the plasma membrane in a process largely controlled by phosphorylation within its cytosolic facing C-terminal domain by casein kinase 1 (CK1) (Walter et al., 2001).

Soon after, BACE2, which has 64% sequence similarity to BACE1, was identified (Solans et al., 2000). However its expression within neurones is extremely low and its cleavage is more reminiscent of the α–cleavage (Yan et al., 2001). However, the final nail in the coffin for BACE2 was that *Bace1*$^{-/-}$ mice crossed with mice that develop plaques are completely devoid of any amyloid species. This concludes that BACE1 is probably the only physiological β-secretase and this initial amyloidogenic cleavage is critical and rate-determining in the generation of Aβ. What was even more impressive was that in these mice the neuronal loss, cholinergic deficits and memory impairment characteristic of AD were rescued (Luo et al., 2001,

Ohno et al., 2004). This and the fact that BACE1 activity is believed to increase in AD brains (Yang et al., 2003, Fukumoto et al., 2002) has lead to numerous therapeutic studies being funded both privately and in academia. Initial studies reported that promisingly in terms of therapy, there was no observable phenotypic side affects resulting from *Bace1* ablation in null mice. However this conclusion has been called into question as recent studies have shown significant reduction in viability of the *Bace1* null mice in the few weeks post-natal if compared to wild-type littermates (Dominguez et al., 2005). As neuregulin-1 is a major target of BACE1, the null mice also suffer from hypo-myelination of nerves within the peripheral nervous system (PNS) (Willem et al., 2006). This results in subtle motor and sensory phenotypes such as reduced grip strength and increased pain sensitivity (Hu et al., 2006). Some behavioural abnormalities that were reminiscent of a schizophrenic phenotype have been reported in the *Bace1* knockout line as well (Savonenko et al., 2008). A plethora of additional cellular substrates again call into question the suitability of BACE1 as a pharmacological target (Vassar et al., 2009).

In addition to an increase of activity in AD brains, BACE1 activity increases have also been reported in normal aging (Fukumoto et al., 2004). There is also evidence to suggest that an increase in activity can be induced by traumatic brain injury (Blasko et al., 2004) and inflammation (Sastre et al., 2008). These observations go a long way to explain at a mechanistic level, why there are increased incidences of AD in persons who were subjected to traumatic brain injury such as boxers and persons involved in car accidents (Gentleman et al., 1997). In addition to the obvious increased activation of microglia and astrocytes that orchestrate the CNS inflammatory response to plaques, a recent hypothesis has also hinted at inflammation being a major driver of the initial AD pathology. The increased activity of the β-secretase may be explained by alterations in the transcriptional output from the BACE1 gene. Numerous *in vitro* studies have indicated that the BACE1 promoter is responsive to a multitude of transcriptional factors signalling related to dampening or promoting the inflammatory response, these include NFκB, STAT and PPARγ (Sastre et al., 2008). In addition to regulation at the transcriptional level, changes in the protein expression of BACE1 without a parallel alteration in the mRNA can also come from post-transcriptional regulation (Willem et al., 2009). These mechanisms include RNA secondary structures within the 5' untranslated region (UTR) and binding of micro RNA (miRNA) species to a 3' UTR that both influence the

translational efficiency from the mRNA transcript (Lammich et al., 2004). As most of these elements are associated with reducing translation (Zong et al., 2011) their loss is correlated with increased BACE1 expression in sporadic AD patients (SAD) (Hébert et al., 2008). A surprising non-coding antisense RNA, *BACE1-AS*, was identified that led to increased stabilisation and translation of *BACE1* mRNA as opposed to increased degradation, which is associated with RNA duplexing (Faghihi et al., 2008). A feed-forward loop is generated through the expression of this RNA element with cellular stress such as Aβ exposure and is elevated in AD patients.

In addition, several adaptor proteins that interact with the C-terminus of BACE and regulate the cellular location can also influence the activity of the β-secretase. An increase in expression of reticulon/Nogo family of proteins leads to retention of BACE1 within the ER, which is too alkaline for optimal β-CTF generation (He et al., 2004, Murayama et al., 2006). Later in the secretory pathway, the Golgi-localized γ-ear-containing ARF-binding (GGA) proteins seem to regulate the retrograde trafficking between the late Golgi compartments and the early endosomes, where changes in the acidity of the respective lumen influences β-secretase activity (Wahle et al., 2005, Wahle et al., 2006).

The membrane-bound Prion Protein (PrP) is an interesting peptide, as when it is processed erroneously it leads to prion diseases but also it has been linked to the pathogenesis of AD. In its physiological state, PrP^c, can inhibit the β-cleavage from BACE1 and reduce Aβ production (Parkin et al., 2007). In sporadic but not familial cases of AD, it appears that this negative regulator is reduced in expression and therefore can provide another explanation for increased β-secretase activity with aging (Whitehouse et al., 2010). The differential linkage can be explained by the observation that a later study illustrated PrP^c only influences the processing of wild-type APP and not familial forms such as APPsw (Griffiths et al., 2011b).

2.5.2.4 γ-secretase processing

Initially identified through genetic analysis, it was later proven in several key studies from several groups to show that presenilin (PSEN1/2) along with three other regulatory proteins, anterior pharynx-defective 1 (APH1), presenilin enhancer-2 (PEN-2) and nicastrin reconstitute the activity of the γ-secretase complex (Edbauer et al., 2003, Kimberly et al., 2003, Takasugi et al., 2003). The different isoforms of the various complex subunits, for example APH1aS/L and APH1b, allow for differential γ-secretase complex formation and activity (Shirotani et al., 2004, Ma et al., 2005). While the generation of the P3 fragment is of no interest as it is rapidly degraded, the more interesting cleavage yielding Aβ happens within the transmembrane region in a highly regulated manner. This kind of proteolysis has attracted much research and several key studies have elucidated the biochemical mechanisms behind its functions. In line with familial linked mutations within the *PSEN* genes, the double knock-in *APP/PSEN1* (expressing the familial human *APPsw* and *PSEN1 M146L* mutants) mouse model accurately recapitulates AD with amyloid pathology that is correlated with memory impairment, cognitive decline and hypometabolism far superior to that of *APP* single knock-in transgenic models (Trinchese et al., 2004). Finally, when combining this background with the human tau familial mutant, *P301L*, it is possible to model the interaction between the amyloid and tau pathology in a single mouse strain (3xTg-AD) (Oddo et al., 2003).

Presenilins, the catalytic unit of the complex, are several-passing transmembrane proteins that are associated with intracellular membranes such as the endoplasmic reticulum (ER), the Golgi apparatus, lysosomes and autophagosomes (Kovacs et al., 1996, Pasternak et al., 2003, Yu et al., 2004). In addition to their catalytic function towards APP, they also have physiological functions towards type-I integral membrane proteins. For instance, its typical cleavage regulates Notch signalling (Schroeter et al., 1998, Vetrivel et al., 2006) and it also cleaves the APP-like proteins (APLP), where the function is less clear (Eggert et al., 2004). In most cases these presenilin cleavage events result in intracellular fragments capable of nuclear shuttling albeit with controversial transactivation function. In addition to this, there are believed to be many more biological functions associated with presenilin activity and functions independent of its secretase role (Parks and Curtis, 2007, Thinakaran et al., 1996b). No doubt, whether they are direct or indirect, biological functions that are associated with presenilins will only gain in number with more

research. Of particular interest was the role of PSEN1 in the acidification of autophagolysosomes through its interaction with the vacuolar-ATPase. FAD relevant mutations in *PSEN1* can result in improper acidification and as such result in reduced proteolysis through autophagy/lysosomes (Lee et al., 2010). This is of note as such dysfunctions have been observed in human AD post-mortem tissue and mouse models of AD such as the *PSEN1/APP* transgenic mouse (Rubinsztein et al., 2005). With the numerous cellular targets, there must be some fairly stringent regulation in order to insulate the many pathways influenced. One prime example of regulation is through the coordinated cycling and location of the complex with its substrate within several intracellular membranes.

The γ-secretase complex is defined by its function, namely the sequential cleavage of APP CTFs to produce varying Aβ fragments and additional metabolites. There are three typical sites that are believed to occur in a sequential order (see figure 2.5):

- The ε-cleavage, which lies closest to the membrane/cytosol boundary, generates the larger $A\beta_{49}$ (Sastre et al., 2001a). This cleavage event is highly analogous to the S3 cleavage of Notch, another major PSEN1 subunit (De Strooper et al., 1999).
- Next, the ζ-cleavage results in the production of the less abundant $A\beta_{46}$ (Zhao et al., 2004).
- Finally γ-cleavage results in the production of the most prominent species $A\beta_{40}$ and $A\beta_{42}$ depending on the exact site.

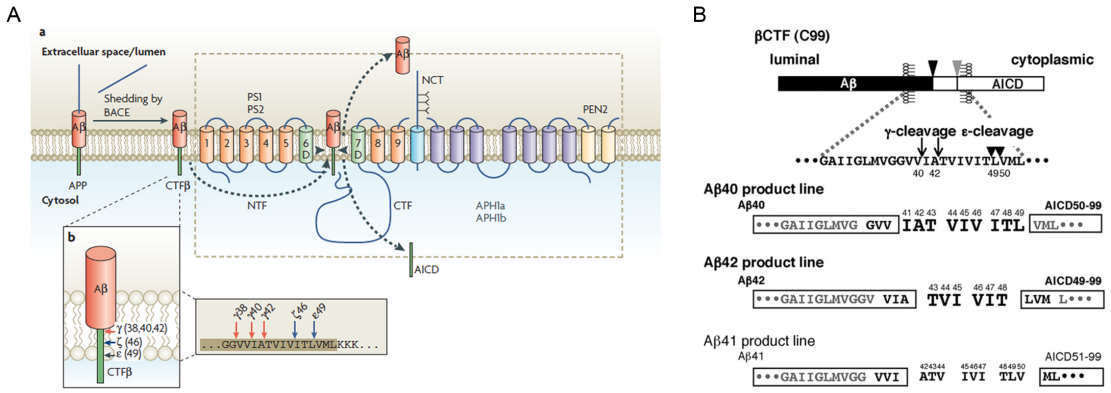


Figure 2.5: The putative topology of PSEN1/2 and the stepwise model for generation of major Aβ metabolites from β-CTF by the γ-secretase complex.

(A) The putative topology of PSEN1/2 and its binding partners. From genetic and biochemical analysis, the topology of PSEN1 was mapped to include 9 TMD domains and a large cytoplasmic loop between TMD 6 and 7 which contains the endoproteolytic cleavage event for activation of PSEN1. Scheme taken from Haass and Selkoe, 2007. (B) Hypothetical schematic put forward by Ihara and colleagues states a stepwise cleavage every three residues starting from the epsilon cleavage either at position 49 resulting in the production of $A\beta_{40}$ or at position 48, which results in the less abundant $A\beta_{42}$. This also results in differential sizes of the released AICDs. Scheme taken from Takami et al., 2009.

Each sequential cleavage event protrudes further into the membrane and allows entry of water molecules for the hydrolytic reaction. Although the exact mechanism by which these varying fragment lengths are generated is unknown, it is believed that they all result from the same γ-secretase molecule (Zhao et al., 2007). The most current line of thinking speculates that $A\beta_{42}$ is generated by a different product line of sequential tripeptide cleavage events to that of the more prominent $A\beta_{40}$ (Takami et al., 2009). Figure 2.5 shows that the typical epsilon cleavage that generates $A\beta_{49}$ (Sastre et al., 2001b) results in the progressive formation to $A\beta_{40}$ through the intermediates, $A\beta_{46}$ and $A\beta_{43}$. In contrast with a differential epsilon cleavage at position 48, $A\beta_{42}$ is generated through the intermediates $A\beta_{45}$ (Takami et al., 2009). Using sophisticated mass spectrometry, the predicted tripeptides that should be released from a stepwise cleavage mechanism were detected from cells over expressing the β–CTF. Most *PSEN1* mutations lead to an increase in specifically $A\beta_{42}$, believed to be the more toxic form of the amyloid peptide due to its increase in hydrophobicity and propensity to aggregate. This observation is formed from experiments in human brains, *ex vivo* cultures (Scheuner et al., 1996) and *in vivo*

transgenic models (Borchelt et al., 1997, Holcomb et al., 1998). Gain in the γ42 cleavage also has a parallel effect to reduce the ε-cleavage of APP and S3 cleavage of Notch (Chen et al., 2002). Unfortunately, the biological mechanism behind the molecular switching of PSEN1 cleavage site preference is still to be elucidated. The functional significance for AD of concomitantly reducing the preference of PSEN1 for its other targets such Notch is also unknown.

PSEN1 undergoes a highly conserved endoproteolytic activation in which the unstable nascent protein undergoes a cleavage event producing a 27-28kDa N-terminal fragment (NTF) and a 16-17kDa C-terminal fragment (CTF) (Thinakaran et al., 1996a). This cleavage, although not completely understood, is believed to occur within the large cytoplasmic loop domain between residues Thr291 and Ala299. This cleavage is dependent on two key aspartate residues, one at position 275 within the putative transmembrane domain (TMD) 6 and another at position 385 in TMD7 (Wolfe et al., 1999) and is largely regulated by the PEN-2 subunit (Luo et al., 2003) (please see figure 2.5). This event is believed to have two main biological outcomes; first and foremost, this is associated with an increased activity of the γ-secretase and secondly that the half-life of the two resulting fragments increase to 24hrs (Podlisny et al., 1997). Interestingly, the *PSEN1ΔE9* variant associated with FAD lacks a region encoded by exon 9 that codes for this cleavage loop and is somehow intrinsically stable and more importantly is capable of γ-secretase activity (Ratovitski et al., 1997, Iwatsubo, 2004).

One major contribution to the regulation of presenilin function is the proximity and access to the different substrates within the cell. The presenilin function requires high cholesterol and sphingolipid content, reminiscent of lipid micro-domains from the major intracellular organelle membranes (Vetrivel et al., 2004) and its activity is found mostly in these compartments. De Strooper and colleagues using an interactome study of PSEN1, identified tetraspanin, which forms the cholesterol-rich lipid raft-like microdomains, as an important interactor and therefore validating the localisation of PSEN1 (Wakabayashi et al., 2009). Using various methodologies, groups have shown there is very little γ-secretase activity associated with the plasma membrane despite its important role in Notch cleavage/signalling (Chyung et al., 2005). In contrast, APP is mainly cleaved in the early endosomes following internalisation from the plasma membrane and the TGN

(Tarassishin et al., 2004). Another possible gain-of-function mechanism for *PSEN1* mutations may be due to the retention of PSEN1 within the intracellular compartments leading to an increased localisation with APP and a concomitant reduction in cleavage of the other substrates.

In addition to the role of cleavage, the PSEN1 subunit is also believed to aid in the trafficking of many key substrates such as APP. In *PSEN1* knockout cells, there are numerous examples of membrane proteins being mislocalised that are not secretase substrates (Vetrivel et al., 2006, Naruse et al., 1998). This provides evidence for PSEN1 being a *bona fide* chaperone. One example interestingly is the α-synuclein protein that is the main component of Lewy bodies dotting the brain from dementia with Lewy bodies and Parkinson's disease patients. In *PSEN1* KO cells this protein is found mainly in autophagosomes but it is not in normal neuronal cells treated with selective γ-secretase inhibitors (GSIs) (Wilson et al., 2004).

Most current GSIs in clinical development have largely failed due to their low therapeutic index that is resulting from the multitude of cellular substrates and events that PSEN1 and the γ-secretase is involved in. For instance, most current therapies are not Notch sparing and as such one particular clinical trial had to be halted owing to an increased cancer frequency risk (Cummings, 2010). Other important targets of presenilin cleavage include cadherin, which is found at tight junctions and influences the stability and turnover of β-catenin (De Strooper and Annaert, 2010, Zhang et al., 2011), the tyrosine kinase ErbB4 that is responsible for the behavioural abnormalities in the *Bace1* knockout studies (Savonenko et al., 2008, Lee et al., 2002) and around 60 other targets

One key question under investigation is what are the potential mechanisms by which the γ-secretase can regulate the cleavage of its multiple cellular substrates? One possibility is that the varying substrates may have different subcellular localisations. Another hypothesis is that the other subunits of the γ-secretase complex are involved in substrate recognition (Bammens et al., 2011). De Strooper and colleagues, whose research focuses on the regulatory roles of the other subunits apart from presenilin in the γ-secretase, have championed this proposal through therapeutics categorised as modulators (GSM) as opposed to inhibitors (Karran et al., 2011). One very promising therapeutic target is the newly identified γ-secretase activating protein (GSAP) (He et al., 2010). This selectively alters $A\beta_{42}$ production without affecting Notch cleavage

by binding directly to the APP CTF and the γ-secretase complex. This activating protein already has a FDA approved antagonist, Gleevec, an anticancer drug already shown to reduce Aβ production independent of Notch (Netzer et al., 2003). Further to this, certain NSAIDs, which have been shown to be protective against AD in certain meta-analyses (Sastre and Gentleman, 2010, Vlad et al., 2008), can also alter the ratio of $A\beta_{40/42}$ favourably rather than inhibit the γ-secretase outright (Eriksen et al., 2003, Weggen et al., 2001).

2.5.2.5 Aβ clearance and degradation

In addition to an amyloidogenic pathway, there is also physiological means to clear Aβ peptides out of the interstitial fluid (ISF) and across the blood-brain-barrier (BBB) into the periphery. Aβ-immunotherapy, whereby parenchyma levels of Aβ are depleted is believed to rely on this shuttling process from the ISF to the peripheral serum, where it accumulates (Morgan, 2011). The efflux is mediated through transporters such as the P-glycoprotein and lipoprotein receptor-related protein 1 (LRP1) transcytosis (Deane et al., 2009). Apolipoprotein-ε (Apoε) isoforms, which are involved in redistribution of cholesterol and phospholipids in the brain, can heavily influence these efflux mechanisms. They are produced and secreted by astrocytes and lipidated by the ATP-binding cassettes transporter A1 to form high-density lipoprotein particles. The three isoforms Apoε2/3/4 vary in their ability for cholesterol efflux, lipidation and receptor binding affinity (Kim et al., 2009a). While the ε3 isoform is far the most common, ε4 is associated with a greater risk of AD progression while ε2 is thought to be protective (Roses, 1996). Subsequent work has illustrated the isoform dependency for predisposition to AD down to the ability for Apoε to clear Aβ species from the brain (Castellano et al., 2011a).

In addition to clearance of soluble forms of Aβ across the BBB, they can also be degraded through proteolysis in the extracellular space. These peptidases include the membrane-bound neprilysin, which is associated with microglia and the insulin-degrading enzyme (IDE) that is secreted from numerous cell types (Iwata et al., 2001, Iwata et al., 2000). A molecular mechanism to explain the link between type-2 diabetes (causing hyperinsulemia) and predisposition for AD in later age might arise from the superior affinity of insulin over Aβ to bind IDE (de la Monte and Wands, 2008).

Activated microglia are capable of up-taking extracellular Aβ that is fibrillar as opposed to the soluble species, which can cross the BBB. This is believed to occur through a phagocytic process, which is believed to result in degradation of the insoluble aggregates however this is not conclusive (Lee and Landreth, 2010). This process is mediated through a spectrum of cell surface receptors to form Aβ-receptor complexes influenced by a cacophony of pro- and anti-inflammatory signalling mediators. Neuronal cells and astrocytes can also uptake extracellular aggregates of Aβ through the receptor for advanced glycation end-products (RAGE) complexes (Lee and Landreth, 2010).

What happens when the Aβ aggregates are endocytosed in the differing cell types within the brain is unknown. In most cases, the various Aβ species remain locked in endosomes that will later fuse with lysosomes for proteolysis if correctly acidified (Majumdar et al., 2007). In addition to the endosome-lysosome pathway, degradation can also occur via the autophagy pathway. For instance, if this pathway is blocked, the Aβ-mediated toxicity observed in most transgenic models of AD is enhanced (Florez-McClure et al., 2007). In terms of AD, great strides have been made recently in understanding the mechanistic basis of the FAD mutations associated with *PSEN1*. Interestingly, these mutations in addition to increasing the ratio to favour the fibrillogenic $A\beta_{42}$, seem to also affect autophagy-lysosomal proteolysis through disrupting the role of PSEN1 as a chaperone for an important vacuolar-ATPase. As a result the fusion events with lysosomes do not result in the correct acidification that is required for protease activity (Lee et al., 2010). A similar phenomenon was observed in a recent paper studying the induction of non-demented and FAD patient fibroblast cells into human induced neurones (hiN) (Ambasudhan et al., 2011). Importantly, this new technique allows the study of cellular events in a direct model of the human disease without having to express human familial forms of APP in mouse cells and transgenic lines. The authors have corroborated previous studies illustrating an increased production of Aβ with the presence of *PSEN1* polymorphisms. In addition, the hiN cells from AD patients when compared to hiN cells of healthy patients showed an altered endosomal compartment phenotype that were often APP-immunopositive (Qiang et al., 2011). This is consistent with previous autopsy analysis of human SAD brains (Cataldo et al., 1997) and certain AD transgenic models (Yang et al., 2008), which have reported the presence of altered endosomal, lysosomal and autophagy compartments (Rubinsztein et al., 2005, Boland

et al., 2008). In addition to Aβ, several studies have shown that the holo-protein APP can be specifically targeted to the autophagosomes. This can be associated with degradation of the holo-protein independent of processing (Vingtdeux et al., 2010) or with amyloidogenic processing of APP (Jaeger et al., 2010); however this latter finding has been called into question (Boland et al., 2010).

2.5.2.6 Physiological functions of APP

While decades of intricate research have deciphered how dysregulation of APP processing and Aβ-neurotoxicity may lead to AD, the physiological function(s) of APP are still not fully known. While this may seem a trivial point, often one can learn a lot of a disease state from first fully understanding the normal physiological state. Whilst the non-amyloidogenic pathway amounts for the majority of APP processing, the amyloidogenic pathway does occur within the brain of healthy humans albeit at a minimal level (O'Brien and Wong, 2011).

The fact that APP resembles a surface receptor, suggests it may function in a receptor role similar to Notch at the plasma membrane. Furthermore it contains the two highly conserved sequences, the ^{667}VTPEER^{672} motif and the ^{681}GYENPTY^{687} motif, situated in the CTD of APP (O'Brien and Wong, 2011), which largely regulate its trafficking and are characteristic of cell surface receptors. These conserved regions provide sites for phosphorylation and regulation of adaptor protein binding. These auxiliary proteins control the amount of processing and the shuttling of the AICD fragment to the nucleus (Kang et al., 1987, von Rotz et al., 2004). A similar intracellular fragment, cleaved from Notch, shuttles to the nucleus to regulate transcription and thus linking an external cue perceived by Notch and gene regulation (Sastre et al., 2001a). While it remains controversial, the AICD is believed to act in a similar fashion and can regulate the expression of multiple genes encoding APP itself and BACE1 (Beckett et al., 2011) and neprilysin (Pardossi-Piquard et al., 2005).

As a means to study the physiological functions of APP there are several *App* and *App/Aplp* knockout models in addition to the numerous knock-in models used to determine the function of the different APP fragments (Guo et al., 2011). Furthermore, conditional KO mice have been used to discern postnatal function from a developmental context. As such the function(s) of APP include axonal transport, cell adhesion, cholesterol metabolism and gene transcription via its nuclear-shuttling AICD fragment (Turner et al., 2003, Belyaev et al., 2010). In response to this, APP

in isolation is not important but the generation of its constituent metabolites is. For instance, signalling in a paracrine manner, sAPPα is believed to play a neuroprotective role and in synaptic plasticity while a novel sAPPβ fragment has recently been found to induce synaptic pruning and neuronal death which is required for sculpting neuronal circulatory during development (Nikolaev et al., 2009). Indeed, rescuing mice with just the sAPPα fragment is capable of attenuating the synaptic dysfunction in *App* KO mice (Ring et al., 2007). Despite the indication of function from knock-in models, the various single knockout and their combinations (including the triple knockout), show very little changes in phenotype. Any resulting phenotype is associated with developmental alterations and is subtle, such as the alteration in the migration of the neurones that make up the layers of the cortex (Herms et al., 2004).

Concerning Aβ, it must have a function by itself, as there is a biological pathway to generate this peptide, and it is produced physiologically in tissues and cell culture, albeit in small quantities. It is tempting to speculate that as sAPPα promotes LTP and Aβ promotes LTD, they could both serve in finely tuning synaptic plasticity (Abramov et al., 2009, O'Brien and Wong, 2011).

Or it could be speculated that, while other metabolites of the amyloidogenic pathway serve functions, Aβ is a by-product that in normal individuals is inconsequential but if generated in excess, as in the case within the brain of an AD patient, it causes irreparable damage. While natural selection generates systems that need not expend energy needlessly, Aβ-mediated toxic events occur decades past the reproductive peak and as such there is simply no selective pressure to eliminate this generating cleavage event.

2.5.3 Amyloid cascade hypothesis

Following the isolation of the Aβ peptide and the identification of the *APP* gene, several familial pedigree analyses of autosomal AD added two key elements. Firstly, although DS could be explained by Aβ deposition it did not necessarily link the peptide to AD genetically. However, this changed with the identification of missense mutations within *APP* itself that lead to an early-onset AD type (EOAD). There are 20 FAD mutations in the *APP* sequence, but this represents only 5% of total FAD mutations. But more specifically, these mutations lie within regions overlapping sites for endoproteolysis that is involved in the production of Aβ. For example, the

London mutation alters a valine residue at position 717 to an isoleucine (V717I) with a concomitant increase in $A\beta_{42}$ production and this specific peptide is believed to be more fibrillogenic and toxic in nature (Goate et al., 1991). Similarly a double substitution mutation isolated from a Swedish family, positioned at the β-secretase cleavage site (see 2.5.2 APP metabolism) results in increased production in both $A\beta_{40}$ and $A\beta_{42}$ (Mullan et al., 1992). The novel $A\beta_{43}$ peptide, which is found in AD brains to a similar extent as $A\beta_{42}$, is also extremely toxic in an overexpressing transgenic model (Saito et al., 2011). It would seem then that the toxicity of Aβ increases with its length (see figure 2.3). Owing to this genetic evidence, it was postulated that the Aβ peptide was the causation of the pathological defects observed at the microscopic scale and the basis of the neurological symptoms. Further studies show that mutations contained within the Aβ domain can, unlike others located at the beginning and end, affect the dynamics of oligomerisation, deposition in the vessel walls (CAA) and clearance from the CNS (Jawhar et al., 2011). This latter point is vital in understanding the hypothesis, as the initial proposal other than acting as a trigger for subsequent events did not actually explain the pathogenic mechanism (Hardy and Allsop, 1991, Hardy and Selkoe, 2002). It should be stated that up until this point there is no evidence that any familial mutations within *APP* alter its function but rather concern themselves with Aβ metabolism. This is important in order to stress that the Aβ is linked and drives the disease as opposed to a gene dosage effect of the physiological function of APP itself. However this is born out from the lack of understanding of native APP biology unrelated to disease. Ultimately further research is required in fully understanding the physiological function(s) (see 2.5.2.5 Physiological functions of APP) of APP and also the amount of redundancy that comes from APLP1/2.

Further evidence was gained with the isolation of mutations within two key genes *PSEN1* (Levy-Lahad et al., 1995) and *PSEN2* (Sherrington et al., 1995) encoding the catalytic unit of the γ-secretase (see 2.5.2 APP metabolism), which ultimately cleaves APP to yield Aβ. Interestingly, these mutations are not only found in FAD resulting in an early onset of the disease but they are also found in the more frequent LOAD cases. This is of note as some may argue that the amyloid hypothesis may only explain the mechanisms leading to FAD and segregate these rare cases as a separate disease. These mutations also have some mechanistic basis, which result in

increased Aβ production. One particular mutation, *PS1ΔE9* was found to completely override the highly regulated endoproteolysis of PSEN1/2, which results in a concomitant increase in γ-secretase activity (see 2.5.2.4 γ-secretase processing) (Iwatsubo, 2004, Ratovitski et al., 1997). And again there are numerous examples of mutations in *PSEN1/2* that lead to a gain of function towards APP with or without a parallel loss of function towards its many other substrates (see 1.6 Variations on a theme: LOAD versus FAD).

Therefore, it is perfectly intuitive to think that if the disease-linked genetic alterations result in increased Aβ production, then it must drive the disease.

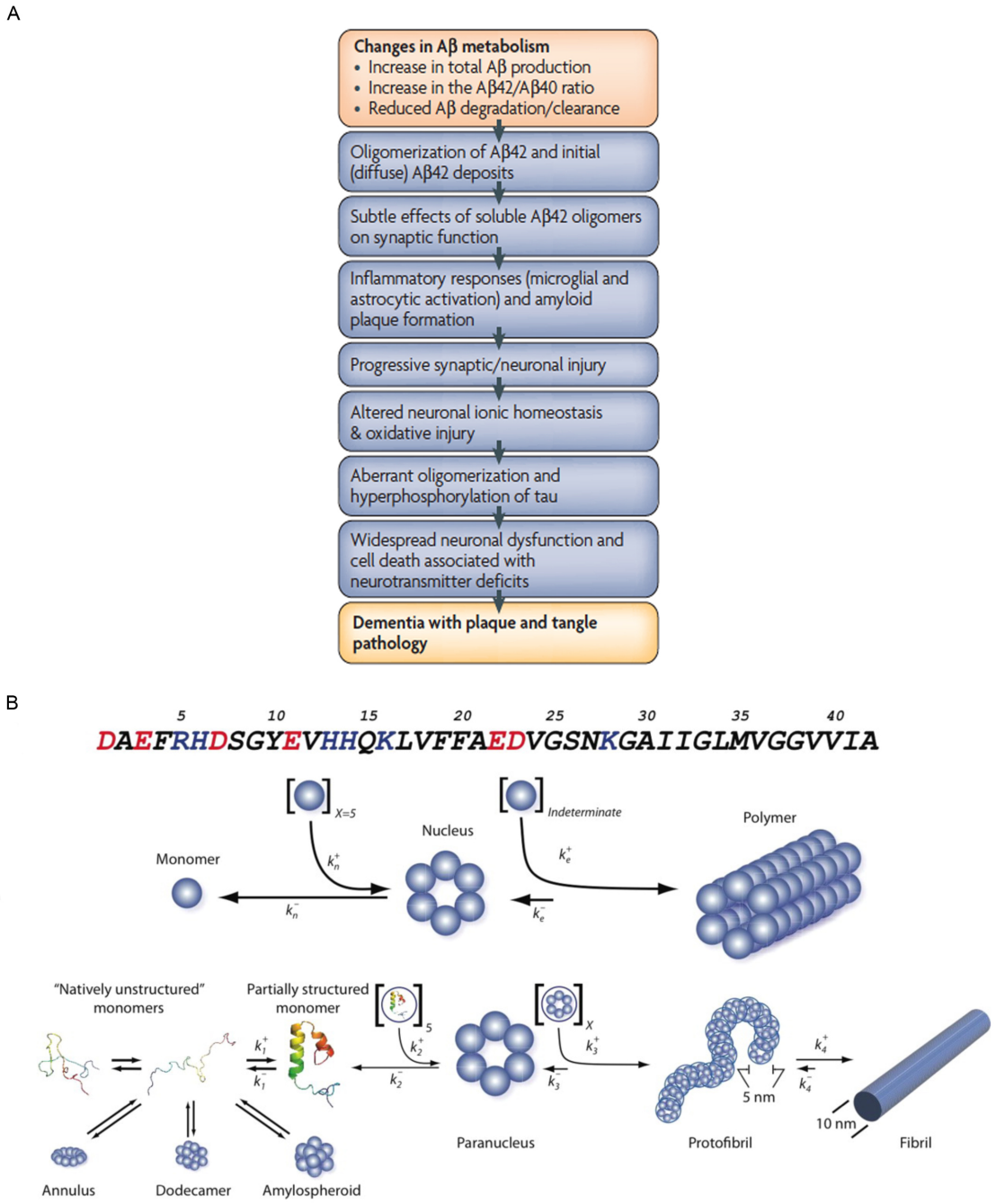


Figure 2.6: Amyloid cascade hypothesis.

(A) The modified amyloid cascade hypothesis presented in the review, Selkoe and Haass (2007), is an update of the original proposed by Hardy and Allsop (1991) and Hardy and Selkoe (2002). The original elucidation of *APP*, a genetic element of Alzheimer's proposed an increase in Aβ production drives the disease. Over time spine densities are reduced, synaptic signalling altered, axonal transport disrupted and programmed cell-death will ensue. Loss of synaptic signalling in addition to loss of whole neurones leads to disruption of cognition, memory and executive functions. (B) The initial production of monomeric Aβ and polymerisation into intermediary oligomers, leading to fibrillation into fibrils, which ultimately form plaques. The process with reversible steps is thermodynamically complicated and can be influenced by the mutations found within the Aβ peptide (Jawhar et al., 2011).

2.5.4 Aβ oligomerisation and toxicity

From the initial proposition of the amyloid cascade hypothesis for AD, some controversial data has come to light, the most noticeable of which is that plaque load correlates very poorly with cognitive decline, unlike the load of neurofibrillary tangle (NFT) pathology (Sloane et al., 1997, Nelson et al., 2009). Complementary analysis has however isolated numerous intermediary amyloid structures that transition monomeric Aβ into the typical AD plaques. As a result, a far more complicated picture has emerged showing a highly dynamic process in which initial dimers and low molecular weight oligomers polymerise to form insoluble fibrils and ultimately the amyloid plaques. Electrophysiology and behavioural experimentation have therefore identified the lower molecular-weight and soluble amyloid species as the toxic component where they disrupt synaptic plasticity (Walsh et al., 2002, Shankar et al., 2008). Furthermore, removal of soluble species and not plaques can alleviate memory impairment typical of several AD transgenic models (Dodart et al., 2002). Plaques rather act either as a source and/ or a sink for these diffusible species of amyloid, depending on how stable the plaque is and the direction of the equilibrium shown in figure 2.6 (Jawhar et al., 2011). In accordance with functional assays, it seems these soluble oligomers correlate far better with cognitive decline (Mc Donald et al., 2010, Villemagne et al., 2010). In addition to the genetic factors altering the $A\beta_{42/40}$ ratio which can influence fibrillogenesis (Irvine et al., 2008), environmental factors such as metal ion concentrations and nitration of Aβ (Kummer et al., 2011) can influence the dynamics of aggregation. Lastly, secondary modifications such as phosphorylation (Kumar et al., 2011), oxidation, isomerisation (Kuo et al., 1998) and racemisation (Mori et al., 1994) of Aβ and the pyroglutamate-modified Aβ ($A\beta_{pE3}$) can also drive aggregation and toxicity (Jawhar et al., 2011). Additionally these modifications can also render the Aβ species resistant to neprilysin and the insulin-degrading enzyme.

Excitation of NMDA receptors at the synapse is believed to be another effect of Aβ. Signalling through this receptor complex has been shown to be responsible for induced spine loss from Aβ. It is of interest that Aβ-neurotoxicity mediated through metabolic glutamate receptors, leads to LTD and Aβ can also inhibit Wnt signalling via the Frizzled-1 receptor (Chacon et al., 2008). Thus it seems likely that varying synaptic receptor subtypes can mediate the varied neurotoxic attributes of soluble Aβ species (Ittner and Götz, 2011).

2.6 Variations on a theme: LOAD versus FAD

From the initial studies of epidemiology and clinical observations it was clear there were two variations of the disease differing by the age of onset:

1) Late-onset AD (LOAD)/SAD is seen as sporadic with perhaps a genetic pre-disposition element. By far this is the most common type, because >99% of the AD-cases do not have a clear familial inheritance pattern. Age constitutes the biggest risk factor for sporadic AD (Swerdlow, 2007). In the population aged 65 or over, 15-25% suffer from AD, rising to 50% in those aged 95 or over. This average varies among populations, ethnic groups and countries associated with different gender/age structures and with lifestyle differences (Wang and Ding, 2008, Korczyn and Vakhapova, 2007, Kalaria et al., 2008). Although LOAD has no genetic linkage *per se,* many researchers believe that there are multiple minor genetic predispositions with effects that are additive to exacerbate the onset, severity and progression of the disease. This has been drawn upon from the age of genome-wide association studies (GWAS) that have only become available to understand these complex, multifactorial diseases through the requirement of sequencing thousands of genomes.

Besides age, risk factors can include head injury, vascular disease, depression and AD is more common in women than in men. A potential molecular connection is suspected between cholesterol metabolism and AD, which has been confirmed by GWAS linking the *APOE4* allele, which encodes Apoε4 to AD (see 2.5.2.5 Aβ clearance and degradation). Inheriting even one ε4 allele increases the risk of developing AD earlier by a factor of 3 to 5. Apoε4 is involved in Aβ clearance, but other mechanisms have been proposed (Holtzman et al., 2011, He et al., 2007). More recent GWAS studies have identified new gene variants associated with increased risk such as the *PICALM* [phosphatidylinositol-binding clathrin assembly protein] gene and *CLU* [clusterin], which are believed to affect the production and clearance of amyloid species (Bertram, 2011, Harold et al., 2009). This has led many to postulate that in addition to the increased production of Aβ, there is also a problem in clearing it from the brain (Yamada et al., 2011, Castellano et al., 2011b) and as such CSF levels of Aβ are negatively correlated with cognitive decline (Barber, 2010, Fjell et al., 2010).

The molecular underpinning of AD is a tangled web of environmental factors, genetic traits and spontaneous genetic mutations that occur with the aging process

itself. As individuals grow old, so do their cells. Rare and spontaneous mutations build-up within terminally differentiated neurones; the chromatin is remodelled to different acetylation and methylation patterns leading to an altered transcriptional profile; cellular processes lose efficiency; faulty protein turnover results in protein aggregation and finally mitochondria become leaky. Ultimately, any one of these factors can induce or contribute to cell-death by the numerous connections within the molecular regulatory pathways. However, something particular in AD separates it from "normal" aging. For one, BACE1 expression and activity may increase more in AD than in aging, which combined with increased inflammation, could result in enhanced Aβ production as the first defect and trigger in AD (Blasko et al., 2004, Rossor et al., 1993, Zhiyou et al., 2009, Zhang et al., 2007).

2) Familial AD (FAD) is typical for its early onset (EOAD) with a dominant familial inheritance pattern. Clear familial linkage to several key genes has been identified and account for <1% of AD cases. The most convincing of these mutations lies in the *APP* gene and also in the genes *PSEN1* and *PSEN2* located on chr14 and chr1 respectively, which encode for essential factors in the γ-secretase complex, responsible for generating $A\beta_{40/42}$ (see 1.5.2 APP metabolism) (Williamson et al., 2009). A key observation was noticed in the similarity with DS sufferers (Glenner & Wong, 1984), where the trisomy of Chr21 confers an increased gene dosage effect of *APP*, and consequently present AD symptoms from an early age (Wang and Ding, 2008). Ultimately these genetics factors exacerbate an underlining AD pathogenesis leading to a much earlier age-of-onset.

Table 2.1: Familial linkage to AD.

Gene	Age of onset	Functional outcome
***APP* trisomy 21 DS**	50s	Increase in total Aβ production
***APP* mutations**	50s	Increase in total Aβ production $A\beta_{42/40}$ ratio increased
***APP* triplication**	50s	Increase in total Aβ production
PSEN1	40s/50s	$A\beta_{42/40}$ ratio increased
PSEN2	50s	$A\beta_{42/40}$ ratio increased

2.7 Tau protein and Braak staging of NFT pathology

The protein tau has long been the focus of AD research since it was known to be hyperphosphorylated and form tangles within neurones of AD patients (Hyman and Gomez-Isla, 1997). At a molecular level, tau functions as a spacer between the microtubules, which form the cytoskeleton along the axonal processes of neurones. Cytoskeletal dynamics allow for cells to polarise, grow and sense its niche whilst also serving as molecular highways for the transport of protein and RNA molecules within the cell. This is of particular importance for neurones whereby a synaptic output can be separated from the soma by a vast distance. However, in a disease setting such as AD there is excessive kinase activity focused on the tau molecule leading to hyperphosphorylation, aggregation and NFT formation. Cyclin-dependent kinase 5 (CDK5) and glycogen synthase kinase-3 (GSK3) (as discussed later) have the ability to phosphorylate tau in a physiological and pathological setting. Hyperphosphorylated tau leads to aggregation, which results in neurofibrillary tangle formation within the neurones. This second major hallmark of AD has been observed in post-mortem brain samples and staged for its progress through the disease. What is prominent is that NFT formation seems to correlate very well with neuronal loss and cognitive decline. Initial NFT formation begins in the allocortical areas such as the entorhinal cortex spreading to limbic centres like the hippocampus and the amygdala. Through later stages, a dramatic spreading occurs through the neocortex invading the parietal, occipital and temporal regions (Nelson et al., 2009). Braak (1991) introduced a system to standardise the severity of this pathology in each AD patient presented at post-mortem as shown in figure 2.7 (Alafuzoff et al., 2008). This ultimately led to the ability to correlate Braak stages with cognitive decline. This is the major downfall of the amyloid cascade hypothesis in that a similar staging of amyloid pathology (Alafuzoff et al., 2009) does not correlate with cognitive decline. This has led to a strengthening of the tau hypothesis. As a final word on this particular matter it should be stated that correlation does not in any means imply causation (Nelson et al., 2009). This neuropathology-centric view on AD has also identified a paradox in that while NFT in late stages are found in numerous regions of the human brain, only certain neuronal types are afflicted. Indeed this is something that has been ignored, if not side-lined.

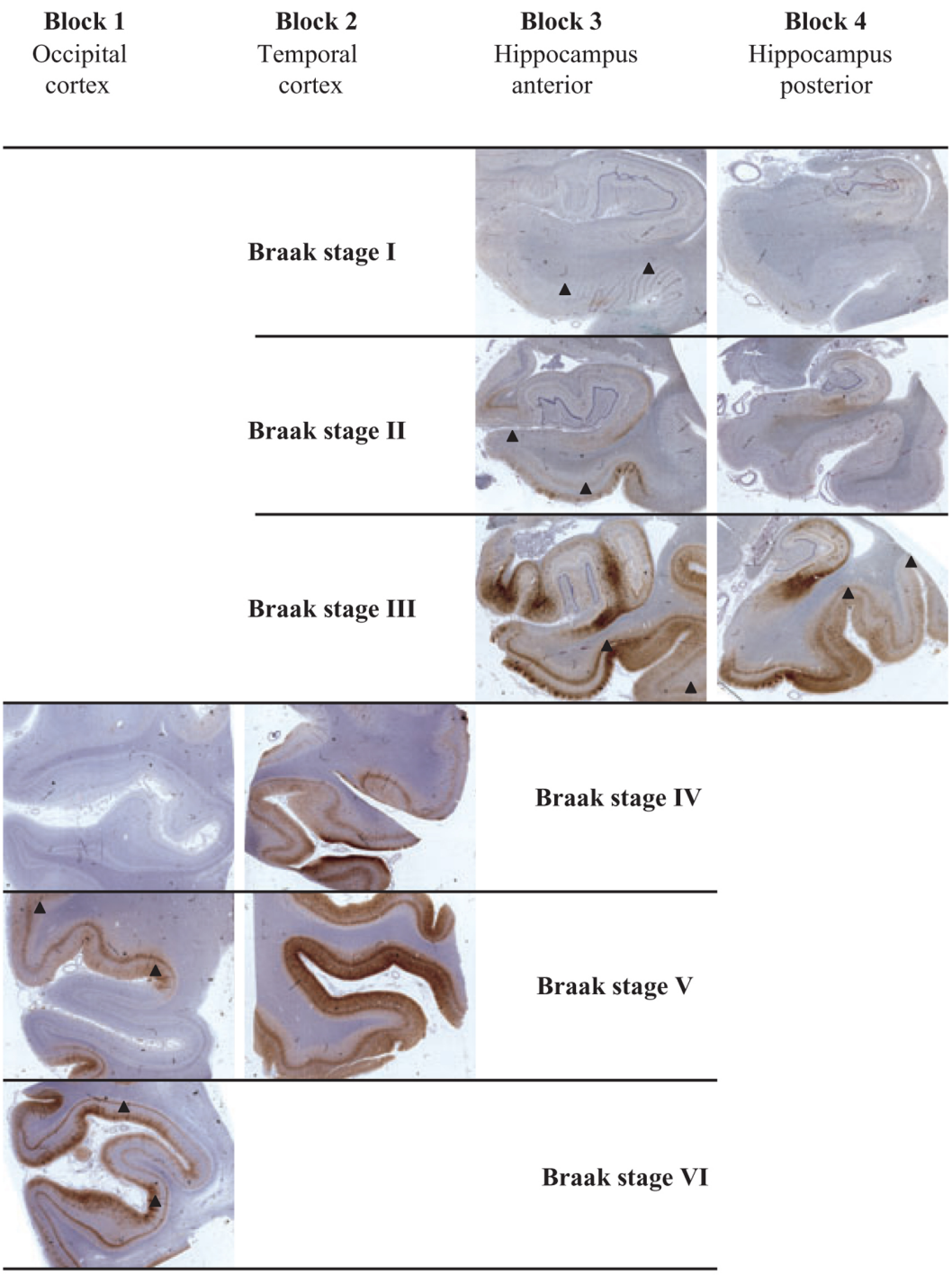


Figure 2.7: Staging of NFT pathology in AD human brains from the BrainNet human consortium.

Figure taken from (Alafuzoff et al., 2008) showing the development of NFT through varying Braak stages in human AD brains. Staining of sections was carried out using typical immunohistochemical techniques against hyperphosphorylated tau with the antibody AT8. Pathology is shown here beginning in the entorhinal cortex (stage 1) spreading through the cortex (stage 2-6).

2.8 Glycogen synthase kinase-3

GSK3 was originally identified for its ability to phosphorylate glycogen synthase in the glycogen biogenesis pathway and as expected is a highly conserved enzyme found in every domain of life (Embi et al., 1980). Several decades of research have now elucidated that there are some 50 known cellular substrates for GSK3 and, therefore, creates a major node within the molecular web of cell signalling. Not surprisingly, GSK3 has been linked with a plethora of syndromes and diseases in humans and therefore is a highly researched drug target (Jope and Johnson, 2004). A set of criteria has been set forward by Frame and Cohen in 2002 as to establish a putative target as a genuine *in vivo* target. This is important to sieve out the physiologically relevant kinase substrates from those that are not (Frame and Cohen, 2001).

Three isozymes are encoded by 2 genes GSK3α and GSK3β, with the latter encoding a splice variant to generate GSK3β-1 and 2. The GSK3β splice variants are preferentially enriched within neurones while GSK3α has a ubiquitous expression in mammalian tissue (Mukai et al., 2002, Woodgett, 1991). The two genes were originally cloned by Woodgett in 1990 and found to be homologous to *shaggy* in *Drosophila,* which is key for the canonical Wnt cascade and targeting β-catenin (Siegfried et al., 1992, Miller and Moon, 1996).

Despite the extent of putative targets, there is some 97% sequence homology within the active site between the three isozymes (Frame and Cohen, 2001). This raises the question of how does GSK3 correctly select its substrate. One would assume that an important enzyme like GSK3 has to be tightly regulated both spatially and temporally for correct development of an organism and also for proper metabolic control in the CNS. This is highlighted by firstly, that *Gsk3β* null mice are embryonic lethal (Hoeflich et al., 2000) and secondly, that dysregulation of GSK3 is linked to a myriad of metabolic disease like cancer and type-2 diabetes. Intriguingly, *Gsk3α* null mice are viable but have a minor behavioural phenotype, which would suggest it plays a more pronounced role in the brain in a developmental context (MacAulay et al., 2007).

2.8.1 GSK3 as the tau kinase

The tau protein kinase 1 (TPK1) extracted from bovine brain was found to be GSK3 and the main proponent as one of, if not the most important kinase for physiological phosphorylation of tau (Ishiguro et al., 1988, Ishiguro et al., 1993). This was confirmed through *in vitro* action of GSK3 on tau and also the correlation between these specific kinase sites within tau and those found in pathological NFT in AD patients (Hanger et al., 1992, Lovestone et al., 1994). Finally, several GSK3 knock-in mouse models have been generated and all seem to generate tau hyperphosphorylation albeit at different rates, sometimes not occurring until a relatively old age (Spittaels et al., 2000, Brownlees et al., 1997, Lucas et al., 2001). Furthermore, hyperphosphorylation of tau can be reversed by chronic administration of LiCl, a non-specific GSK3 inhibitor in the *TauFDP-17/GSK3β* double knock-in transgenic mouse (Engel et al., 2006a).

2.8.2 Regulation of GSK3

2.8.2.1 Regulation by phosphorylation

The basal level of GSK3 in resting cells appears to be high and is usually negatively regulated upon stimulation from an internal or external signal. The main means of regulation comes from the upstream kinase phosphorylation of two key residues; serine 9 of GSK3β and serine 21 of GSK3α that both lie within the N-terminus. Numerous signalling pathways use this regulation including insulin signalling, through the PI3K/Akt pathway (Sutherland et al., 1993) (see 2.8.4 GSK3 and Wnt signalling). However, other mechanisms include a tyrosine autophosphorylation event at position Y216 (Lochhead et al., 2006) and with a GSK3 β-specific serine-phosphorylation within the C-terminus (Thornton et al., 2008). This latter example of phosphorylative regulation is mediated through the p38 MAPK axis and illustrates the principle of multiple pathways converging onto a singular node such as GSK3. However the downstream physiological outcome does alter despite using most of the same mediators in that the MAPK pathway leads to the promotion of cell survival while through the insulin axis, GSK3 alters the anabolic/catabolic switch in the cellular metabolism.

2.8.2.2 Primed substrate prerequisite

Another intriguing property of GSK3 is that its kinase activity usually requires a primed substrate, in which a key serine/threonine residue situated 4aa upstream from the target residue within its consensus sequence, Ser/Thr-Xaa-Xaa-Xaa-pSer/pThr, is phosphorylated by an additional kinase (Frame and Cohen, 2001, Fiol et al., 1987). This ultimately leads to a concerted action needed for GSK3 signalling and can add a complex level of regulation as both kinases have to be active, act in the right order and in the same vicinity for a specific response.

2.8.2.3 Subcellular pooling

Despite the classical functions within the cytosol, GSK3 can also function within organelles such as the mitochondria and the nucleus where it appears to have an even elevated activity (Jope and Johnson, 2004, Bijur and Jope, 2003). These membranous organelles form a clear and distinct sub-pool of GSK3 molecules, which may undergo differential local regulation. For example, the activity of GSK3 within the nucleus follows the cell-cycle and peaks in the S-phase where it acts on several transcription factors such as cyclin D1 (Diehl et al., 1998). It has already been noted that GSK3β2 has a preferential location within the processes of the neurone although the mechanism for its restriction to these areas is not fully understood. Presumably this may well have to do with interactions with other binding partners.

However, one could envisage that molecules of the same isoform may have differential activity and substrate specificity depending on the immediate cellular niche in which it finds itself. Signalling can be localised and insulated within certain parts of the cell, especially events occurring close to the plasma membrane whereby secondary modifiers coalesce around the immediate site of stimulation i.e. a receptor. Indeed Wnt stimulation on the Frizzled/LRP co-receptor complex forms a perfect paradigm for this.

2.8.2.4 Differential isoform expression and substrate specificity

However, there are two indications that there is some intrinsic ability for substrate specificity. The first is that outside of their respective catalytic domains, the isozymes vary dramatically to the extent that GSK3α has an extended N-terminal glycine rich domain with respect to the GSK3β variants (Frame and Cohen, 2001). Further to this, the major structural difference between the two splice variants of GSK3β is a 13aa insert. Interestingly GSK3 kinase activity can be differentially distributed with

GSK3β2 expression restricted to the soma while its GSK3β1 counterpart is found in both the soma and its processes (Mukai et al., 2002).

The second indication of substrate specificity comes from a recent study from Soutar (2010) and colleagues in which they report substrate selection from single and double knockouts of the varying GSK3 isoforms. When comparing cortical-lysates from the varying combinations of single and double *Gsk3* KO embryos and age-matched controls harvested at E15, it was noticed that there were differences in phosphorylation of a spectrum of substrates. Interestingly, the 13aa insert of GSK3β2 that is situated in a linker region between alpha helices X and XI in the catalytic domain seems to reduce its ability to phosphorylate numerous targets compared to GSK3β1, including the protein tau. This was previously observed with the initial cloning of this splice variant from Mukai et al, 2002. However other substrates such as *c-Myc* and *c-Jun* are phosphorylated without preference from all isotypes of GSK3 (Soutar et al., 2010).

2.8.3 GSK3 hypothesis of AD

As mentioned earlier, the first link of GSK3 playing a role in AD pathogenesis was its homology to the TPK1 (Ishiguro et al., 1988, Ishiguro et al., 1993). However, many approaches have produced a long list of evidence that not only implicates GSK3 at several stages of AD development but also incriminates it as a major orchestrator leading to a hypothesis postulated by Small and Duff in 2008. In this persuasive paper, the authors suggest that it is neither the amyloid nor the tau hypothesis that accounts for AD but rather they run in parallel and are connected at various points by GSK3 as explained in this section. It should be noted that Hooper, Killick and Lovestone put forward an equally convincing argument in 2008 in which they state that GSK3 can be linked to every hallmark observed in the progression of AD.

2.8.3.1 GSK3 activity and aging

A consequence of aging is a dysregulation of usually highly in-tuned homeostatic processes. Indeed, kinases, which heavily rely on upstream regulation as well as autoregulation, are often altered in their activity in an aging organism. There are some controversial phenotypic findings describing altered glycogen metabolism in aging and aging-related diseases. A decrease of glycogenic activity was shown to be associated with aging (Kurokawa et al., 1997), while increased glycogen accumulation was also observed in cellular senescence and aged tissues (Gertz et al.,

1985). The potential role of GSK3 as modulator of cell senescence is still disputed (Liu et al., 2008, Seo et al., 2008).

Pei and colleagues published in 1997 elevated expression of GSK3 in the post-synaptosomal fractions from the brains of AD patients and Blalock et al, found an upregulation of GSK3 in the hippocampus of AD patients (Pei et al., 1997). A more recent study from 2007 by Leroy and colleagues found GSK3 to be highly activated in AD patients. Interestingly, a genetic polymorphism in the promoter of *GSK3* is a risk factor for LOAD (Mateo et al., 2006). In addition, increased Aβ production can aggravate the tau pathology by hyper-activating GSK3 (Terwel et al., 2008). Further to this, expression of the familial linked mutations in *PSEN1* also leads to activation of GSK3 (Weihl et al., 1999, Zhang et al., 1998a, Baki et al., 2004). Several molecular mechanisms have been postulated for this observation and reviewed elsewhere (Hernández et al., 2009). But one evocative explanation is that the increased Aβ production blocks the PI3K/Akt cascade leading to less negative regulation on GSK3 (Takashima et al., 1996).

Other metabolites of APP can also influence the expression and activation of GSK3. Firstly, the product of the BACE1 cleavage, the β-CTF, resulted in an increase in GSK3 activity, tau phosphorylation and subsequent apoptosis (Kim et al., 2003). There is evidence that GSK3 transcription is positively regulated by the AICD fragment whose production would increase in the context of the familial cases of AD (Gao and Pimplikar, 2001). This was in line with the AICD transgenic mice having activation of GSK3β compared to wild-type mice (Ryan and Pimplikar, 2005).

The upshot of this is that GSK3 can influence the processing and activity of PSEN1 (Takashima et al., 1996). Indeed, this appears to be a common theme throughout the GSK3 hypothesis in that while its activity can affect every step of AD pathogenesis, in turn these events themselves influence GSK3 activity, which may result in a feed-forward cycle (see 2.5.3 Amyloid cascade hypothesis). Again there is a chicken and egg paradox as to what comes first, which is so often the case in AD research.

2.8.3.2 GSK3 and APP processing

Several key studies have shown that increased GSK3 activity is associated with increased production of Aβ species and lowered by GSK3 inhibitors in both *in vitro* and *in vivo* studies (Phiel et al., 2003, Sun et al., 2002, Su et al., 2004). However the mechanism(s) by which this occurs is largely unknown, apart from a key observation that APP can be phosphorylated by GSK3 (Aplin et al., 1997), which in turn might regulate the modification and maturation of APP (Rockenstein et al., 2007) (see 2.5.2 APP metabolism). Secondly, GSK3 can also interact and affect the activity of PSEN1 (Takashima et al., 1998). Phiel and colleagues claimed in their paper that the decrease in Aβ detected by LiCl treatment is the result of GSK3α inhibition, as they only observed the effect using siRNA specific to the α-form. Furthermore, they postulated that this effect is mediated through alterations in the PSEN1 complex. To complicate matters, Feyt et al (2002) published that LiCl can indeed increase the formation of the β-CTF and therefore, increase Aβ load, although it must be stated that this effect was independent of its role as a GSK3 inhibitor (Feyt et al., 2005). Summarising the above data, the role of GSK3 on APP processing appears far from clear and to date, any mechanistic understanding is lacking.

2.8.3.3 Aβ toxicity, apoptosis and GSK3

In addition to the role of GSK3 on metabolism of APP, there is evidence that GSK3 is actually required for Aβ-induced neurotoxicity on neurones. Numerous studies in primary neuronal cultures and tissue slices have shown that Aβ of varying species, with particular prevalence to oligomeric forms, results in morphological changes in combination with axonal and dendritic dystrophy and finally apoptosis (Pike et al., 1991, Loo et al., 1993, Fuentealba et al., 2004). This cell death can be prevented through LiCl treatment. At the molecular level, a concomitant activation in GSK3, hyperphosphorylation of tau and destabilisation of the cytoskeletal network occurs (Busciglio et al., 1995). Work from Takashima and colleagues (Takashima et al., 1993, Takashima et al., 1995) shows convincing evidence that without GSK3 the neurotoxicity from Aβ is ameliorated and the apoptosis induced by Aβ can be blocked by LiCl treatment in cultured neurones (Alvarez et al., 1999). Experiments have illustrated that heightened GSK3 activity leads to an inactivation of the key mitochondrial enzyme, pyruvate dehydrogenase, which catalyses the production of acetyl-coA, an intermediate to acetylcholine production. This not only results in

mitochondrial dysfunction, but also leads to a lack of acetylcholine production within cholinergic neurones. This could be an explanation for the specific loss of cholinergic neurones in AD (Hoshi et al., 1996). GSK3, therefore, plays a central mediator in connecting and synergising the amyloid and tau toxicity, particularly at the synapse (Ittner and Götz, 2011, Ittner et al., 2010).

During apoptosis, an atypical cleavage event is believed to occur at Asp^{664} of APP, which is mediated by activated caspase-3. The resulting fragment C31 is released intracellularly and subsequent γ-secretase cleavage releases the fragment Jcasp (see figure 2.2) (Gervais et al., 1999). Intriguingly, this caspase-mediated cleavage is a prerequisite for Aβ-mediated toxicity, as transgenic mice for a mutation at this Asp^{664} site had alleviated synaptic, behavioural and electrophysiological abnormalities whilst still having a high Aβ burden (Galvan et al., 2006). In this scenario, C31 is believed to complex with FL-APP to recruit cellular toxicity mediators (Park et al., 2009). The fundamental molecular mechanism(s) behind such pathway(s) are still under investigation and may decipher why AD pathology appears to rely so heavily on the genetics of APP processing, but at the same time plaque burden not correlating with cognitive decline.

2.8.3.4 GSK3 and memory impairment

In conjunction with the induced apoptosis, GSK3 appears to have connections with impairment to memory formation, which is highlighted by clear degeneration of the dentate gyrus in GSK3 transgenic mouse models (Engel et al., 2006a). This can lead to memory impairment as measured by the Morris water maze test (Hernández et al., 2002) and object recognition testing (Engel et al., 2006b). In addition to the apoptosis, it should be made clear that this degeneration has as much to do with the lack of neurogenesis from the subventricular and subgranular zones (SVZ and SGZ) of the dentate gyrus (Hernández et al., 2009, Sirerol-Piquer et al., 2010). This is likely due to the increased negative regulation on the β-catenin axis, which is important for maintenance of the stem-cell niche (Adachi et al., 2007, He and Shen, 2009). Interestingly, similar results have been obtained from the 3xTg-AD model, which do not have any overexpression of GSK3β. This suggest once more that GSK3 hyperactivity lay downstream of the APP and tau pathology (Rodríguez et al., 2008). This is reminiscent of a study from He and Shen (2008) that found lower neurogenesis capability of glial progenitor cells (GPC) taken from cortices of AD

patients compared to those from healthy controls when both were treated with Aβ. This was due to disrupted β-catenin signalling with lower levels of nonphosphorylated/stable β-catenin. This pathway is thought to be necessary for learning and short-term acquisition as stated in the review from Zhao et al, 2008.

Aβ–neurotoxicity can also inhibit LTP via activation of caspase-3 (Walsh et al., 2002, Shankar et al., 2008), along with memory formation and also elevate LTD (Hsieh et al., 2006). Lo and colleagues (2011) found that Aβ inhibition of LTP is reversed by blockade of GSK3. They speculated that caspase-3 could inhibit LTP by the cleavage of Akt1, resulting in activation of GSK3. In addition to this *ex vivo* study, caspase-3 has been found activated in the hippocampal dendritic spines in the AD mouse model, Tg2567 (overexpressing the APP Swedish familial variant). This study shows eloquently that this activation is pre-emptive to the plaque formation and therefore based on oligomeric forms of Aβ and intriguingly this caspase-3 activation is not associated with apoptosis, confirming that caspase-3 is required for physiological LTD (Li et al., 2010b). It has been noticed that while Tg2567 provides an excellent model for amyloid pathology, mice do not suffer overtly from neuronal loss. This may be due to sub-optimal activation of caspases to induce LTD but not apoptosis. However, that does not mean that the activated caspase-3 is not detrimental. The authors observed dramatic changes in the AMPAR subunits at the synapse, which led to alterations in glutaminergic signalling and plasticity, spine degeneration and memory impairment (D'Amelio et al., 2011).

The above observations raise the rather intriguing point that cognitive decline may not have to correlate with neuronal loss, and indeed large cognitive deficit can come from sub-optimal caspase levels for apoptosis, but which result in local synaptic remodelling and degeneration. However, it is unsure whether this can be extrapolated to the human disease but there does appear to be evidence for activated caspases in the AD brain reviewed in Hyman, 2011.

2.8.3.5 GSK3 and inflammation

Another important feature of AD is an increase in brain inflammation. Indeed excessive inflammation is a common theme in most neurodegenerative diseases, whereby an inflammatory response is mounted to engulf the apoptotic neurones. Such a response at first would be beneficial to a system under stress, however over stimulation can lead to exacerbation of the pathology. Such topics have been

reviewed comprehensively elsewhere (Sastre et al., 2008, Sastre et al., 2006b, Sastre et al., 2011). Whether a prolonged inflammatory response is, firstly a bystander effect and secondly, beneficial or detrimental to neurodegeneration, are hotly debated topics.

Briefly, there appears to be a mass encroachment of plaques by activated microglia (the main immune cell of the CNS) in AD patients and animals models, which presumably phagocytose the aggregated material (Christie et al., 1996, Stalder et al., 1999). Indeed, this mechanism is believed to underlie the clinical trials for Aβ immunotherapy clearance of plaques in AD patients through Fc-recognition. Secondly, certain key pro-inflammatory cytokines are heavily upregulated in the brains of AD patients (McGeer and McGeer, 1996, Griffin et al., 1989).

Not surprisingly, GSK3 is documented to have a major regulatory role on inflammation both in a physiological and disease setting. Jope, Yustaitis and Beurel (2007) have reviewed this topic in great detail. In the periphery, migration, activation and secretion of pro-inflammatory cytokines/ chemokines from leukocytes are greatly dependent on proper GSK3 function (Rodionova et al., 2007). Whether the same can be true in the CNS is simply not known, as the brain, which is separated from the periphery by the BBB, has its own inflammatory and immune responses. However, these can be bolstered by relaxation of the barrier and infiltration of immune cells from the periphery, a process in which GSK3 seems to have some function.

LiCl has long been used for decades as mood stabilisers for psychiatric conditions despite its therapeutic target not being known. Furthermore, mood disorders such as depression and bi-polar disorder are dominated by inflammation (Licinio and Wong, 1999) and many classical mood stabilisers have anti-inflammatory properties (Schiepers et al., 2005).

It has only been very recently that GSK3 regulation on inflammation has been discovered in the CNS. It has a profound effect on activation, migration (Yuskaitis and Jope, 2009) and phagocytosis from microglia cells both *in vitro* and *in vivo*. These actions are based on GSK3 signalling within multiple pathways including the pro-inflammatory, NF-κB pathway as reviewed elsewhere (Koistinaho et al., 2011).

One could hypothesise that the hyper-activated GSK3 induced from Aβ-neurotoxicity could explain the several pro-inflammatory responses observed in AD.

If so, again, GSK3 provides the link between the amyloid cascade hypothesis and another hallmark of AD, inflammation.

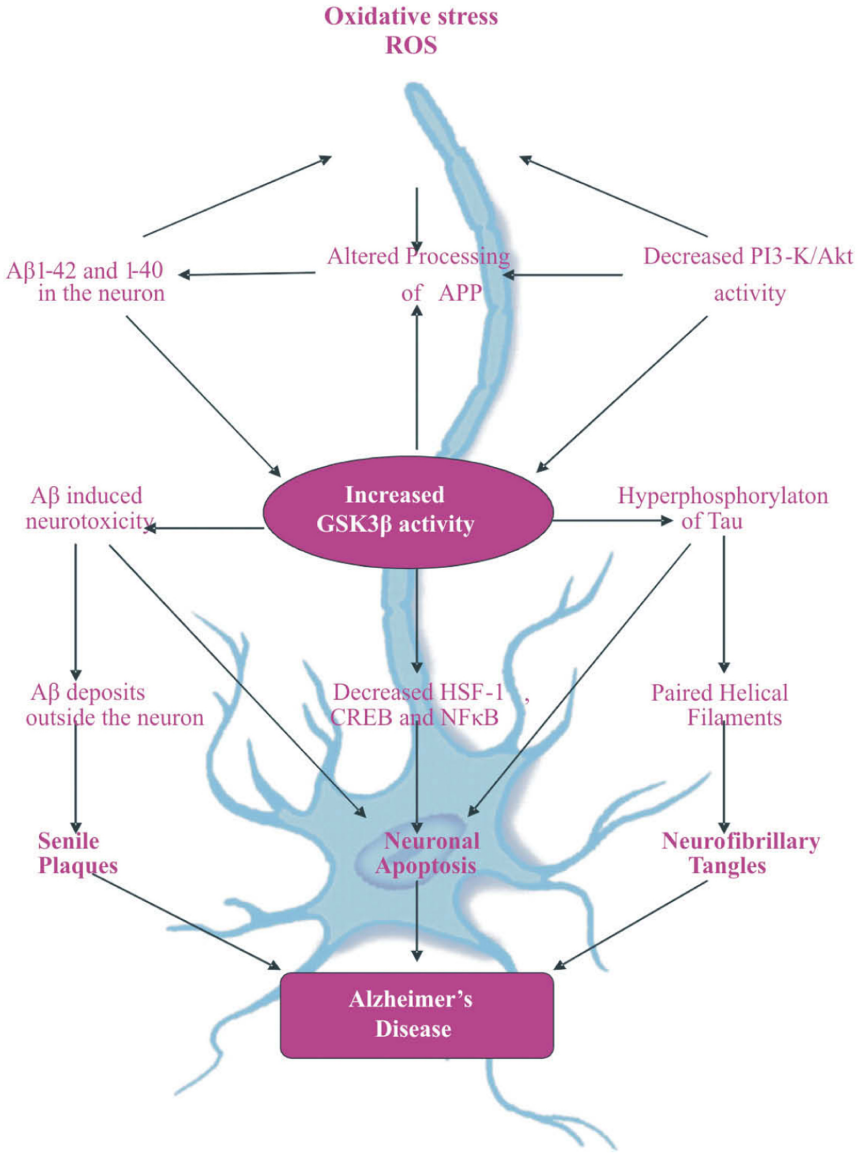


Figure 2.8: Increased GSK3 activity links several aspects of AD pathogenesis.

This schematic was taken from (Fuentealba et al., 2004) and shows the central remit of GSK3 in the parallel pathways leading to AD.

2.8.4 GSK3 and the canonical Wnt signalling

Due to the prevalence of GSK3 targets it is not surprising that it is found to be an effector molecule in numerous signalling pathways controlling many physiological functions within the cell. Apoptosis, cell polarity, cell migration, cytoskeleton and membrane dynamics, cell cycle, cell survival and cell-fate determinism are all influenced in part by this enzyme (Jope et al., 2007). To go into detail of each would be beyond the scope of such a thesis however the intricate detail of its crucial role within the canonical Wnt cascade will be discussed and serves as a perfect example for the various regulation mechanisms mentioned previously (see 2.8.2 Regulation of GSK3).

The canonical Wnt cascade in a developmental context is vital for axis formation and cell-fate determination. However, in the adult form it is required for stem-cell maintenance, tissue regeneration and is causal for a high percentage of cancers (Logan and Nusse, 2004, Nusse, 2008). Given its developmental context, the canonical cascade has been deciphered over a decade with eloquent genetic manipulation in model systems like *Drosophila* but each key protein has a well-conserved homologue in mammalian systems.

In the resting state, a destruction complex made up of GSK3, casein kinase 1α (CK1α) (Liu et al., 2002), and the structural proteins, adenomatous polyposis coli (APC) and axin (Kishida et al., 1998), enable the sequestration of β-catenin leading to its phosphorylation. CK1 provides the primed phosphorylation on serine 45 (Amit et al., 2002) for the subsequent GSK3 phosphorylation on serine 33, 37 and 42 of β-catenin. These phospho-sites provide molecular cues for recognition from the ubiquitination mediator, β-TrCP (Liu et al., 1999, Aberle et al., 1997) and its subsequent degradation through the 26S proteasome (see figure 2.8).

Stimulation of the canonical Wnt cascade ultimately leads to the break up of this destruction complex and inactivation of GSK3. The stabilisation of β-catenin leads to its translocation to the nucleus (Miller and Moon, 1997). Within this compartment, it partners with LEF/TCF transcription factors, which are usually repressed by Groucho (transcriptional repressor) and therefore upregulates the Wnt target genes (Behrens et al., 1996, van de Wetering et al., 1997). How this stabilisation event occurs by stimulation of the Frizzled/LRP5/6 co-receptor complex is unknown but several mechanisms prevail. Despite this ambiguity, two key attributes provide clues. As pharmacological inhibition of GSK3 perfectly mirrors

stimulation of the canonical Wnt axis, GSK3 must be inactivated during Wnt stimulation (Wu and Pan, 2010). And secondly, the stimulated complex of Frizzled/LRP5/6 and the Wnt ligand must be internalised (Blitzer and Nusse, 2006, Yamamoto et al., 2006). This is usually associated with the sequestration of a protein called *Dishevelled* (*Dsh*) and axin from the destruction complex to the plasma membrane surrounding the receptor complex (Bilic et al., 2007, Zeng et al., 2008). Classically, *Dsh* was thought to inactivate GSK3 by is N-terminal phosphorylation.

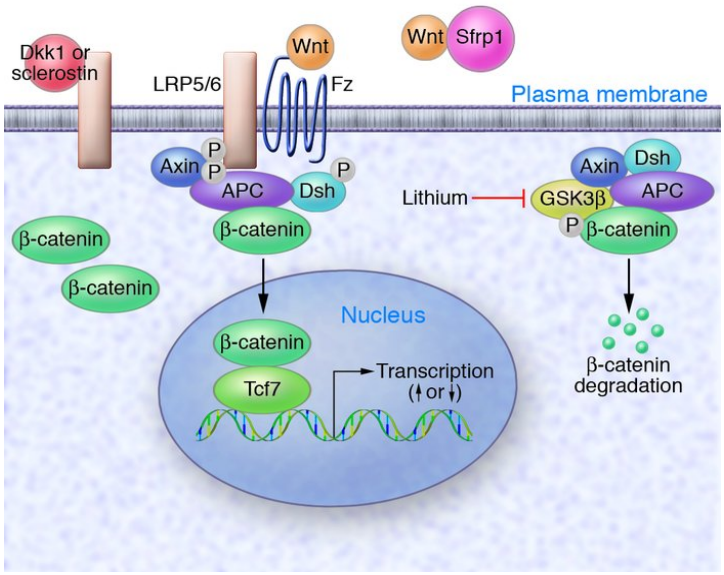


Figure 2.9: Schematic of canonical Wnt signalling in metazoa.

Canonical Wnt signalling leads to the stabilisation of β-catenin and translocation to the nucleus, upon which it interacts with various LEF/TCF activators and the regulation of target genes.

A recent study from Taelman et al., 2010 with a *tour de force* illustrated a unique mechanism for how GSK3 is inactivated by sequestration from the cytosol into a multivesicular body (MVB), rather than direct inactivation through GSK3 phosphorylation. In addition to this, they show that Vps27 and Vps4, which aide in the formation of MVBs are a requisite for canonical Wnt stimulation (Taelman et al., 2010). However, certain questions still remain unanswered as to how β-catenin escapes the firm grip of the destruction complex (see figure 2.10).

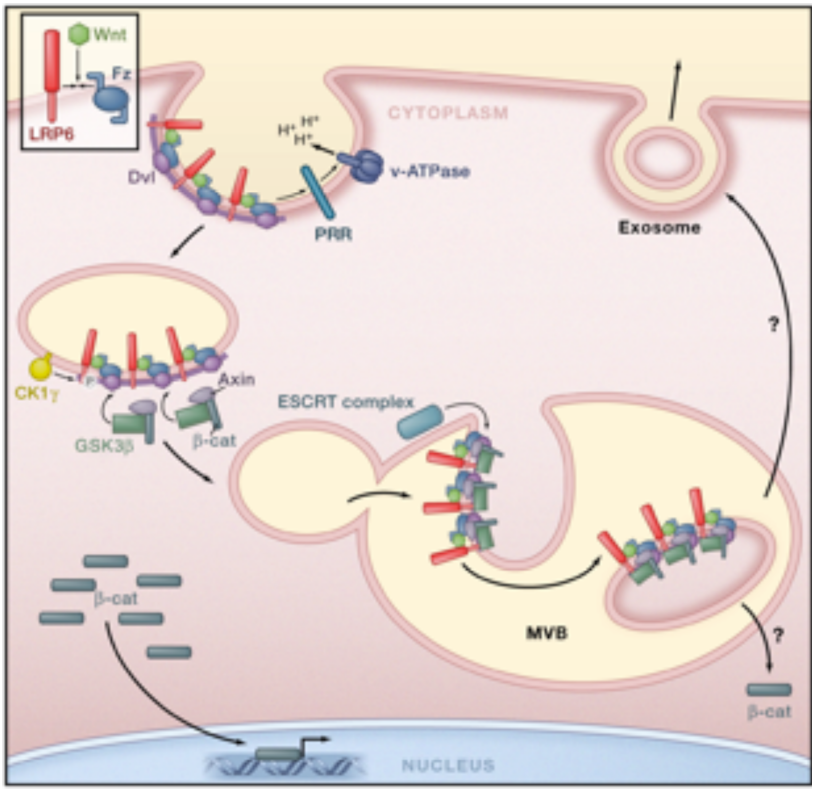


Figure 2.10: Schematic of signalling sequestrome upon canonical Wnt stimulation.

The schematic shown illustrates the signalling sequestrome as a result of the endocytosis into an MVB, which results in the inactivation of GSK3 from the cytosol and stabilisation of β-catenin. This image was taken from a comment article written by Niehers and Acebron, 2010.

2.9 The canonical Wnt cascade and AD

Dysregulation of the canonical Wnt cascade has been heavily implicated in neuro-developmental disorders such as autism and schizophrenia, due to its importance in developing the CNS. However, supported by enormous data from mouse models and some limited data from humans, the canonical Wnt cascade adopts different function(s) in the adult form. For instance, in adult mice it regulates the development of hippocampal neurones from the neural stem-cell niche within the subventricular and subgranular layers of the dentate gyrus. Of interest is a study from Mao in 2009 that looked into the role of the Dissociated in schizophrenia-1 (Disc1) protein. They focused on its role in progenitor cells of the SVZ and SGZ, in both the embryo and in adult mice. Consistently, neurogenesis was majorly disrupted at both time points. In conjunction they found that not only can Disc1 regulate the levels of β-catenin but also it is required for the Wnt3a induced activation of LEF/TCF targeted genes leading to proliferation of cultured adult progenitor cells. The story was completed with *in vitro* binding assays, which reveal GSK3 can bind to a N-terminal domain on Disc1. The physiological relevance is to block GSK3 activity, as specific GSK3 inhibition can restore the proliferative capabilities of *Disc1*$^{-/-}$ embryonic and adult neural progenitors. In a separate study it was shown that the mutant Disc1 protein, from the mutant L100P mouse (expressing a Scottish pedigree familial mutation leading to schizophrenia), has a dramatic reduction in its affinity for GSK3. Lastly genetic and pharmacological inhibition of GSK3 rescued the schizophrenic phenotype of this mouse model (Lipina et al., 2011) (Ming and Song, 2009, Chubb et al., 2008).

Neurogenesis of progenitors and subsequent positioning is key to provide the cells that form working circulatory for learning and memory (both of which are afflicted in AD) and for mood regulation (the basis of mood disorders such as schizophrenia and depression) (Zhao et al., 2008). Such studies reveal beautiful connections between varying syndromes and diseases to the SVZ and SVG of the dentate gyrus, a region classically linked to AD. An emerging picture speculates that the age related increase in activity of GSK3 could lead to this disruption only later in life. However seeing as this Disc1/GSK3 pathway plays both a role in embryogenesis and adulthood, alterations during the former could set in place a predisposition for psychiatric illness or dementia later in life.

In addition, there is a requirement for synaptic plasticity, involving highly dynamic mechanisms being tightly regulated throughout the lifespan (Speese and

Budnik, 2007). Therefore a growing body of evidence implicates this cascade and synaptic plasticity in the aetiology of neurodegenerative disorders such as AD (Boonen et al., 2009).

2.9.1 Receptor-level alterations in the Wnt cascade with sporadic AD

SAD cases, which account for the overwhelming majority of AD patients, is closely linked to the Wnt cascade at the receptor level, in particular the LRP5/6 co-receptor.

Dickkopf-1 (DKK1), an extracellular negative regulator of the Wnt receptor complex (Mao et al., 2001) is elevated in response to cellular stressors such as in models of neurodegeneration (Rosi et al., 2010, Caricasole et al., 2004). Its absence in healthy control patients only compounds its identity as a marker of cellular stress (Caricasole et al., 2004). In this scenario, the canonical Wnt cascade disruption is a consequence of Aβ-neurotoxicity and there is a widely known phenomenon of ectopic cell-cycle entry in post-mitotic neurones of AD patients. Post-mortem observations have shown numerous examples or aborted cell-cycle events at S-phase in hippocampal and cortical neurones (Yang et al., 2001). Subsequent genome duplication without mitotic division would prevail as a strong apoptotic inducer. In agreement, when blocking the G1/S phase, Aβ induced apoptosis is attenuated (Herrup et al., 2004, Copani et al., 2006, Copani et al., 2002).

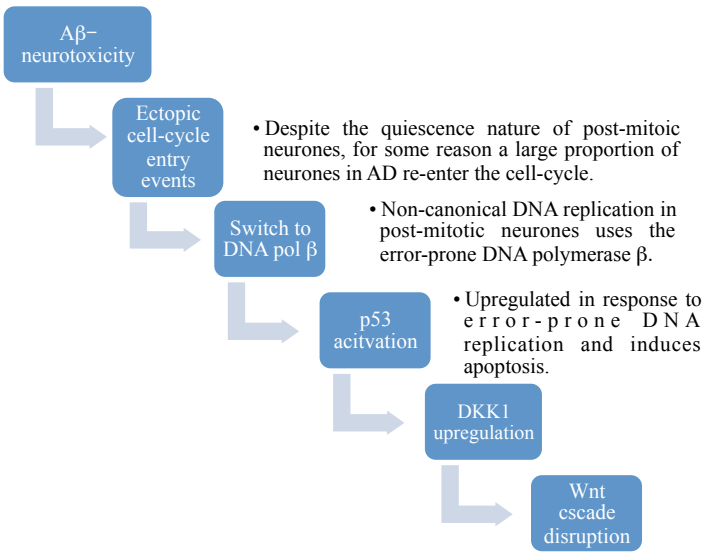


Figure 2.11: Signalling events connecting Aβ neurotoxicity to Wnt cascade disruption.

Interestingly, the DKK1 upregulation has a compounding effect on the induced apoptosis, resulting in the stimulation of the pro-apoptotic Bax and limiting the action of the anti-apoptotic Bcl-2 and results in tau hyperphosphorylation (Scali et al., 2006).

It is worth noting that, while in this scenario Aβ has a very indirect effect on the eventual outcome of the canonical Wnt cascade, there is evidence that Aβ can bind to the conserved cysteine-rich domain (CRD) within the Frizzled receptor and functionally block Wnt signalling resulting in less gene target transcription (Magdesian et al., 2008).

Two single nucleotide polymorphisms within the *LRP6* gene at exon 14 and 18 are associated with a vastly increased risk of developing AD (De Ferrari et al., 2007). The functional significance of these genetic variants and the associated risk results from a reduction in β-catenin signalling. In conjunction, allele dosage of the low-density lipid-binding protein subtype Apoε4, which provides the greatest risk for SAD, can synergise with the above *LRP6* polymorphisms to alter Wnt signalling. The mechanism by which the Apoε4 dosage has an effect on the incidence of AD comes from the different ability to clear Aβ from the CNS into the circulating plasma (Castellano et al., 2011a, Kim et al., 2009a). However, Apoε4 might also serve to promote neurodegeneration by dampening the canonical Wnt cascade, having a greater potency than the other three isoforms of Apoε (Caruso et al., 2006), reminiscent of the isoform dependency for Apoε to acts as an AD risk factor.

2.9.2 *PSEN1* mutations and regulation of cytoplasmic β-catenin

The steady-state level of β-catenin controls the transcription of gene targets that are downstream of the canonical Wnt cascade. For LEF/TCF mediated transactivation of target genes, Groucho must be displaced by β-catenin and the chromatin remodelled. Such an event is therefore dependent on the concentration of unphosphorylated β-catenin and its subsequent translocation to the nucleus. As pointed out in previous sections, β-catenin steady-state levels are controlled through a destruction complex involving kinases and scaffold proteins. PSEN1, the catalytic subunit of the γ-secretase, functions outside of this remit to alter the biology of β-catenin (Kang et al., 2002). Physiologically, these two crucial proteins are found associated in complexes with cadherins within tight junctions. Therefore this illustrates that the function of a protein can be regulated more than anything by its subcellular location. As such, this interaction can also lead to the destruction of β-catenin independently of the canonical Wnt cascade by bringing it to be primed by protein kinase A (PKA) at Ser45 (Kang et al., 1999, Kang et al., 2002).

It has become evident that the FAD linked mutations within *PSEN1* seem to illicit alterations in its constitutive action on β-catenin levels (Zhang et al., 1998b). It should be stated however that the current evidence does not dictate a simple and direct link whereby familial mutations in *PSEN1* link to disruption in the canonical Wnt cascade, but rather it could be the case that some actually increase the level of Wnt induction. A comprehensive review from Boonen, Tijn and Zivkovic (2009) has summarised the many studies in which groups have investigated the outcomes of FAD *PSEN1* mutations on β-catenin levels.

Briefly, FAD *PSEN1* mutations that disrupt the PSEN1/β-catenin interaction will lead to stabilisation in cytoplasmic levels of both proteins (Kang et al., 1999, Nishimura et al., 1999, Chevallier et al., 2005). However, it should be firmly stated that several studies of this nature have not considered the physiological outcome, i.e. the induction of the canonical Wnt cascade and have only documented an increase in cytoplasmic β-catenin irrespective of its phosphorylation state. This is a worthy consideration, as any increase in its protein levels maybe the result of the well-established proteasomal dysfunction in neurodegenerative diseases. As such, the resulting increased pool of β-catenin might be in a phosphorylative state that is therefore incapable of nuclear translocation and transactivation (Staal et al., 2002).

In contrast, there are just as many examples of FAD *PSEN1* mutations that lead to destabilisation and increased destruction of β-catenin. The major difference in whether there is attenuation or potentiation of the canonical Wnt cascade could come from subtle mechanistic differences between the types of *PSEN1* mutation. For instance, whether it increases or decreases the association with β-catenin. However, one has to consider that the numerous studies reported here used differing contexts, namely in that when it was found that FAD *PSEN1* mutations decreased β-catenin levels, there was some form of extracellular stimulation of the cascade.

In conclusion, it would be wise to elucidate the biological relevance of the *PSEN1* FAD mutations and also to standardise the paradigms being used to assess their regulation of canonical Wnt signalling. At this juncture it is not known, other than that this pathway is dysregulated, its association with AD pathogenesis. Furthermore, in terms of a timescale, our current understanding is a confused picture as to whether the aberrant Wnt signalling is the result or cause of Aβ-neurotoxicity.

CHAPTER 3 : MATERIALS AND METHODS

3.1 Antibodies and reagents

In this study different APP antibodies raised against different epitopes of APP were used. The colour coding is to illustrate which APP antibody was used to detect the FL-APP and APP-CTFs from cell lysates and Aβ as well as sAPP in the medium and are listed below and shown in figure 3.1:

- The mouse monoclonal 6E10 from Covance (against Aβ1-16).
- The mouse monoclonal 4G8 from Covance (against Aβ17-24).
- The clone 2D8 from Dr Michael Willem (against Aβ1-16).
- The rabbit polyclonal 192swe from Elan Wyeth Pharmaceuticals (against sAPPβ).
- The mouse monoclonal 22C11 from Millipore (against N-terminus of APP).
- The rabbit antisera 140 against CT-APP (Wahle et al., 2006) from Dr Jochen Walter, University Bonn.
- The rabbit antisera R1_57 against the C- terminus of APP (Anderson et al., 1989) from Dr Mehta, the Institute of Basic Research in Developmental Diseases, New York.

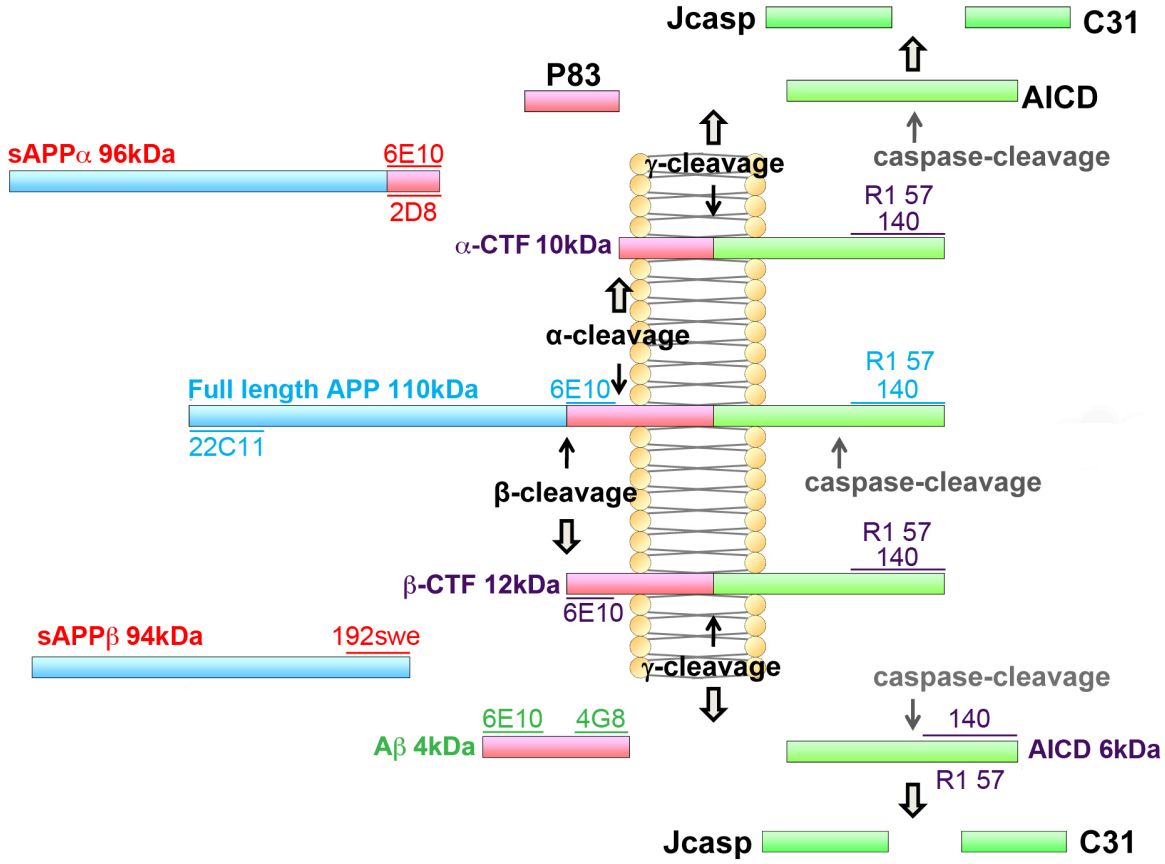


Figure 3.1: Schematic of APP metabolism and antibody epitopes.

This schematic shows APP metabolism and epitopes for membrane-bound FL-APP and C-terminal fragments, intracellular fragments (AICD) and secreted Aβ and sAPPα/β. The approximate molecular weight for each metabolite is also shown. Both amyloidogenic and non-amyloidogenic processing are shown, the α-cleavage precludes any Aβ production. Illustration reproduced from Zhang et al., 2011.

Other antibodies used in this study are shown in the table below.

Table 3.1: List of antibodies.

Antigen	Clone/Code	Company/ Source	Species	Monoclonal/ Polyclonal	Dilution
APP-CTD	140	Dr J. Walter	Rabbit	Antisera	WB 1/2000
APP-CTD	R1 57	Dr Mehta	Rabbit	Antisera	WB 1/2500 and ICC 1/500
APP-NTD	22C11	Millipore	Mouse	Monoclonal	WB 1/1000
APP-Aβ17-24	4G8	Covance	Mouse	Monoclonal	IP 1/1000
APP-Aβ1-16	6E10	Covance	Mouse	Monoclonal	WB 1/1000, ICH, 1/500, ICC 1/500 and IP 1/10 000
BACE1	Ab5940	Millipore	Rabbit	Polyclonal	WB 1/500
Beclin-1	612112	BD Biosciences	Rabbit	Polyclonal	WB 1/2000
FLAG-tag		Sigma Aldrich	Mouse	Monoclonal	WB 1/1000
GSK3α/β	44610	BioSource	Mouse	Monoclonal	WB 1/1000
pS9-GSK3β	9336	Cell Signalling	Rabbit	Polyclonal	WB 1/1000
H4	04-858	Millipore	Rabbit	Monoclonal	WB 1/1000
LAMP1	Ab25630	Abcam	Mouse	Monoclonal	ICC 1/200
LC3		Dr M. Koike	Rabbit	Polyclonal	WB 1/500
LC3	Ab48394	Abcam	Rabbit	Polyclonal	WB 1/1000
p62/SQMST1	P0067	Sigma Aldrich	Rabbit	Polyclonal	1/2000
pS33/37 β-catenin	BC-22	Sigma Aldrich	Mouse	Monoclonal	IHC 1/500, ICC 1/250
sAPPα	2D8	Dr Michael Willem			WB 1/1000
sAPPβ	192swe	Elan	Rabbit	Polyclonal	WB 1/2000
TFEB	AB1	Sigma Aldrich	Rabbit	Polyclonal	WB 1/1000
Ubiquitin	PD41	Santa Cruz	Rabbit	Polyclonal	WB 1/500
β-actin	AC-15	Abcam	Mouse	Monoclonal	WB 1/10 000
β-catenin	C2206	Sigma Aldrich	Rabbit	Antisera	WB 1/500, IP 1/250, ICH 1/100 and ICC 1/200
β-catenin	610153	BD Biosciences	Mouse	Monoclonal	WB 1/1000

Table 3.1: Dilutions of antibodies used are given for the separate techniques they are used for, including Western blotting (WB), immunoprecipitation (IP), immunohistochemistry (IHC) and immunocytochemistry (ICC).

All other chemicals and solutions were obtained from Sigma Aldrich (US) or unless stated throughout text or in the appendix.

3.2 Human post-mortem brain samples

Human brains were obtained from routine autopsies at the Huddinge Brain Bank in accordance with the laws and the permission of the ethical committee. The control group included frontal-cortex from subjects who died either of non-neurological diseases or traffic accidents and had no history of long-term illness or dementia (85yrs ±8: 3F, 3M). The sporadic AD group included the frontal-cortex samples from patients with clinically and pathologically confirmed AD (81yrs ±5: 4F, 3M). The case history of each post-mortem is summarised in table 2.2. The frozen tissue was crudely fractionated to give a nuclear, membrane and cytosolic fraction. Samples were kept at -80°C until used. Preliminary Western analysis showed the nuclear fraction was absent for β-actin and β3-tubulin but positive for histone 4 (H4) while the cytoplasmic fraction was positive for β-actin and β3-tubulin but very little H4 expression. The membrane fraction did stain positive for β-actin but this was less abundant than the cytoplasmic fraction.

Table 3.2: Case histories of the different sporadic AD patients.

Case	Age	Sex	Cause of death	Dementia	Braak-Stage	CERAD-Score	Aβ-Phase	CAA-Stage
SWE28	73	F	Cardial insufficiency/ Hypertension	N	0	0	0	0
SWE64	90	M	Pneumonia	N	0	0	0	0
SWE70	91	F	Cardiomyopathy	N	0	0	0	0
SWE71	91	M	Cardial insufficiency	N	0	0	0	0
SWE72	78	M	Cardial infarct	N	0	0	0	0
SWE73	85	F	Cardial insufficiency/ DM type-II	N	0	0	0	0
SWE19	81	M	AD/ Cardial insufficiency	Y	4	B	3	1
SWE20	74	M	AD/ Pneumonia	Y	5	C	4	2
SWE45	78	F	AD/ Cardial insufficiency	Y	5	C	4	2
SWE57	80	F	AD/ Mycocardial infarction	Y	5	C	4	2
SWE58	80	F	AD/ Cardial insufficiency	Y	4	B	3	1
SWE74	84	M	AD/ Cardial insufficiency/ Hypertension	Y	4	B	3	1
SWE78	93	F	AD/ Pneumonia	Y	5	C	4	2

3.3 Mouse tissue homogenisation

C57Bl/6 mice of three different ages were used (1.5, 9.5 and 15 months of age). The brains were rapidly dissected, snap-frozen in liquid nitrogen and stored at -80°C until used. The frontal-cortex was homogenised with a glass Dounce homogeniser in radioimmunoprecipitation assay buffer (RIPA) (see Buffers) with Roche Complete protease® inhibitor cocktail. This suspension was left on ice for 15mins and separated into a soluble total-lysate and insoluble nuclear fraction by centrifugation at 15, 000RPM for 15mins. 30μg of protein from the supernatant were run on a 10% SDS-PAGE gel (see 3.7 Western blotting).

3.4 Cell culture

A murine neuroblastoma cell-line stably transfected with APPsw.695 [K595N/M596L] (Swedish familial variant), is herein referred to as N2aSw. The original cloning of this gene fused with a c-Myc tag was described by Lo et al in 1994. The expression of the clone within a pCB6 vector and subsequent selection with 0.4mg/ml geneticin/ G-418 generated the stable cell-line N2aSw.10.

The cells were maintained in a selective state using the antibiotic G-418 at a final concentration of 0.2mg/ml in a 1:1 mix of Dulbecco's Modified Eagle's Medium (DMEM) and OPTI-MEM (GIBCO, US), supplemented with 5% foetal bovine serum (FBS) and penicillin/streptomycin. Cells were grown in a 5% CO_2 incubator at 37ºC. This cell-line was a kind gift from Dr Gopal Thinakaran at the University of Chicago (Thinakaran et al., 1996b). The authors originally stated that this cell-line secretes 6-8 times higher levels of Aβ compared to cells overexpressing wild-type APP into the media. This is due to the increased selectiveness by the β-secretase. With this genetic manipulation, the Aβ secreted into the media is above the detectable threshold for Western blotting.

Some experiments were carried out in parallel in untransfected N2a cells. The cells were maintained in 1:1 mix of DMEM and OPTI-MEM supplemented with 5% FBS and penicillin/ streptomycin mix but lacking G-418.

Human embryonic kidney (HEK) 293 cells and COS-7 cells were grown in the usual DMEM supplemented with 10% FBS and penicillin/ streptomycin mix. A HEK293 cell-line stably over expressing APPsw.695 variant, herein referred to HEK293sw was a kind gift from Dr Jochen Walter at the University of Bonn. Finally

we used a HEK269 cell-line over expressing the wild-type variant of human APP herein referred to HEK269, was a kind gift from Dr Anja Capell and Dr Christian Haass at the University of Munich. Both HEK293sw and HEK269 were cultured in DMEM supplemented with 10% FBS, penicillin/streptomycin mix and a final concentration of 0.2mg/ml of G-418.

3.5 Cell treatments

Cells were treated with two specific (Calbiochem GSK3 inhibitors VIII and XI) and one non-specific (LiCl) GSK3 inhibitors. The Calbiochem inhibitors were dissolved in DMSO and used at 5μM and 10μM, respectively, to give maximum GSK3 inhibition with the least cell death (Bhat et al., 2003). These inhibitors are known to not inhibit the structurally similar CDK2 and protein kinase A. LiCl was used at 5, 20 and 40mM. Cells were incubated with the drugs in fresh medium overnight, which was harvested for subsequent analysis. The GSK3 inhibitor VIII, chemically referred to as AR-1014418, is highly specific for the GSK3β isoform as shown through co-crystallisation with the recombinant protein but it cannot be ruled out that it also inhibits the GSK3α isoform. As these inhibitors compete for the ATP-pocket within the kinase domain, which share 98% sequence identity between the two isoforms, it is highly likely that they inhibit both GSK3 isozymes. Therefore, these inhibitors are referred to as GSK3 inhibitors (cfr Calbiochem website).

The proteasomal inhibitor, MG132, was obtained from Sigma Aldrich and dissolved in DMSO. Working concentrations were varied to find optimal inhibition at 50μM. The additional proteasomal inhibitor, PS1 (Peptide Institute) was used at the recommended concentration of 10μM. The autophagy regulators 3-methyladenine (3-MA) and rapamycin were used at 500μM and 25nM, respectively. The former had to be dissolved in distilled, sterilised water and warmed in a water bath to aid suspension. Cycloheximide was used in order to block *de novo* protein synthesis for varying time points to determine the stability of FL-APP with GSK3 inhibition. Protein synthesis was blocked 30mins at a concentration of 50μg/ml, prior to addition of other chemical compounds.

Leupeptin (Sigma Aldrich) was used to inhibit key lysosomal peptidases at a concentration of 100μM/200μM and was dissolved in sterilised water. Bafilomycin A1 (Sigma Aldrich) and $NHCl_4$ (Sigma Aldrich) were used at 10nM and 20mM

respectively to prevent the correct acidification of lysosomes and therefore prevent broad lysosomal proteolysis.

3.6 Cell transfection of plasmid constructs and siRNA

Cells were transfected using the standard calcium phosphate method (Kingston et al., 2001) or using Lipofectamine™ 2000 (Invitrogen). Plasmid constructs used throughout were as follows: GSK3βS9 (constitutively active form, a kind gift from Professor Fred Van Leuven, Katholeike Universiteit Leuven), rat BACE1 promoter (a kind gift from Dr Steffen Rossen, University of Leipzig), scramble and β-catenin shRNA (a kind gift from Dr Patricia Salinas, UCL), β-catenin serine 33 (a kind gift from Professor Hans Clevers, The Hubrecht Institute), Wnt3a (Addgene, US), bif-1 shRNA (a kind gift from Professor Beniyi Li, University of Kansas Medical Centre) and TOPflash and FOPflash reporter constructs (a kind gift from Professor Simon Lovestone, Kings College London).

A GFP-tagged LC3 construct was used to observe GFP puncta formation upon autophagy stimulation (kind gift from Professor Stefan Grimm, Imperial College London). A FLAG-tagged version of TFEB was a kind gift of Andrea Ballabio (Telethon Institute of Genetics and Medicine, Naples) and was used to assess the subcellular localisation of TFEB. For the above experiments an empty pcDNA3, GFP- and FLAG-tag plasmids, scramble shRNA or control siRNA were used as controls.

The bacteria containing the cDNAs were stored as glycerol stocks at -80°C and amplified using the PureLink™ HiPure plasmid filter Maxiprep kit (Invitrogen) following the protocol available online. The concentration and purity was measured on the Nanodrop (Thermo Scientific) and aliquots were stored at -20°C, while a working aliquot was stored at 4°C for up to a month to avoid repeat freeze-thawing cycles of the sample which would lead to nicks and degradation of the plasmid cDNA.

For the transfection of siRNA specific for GSK3α/β (Cell Signalling, US), Lipofectamine™ 2000 (Invitrogen) was used in OPTI-MEM medium (GIBCO). The final concentrations of siRNA used were 10nM and 50nM within 2ml of OPTI-MEM medium. This was mixed with 5µl of Lipofectamine™ 2000 per well/sample of a 6 well plate, as summarised in Table 3.3 below.

Table 3.3: Beclin-1 and GSK3α/β siRNA transfection with Lipofectamine™ 2000.

siRNA	Culture vessel	Surface area	Volume of plate medium	Volume of dilution medium	[siRNA]	Reagent
Signal Science® GSK3α/β	6 well plate (1 well)	10cm^2	2ml	2x250µl	10-50nM	5µl
BECN1 Stealth RNAi™ siRNA	6 well plate (1 well)	10cm^2	2ml	2x250µl	10-50nM	5µl

Table 3.3: All volumes are scaled for the number of repeats for each treatment and the volume was split evenly between the replicate wells. This table is adapted from the one shown with the Invitrogen data sheet available at the following web address: http://tools.invitrogen.com/content/sfs/manuals/lipofectamine2000_man.pdf.

The Lipofectamine™ 2000 reagent was equilibrated in the OPTI-MEM medium for 5mins and siRNA was added afterwards. Once mixed with the siRNA, the complex is stable for up to 45mins but was added to the plate after 20mins in a drop-wise fashion. Silencing of the mRNA lasted up to 48hrs upon which protein or mRNA was harvested as detailed elsewhere. Initially, the protein expression of GSK3α/β and β-catenin from total-lysates were used to assess the effectiveness of the knockdown of GSK3.

3.7 Western blotting

3.7.1 Cell lysis and eletrophoresis of SDS-PAGE gels

Proteins were extracted from cells and tissue using RIPA buffer (see Buffers) supplemented with Roche Complete protease® inhibitor cocktail. The insoluble nuclear fraction was separated from the solubilised total-lysate by centrifugation at 13, 000RPM for 15mins at 4°C. Protein levels were determined using the Bradford method with the G-250 Coomassie brilliant blue reagent (Sigma Aldrich). Volumes of samples were adjusted to give equal loading of total protein into equal volumes of 2X sample buffer (see Buffers). To denature the protein, the samples were boiled at 96°C for 10mins, spun briefly and then stored on ice before loading. 50µg of the

protein sample were separated in 8% or 10% SDS gels. The Invitrogen Prestained SeeBlue® Plus2 marker was used to assess the molecular weights.

The protein was transferred to Immobilon®-P PDVF (Millipore, US) membranes or Hybond™-C Extra nitrocellulose (Amersham, UK) for Aβ and the C-terminal fragments of APP. The transfer was carried out in 1X tris-glycine buffer with 10% methanol at a constant 400mA for 60mins. Membranes were blocked in 5% non fat dried milk (NFDM) in TBST for 1hr at RT, with the exception for the antibody R1 57 which was blocked in 5% FBS at 37ºC for 30mins. Membranes were blotted with primary antibody overnight at 4°C. Primary antibodies were diluted in 1% BSA/ 0.1% sodium azide in TBST unless stated. Membranes were then incubated with a HRP conjugated secondary antibody in 5% NFDM in TBST for 1hr at room temperature.

After thoroughly washing, membranes were developed using ECL reagent (see Buffers), which was used to detect luminescence and were exposed to Hyperfilm ECL™ film. Films were developed with an automated developer from Konica, SRX 101A. The intensity of banding was quantified by densitometry scanning with Image J (NIH) and normalised to β-actin in most cases or to the subcellular marker for fractionation studies. In addition, the protein of level of GAPDH and β3-tubulin were used to ascertain the stability of the total protein levels. The housekeeping protein, β3-tubulin, is also more sensitive to neuronal death and closely correlated with total protein concentrations, to confirm that the treatments used were not associated with cell death. All equipment used for both SDS-PAGE and the transfer was obtained from Bio-Rad using the Mini-Protean® tetra cell system.

3.7.2 Determination of secreted Aβ and sAPPα ectodomain

Secreted soluble APPα (sAPPα) and Aβ were measured from the medium of N2aSw cells. The volume of medium loaded was adjusted to protein concentrations measured from the total-lysate of the corresponding cells. An aliquot of the medium was either run straight away on a NuPage 4-12% tris-glycine gel (Invitrogen) or Aβ was pulled down overnight at 4ºC using Sepharose Protein A beads (Invitrogen) and the antibody 4G8, a monoclonal antibody raised against amino acids 17-42 of human Aβ (Covance, US). 40µl of sample buffer 2 (see Buffers) was added to each sample. Samples were vortexed and then boiled for 10mins. The samples were loaded onto a NuPage 4-12% Bis-Tris gel with MES buffer and subsequently transferred onto a

nitrocellulose membrane. The membrane was boiled in 1X PBS for 5mins[3], blocked with NFDM and incubated with 6E10 antibody at 1/1000 overnight at 4°C (Covance). After incubation with HRP-conjugated secondary antibody, the blot was developed using an ECL reagent (see Buffers) and exposed to Hyperfilm ECL™ film and developed in an automated developer from Konica, SRX 101A. The area of protein bands were scanned and quantitated using the Image-J program (NIH). Changes in sAPPα and Aβ levels expressed as percentage change from control at 100%.

3.7.3 Subcellular fractionation

Cells were washed twice in ice cold 1X PBS, scraped and left on ice for 10mins in hypertonic buffer containing Roche Complete® protease inhibitor cocktail (see Buffers) and sodium fluoride and sodium orthovanadate, two established phosphatase inhibitors. The cells were mechanically ruptured when they were passed through a 0.6ml gauge needle several times. Then, samples were centrifuged at 5, 000RPM for 5mins to pellet the nuclear fraction. The supernatant pertaining the membrane and cytosol was transferred to a fresh tube and subsequently centrifuged at 13, 000RPM for 45mins. The pellet containing the membrane fraction was taken for further analysis for measuring enzymatic activity and APP CTFs. The cytosolic fraction was then precipitated by adding 20% trichloroacetic acid (TCA) in a 1:1 ratio to give a final concentration of 10%. After incubating for 45mins on ice, this fraction was spun at 13, 000RPM for 30mins. The pellet was washed firstly in ice cold 90% acetone and then 100% acetone, spinning at 13, 000RPM for 10mins between the washes. The final pellet was resuspended in 2X loading buffer 1, adding tris-HCl pH8 to neutralise the acid. All steps of this procedure were carried out on ice, to avoid protein degradation.

[3] Boiling the membrane was found to be effective in increasing the detection limit of Aβ presumably by unmasking epitopes to the detection antibody in a mechanism analogous to antigen retrieval in IHC techniques KLAFKI, H. W., WILTFANG, J. & STAUFENBIEL, M. 1996. Electrophoretic separation of betaA4 peptides (1-40) and (1-42). *Anal Biochem.* United States, SASTRE, M. 2010. Troubleshooting methods for APP processing in vitro. *J Pharmacol Toxicol Methods.* United States: 2010 Elsevier Inc.

3.7.4 Analysis of APP C-terminal fragments

Measurement of the CTFs of the various secretases is an indirect measurement of their activity. The CTFs were analysed by immunoblotting with the antibody 140 of membrane extracts from N2aSw, as described previously (Sastre et al., 2001). The α- and β-CTF, were detected from the membrane fractions obtained by the subcellular fractionation method. The membrane pellet was resuspended in an appropriate volume of sample buffer 2 (see Buffers), boiled for 10mins and run in 4-12% NuPAGE gels. The α-CTF (10kDa) and β-CTF (12KDa) were detected using the antibody 140. For detection of β-CTF alone the antibody, 6E10 was used.

The AICD fragment was generated using an *in vitro* assay from membrane preparations, according to procedures described previously (Sastre et al., 2001b). Membranes were pelleted by centrifugation for 20mins at 15, 000RPM at 4°C, washed, and resuspended in the assay buffer (150mM sodium citrate, pH6.4). To allow the generation of the AICD, samples were incubated with shaking at 37°C for 2hrs. After termination of the assay on ice, samples were spun at 15, 000RPM at 4°C for 1hr. The supernatant was collected and an equal volume of sample buffer 2 (see Buffers) was added and boiled for 10mins. Proteins were separated by electrophoresis using 4–12% Bis-Tris NuPage gels in 1X MES buffer using the XCell *SureLock II*™ system (Invitrogen). Proteins were transferred to a nitrocellulose membrane as stated. The membrane was boiled for 5mins in 1X PBS before blocking in 5% FCS in TBST at 37ºC for 30mins. The APP C-terminal specific antibody, R1 57 or the 140 were used to detect the 6kDa AICD fragment. Two negative controls were used to assess the specificity of the antibody for the AICD. Firstly, a sample "ice" control was kept at 4ºC on ice, where no enzymatic activity of the γ-secretase should be present. The specificity of the assay was further demonstrated by incubating a membrane sample at 37ºC with 250nM DAPT, a specific γ-secretase inhibitor.

3.8 Pulse-chase analysis

The following procedure was carried out within a class 2 culture hood situated in a "hot room" and the cells were incubated in a 5% CO_2 humidified incubator at 37ºC. N2aSw cells were starved in methionine-free medium supplemented with glutathione and 5% dialyzed serum for 30mins at 37°C. The cells were then pulsed with the same kind of media containing [S^{35}]-methionine at 300µCi/ml for 20mins at 37°C. After this, the cells were washed twice in PBS to remove excess radioactivity and chased with normal DMEM with an excess of methionine, 150µl/ml at 37°C for different periods. The cells were lysed on ice at different time points (0, 2, 4, 8hrs) with RIPA supplemented with the Roche® complete protease inhibitor cocktail mix. Similar amounts of protein in lysates were immunoprecipitated overnight at 4°C with either 1µl of 6E10 or 5µl of R1 57 with 30µl of 50% Protein G or A beads, respectively in a total volume of 500µl made up with RIPA buffer. The beads were washed in ice cold buffer B (see Buffers) for 3x10mins and resuspended in 40µl of 2X sample buffer and incubated at 95ºC for 10mins. Samples were run on an 8% SDS-PAGE gel. The gel was firstly fixed in 50% isopropanol/ 10% acetic acid for 30mins. The signal was then enhanced by soaking the gel in a 1M sodium salicylate solution for 30mins in the dark. The gel was dried for up to 2hrs with a gradient increase of temperature to 85ºC on a gel drier (Bio-Rad, US). The signal was detected by exposing to a Hyperfilm MP (GE Healthcare) autoradiography film at -80ºC to maintain linearity and to reduce the background noise of the signal. An initial overnight exposure was used followed by longer times, depending on signal strength. The protein bands were scanned and quantitated using the Image-J program. Relative intensity of the bands was calculated as a percentage of the intensity of the protein band in cell-lysates at time 0hr of the chase.

3.9 Autophagy assessment/LC3-II production

LC3-II (16kDa) production was assessed by Western blotting from N2aSw total-lysates on a 16% tris-glycine gel and normalised to levels of LC3-I (18kDa). The antibodies used were an anti-rabbit LC3, which was a kind gift from Dr. M. Koike (Juntendo University Graduate School of Medicine) and a rabbit polyclonal anti-LC3 from Abcam. Any changes with respect to control were expressed as LC3-II/LC3-I ratio. The specificity of the bands was confirmed with the following positive

controls: 3-methyladenine, a negative repressor and rapamycin, a known positive regulator. In addition both N2aSw and COS-7 cells were transfected with a GFP-tagged LC3 construct and assessed for puncta formation owing to autophagosome formation by normal epifluorescence (Klionsky et al., 2008). Cellular conditions are detailed in figure legends.

In order to show whether specific GSK3 inhibition leads to increased autophagy flux, the levels of LC3-II were measured in cells additionally treated with both 200μM leupeptin and 20mM NH_4Cl, which completely blocks lysosomal degradation.

3.10 Enzymatic activity of the β- and α-secretases

The enzymatic activities of the β- and α-secretases were measured by a fluorimetric reaction kit (R&D Systems). Membrane fractions from N2aSw cells were resuspended in 200μl of the "Cell Extraction Buffer". 50μl of the sample was incubated with 50μl of the 2X "Reaction Buffer" and 3μl of substrate at 37ºC for 2hrs with mild shaking in the dark. The fluorescence was measured using a fluorimeter, with excitation between 335-355nm and emission detection between 495-510nm.

The substrates are patented peptides mimicking the native substrates for either the α- or the β-secretase. These peptides are homologous to amino acids 681-689 and 668-675 of APP for the α- and β-cleavage respectively. Conjugated to theses peptides, are an EDAN and a DABCYL moiety flanking the cleavage site. Upon enzymatic activity and cleavage of the peptide, the EDAN moiety is allowed to fluoresce with the physical separation from the DABCYL moiety, a quencher.

The background fluorescence obtained from a "No cell lysate" negative control was subtracted from values and the raw fluorescence was normalised to protein levels. The results were expressed as a percentage of the control.

3.11 Microscopy

3.11.1 Lysotracker®-Red DN-99 staining

N2aSw and COS-7 cells were seeded on glass coverslips and treated with inhibitor VIII overnight. Cells were treated with or without Lysotracker®-Red DN-99 (Invitrogen) at a final concentration of 75nM for 2hrs at 37°C. The medium was aspirated and washed once quickly in PBS to remove unbound Lysotracker®-Red DN-99 and coverslips were fixed in 2% PFA for 15mins[4]. The coverslips were counterstained with DAPI and mounted straight in ProLong® Antifade (Invitrogen) overnight at room temperature before sealing with nail varnish and storing at 4°C.

3.11.2 Immunocytochemistry

Immunocytochemistry was used for subcellular localisation of APP and the lysosomes. The cells were fixed as above upon which they were blocked in 3% BSA in 0.025% saponin for 1hr. Primary antibodies were used in combination or separately: rabbit polyclonal anti-APP (140) at 1/500 and mouse monoclonal anti-LAMP1 at 1/200 were incubated for 1hr at RT in 1% BSA/0.025% saponin at room temperature. After 5x5mins washes with PBS, Alexa Fluor® secondary antibodies (488 and 594) were incubated for 1hr at RT in 1% BSA/0.025% saponin at a dilution of 1/750. After the final PBS washes, the cells were counterstained with DAPI and mounted in the same ProLong® Antifade mountant.

For the cellular localisation of TFEB, N2aSw cells that transiently overexpressed the TFEB-FLAG construct were grown on coverslips and permeabilised and fixed in methanol at -20°C for 10mins. The cells were washed in 1XPBS, blocked with 1% BSA in 1XPBS for 10mins and incubated with primary antibody, anti-FLAG at 1/200, in blocking buffer for 1hr at 37°C. The secondary antibody, Alexa Fluor® 594 anti-mouse secondary antibody, was incubated for 1hr at room temperature at 1/500 in the same blocking solution. The coverslips were mounted on glass slides using Vectashield mounting medium (Vector Laboratories), sealed with nail varnish and stored at 4°C.

---

[4] It should be noted that Lyostracker probes are intended for live cell imaging but Lysotracker®-Red DN-99 has been successfully used in fixed cells. Please refer to Invitrogen website (cfr http://www.invitrogen.com/site/us/en/home/References/Molecular-Probes-The-Handbook/Probes-for-Organelles/Probes-for-Lysosomes-Peroxisomes-and-Yeast-Vacuoles.htmland) and Lee et al, 2010.

3.11.3 Image capture and analysis

Z-stacks with a 0.42µm step were captured on a Leica LAS AF SP5 confocal with a x63 optical oil immersed lens and x2.5 digital zoom with a sequential scan between channels, averaging over 4 frames for each scan and saved at 1024x1024 pixel ratio:

- Scan 1: An Argon laser set to 20% was used for Alexa Fluor® 488 and with a Bright field image.
- Scan 2: A Xenon laser set to 52% was used for Alexa Fluor® 594, TFEB-FLAG and Lysotracker® Red DN-99.
- Scan 3: A Diode laser set 10% was used for the DAPI counterstain.

Five randomly selected fields were captured per treatment with roughly 10-20 cells per field. For total APP, using the "Measure stack" function in Image J, an average mean intensity was taken from each stack, which was then further averaged to give the mean of the entire Z-stack. This was either based on the entire field or a threshold of the cell area. For counting vesicle numbers for both LAMP1 and Lysotracker®-Red staining, the "Analyse particle" function from Image J was used. A region of interest was drawn to include the maximum area through the Z-stack for each cell within the field as governed by the Bright field image taken. The limits were set for a size from 1 to infinity and a circularity from 0 to 1 and therefore not dictated by its shape. A sum was taken from the number of particles of each stack within the Z-stack series and then divided by the number of cells within the ROI.

The Imaris CoLoc plugin was used to assess the significance of the colocalisaiton between APP and LAMP1 within the field of view using the Pearson's Correlation Coefficient (PCC) and Mander's coefficient (M1 and M2) for each randomly sampled field. In addition the percentage of the field that was colocalised was also expressed.

10 randomly selected fields were captured for the localisation of TFEB within N2aSw cells transiently transfected with a FLAG-tagged TFEB construct. The numbers of nuclear-positive cells were counted and expressed as a percentage of the total number of TFEB-positive cells.

3.11.4 Transmission electron microscopy

Cells incubated on coverslips were washed thrice in serum-free DMEM media, and fixed in 4% paraformaldehyde and 1% glutaraldehyde in 0.1M sodium cacodylate buffer (pH 7.2) for 30mins at RT. Following fixation, coverslips containing cells were treated with reduced 1% osmium followed by 1% tannic acid. Samples were processed for en-face embedding in epon. Ultrathin sections of 70nm were collected from various depths from the block and then were stained with a 2% aqueous solution of uranyl acetate and Reynold's lead citrate and observed using a transmission electron microscope (Tecnai G2 Spirit, FEI). Images were captured on a digital camera (Eagle, FEI). Initial low magnification images were captured of cells that were to be surveyed and imaged at X6, 500 in order to give enough resolution to identify the organelles but also to be able to cover the entire cytoplasm of the cell. More than 30 cells were analysed per section from each treatment and multiple sections were analysed so as to have some representation from the different depths through the Z-plane.

Organelles counted included: The total number of autophagosomes (AVs) and autophagolysosomes (AVLs), primary lysosomes (PL), mature lysosomes (ML), mitochondria and multivesicular bodies (MVBs). The identification based on morphology from the micrographs used previously established criteria. Briefly, AVs (vesicles greater than 300nm) were classified as autophagosomes when they met two or more of the following criteria: double membranes (complete or at least partially visible), absence of ribosomes attached to the cytosolic side of the membrane, luminal density similar to cytosol, and identifiable organelles or regions of organelles in their lumen. AVLs were merely classed as being more mature versions than what was previously described, sometimes containing a singular enveloping membrane and/or some already partially digested material within it. Such criteria were based on highly critical peer reviews from several established groups within the autophagy field (Eskelinen, 2008, Klionsky et al., 2008, Ylä-Anttila et al., 2009).

3.12 mRNA extraction and RT-PCR

N2aSw cells were subjected to reverse-transcription quantitative PCR (RT-qPCR) analysis using a 2-step method with an initial reverse transcription and subsequent real-time cycling using a Strategene Mx3000p block cycler.

Total RNA was extracted using the RNeasy® mini kit (Qiagen) with the additional step of sample homogenisation with a 20G needle and the removal of contaminating DNA by passing through a DNA capture column. RNA integrity was confirmed by relative abundance of the 28S to18S rRNA (2:1) on a 1.5% agarose gel and a spectrophotometric 260/280 ratio of =1.9. Quantification of RNA was determined by reading on a Nanodrop (Thermo Scientific) to normalise the RNA input to 1µg for the RT step. Total RNA was amplified by priming with 10X random hexanucleotide mix (Roche, Switzerland) as detailed in Table 3.4 and 3.5 below. The SuperScript®II reverse transcriptase (Invitrogen) was provided with 5X first strand buffer and 0.1M DTT and the 25mM dNTP mix was provided by Fermantas (US).

Table 3.4: Step 1a.

Reagent	Volume	Final concentration/ Volume
RNA input	Xµl	1µg/20µl
ddH_20	Xµl	10µl
10X random hexanucleotides	2µl	1X
Total (per reaction)	**12µl**	

Priming:

-95°C for 2mins

-72°C for 10mins

-8°C pause

Table 3.5: Step 1b.

Reagent	Volume	Final concentration/ Volume
5X first strand buffer	4µl	1X
0.1M DTT	2µl	10mM
(10mM each) dNTPs mix	1µl	1mM each
Reverse transcriptase 200U/µl	0.5µl	100U
ddH_20	0.5µl	
Total (per reaction)	**8µl**	

First strand synthesis

-25°C for 5mins

-42°C for 1hr

-95°C for 5mins

-8°C paused

The resulting cDNA was then immediately frozen or used for subsequent PCR analysis.

Semi-quantitative RT-PCR was performed for APP mRNA levels from N2aSw cells treated with the GSK3 inhibitor VIII overnight. The primers used were: human *APPsw* (Forward: 5'-GCTTGCACCAGTTCTGGATGG-3'; Reverse: 5'-GAGGTATTCAGTCATGTGCT-3'), mouse *App* (Forward: 5'-GGTGGACTCTGTGCCAGC-3': Reverse: 5'-TCCGTTCTGCTGCATCTTGG-3') and mouse *Gapdh* (Forward: 5'-ACCACAGTCCATGCCATCAC-3'; Reverse: 5'-TCCACCACCCTGTTGCTGTA-3'). This was taken through:

Initial denaturation 95°C for 5mins

-Initial denaturation 94°C for 30secs

-Annealing 53°C for 30secs

-Extension 72°C for 1min

Final extension 72°C for 3mins

Pause at 8°C

-25 cycles

After the addition of loading dye, 10µl of reaction product was then resolved on a 0.8% gel and the density of the bands corresponding to both human and mouse APP were normalised to that of mouse *Gapdh* and expressed as percentage of the control.

Real time cycling was carried out with the Quantifast® SYBER green (Qiagen) and Quantitect® Primer assays (Qiagen) for mouse *Bace1* and for the reference gene mouse *Gapdh* (Forward: 5'-ACCACAGTCCATGCCATCAC-3'; Reverse: 5'-TCCACCACCCTGTTGCTGTA-3'), which were a kind gift from Dr. Egle Solito (William Harvey Research Institute). Cycling conditions were as stated in the Quantifast® handbook with 40 cycles on a Stratagene Mx3000p thermocycler (see figure 3.4).

Table 3.6: Cycling conditions and reaction mastermix.

Reagent	Volume	Final concentration/ Volume
cDNA 50ng/µl	Xµl	1-100ng
10X Quantitect® primer	2.5µl	1X
2X Quantifast® SYBR green	12.5µl	1X
ddH_20	Xµl	
Total volume	**25µl**	

Cycling:

-Initial denaturation 95°C for 5mins

-Denaturation 95°C for 10s

-Annealing/ Extension[5] *60°C for 30s*

-35-40 cycles[6]

A post melt-curve analysis revealed the absence of primer dimers for all primer sets as shown in figure 3.4. For each experimental repeat/RNA extraction, a calibration curve (100, 10 and 1ng) was produced for each transcript to ascertain the primer set efficiency and the cDNA input. The efficiency is described by equation (1).

$$(1)\ E = 10^{\left(\frac{-1}{gradient}\right)}$$

A no RT and template control was used to set the fluorescence threshold above the background and in each case a no Ct value was obtained for all three replicates. The baseline and reference dye normalised (dRn) Ct values were analysed using the Pfaffle method and elaborated upon in 2000 (Vu et al., 2000).

This is described by the mathematical equation (2) and normalises differences in a control case and test case for a particular gene of interest to a difference in a control case and test case of a stable reference gene. More importantly these two variables are weighted to the efficiency of the primer set that generated them. This is an important addition as theoretical bias would dictate that the DNA/ fluorescence content after each cycle should double however as the reaction is not a *perfect* system,

[5] The Quantifast® SYBR contains a patented polymerase that enables a joint annealing and extension phase during the cycling thus reducing the programme time.

[6] As the reaction is followed in real-time by measurement of fluorescence it is not important whether the reaction reaches saturation or not.

the actual content maybe less or more than double with each cycle thus the E function can be used to normalise for less than perfect primer sets.

(2) $E^{Expt(Ct\ control-Ct\ test)}/E^{Ref(Ct\ control-Ct\ test)}$

(3) $\frac{E^{Expt(\Delta Ct)}}{E^{Ref(\Delta Ct)}}$

This method also has the bonus of the calibration step. In this way the input can be ascertained so as to give results in the linear range of the reaction and therefore will be quantitative. And thus the input can be varied for each transcript owing to the differences in the relative abundance from the original source.

Mouse *Gapdh* was chosen as the reference gene after an initial screen of different references genes for stability with treatments including *18Srna* (Qiagen), *Cyclophilin-b and Actin-f* (Invitrogen)[7].

[7] This was based on an algorithm (GeneNorm) that assesses the most stable data set with varying treatments which is made freely available at: http://medgen.ugent.be/~jvdesomp/genorm/.

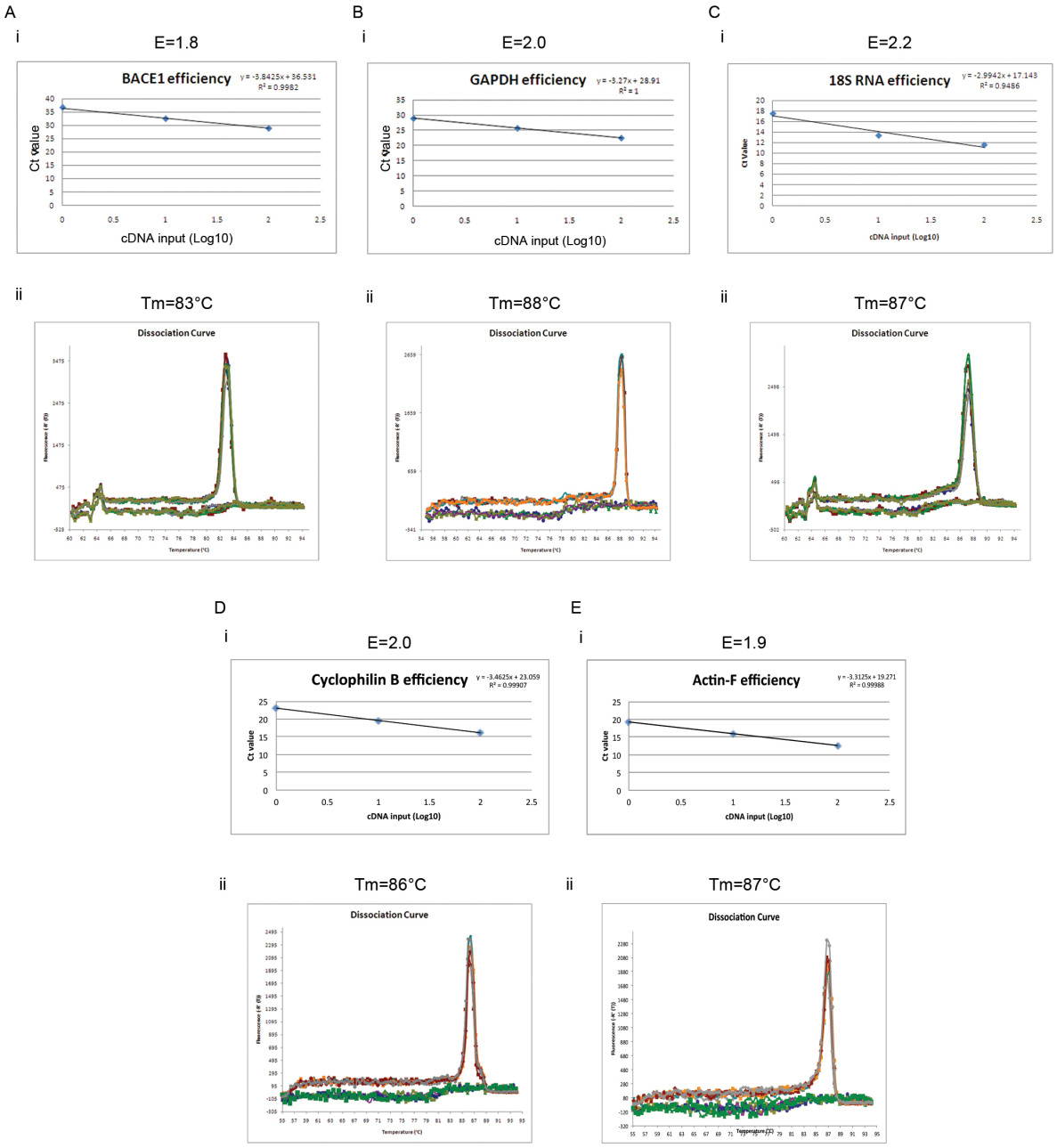


Figure 3.2: Efficiency and post melt-curve analysis of primer sets.

Primer sets (A) *Bace1*, (B) *Gapdh*, (C) *18Srna*, (D) *Cyclophilin-b* and (E) *Actin-f* were tested for their efficiency (i) and their specificity (ii) from a melt-curve analysis. The efficiency was determined by plotting the Ct value against the log of the cDNA input and is equal to the gradient of the slope. In each case the melt-curve gives a specific peak for the meting temperature and the approximate *Tm* is given for each primer set.

Figure 3.4 shows that every primer set used throughout gave good efficiency values and that in each case a single *Tm* peak was produced from the resulting melt-curve analysis. This would suggest that the specificity of the primers is perfect producing one specific amplicon. This was later confirmed by running a fraction of the product out onto a 2% agarose gel resulting in the migration of one band of the expected size when compared to the standard DNA ladder.

3.13 Luciferase dual reporter assays

The activity of the BACE1 promoter was determined by measuring luciferase activity in a luminometer. N2aSw cells were transfected with the rat BACE1 promoter fused to the Firefly luciferase reporter gene and co-transfected with the CMV-*Renilla* luciferase normalising construct in a 400:1 ratio. The 1.5kb BACE1 promoter region was originally cloned from a highly conserved region upstream of the rat BACE1 coding region. Homologous sequences from rat, mouse and human are highly conserved and contain multiple putative binding sites for transcriptional regulators (Lange-Dohna et al., 2003). Therefore this luciferase construct is and has been a reliable method for assaying BACE1 promoter activity in both mouse and human cells and has done so before (Sastre et al., 2006a, Bourne et al., 2007).

BACE1 promoter activity and TOP/FOPflash reporter assays were carried out on a luminescence reader following the protocol for the Promega dual reporter assay®. The data was normalised to the *Renilla* luciferase expression to allow for varying transfection efficiencies.

3.14 Statistical analysis

The statistical analysis used throughout this study was done with the advice from the Statistical Advisory Service based at Imperial College London. Columns in graphs represent the mean values ±SEM and expressed as percentage of control, unless stated otherwise, in GraphPad's Prism v5.0. For *in vitro* experiments at least three samples were run for each treatment group and each experiment was reproduced at least three times, the n-number is therefore equal to the number of samples per treatment group multiplied by the number of times the experiment was repeated (3 samples per group and with the experiment repeated 3 times is equal to n=9). The n-number for which a particular statistical analysis was based on is given in the body text and the figure legend. For *in vivo* data, each n-number is equivalent to the number of animals or human cases (6 animals is equivalent to n=6). An unpaired t-test or a one-way ANOVA were used to show any significant statistical difference between means of two or more groups respectively. A Dunnett's post-hoc test was used to assess significance in reference to the control group only and a Tukey's post-hoc test if comparing between all groups, both of which correct for multiple comparisons. In the case of Wnt3a and β–catenin S33 overexpression in chapter 5, individual t-tests were used to assess the difference in the means of treatment to control (see figure 6.3 and 6.4).

Table 3.7: List of drugs and concentrations

Drug name	Function	Company	Solvent	Stock concentration	Working concentration
3-MA	Autophagy repressor	Sigma Aldrich	Sterilised ddH_20[8]	10mM	500µM
Actinomycin-D	Transcription inhibitor	Sigma Aldrich	DMSO	1mg/ml	1µg/ml
Bafilomycin A1	Vacuolar-ATPase inhibitor	Sigma Aldrich	DMSO	1mM	10nM
Cycloheximide	Translational inhibitor	Sigma Aldrich	DMSO	5mg/ml	50µg/ml
DAPT	γ-secretase inhibitor		DMSO	10µM	0.25µM
GSK3 inh VIII	GSK3 inhibitor	Calbiochem	DMSO	10mM	5µM
GSK3 inh XI	GSK3 inhibitor	Calbiochem	DMSO	10mM	10µM
Leupeptin	Peptidase inhibitor	Sigma Aldrich	Sterilised ddH_20	2mM	100µM/200µM
LiCl	Non-specific GSK3 inhibitor	Sigma Aldrich	Sterilised ddH_20	1M	5-40mM
MG132	Proteasomal inhibitor	Sigma Aldrich	DMSO	10mM	50µM
$NHCl_4$	Lysosomal inhibitor	Sigma Aldrich	Sterilised ddH_20	1M	20mM
PS1	Proteasomal inhibitor	Peptide Institute	DMSO	10mM	10µM
Rapamycin	Autophagy inducer/mTOR inhibitor	Sigma Aldrich	DMSO	1mM	25nM
Tunicamycin from *Streptomyces Sp.*	N-glycosylation inhibitor	Sigma Aldrich	DMSO	10mg/ml	10µg/ml

[8] 3-methyladenine requires heat and agitation to obtain solubility in ddH_20 with concentrations up to 10mg/ml.

Buffers

Buffer 2: 150mM NaCl, 0.1% triton X-100, 10mM tris-HCl pH8.3 and 5mM EDTA pH6.8 made up in ddH_20.

ECL reagent A: 50ml 0.1M tris-HCl pH8.5, 0.22ml p-columeric acid and 0.5ml luminol.

ECL reagent B: 50ml 0.1M tris-HCl pH8.5 and 30µl H_20_2.

Erasing buffer: 62.5mM tris-HCl pH8.0, 2% SDS and 100mM β- mercaptoethanol in ddH_20.

2X HEB: 50mM HEPES, 280mN NaCl and 1.5mM Na_2HPO_4 at pH7.09.

Hypertonic buffer: 10mM Tris-HCl pH8.0, 1mM EDTA pH8.0, 1mM EGTA pH8.0 and Roche Complete protease inhibitor cocktail (1 pill per 50ml of buffer). 50mM NaFl and 1mM sodium orthovanadate were added just before use if studying phosphorylated protein levels.

Loading buffer 1: For 1ml, 300µl of NuPage 4X LDS loading buffer (Invitrogen), 600µl of ddH_20 and 100µl β-mercaptoethanol.

Loading buffer 2 X1: 50mM Tris-HCl pH 6.8, 2% sodium dodecylsulfate, 10% glycerol and few grains of bromophenol blue made up in ddH_20. For 2X double the amount of each constituent. β-mercaptoethanol added before use, 5% of total volume.

Running buffer 10X: 30g of trizma base and 143.4g of glycine in 1L of ddH_20. Diluted 1 in 10 with ddH_20 to give 1X and 10ml of 10% SDS to give final concentration of 0.1% in 1L.

Sodium Citrate Buffer: 150mM tris HCl, pH6.4.

10X TBE: pH 8.3; For 1 L, 108g of Trizma, 55g of boric acid and 9.3g of EDTA in ddH_20.

TBST: 8.8g of NaCl, 10ml of 1M Tris-HCl pH8.0 and 500µl of Tween-20 up to 1L with ddH_20.

TE: 10mM Tris pH 7.4, 1mM EDTA.

CHAPTER 4 : ROLE OF GSK3 ON APP PROCESSING

4.1 Introduction

As outlined previously, there is evidence indicating that GSK3 plays a crucial role during the pathogenesis of AD. For every aspect of AD pathology, GSK3 hyperactivity is shown to drive and connect the varying aberrant events that occur throughout the lifetime of a patient. It has been postulated that dysregulation of GSK3 activity occurs with aging, although it remains unclear whether such effects may occur in nervous tissue. The effects of aging on GSK3 expression in the CNS have not yet been defined. This could have consequences in the development of age-related disorders, such as AD.

There is an enormous amount of literature referring to GSK3 regulating Aβ toxicity, tau pathology, inflammation, apoptosis and memory impairment (see 2.8.3 GSK3 hypothesis of AD). However, what is lacking is any consistent data on the mechanism in which GSK3 regulates the processing of APP. Certain studies have hinted at a possible link showing altered Aβ load with GSK3 inhibition in both *in vitro* and *in vivo* models. However, taken together there appear to be inconsistencies and any mechanistic understanding is still lacking. Some of the inconsistency may have come from the use of LiCl, a non-specific inhibitor of GSK3 in the earlier studies (Feyt et al., 2005, Phiel et al., 2003, Sun et al., 2002). While some reports show GSK3 promotes Aβ production and others the very opposite, neither show any mechanism behind this alteration.

What is required within the field is some clarity on the mechanistic understanding by which GSK3 inhibition affects Aβ generation. One obvious application of basic biological research is that of medical research. Nonetheless, a more complete insight of these principles is required in order to make informed decisions and produce effective therapies. Intuitively, if inhibition of GSK3 function does reduce Aβ load this would prove a beneficial role. However, if the mechanism underlying the regulatory role of GSK3 on APP processing is mediated through regulation of the γ-secretase (Phiel et al., 2003), then caution should be taken as negative effects from increased CTF accumulation with γ-secretase inhibitors have been observed (Bittner et al., 2009). Therefore, a need to understand the molecular

basis of GSK3 inhibition using an *in vitro* or cell based model with specific pharmacological inhibition. It is important to verify any mechanistic findings later on in an *in vivo* setting. To this end, the role of GSK3 in regulating APP processing was investigated in a well-documented cell-based model for APP processing, the N2aSw cell-line (Thinakaran et al., 1996b, Sastre, 2010). In addition to LiCl, which has produced inconsistent results, two cell-permeable and specific inhibitors of GSK3 were used. Furthermore GSK3α/β knockdown was performed using a siRNA strategy.

The first aim of this project was to determine the potential changes of GSK3 with aging and to ascertain if the processing of APP is affected by GSK3 and, if so, what are the potential mechanism(s)

4.2 Results

4.2.1 GSK3 expression and activity increases with age

To define the effect of aging on GSK3 in the CNS, the expression of GSK3 and serine-9 phosphorylated-GSK3 (p-GSK3) in lysates (frontal-cortex) from C57Bl/6 mice at different ages was determined. As shown in figure 4.1, there was an increase in the levels of GSK3β in old mice (9.5 and 15 months of age) compared to young mice (1.5 months of age), while GSK3α expression remained unchanged during aging. Conversely, the levels of the inactivated form p-GSK3 were decreased in 9.5 months old mice compared to young mice (n=4 per group).

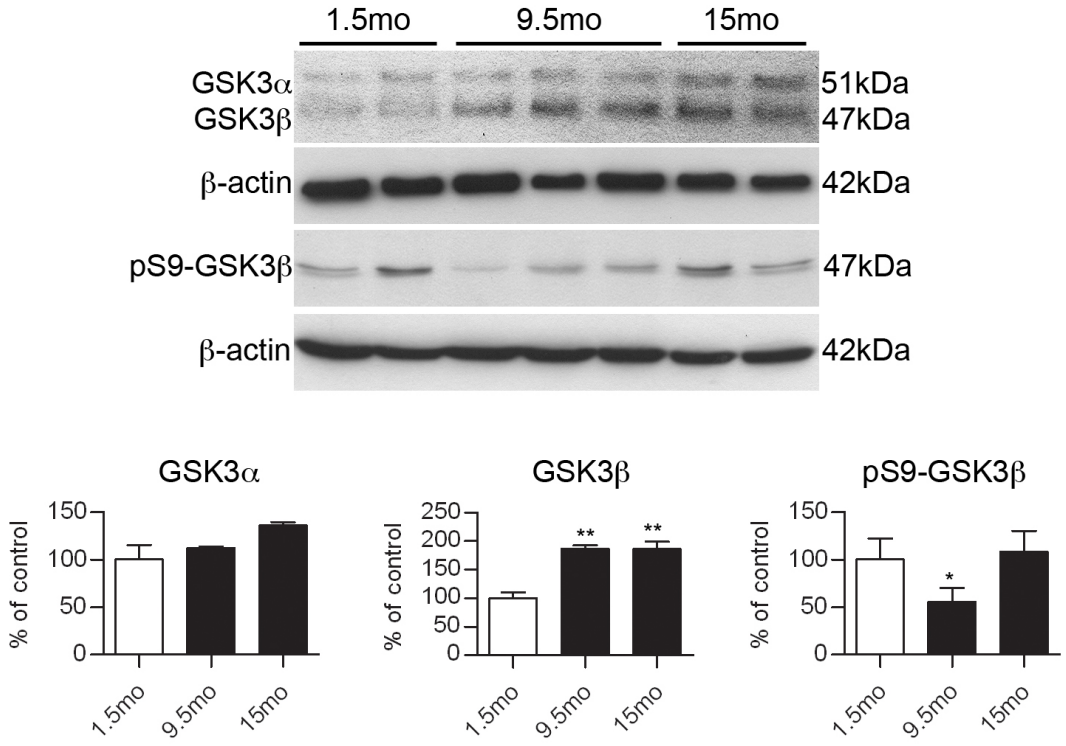


Figure 4.1: GSK3 expression and activity increase with age.

Western blots and their quantification for GSK3β and its phosphorylated form at serine 9, in brain homogenates from young and old C57Bl/6 mice. Compared to young mice at 1.5mo of age, there was a significant increase in the expression of GSK3β but not GSK3α at 9.5mo and 15mo. Additionally when compared to mice of 1.5mo there was a significant decrease in the amount of phosphorylated GSK3β at serine 9 at 9.5mo, indicative of increased activity (n=4 per group). Values shown in graphs represent the mean value ±SEM and are expressed as a percentage of control. Statistical analysis included one-way ANOVA with a post-hoc Dunnett's test, *P<0.05 and **P<0.01.

4.2.2 Changes in GSK3 activity lead to alterations in the amyloidogenic processing of APP

The initial line of investigation was to firstly ascertain whether specific pharmacological inhibition of GSK3 does indeed result in reduced amyloidogenic processing of APP, as shown previously elsewhere. And as further confirmation to this, a second approach was to determine whether genetic silencing of GSK3 also results in the same changes. To this end, a simple *in vitro* cell system was used whereby different GSK3 inhibitors were added to the culture medium of N2aSw cells overnight. Subsequently harvesting the cells for further analysis, the conditioned medium was assayed for Aβ production by Western blotting. To verify the inhibition of GSK3 and to determine the appropriate concentrations of GSK3 inhibitors to be used in this assay, the levels of total β-catenin expression by Western blotting from total-lysates of N2aSw cells were determined. Any inhibition of GSK3 should lead to an increase in the levels of β-catenin in the cytoplasm and nucleus due to a reduction in proteasomal degradation. In addition to the two specific inhibitors VIII and XI (Calbiochem), LiCl was also used at concentrations stated from other studies as a means to corroborate previous findings in this paradigm. As expected, LiCl and the commercial GSK3 inhibitors significantly increased the expression of β-catenin in the nucleus (figure 4.2) thus confirming the inhibition of GSK3.

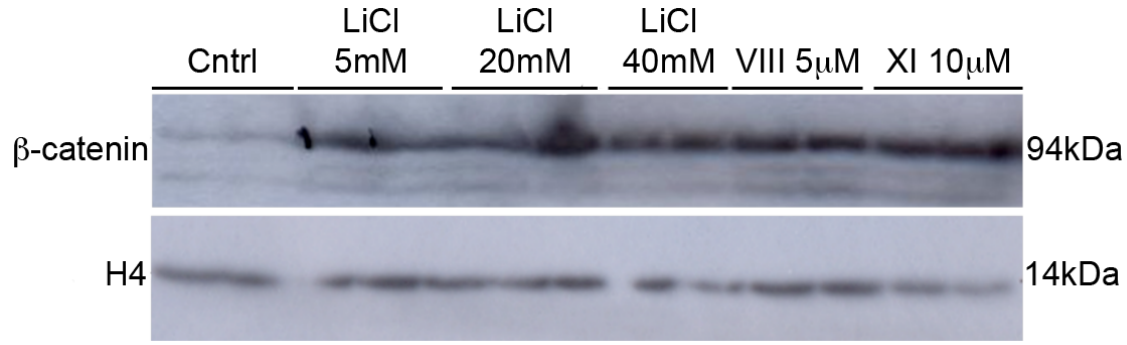


Figure 4.2: GSK3 inhibition with various inhibitors leads to stabilisation of β-catenin.

Figure depicts a Western blot showing the increased level of β-catenin from nuclear fractions of N2aSw when treated with numerous GSK3 inhibitors. H4 was used as marker of the nucleus and to show equal loading when running the gel.

From this preliminary data it was established that inhibitors VIII and XI should be used at concentrations of 5μM and 10μM respectively.

Both of these structurally diverse inhibitors significantly reduced the amount of Aβ produced and secreted into the medium (see figure 4.3A) by 52.89% ±9.21 and 34.76% ±10.27 respectively (mean value ±SEM. ***P<0.001 and **P<0.01 respectively based on n=12 per group). In contrast to other studies, with this cell model, there was no reduction in amyloidogenic processing using the same concentrations of LiCl taken from previous reports. If anything, a non-significant increase in Aβ production was observed with the highest concentration of 40mM (see figure 4.3B).

To dispel any criticism of specificity, a siRNA silencing approach was also employed in this study. The GSK3α/β siRNA was transfected into the cultured cells using the Lipofectamine™ 2000 reagent protocol at a final concentration of 10nM, which was found to reduce the levels of both GSK3 subtypes and significantly increase the steady-state level of β-catenin (see figure 4.3C). Confirming the results obtained with specific pharmacological inhibition, silencing the GSK3 enzyme resulted in a significant decrease in the generation and secretion of Aβ (see figure 4.3D) by 34.75% ±13.13 (mean value ±SEM. ***P<0.001 based on n=9 per group).

In addition to measuring Aβ secreted in the medium, intracellular Aβ levels in cell-lysates were also determined. From figure 4.3E, consistent with figure 4.3A, there was a clear and significant reduction of 57.00% ±5.00 (mean value ±SEM. **P<0.01 based on n=8) in the amount of intracellular Aβ produced in N2aSw cells after specific GSK3 inhibition. Therefore, the reduced Aβ level detected in the cell media is not based on simply reduced secretion but on Aβ production.

In contrast, when the activity of GSK3 was over-stimulated by transiently transfecting a constitutively active form of GSK3β (see figure 4.3F), namely GSK3βS9 (due to mutation at the serine 9 residue to alanine, which cannot be phosphorylated), there was a significant increase of 29.54% ±7.72 (mean ±value SEM. **P<0.01 based on n=9 per group) in the generation of Aβ (see figure 4.3G). Therefore, overexpression of active GSK3β S9, resulted in an increased production of Aβ. Interestingly, increased GSK3 activity is associated with aging and even more so with AD patients, who are clearly afflicted by aberrant amyloidogenic processing of APP (see 2.8.3 GSK3 hypothesis of AD).

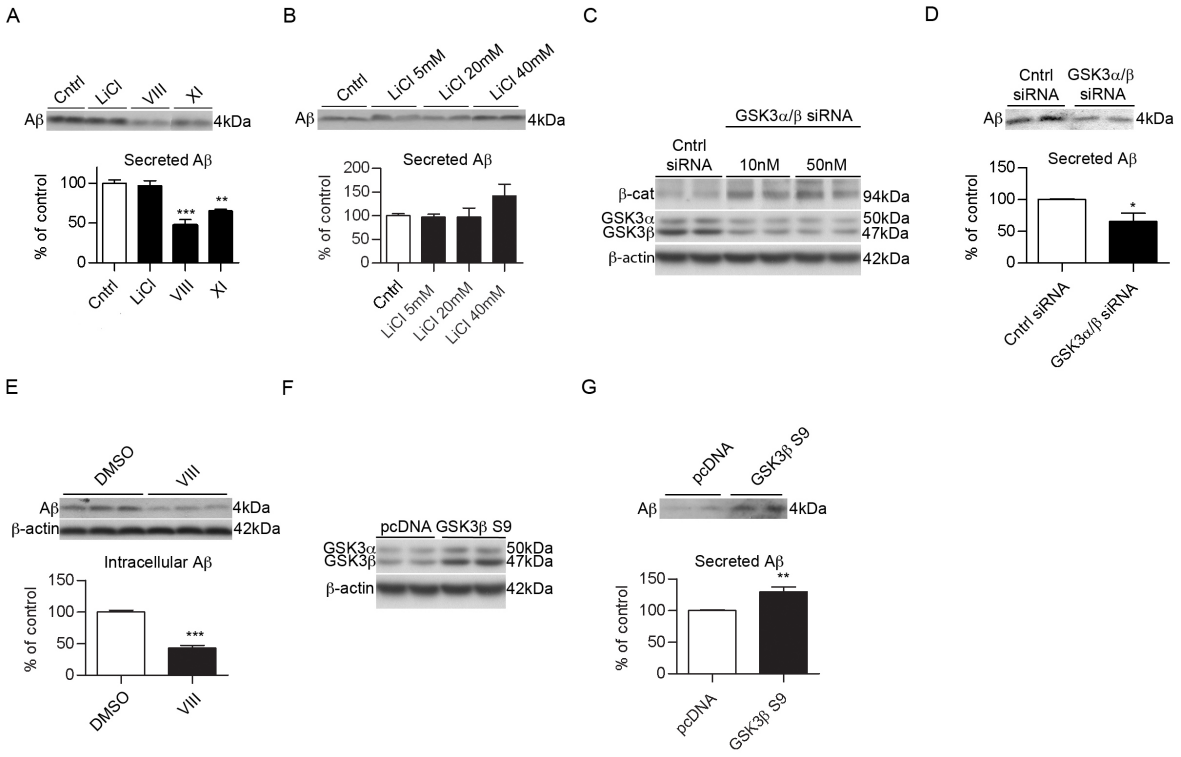


Figure 4.3: Changes in the activity of GSK3 led to alteration in the amyloidogenic processing of APP.

Representative blots and quantification. Secreted Aβ (4kDa) was measured in the conditioned medium and total-lysates by Western blotting with an anti-human Aβ antibody, 6E10 and shown in the above representative blots. (A and B) There was a significant decrease by 52.89% ±9.21 and 34.75% ±10.27 in the amount of secreted Aβ when GSK3 activity was inhibited specifically with VIII (5μM) and XI (10μM), respectively but not with any concentration of LiCl (n=12 per group). (C) Preliminary experiments show that 10nM GSK3α/β siRNA is capable of markedly reducing GSK3 and increasing β-catenin levels. (D) When inhibiting the activity of GSK3 by silencing its expression, there was a 34.75% ±13.13 decrease in the production of Aβ (n=9 per group). (E) The level of Aβ detected from the total-lysate was also significantly reduced by 57% and ±5 with VIII treatment (n=8 per group). (F) Transient transfection of GSK3β S9 leads to an increase in GSK3 expression. (G) Transiently transfected N2aSw cells with constitutively active GSK3βS9 had increased levels of Aβ by 29.54% ±7.72. Values shown in graphs represent the mean value ±SEM and are expressed as a percentage of control. Statistical analysis included one-way ANOVA with a post-hoc Dunnett's test (A-B) and an unpaired t-test (C-E), *P<0.05, **P<0.01 and ***P<0.001.

4.2.2 Altered GSK3 activity does not result in changes in the activities of the α-secretase and the γ-secretase

A reduction of amyloidogenic processing could result from a concomitant increase in non-amyloidogenic processing, as the α-cleavage precludes any amyloidogenic cleavage events. However, it was observed that there was a significant decrease in the amount of secreted sAPPα by specific GSK3 inhibition (41.21% ±4.91 reduction, ***P<0.001 based on n=9 per group). In contrast, incubation with LiCl did not reveal any change in the levels of sAPPα detected in the medium (see figure 4.4A). In addition to specific chemical inhibition of GSK3, there was also a reduction in sAPPα when cells were transiently transfected with the GSK3α/β siRNA. However, while specific GSK3 inhibition led to reduced production and secretion of sAPPα in N2aSw cells, overexpression of the constitutively active form of GSK3 did not seem to affect the production and secretion of sAPPα (see figure 4.4C, based on n=9 per group).

In addition to measuring the steady-state levels of sAPPα, the α-secretase activity was assayed with a commercial R&D kit. This kit is based on the cleavage of a fluorescent synthetic peptide containing the α-secretase cleavage sequence. In contrast to the steady-state levels of sAPPα, no change was detected in α-secretase activity by specific GSK3 inhibition (based on n=9 per group) (see figure 4.4D). Furthermore, transient transfection with GSK3βS9 did not influence α-secretase activity (see figure 4.4E).

To determine whether the reduced production of Aβ by specific GSK3 inhibition was the result of altered γ-secretase cleavage, the final event of Aβ production, an *in vitro* γ-secretase assay was used (Sastre et al., 2001a). The generation of the 6kDa AICD fragment was unaltered by specific GSK3 inhibition (based on n=9 per group) (see figure 4.4F). To confirm the specificity of the γ-secretase assay, DAPT, a specific γ-secretase inhibitor was used at 250nM, which dramatically reduced the production of AICD. Furthermore, samples incubated on ice instead of 37°C showed no production of the AICD fragment.

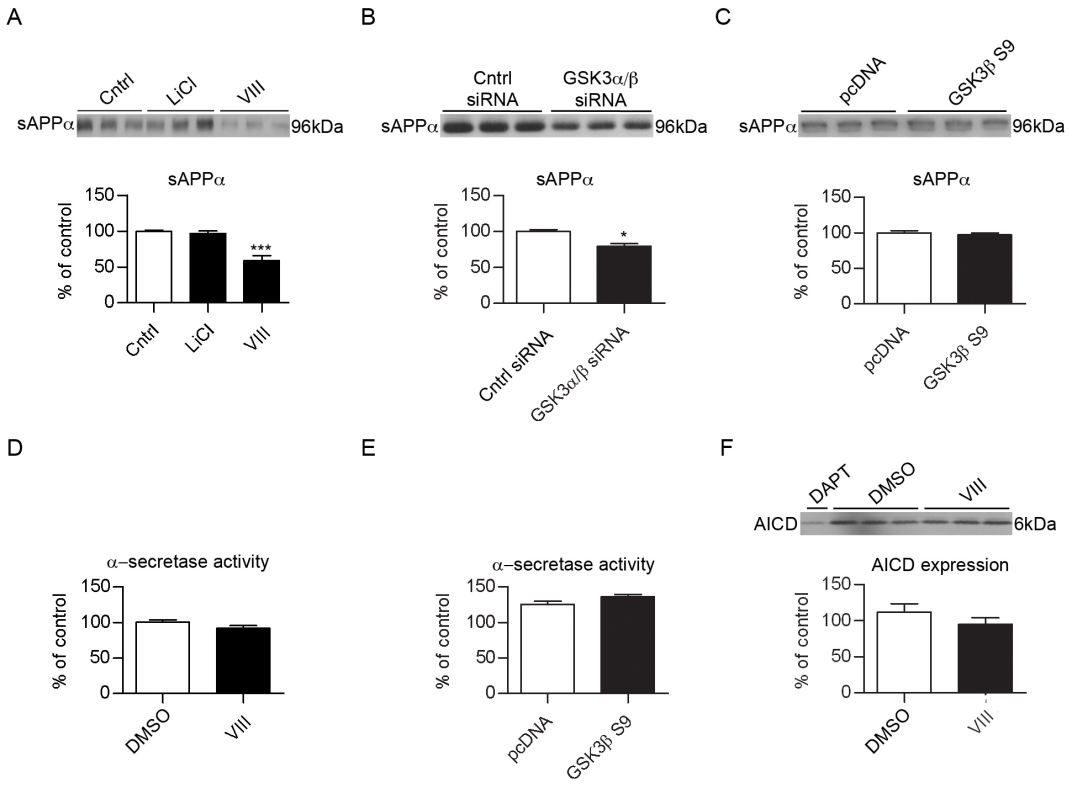


Figure 4.4: Changes in GSK3 activity do not affect the α-secretase or the γ-secretase activity.

Representative blots with quantification. Alterations in the non-amyloidogenic processing of APP while perturbing GSK3 activity was assessed by measuring the production of sAPPα and α-secretase activity and shown in the representative blots above (A-D). (A) N2aSw conditioned medium was assessed for the amount of sAPPα (96kDa) produced by probing with the antibody 6E10. Cells treated with 5μM VIII overnight resulted in a 41.21% ±4.91 reduction of secreted sAPPα (n=9 per group). (B) Similarly there was a significant decrease of sAPPα by GSK3 siRNA knockdown (n=9 per group). (C) In contrast, transient transfection of the constitutively active GSK3βS9 resulted in a non-significant change in the secretion of the sAPPα fragment (n=9 per group). Neither GSK3 inhibition (D), nor GSK3βS9 transfection (E) resulted in alterations in the activity of the α-secretase activity using a commercial activity kit (n=9 per group). (F) Finally the production of the AICD fragment from membrane preparations of N2aSw using an *in vitro* assay was used, as an indicator of γ-secretase activity. No changes were detected using 5μM VIII treatment for 2hrs (n=9 per group). Values shown in graphs represent the mean value ±SEM and expressed as a percentage of control. Statistical analysis included one-way ANOVA with a post-hoc Dunnett's test (A) and the unpaired t-test (B-F), *P<0.05 and ***P<0.001.

4.2.3 GSK3 regulation of the β-secretase

Having excluded the γ-secretase and α-secretase as the targets modulated by GSK3, the next step was to evaluate the effect of GSK3 inhibition on the β-secretase (BACE1) activity, i.e. the enzyme responsible for the cleavage of APP at the N-terminal of the Aβ-domain. Seeing as this cleavage event is the rate-determining step in Aβ production, small alterations can have a dramatic effect on Aβ production, as illustrated with *Bace1* null mice that are devoid of plaques.

4.2.3.1 Specific GSK3 inhibition results in a decrease in β-secretase activity, transcription and expression of BACE1

To this end, the activity of the β-secretase was measured in N2aSw cells incubated in the presence or absence of the specific GSK3 inhibitor. Firstly, the activity was determined by analysing the levels of the β-C-terminal fragment (β-CTF), which is generated from the cleavage of APP by the β-secretase. Membrane preparations from cell-lysates were probed with the antibody 6E10 by Western blotting. This antibody does not react with the α-CTF that is produced by the α-secretase. The level of the β-CTF was decreased in cells incubated with the specific GSK3 inhibitor, VIII by 27.69% ±10.68 (mean value ±SEM. *P<0.05 based on n=9) but not by LiCl. To confirm this, a fluorescence enzymatic assay was used, using a synthetic peptide containing the specific β–cleavage site and which has previously been shown to be highly specific (Heneka et al., 2005). This assay showed a reduction in the specific activity of the β-secretase by 10.46% ±3.00 with incubation of VIII (see figure 4.5A and B) (mean value ±SEM. ***P<0.001 based on n=12). While secondary modifications, maturation and trafficking events of BACE1 can explain an alteration in its activity, these were all shown to be unaffected by GSK3 inhibition (data not shown).

To define whether changes in β-secretase activity were due to alterations in BACE1 expression, BACE1 protein was measured by Western blotting. Originally published in Katsouri, Parr et al., 2011, figure 4.6 demonstrates the specificity of the rabbit polyclonal anti-BACE1 antibody (Millipore). This antibody was assessed for its specificity of this BACE1 antibody from Millipore. It is clear from cell membrane preparations or tissue homogenates, that a specific band migrating to 64kDa is either reduced or absent when mouse *Bace1* is knocked-down of knocked-out respectively. The *Bace1* double knockout mice (B6.129-Bace1tm1Pcw/J) were purchased from Charles River and compared to aged-matched C57B16 littermates. For mouse *Bace1*

knockdown experiments, N2aSw cells were either transiently transfected with 300pmol BACE1 siRNA (Dharmacon-003747-01-50) or a non-specific siRNA (Dharmacon-004503-01-50). The lower panel of figure 4.6B shows the specificity and the effectiveness of the RNA silencing as there was a decrease in production of sAPPβ (specific β-secretase cleavage) detected from the conditioned medium using the antibody 192swe (Elan). By comparison, when ADAM-10 (α-secretase) was knockdown there was no such decrease. This data was collated with the collaboration with Dr Michael Willem from the University of Munich.

BACE1 protein was reduced using increasing concentrations of the GSK3 inhibitor VIII (see figure 4.5C). There was also a similar reduction in the level of BACE1 protein when N2aSw cells were transiently transfected with GSK3α/β siRNA (see figure 4.5D). While under several conditions the half-life of the BACE1 protein can be destabilised by being targeted to the proteasome, as shown in several studies (Gong et al., 2010), no such phenomenon was observed with specific GSK3 inhibition. Moreover, this decrease was due to changes in its transcription, because quantitative RT-PCR experiments showed a reduction in mouse *Bace1* mRNA levels by specific GSK3 inhibition (see figure 4.5E) in a dose-dependent manner, showing a significant reduction of 36% ±10 and 76% ±18% in *Bace1* mRNA levels. Additionally, we determined whether BACE1 promoter activity was modulated by GSK3 using a luciferase Firefly reporter gene driven by the rat BACE1 promoter transfected in N2aSw cells. This data shows specific GSK3 inhibition induces a significant decrease in the promoter activity of BACE1 (see figure 4.5F) in a dose-dependent manner by 36.05% ±15.04 and 60.16% ±31.84 at concentrations of 5μM and 10μM of the inhibitor VIII respectively (mean value ±SEM. **P<0.01 based on n=9 per group). This data was confirmed by reducing GSK3 levels using siRNA approach, validating the specificity of GSK3 inhibitors on BACE1.

4.2.3.2 Transient overexpression of GSK3 led to an increase in BACE1 expression

In addition to specific GSK3 inhibition, transient transfection of GSK3βS9 resulted in an increase of BACE1 protein expression by 61.37% ±27.82 (mean value ±SEM. *P<0.05 based on n=9 per group) (see figure 4.5G). Again this would indicate that the transcription and expression of BACE1 is under the regulation of GSK3. However, there were no significant changes in the *Bace1* mRNA level or the activity of its promoter in cells overexpressing GSK3β S9 (see figure 4.5H and I).

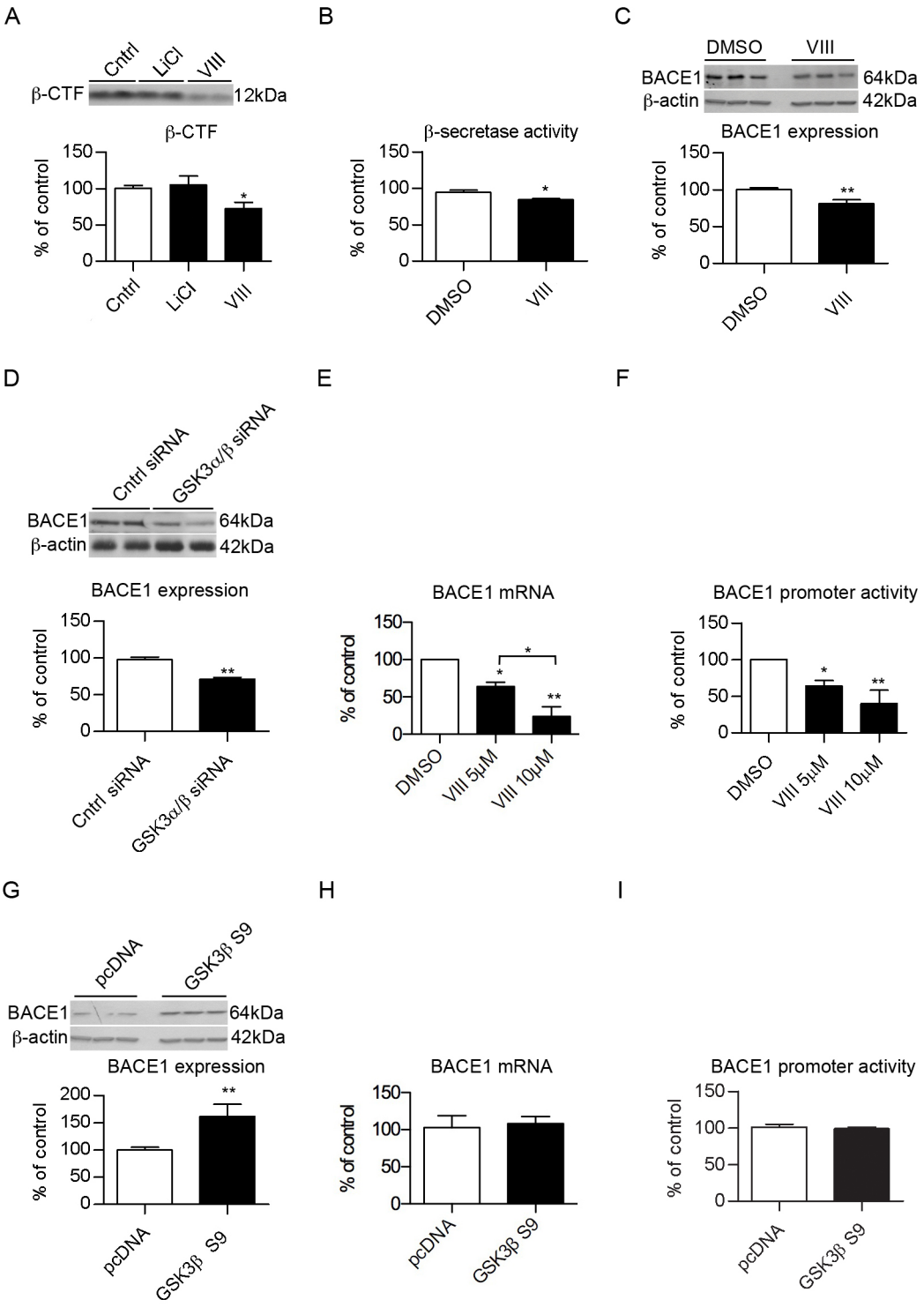

A
Cntrl
LiCl
VIII
β-CTF
12kDa
β-CTF
% of control
150
100
50
0
Cntrl
LiCl
VIII
B
β-secretase activity
% of control
DMSO
VIII
C
DMSO
VIII
BACE1
64kDa
β-actin
42kDa
BACE1 expression
% of control
DMSO
VIII
D
Cntrl siRNA
GSK3α/β siRNA
BACE1
64kDa
β-actin
42kDa
BACE1 expression
% of control
Cntrl siRNA
GSK3α/β siRNA
E
BACE1 mRNA
% of control
DMSO
VIII 5μM
VIII 10μM
F
BACE1 promoter activity
% of control
DMSO
VIII 5μM
VIII 10μM
G
pcDNA
GSK3β S9
BACE1
64kDa
β-actin
42kDa
BACE1 expression
% of control
200
150
100
50
0
pcDNA
GSK3β S9
H
BACE1 mRNA
% of control
pcDNA
GSK3β S9
I
BACE1 promoter activity
% of control
pcDNA
GSK3β S9

Figure 4.5: Changes in the GSK3 activity led to reduced β-secretase activity and BACE1 expression.

The activity of the β-secretase and the expression of its coding gene, BACE1, were assessed in N2aSw cells when GSK3 was inhibited with VIII overnight or by GSK3 siRNA transfection (A-F) and with transient transfection of the constitutively active GSK3βS9 form (G-I). (A) The activity of the β-secretase was assessed by the generation of the β-CTF in membrane fractions of N2aSw cells treated with 20mM LiCl or 5μM VIII overnight as shown in the representative blot. Specific GSK3 inhibition with VIII led to a 27.69% ±10.68 reduction in the production of the β-CTF (n=9 per group). (B) A 10.46% ±3.00 reduction in the activity of the β-secretase activity was detected in membrane fraction of N2aSw cells treated with 5μM VIII (n=12 per group). (C) BACE1 expression was reduced by specific GSK3 inhibition using 5μM VIII treatment overnight or GSK3α/β siRNA as shown in the respective representative blots (D) (n=9 per group). (E) RT-qPCR revealed that there was a significant decrease of 36% ±10 of *Bace1* mRNA with 5μM VIII treatment (n=9 per group). (F) In line with this, there was a significant reduction in the BACE1 promoter activity by 36.05% ±15.04 with VIII treatment (n=9 per group). (G) While GSK3βS9 transfection led to a significant increase of 61.37% ±27.82 in BACE1 protein expression as shown in the representative blot, there was no significant alteration in either the mRNA (H) or the promoter activity of BACE1 (I) (n=9 per group). Values shown in graphs represent the mean value ±SEM and expressed as a percentage of control or fold change (E and H). Statistical analysis included one-way ANOVA with a post-hoc Dunnett's test (A) a post-hoc Tukey's test (E and F) and an unpaired t-test (B-D, G-I), *$P<0.05$ and **$P<0.01$.

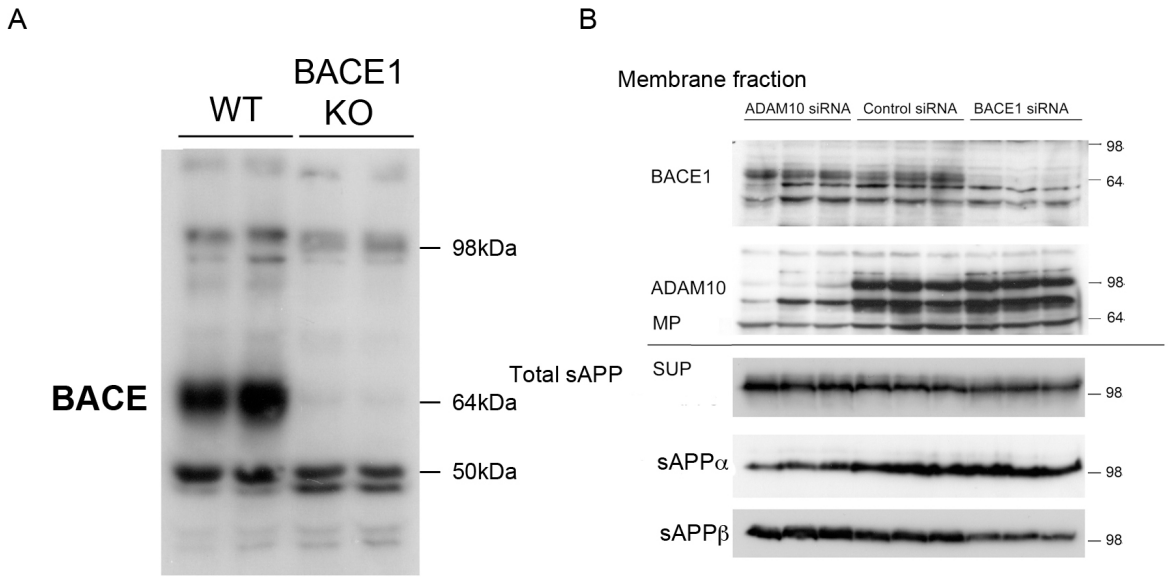


Figure 4.6: Specificity of the Millipore rabbit polyclonal anti-BACE1 antibody.

(A) Representative western for BACE1 from WT (lanes 1-2) and *Bace1*$^{-/-}$ mice (3-4). A specific band at 64kDa represents the mouse BACE1. (B) *UPPER PANEL:* Representative Western of membrane preparations of N2aSw cells that were transiently transfected with control, ADAM-10 or BACE1 siRNA (Dharmacon). Similarly there is a reduction in a band migrating to 64kDa when BACE1 was silenced. *LOWER PANEL:* Conditioned medium from the same cells was measured for total- (22C11), alpha- (2D8) and beta- (192swe) soluble APP. Mouse *Bace1* silencing effectively reduced sAPPβ production when comparing to control or ADAM-10 siRNA treated cells. This data was collated with great help from Dr Michael Willem (University of Munich) and published in Katsouri and Parr et al., 2011.

4.2.4 GSK3 regulation of full-length APP

As there appears to be both a reduction in the production of Aβ and also sAPPα, without changes in α-secretase activity, it might be the case that there is an overall reduction in the steady-state levels of FL-APP. In order to determine whether the decrease in Aβ also involves changes on its precursor protein APP, the expression of FL-APP was measured in total-lysates from N2aSw cells.

4.2.4.1 Steady-state levels of FL-APP are reduced when GSK3 is inhibited specifically

Western blotting experiments using an antibody against the C-terminus of APP (antibody 140) demonstrated a reduction of 53.09% ±9.5 in the expression of FL-APP in total-lysates from N2aSw cells incubated with the GSK3 inhibitor VIII (mean value ±SEM. ***P<0.001 based on n=9 per group) (see figure 4.7A). Because different antibodies against APP might detect multiple mature and immature forms of the FL-

APP protein, another monoclonal antibody raised against the amyloid domain of human APP.695 (6E10) was used, confirming this result. A reduction of 48.40% ±14.22 in the level of FL-APP protein was also observed after transient transfection of GSK3α/β siRNA in N2aSw cells (see figure 4.7B) (mean value ±SEM. *P<0.05 based on n=8 per group).

Additionally, it was determined whether the effect of specific GSK3 inhibition on APP was dependent on the APP isoform being expressed. Both human wild-type APP.695aa and APP.751aa isoforms overexpressed in HEK 293T cells were also reduced by specific GSK3 inhibition, as well as the endogenous APP (pcDNA control transfection) in the same cell-line (see figure 4.7C). In figure 4.7C, the human wild-type APP.751 shows a similar migration pattern to that of the endogenous APP in the HEK 293T cell (compare lanes 1-4 with 9-12). This is in keeping with previous findings in the literature. Both human wild-type APP.695 overexpressed in HEK 293T and the familial mutant APPsw expressed in the N2aSw cell-line showed a similar migration pattern (compare lanes 5-8 with 13). In each case, the level but not the migration of APP was affected by specific GSK3 inhibition (compare lanes 1-2 with 3-4, 5-6 with 7-8 and 9-10 with 11-12). This latter observation indicates that the specific GSK3 inhibition does not affect the maturation of APP, regardless of the isoform or mutation of APP being overexpressed, because both mature and immature bands were reduced.

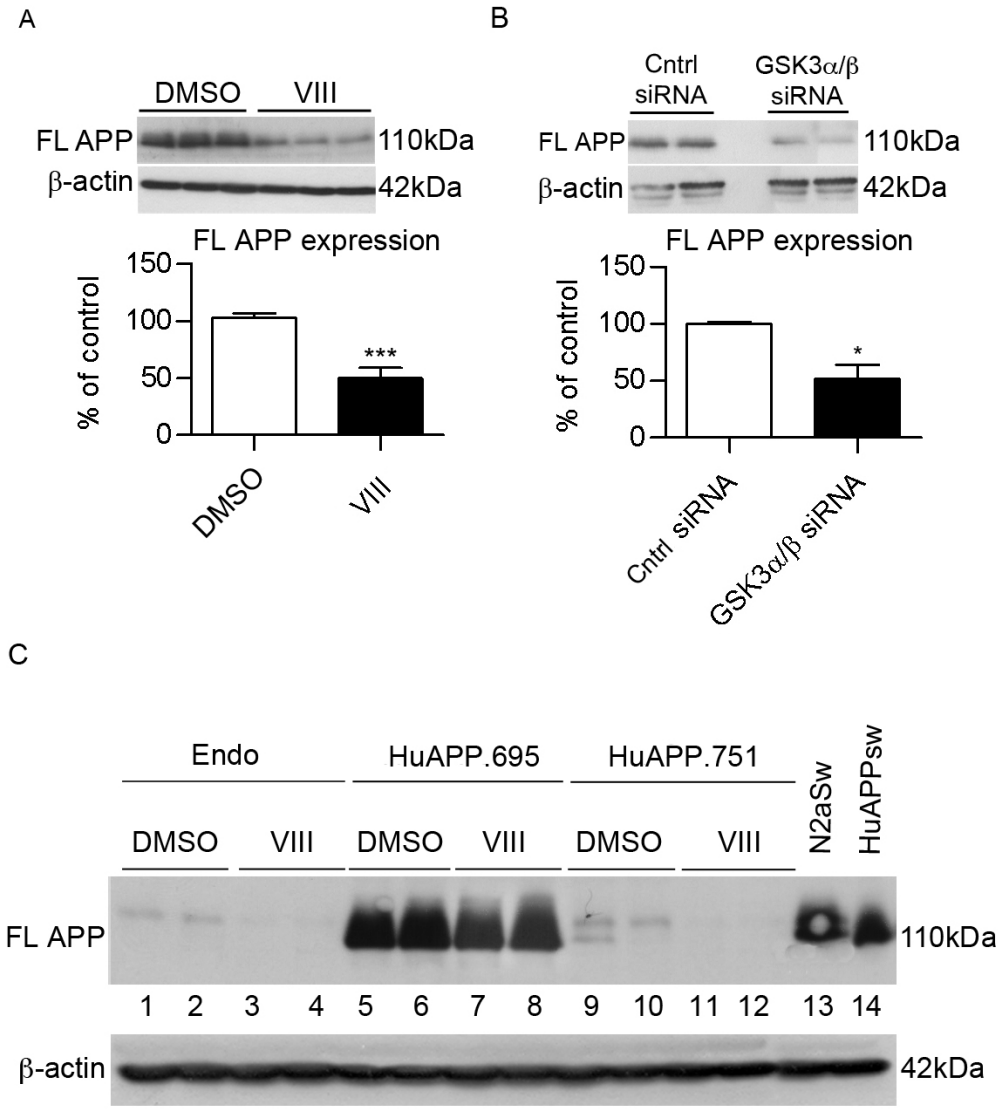


Figure 4.7: Steady-state protein level of FL-APP is reduced in N2aSw cells by specific GSK3 inhibition.

Shown above are representative blots along with quantification. (A) Specific GSK3 inhibition with 5μM VIII overnight in N2aSw cells results in a significant reduction of the FL-APP protein (110kDa) level by 53.09% ±9.50 (n=9 per group). (B) A similar reduction of 48.40% ±14.22 in the FL-APP protein level was observed when the GSK3 activity was inhibited by silencing the expression of GSK3 with siRNA in N2aSw cells (n=8 per group). (C) HEK 293T cells were transiently transfected with either pcDNA3, human wild-type APP.695 or human wild-type APP.751 and treated with either DMSO or 5μM VIII overnight. The total-lysates were probed with the antibody 140 and compared to total-lysate from N2aSw cells overexpressing human APPsw and the HEK 293T overexpressing human APPsw. In each case, treatment with VIII resulted in a reduced level of FL-APP protein of the same molecular weight, expressed from the varying isoform constructs. Values shown in graphs represent the mean value ±SEM and expressed as a percentage of control. Statistical analysis included the unpaired t-test, *P<0.05 and ***P<0.001.

4.2.4.2 Specific GSK3 inhibition does not result in reduced APP transcription

The next step was to ascertain whether the reduced protein expression of FL-APP by specific GSK3 inhibition was the result of changes in transcriptional regulation, as was the case for BACE1. To this end, actinomycin-D (an inhibitor of transcription) was used to determine whether changes in the FL-APP protein level were dependent on alterations in the transcriptional activity of the APP gene. Actinomycin-D treatment overnight in N2aSw cells resulted in a reduction in FL-APP protein of 38.00% ±3.22 independent of specific GSK3 inhibition (mean value ±SEM. **P<0.01) (see figure 4.8A). When actinomycin-D was used in combination with specific GSK3 inhibition, there was a further reduction of 26% ±4.76 on the FL-APP protein level (mean value ±SEM. **P<0.01), compared to cells only treated with actinomycin-D alone.

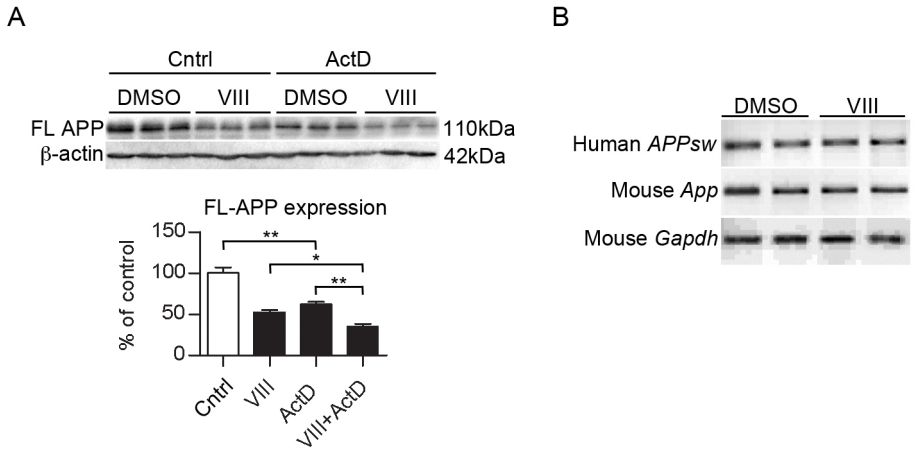


Figure 4.8: Specific GSK3 inhibition does not affect transcription of APP.

N2aSw cells were treated with either DMSO or 5μM VIII overnight and in combination or without 1μg/ml actinomycin-D. Representative blot and quantification of FL-APP shows a reduction of 38% ±3.22 with actinomycin-D blockade of transcription. In combination with specific GSK3 inhibition, there was a further reduction of 26% ±4.76 in FL-APP protein (n=9 per group). (B) Representative gel from a semi-quantitative RT-PCR carried out on mRNA harvested from N2aSw treated with DMSO or 5μM VIII overnight, showing no changes in the level of endogenous mouse *App* and human *APPsw* expression. Values shown in graphs represent the mean value ±SEM and expressed as a percentage of control. Statistical analysis included one-way ANOVA with a post-hoc Tukey's test, *P<0.05 and **P<0.01.

In addition, semi-quantitative PCR analysis was performed, demonstrating no changes in APP mRNA levels for both the endogenous mouse and exogenous human *APP* mRNA by specific GSK3 inhibition (see figure 4.8B). This data suggests therefore that the effects of specific GSK3 inhibition on FL-APP is not based on transcriptional regulation but this would require further RT-qPCR analysis to verify.

4.2.4.3 Specific Inhibition of GSK3 results in increased degradation of FL-APP

One possible explanation for the reduced steady-state levels of FL-APP could be a decrease in its half-life owing to increased degradation. FL-APP following its trafficking through the classical secretory pathway is processed and transported to the plasma membrane, but ultimately APP ends up being degraded in lysosomal compartments in the ESCRT pathway, by internalisation into endosomes (Estus et al., 1992, Golde et al., 1992). It has been estimated that the protein half-life of FL-APP is approximately 8hrs (Morales-Corraliza et al., 2009).

To examine whether GSK3 regulates the stability of FL-APP, the expression of FL-APP was determined by co-incubating the cells with the specific GSK3 inhibitor plus 50μg/ml cycloheximide for up to 16hrs, which blocks *de novo* synthesis. This gives the ability to investigate the stability of pre-existing molecules of APP. Western blot analysis for FL-APP revealed that specific GSK3 inhibition influenced the FL-APP degradation rate (see figure 4.9A). After 16hrs there was a 22% ±1.71% decrease in the total amount of APP protein when GSK3 was inhibited compared to the control, where DMSO was added at the same time-point (mean value ±SEM. **P<0.01 based on n=9 per group). Thus, it would appear from this that there is a destabilisation in FL-APP by specific GSK3 inhibition. To confirm these results, pulse-chase analysis was carried out. N2aSw cells transfected with a control siRNA or GSK3α/β siRNA molecule, were labelled with [35S] methionine/cysteine for 20mins and chased for periods up to 8hrs. Results of the SDS-PAGE temporal profile of FL-APP expression are shown in figure R4.9Bi. Immunoprecipitation of APP species from the total-lysates revealed that GSK3 knockdown significantly decreased the stability of FL-APP. This difference was statistically significant at 2hrs and 4hrs (*P<0.05 based on n=4 for all groups). This result was also replicated by incubating N2aSw cells during the pulse-chase analysis with 5μM of the GSK3

inhibitor VIII (see figure 4.9D). There were statistically significant differences in the FL-APP degradation rate between the two treatments from 1hr up to 4hrs.

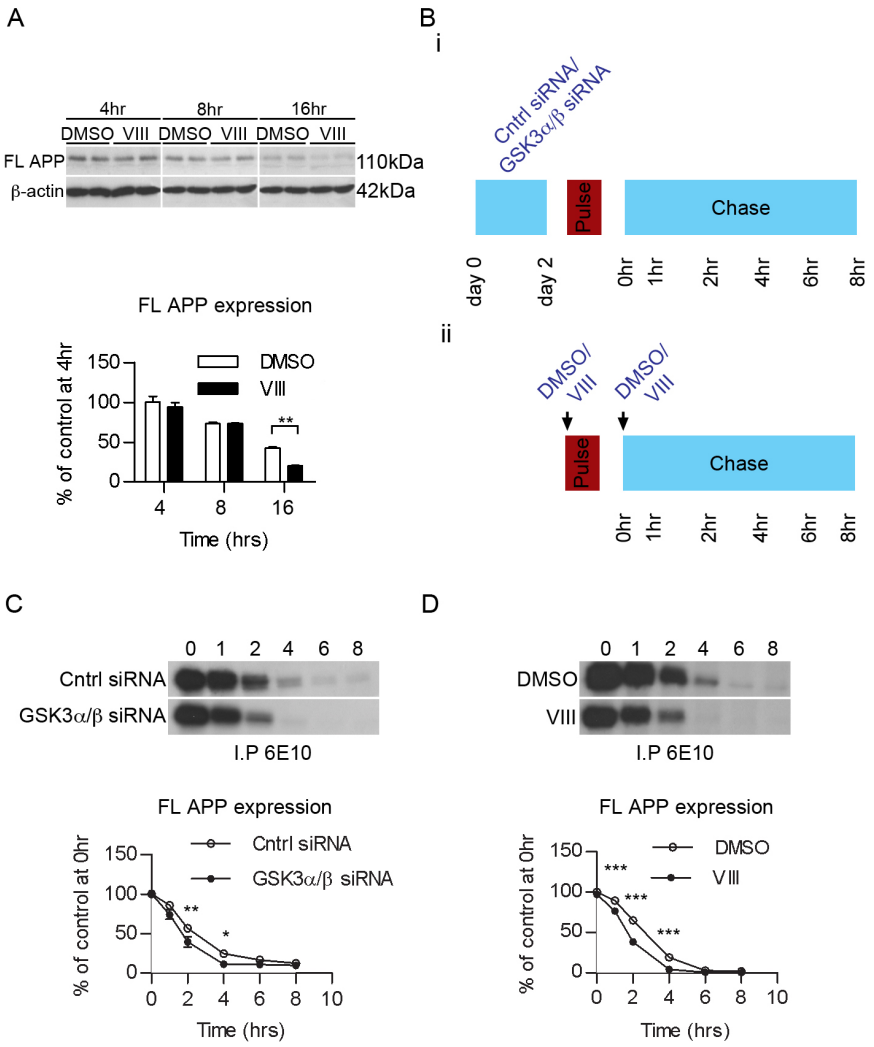


Figure 4.9: Specific inhibition of GSK3 results in increased degradation of FL-APP.

(A) *De novo* protein synthesis was blocked in N2aSw with 50µg/ml cycloheximide with or without 5µM VIII and the total-lysates were harvested at 4, 8, 16hrs as shown in the representative blot. After 16hrs there was a 22% ±1.71% decrease in the protein level of FL-APP when GSK3 was specifically inhibited. (B) Illustrated above is the experimental design of the pulse-chase analysis when GSK3 activity was reduced by siRNA silencing (i) or with 5µM VIII treatment (ii). (C) Representative blot showing that GSK3 silencing for up to 48hrs results in an increased degradation rate of FL-APP showing a significant difference relative to the control of 17% after 2hrs (n=4 per group). Significant differences were also seen at 4hrs but then the signals level out at 6hrs to 8hrs. (D) From the representative blot, a similar observation of increased degradation rate of FL-APP by specific GSK3 inhibition was detected in N2aSw cells by pulse-chase analysis. A significant difference in the rate of degradation was seen from 1hr up to 4hrs (n=4 per group). Values shown in graphs represent the mean value ±SEM and expressed as a percentage of control. Statistical analysis used includes an unpaired t-test for each time point (A, C and D), *P<0.05, **P<0.01 and ***P<0.001.

4.2.5 Destabilisation and degradation events of FL-APP

The decreased half-life of FL-APP could be the result of cellular degradation pathways that are maybe induced with specific GSK3 inhibition. Therefore, the possibility that GSK3 activity stimulates an alternative, proteasome-dependent, processing pathway of APP, consequently decreasing the production of Aβ was investigated.

4.2.5.1 Inhibition of the 26S proteasome partially attenuates the effect of specific GSK3 inhibition on FL-APP stability

N2aSw cells were incubated with the GSK3 inhibitor VIII in the presence or absence of the proteasome inhibitors MG132 at 50μM or PS1 at 10μM. The blockade of the proteasome overnight resulted in a significant increase in the protein level of FL-APP by 93% ±8.56 (see figure 4.10A) (mean value ±SEM. ***P<0.001). This increase was of 79.33% ±10.67 when cells were incubated with MG132 together with inhibitor VIII (mean value ±SEM. ***P<0.001). Because MG132 did not completely abolish the effect of specific GSK3 inhibition, we concluded that proteasomal degradation was not responsible for the effects of GSK3 on FL-APP degradation. These observations were replicated with another 26S proteasome inhibitor, PS1 (Peptide Institute) (see figure 4.10B).

Because proteasome-dependent degradation pathways involve multiple steps, including ubiquitination of proteins targeted for proteolysis, the effect of specific GSK3 inhibition on the formation of ubiquitinated-APP was investigated. N2aSw cell extracts were immunoprecipitated with a polyclonal anti-human APP antibody. Immunoprecipitated proteins were analysed by immunoblotting with an anti-ubiquitin antibody. Figure 4.10C shows that specific GSK3 inhibition did not result in an increased ubiquitination of FL-APP. This is shown by the absence of accumulation in higher molecular weight species on SDS-PAGE, when probing with an anti-ubiquitin antibody. As a positive control, to check the reliability of the assay, N2aSw cells were transiently transfected with PPARγ, which has been shown to increase the degradation of FL-APP via proteasomal targeting (d'Abramo et al., 2005). A negative control was used, containing total-lysate incubated with just protein-A sepharose beads and isotype antibody control (Neg).

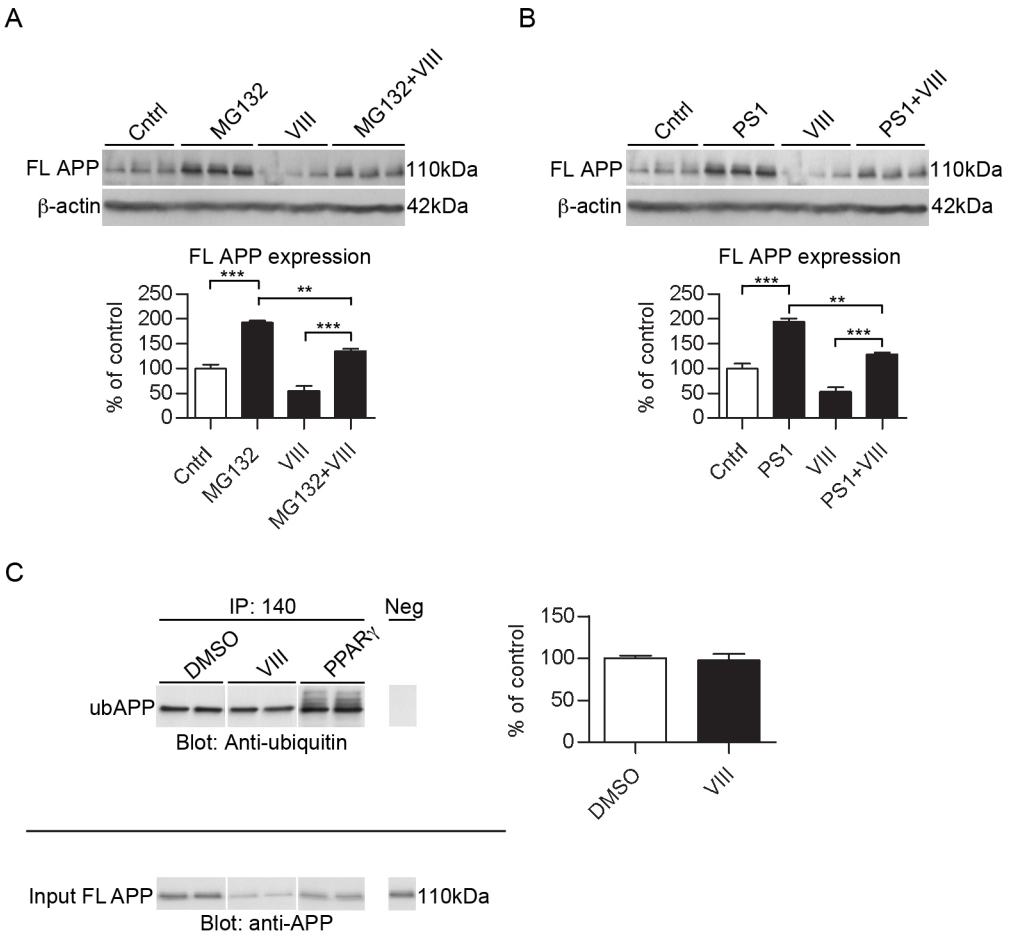


Figure 4.10: The reduction of FL-APP with specific GSK3 inhibition was partially rescued by proteasome blockade.

Representative blots with quantification. (A) N2aSw cells were treated with or without GSK3 inhibitor 5μM VIII and proteasomal inhibitor MG132 50μM overnight. There was an increase of 79.33% ±10.67 in the protein level of FL-APP when comparing cells treated with VIII alone to those co-incubated with MG132. However there was a significant difference between MG132 at 192.3% ±3.33 of control and VIII in combination with MG132 at 134.7% ±4.81 (n=9 per group). (B) This result was verified by cells treated with the proteasome inhibitor PS1 10μM (n=9 per group). (C) Cells treated with DMSO or VIII were lysed in RIPA buffer and FL-APP species were immunoprecipitated with the anti-human APP CTD antibody, 140. *UPPER PANEL:* Subsequent SDS-PAGE separation and probing with an anti-ubiquitin antibody (Santa Cruz) showed no difference in the ubiquitination of FL-APP by specific GSK3 inhibition. *LOWER PANEL:* Total-lysates were run to show the input for the I.P. Values shown in graphs represent the mean value ±SEM and expressed as a percentage of control. Statistical analysis included one-way ANOVA with a post-hoc Tukey's test (A and B) or an unpaired t-test (C), **P<0.01 and ***P<0.001.

4.2.5.2 Inhibition of autophagy induction reverses the effects of specific GSK3 inhibition on FL-APP

The next step was to explore the hypothesis that specific GSK3 inhibition could favour APP degradation via the autophagy-lysosomal pathway. Autophagy is another ubiquitous pathway used by the cell to lyse and recycle cellular constituents. This is often upregulated in response to cellular stress and starvation resulting in breakdown of cellular constituents to recycle for further anabolic functions within the cell. Macroautophagy results in the enveloping of cytoplasmic material which later fuses to lysosomes for its degradation. Previous studies have shown controversial data regarding APP degradation in autophagy (Jaeger et al., 2010, Boland et al., 2010).

To show that APP can be targeted and degraded in the autophagy pathway physiologically, cells were incubated in the presence of the autophagy inhibitor 3-MA (500μM), which increased the levels of FL-APP by 123.9% ±31.81 (mean value ±SEM. **P<0.01) (see figure 4.11A). 3-MA partially reversed the effect of the GSK3 inhibitor on the protein level of FL-APP. There was no-significant difference between 3-MA treatment at 223.9% ±24.64 of control and 3-MA in combination with VIII at 163.8% ±15.22 of control (mean values ±SEM. Based on n=9 per group).

To study the consequences of disrupting autophagy induction, N2aSw cell cultures were treated with beclin-1 siRNA. There was a complete rescue of FL-APP protein levels when autophagy was blocked by knocking down the expression of beclin-1, a protein that is vital for the induction of autophagy (see figure 4.11B). It is also of interest that VIII treatment did not alter beclin-1 protein levels. These results suggest that indeed FL-APP degradation is mediated through autophagy.

Under specific GSK3 inhibition both the altered stability of FL-APP and the reduced transcriptional expression of BACE1 could account for the reduced production in Aβ. To see if blockade of autophagy induction could also rescue the level of Aβ under specific GSK3 inhibition, beclin-1 was knocked down with siRNA (see figure 4.11C). There are some papers that show Aβ can be degraded by autophagy. When induction of autophagosome formation is blocked with beclin-1 knocked down there is an increase in the amount of secreted Aβ by 80.7% ±10.59 (***P<0.001 based on n=12 per group). This shows that autophagy in the basal state can degrade Aβ. Even when autophagy induction was blocked and there was specific GSK3 inhibition, the production level of Aβ was still dramatically reduced. The level of Aβ when cells were treated with specific GSK3 inhibition alone, is

statistically no different from the level in combination with beclin-1 knocked down. Therefore the reduction in Aβ is mainly from decreased activity in the β-secretase activity as opposed to reduced FL-APP being fed into the amyloidogenic pathway.

4.2.6 Bif-1 silencing does not prevent degradation of FL-APP by specific GSK3 inhibition

It has been shown by Yang et al (2010) that the autophagy induction resulting from specific GSK3 inhibition is dependent on bif-1 expression (Yang et al., 2010). Therefore, the role of bif-1 on FL-APP degradation was investigated by transfection of bif-1 shRNA in N2aSw cells, under both starvation and serum-supplemented conditions. In either condition, bif-1 silencing did not reverse the effect of specific GSK3 inhibition on FL-APP levels (see figure 4.11D). Furthermore, the basal level of FL-APP did not increase at the same level as with 3-MA or beclin-1 silencing.

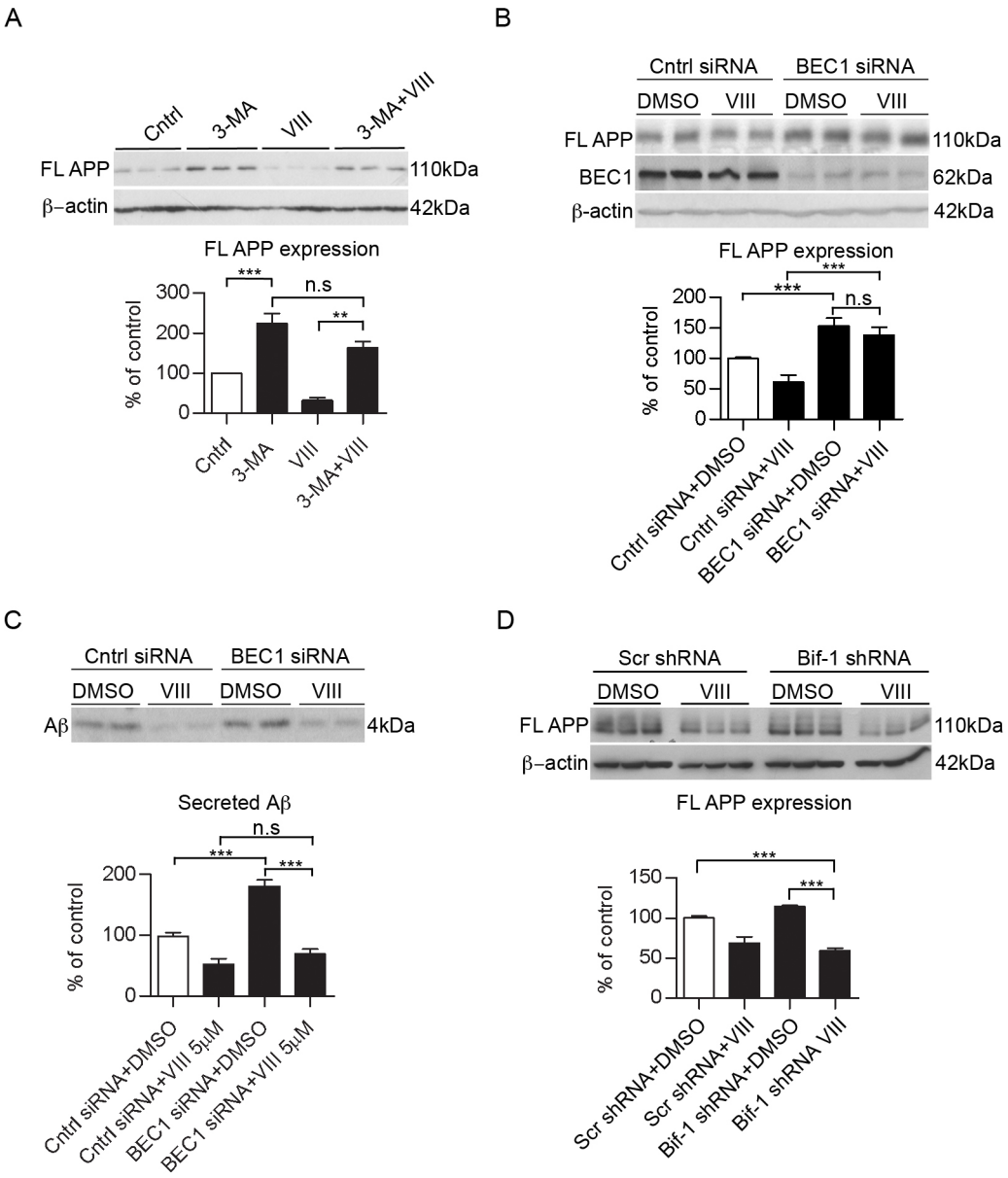


Figure 4.11: Blockade of autophagy reverses the effect of specific GSK3 inhibition on FL-APP.

Representative blots and quantification. (A) Autophagy blockage with 3-MA (500μM) in combination with VIII treatment overnight increased the FL-APP protein level by 131.2% ±16.58 compared to the level in cells treated with VIII alone. Unlike blockade of the proteasome, there was no significant difference between the protein levels of FL-APP in cells treated with 3-MA alone and those treated with 3-MA in combination with VIII (n=9 per group). Results from 3-MA treatment in (A) were reproduced with specific silencing of beclin-1 (B). (C) The medium from cells treated as in (B) was probed for the amount of secreted Aβ. (D) When bif-1 was silenced in N2aSw cells there was no recovery of the FL-APP protein level that was reduced by specific GSK3 inhibition (n=9 per group). Values shown in graphs represent the mean value ±SEM and expressed as a percentage of control. Statistical analysis included one-way ANOVA with a post-hoc Tukey's test (A-D), **P<0.01 and ***P<0.001.

4.3 Discussion

4.3.1 GSK3 can regulate the processing of APP

Activation of GSK3 is found in a number of diseases including Alzheimer's disease (AD), Parkinson's disease, Huntington's disease, schizophrenia, and diabetes (Frame and Zheleva, 2006; Hooper, 2007). Insulin induces inactivation of GSK3, which can contribute to stimulation of glucose uptake and glycogen synthesis (Jope and Johnson, 2004). There is the hypothesis that failure to inactivate GSK3, as a result of insulin deficiency and impaired insulin signalling (insulin resistance) could lead to increased inflammation and cell death (Hooper, 2007). Factors such as excessive caloric diet, hypertension and aging, which have been associated with deficiency in insulin signalling and higher GSK3 activity, could affect the accumulation of aggregated proteins that have been involved in neurodegenerative disorders, such as AD (Jope and Johnson, 2004). Therefore, GSK3 has become an interesting target, since it links aging, metabolic disease, inflammation, protein aggregation and cell death. Indeed, in this study it is shown that in the brain GSK3β levels increase with age and in particular the phosphorylation at serine 9 on GSK3β (associated with GSK3 deactivation) is also reduced, which may have consequences for protein aggregation, Aβ generation and synaptic loss.

Initially, the aim was to conclusively understand the role of specific inhibition of GSK3 activity on APP processing in a well-established cell-line model of these events (Sastre, 2010, Thinakaran et al., 1996b). Previous studies have shown that LiCl, a drug already in use for its mood stabilising properties, reduces Aβ production, presumably by inhibiting GSK3 (Su et al., 2004, Ryder et al., 2003a, Phiel et al., 2003, Sun et al., 2002). GSK3α silencing experiments revealed the same results, suggesting that the action of LiCl on APP processing was likely through GSK3 regulation, particularly the α-isoform. However, there are other studies that show that LiCl treatment can lead to an increase in amyloidogenic processing of APP (Feyt et al., 2005). Ultimately, variations in experimental design such as the paradigm used, the isoform of APP studied, the presence of familial mutations within that APP isoform, the cell-line and finally the concentration of drug can account for the inconsistencies seen. Firstly, the dose of LiCl when treating cells and animals in these studies, as admitted by the authors, was at non-physiologically relevant levels. Secondly, the cell-line used to demonstrate the implication of GSK3α in regulating

APP processing previously suggested (Phiel et al., 2003), was the Chinese Hamster Ovary (CHO) cell-line, while evidence that implicates the β-isoform in regulating APP processing comes from HEK293 cells (Ryder et al., 2003b). Furthermore, it is known from the literature that varying tissues and the culture lines representing these tissues express different APP and GSK3 isoforms. In particular, neurones are believed to express mainly the GSKβ1/2 isoforms (Kremer et al., 2011).

In order to provide a paradigm with more physiological relevance, the neuronal line, N2aSw, which overexpress the human APP.695 isoform with the Swedish double mutation, was used. The advantages and the relevance are illustrated as follows:

1. The Swedish mutation is more easily cleaved by β-secretase and therefore detectable levels of Aβ can be reproducibly measured. Therefore, it provides a good model for studying APP processing (Thinakaran et al., 1996b, Haass et al., 1995, Lo et al., 1994, Citron et al., 1992).

2. The use of a stable clone maintains that the initial levels of APP expression are similar in all the treatments.

3. The effect of GSK3 inhibition is independent of the Swedish mutation (Su et al., 2004, Phiel et al., 2003). As a consequence, this N2aSw cell-line is a valid resource for studying the processing of APP in general. Notwithstanding this, every effort has been made to corroborate findings shown here by using different cell-lines and different APP mutants.

Results shown in figure R3B demonstrate that well-documented concentrations of LiCl (including 40mM) have either no effect or increase Aβ generation in the N2aSw cell-line. While these LiCl concentrations do not alter amyloidogenic processing they can increase β-catenin stabilisation (see figure 4.2) and lead to decreased tau phosphorylation (Feyt et al., 2005). Thus, it must be presumed that any effect on LiCl promoting amyloidogenic processing is independent of GSK3. This is not surprising as LiCl is far from being a specific inhibitor of GSK3. This is probably the result from non-specific targeting of other key signalling mediators, such as Akt. Since these initial studies, efforts have been made to create specific inhibitors that act at the micromolar range and that do not inhibit the structurally similar kinases, CDKs (Bhat

et al., 2004). As shown in figure 4.3A, two structurally diverse chemicals, VIII and XI used at sub-toxic concentrations treated for up 24hrs (Bhat et al., 2003) show a significant reduction in the production of Aβ. The GSK3 inhibitor, VIII (AR-A014418), was used throughout as it gave the most potent response and without significant toxicity at the concentrations used (data not shown). To date this is the only specific GSK3 inhibitor that does not inhibit the structurally similar CDK2 and CDK5 (Bhat et al., 2003). The latter kinase has also been implicated as a tau kinase and roscovitine inhibition of CDK5 seems to lead to increased Aβ production (Ryder et al., 2003a). Thus, it is important to use an inhibitor of GSK3 that is as specific as possible in order to avoid combinatorial effects that may confuse the results. Transient transfection of the GSK3α/β siRNA replicates the results seen with the inhibitor, VIII and therefore illustrates the specificity. This specificity is established in the field and has been noted in many reviews and primary papers. It is also demonstrated that the effect of GSK3 inhibition was not the result of decreased secretion of Aβ, as there was a decrease in intracellular Aβ.

With the exception of Phiel et al (2003), all other studies did not investigate the mechanism behind LiCl action on Aβ generation (Ryder et al., 2003a). The reduction in Aβ by LiCl treatment observed by Phiel and colleagues coincided with a concomitant increase in the β-CTF. As they also saw changes in the $A\beta_{40/42}$ ratio, the authors concluded that GSK3 inhibition likely led to an inhibitory regulation on the γ-secretase activity. Interestingly, there is literature suggesting a dual regulation between PSEN1 and GSK3 (Takashima, 2010). In the present study, it is shown that altering the activity of GSK3 does not affect the activity of the γ-secretase. Figure 4.4A illustrates that specific GSK3 inhibition with VIII but not LiCl led to a decrease in the accumulation of the β-CTF. This is an indication that the observed Aβ reduction is independent of any γ-secretase activity decrease, which would result in an increased accumulation of the β-CTF. In addition to this, the production of the 6kDa AICD fragment (a specific γ-secretase-dependent cleavage event) in the assay from membrane preparations of N2aSw cells was measured. This assay has been used widely with slight variations from numerous groups as an indicator of γ-secretase activity (Sastre et al., 2001b, Sastre, 2010, Chang et al., 2003, Pinnix et al., 2001) (see 2.7.4 Analysis of APP C-terminal fragments). This assay shows only the direct effect of GSK3 inhibition on the γ-secretase complex, because the VIII was only added during the assay with membrane preparations. However, similar results have been

shown when incubating whole cells overnight with inhibitor VIII. Although a close structural link has been shown between GSK3 and PSEN1, this may only influence γ-secretase-independent functions. In agreement with this data, Feyt et al, also observed no effect of LiCl treatment on the γ-secretase activity, and the likely cause of the Aβ increase in that study was the result of increased β-secretase activity. However, the authors concluded that further investigation was required to fully understand this phenomenon.

4.3.2 Changes in GSK3 activity can alter the expression and activity of the β-secretase

In the present study, it is demonstrated for the first time that specific GSK3 inhibition leads to a reduction of the β-secretase activity by using a fluorimetric commercial kit, as well as by detection of the levels of the β-CTF. These results are in agreement with the reductions of the β-CTF found in cells transfected with RPS23R1, a protein that inhibits GSK3 (Zhang et al., 2009). There was no observable alteration in the localisation or trafficking of BACE1, but rather the decreased activity is the result of decreased BACE1 expression. In response to an initial observation of decreased mRNA expression by semi-quantitative RT-PCR, quantitative real-time RT-PCR was employed to validate and quantify the degree of *Bace1* mRNA down regulation. While there only appears to be a small but significant change in the activity of the secretase, this can account for vast changes in the amyloidogenic processing of APP, as the initial amyloidogenic cleavage is the rate-determining step in producing Aβ.

To determine whether the amyloidogenic processing can be driven by increased activation of GSK3, a phenomenon that may replicate AD pathogenesis, GSK3βS9 was overexpressed in the N2aSw cell-line. This approach has been taken before in numerous studies with dubious effect. Many have argued that owing to the fact that GSK3 activity is constitutively high, any further stimulation of GSK3 is hard to accomplish. Furthermore, as GSK3 activity is dependent on primed substrates, there is often a requirement to over stimulate the concerted priming kinase. In other words, the kinase activity of GSK3 is often saturated. Despite this, a significant increase in the production of Aβ in the N2aSw cell-line was observed. A modest GSK3 activity increase in a transgenic line overexpressing GSK3βS9 also resulted in an increase in accumulation of Aβ in the hippocampus (Su et al., 2004). However,

this observation has not been reproduced in the many other GSK3 knock-in transgenics, largely because the attention has been focused on the tau pathology.

In addition, in the present study there was no change in the secretion of sAPPα in cells transfected with GSK3βS9, which was confirmed by the α-secretase activity assay. This was also the same outcome as with specific GSK3 inhibition, and therefore it seems that the decrease in amyloidogenic processing of APP is not the result of an increase in α-secretase activity.

4.3.3 Specific GSK3 inhibition led to increased degradation of FL-APP

Some groups have claimed that the decrease in Aβ by GSK3 inhibition could be due to differences in APP phosphorylation, since it was noticed a decrease in the levels of the phosphorylated form of APPThr668 in mice treated with LiCl (Rockenstein et al., 2007). Aplin et al (1996) showed that GSK3 was capable of phosphorylating the residue Thr743, which resides in the CTD of the isoform, APP.770. However the biological significance of these kinase events is unknown. Subsequent papers from 2003 (Lee et al., 2003) and 2006 (Pierrot et al., 2006) showed that Thr668 of human wild-type APP.695 could also be phosphorylated by GSK3 owing to its sensitivity to the GSK3 inhibitor SB415286. Indeed this phosphorylation event is increased in AD patients compared to age-matched controls. Functionally, the phosphorylation event appears to increase the localisation of APP with BACE1 in endosomal compartments and promotes the intraneural production of Aβ. As such, there is a reduction in Aβ production when this threonine residue is mutated or the kinases responsible for this phosphorylation are inhibited (Sano et al., 2006).

In the present study, cells transfected with the APPsw variant were used. It has been shown that APPsw is preferentially processed in the TGN compartments through the secretory pathway whilst the wild-type protein is mainly processed in endosomal compartments following endocytosis (Griffiths et al., 2011a, Lorenzen et al., 2010). Thus, it is unclear whether the phosphorylation events may differ between the wild-type and the Swedish mutant and therefore, GSK3 inhibition would have differing outcomes on the familial variants of APP. However, as shown in figure R6, the reduction in the steady-state levels of FL-APP in response to specific GSK3 inhibition not only occurs on the APPsw variant but also wild-type variants of both APP.695 (lanes 5-8) and APP.751 isoforms (lanes 9-12). And as such, there appears to be a general GSK3 regulation on any APP isoform.

Ultimately, specific GSK3 inhibition led to a destabilisation of APPsw resulting from a reduced half-life (see figure 4.9). Although not fully investigated, it appears that GSK3 inhibition has no effect on the maturation and trafficking of FL-APP. This may be counter-intuitive as the phosphorylation of its CTD mediated by kinases such as GSK3 largely control its interaction with adaptor proteins, which in turn regulate its trafficking. However, if comparing both N2aSw cells with or without specific GSK3 inhibition, the staining pattern of APP looks identical, albeit being less intense with specific GSK3 inhibition (see figure 4.18). Furthermore, the migration pattern of the FL-APP by Western blotting appears to be unaltered by specific GSK3 inhibition (see figure 4.7C).

There was however a dramatic increase in degradation of the FL-APP protein, as shown from cycloheximide and pulse-chase analysis. In response to this, two major degradative pathways, namely the proteasomal and autophagy-mediated degradation, were investigated. Thus, it was hypothesised that increased targeting of FL-APP through either or both pathways could account for the observed decrease in the steady-state level of FL-APP with specific GSK3 inhibition.

4.3.3 Proteasomal and autophagy targeting of FL-APP upon specific GSK3 inhibition

The 26S proteasome is a highly conserved multi-subunit molecular machine that serves within the ubiquitin-proteasome system (UPS) to break down and recycle proteins that are often misfolded during their maturation through the ER and TGN compartments. Correct folding and trafficking of a protein are one in the same thing and are heavily influenced by adaptor proteins called chaperones (Koren et al., 2009). Trafficking of misfolded proteins are often retained within the ER and delivered to the UPS in a mechanism known as ER-associated degradation (ERAD). If this pathway is disrupted then APP can accumulate within cells and Aβ production increases (Kaneko et al., 2010).

In addition to misfolded proteins, the UPS can be used to maintain general protein turnover and homeostasis that can be up or down regulated to alter the half-life in response to cell signalling. The regulation of the transactivating NFκB (Orian et al., 2000) is one such example. This kind of tailored UPS event has also been discovered for BACE1 recently (Gong et al., 2010). It was demonstrated that autophagy compartments contain Aβ and APP-CTFs (Yu et al, 2005; Boland et al.,

2010; Jaeger et al., 2010; Tamboli et al, 2011). However, it remains controversial whether FL-APP is processed in autophagy. Recently, it was shown that APP can be found accumulated in autophagy compartments and that FL-APP is a substrate for autophagy (Jaeger et al., 2010). Besides, it was found that beclin-1 reduces cellular APP levels and its deficiency alters APP metabolism (Jaeger et al., 2010). However, another study disagrees and showed no changes in FL-APP after induction of autophagy with rapamycin (Boland et al., 2010). Experiments presented here show that FL-APP can indeed undergo targeting to both these degradative pathways, as inhibition of the proteasome and autophagy independently of each other by MG132 and 3-MA respectively, resulted in increased FL-APP expression (see figure 4.10 and 4.11). It is interesting that a recent study showed that neuronal stress resulting from proteasomal blockade with MG132 led to an actual increase in APP turnover. This was due to the fact that there was a concomitant increase in an autophagy response and targeting of FL-APP to this degradative compartments (Zhou et al., 2011). The protein level of FL-APP could be restored by further 3-MA treatment to block the autophagy response induced by the proteasome blockade. This could explain why the blockade of the UPS only partially restores the FL-APP protein level as the MG132 inhibition stimulates an autophagy degradation response. Of great interest is that Zhou and colleagues reported a direct interaction between LC3-I/II and APP/APLP. It would be prudent to explore if the targeting of FL-APP to the autophagy pathway may be mediated through a direct binding to LC3. Such a mechanism would constitute the basis for chaperone-mediated autophagy (CMA), a more specific autophagy response than the better understood macroautophagy, which is associated with general cytoplasmic and organelle digestion.

It seems that both proteasomal and autophagy blockade led to a partial if not complete, in the case of autophagy, attenuation on the effect of specific GSK3 inhibition on FL-APP levels (see figure 4.11). Unfortunately, it is challenging to determine the synergistic effects of blocking both pathways at the same instance, as this resulted in a high degree of toxicity and unworkable cell death. Despite this, it is reasonable to assume that both contribute to the destabilisation effect. Classically, increased proteasomal targeting of a protein is accompanied by increased ubiquitination, necessary for the correct chaperone recognition and trafficking. β-catenin is a prototypical example of this being targeted by the β-TrCP ligase leading to its destruction by the 26S proteasome. However, upon specific GSK3 inhibition

there appears to be no increase in ubiquitination of the FL-APP molecule and thus, the mechanism in which it is targeted to the proteasome under these conditions would require further analysis. Briefly, a recent study has shown a specific ligase, termed HRD1 which is reduced in AD patients, mediates proteasomal targeting of FL-APP to the UPS (Kaneko et al., 2010) and its depletion is associated with increased Aβ production. HRD1 is upregulated upon ER-stress and the unfolded protein response and as such some of its other substrates include the poly-glutamine expanded Huntingtin protein (Huntington's disease), PrP protein (Prion disease) and Pael-R protein (Parkinson's disease) (Apodaca et al., 2006, Yang et al., 2007, Omura et al., 2006). Further lines of investigation could look into the levels and interactions of this E3 ligase with FL-APP in response to specific GSK3 inhibition leading to increased UPS targeting and CMA.

In another study, GSK3 inhibition was found to induce autophagy, but only under serum starvation conditions during periods of up to several days, when there was significant necrosis (Yang et al., 2010). Furthermore, blocking autophagy did not increase cell survival, but merely converted the necrosis-mediated cell death to apoptotic cell death. As a result, GSK3 inhibition induced a dramatic increase of bif-1, which promotes the apoptotic function of beclin-1, which can be attenuated by silencing bif-1. In this context, GSK3 activity is protective against cell death under starvation conditions by preventing the pro-apoptotic functions of bif-1 and beclin-1. In addition to previous literature (Bhat et al., 2003) and preliminary toxicity studies of the GSK3 inhibitors in this study, the putative induction of autophagy observed here with specific GSK3 inhibition is independent of cellular death. From figure R10C, it can be concluded that the FL-APP degradation induced from specific GSK inhibition is independent, firstly of bif-1 activity and lastly, of cellular stress, as it occurs in both serum supplementation and starvation conditions. From accumulated data, it is clear that inhibition of GSK3 activity has a direct role in inducing autophagy and not just an indirect effect, such as cell toxicity. Alterations of GSK3 levels during aging (see figure 4.1) therefore could have implications in the functionality of autophagy-lysosomal pathway and affect neuronal survival and Aβ generation. This is relevant since there is evidence of endosomal/lysosomal system dysfunction in AD (Nixon, 2007).

CHAPTER 5 : SPECIFIC GSK3 INHIBITION ALTERS AUTOPHAGY-LYSOSOMAL DEGRADATION OF FL-APP

5.1 Introduction

Evidence shown in the previous chapter establishes that specific alteration of GSK3 activity can regulate APP processing by affecting Aβ generation and the intermediary metabolites, such as the β-CTF fragment. This regulation is mediated, firstly by control of the mouse *Bace1* transcription and secondly, by reducing the stability of the holo-protein FL-APP, which feeds into the two processing pathways of APP. Further analysis has illustrated that the decreased APP stability is associated with a response from both the proteasome- and autophagy-mediated degradation systems. There was, however, no significant increase in the ubiquitination of FL-APP that could explain the increased targeting of FL-APP to the proteasome. In contrast, there was an almost complete rescue of FL-APP levels with specific GSK3 inhibition when autophagy induction was blocked with 3-MA and beclin-1 knockdown. Therefore, these data would suggest that specific GSK3 inhibition could affect autophagy-mediated degradation of APP. Consequently, the next aim was to determine whether GSK3 might play a role in cellular signalling affecting autophagy regulation.

5.1.1 Autophagy and metabolic sensing

Autophagy, through the formation of autophagosome vesicles (AV), is a conserved degradative mechanism established through eukarya as a means to harvest energy from the cell constituents and long-lived proteins and as such is promoted in times of starvation or cellular stress (Cuervo, 2011). Therefore, metabolic processes and autophagy go hand in hand and the cell signalling pathways underlying both are heavily intertwined. This ultimately allows for cellular life to switch between anabolism and catabolism depending on the availability of resources from the immediate environs. As such the main activators of autophagy are involved in metabolism and are molecular sensors of the overall activity of the cell (Meijer and Codogno, 2011).

The elucidation of autophagy cellular signalling was largely centred on the action of a drug named rapamycin, which came to prominence for its life-extending properties. It later turned out that rapamycin was in fact a potent inhibitor of mTOR (mammalian target of rapamycin), a negative regulator of ULK (UNC-51 like kinase)

complex that is required for autophagy induction (Meijer and Codogno, 2011). Activity of mTOR usually promotes anabolic processes such as protein synthesis and thus one of its main roles is to activate key mediators such as the eukaryotic initiation-factor 4 (eIF4) (Meijer and Codogno, 2009). Upstream of the mTOR complex (mTORC) are numerous molecular sensors that are indicative of a high or low energy state, for example the NAD/NAD^+ and ATP/ADP ratios in addition to cellular constituents such as amino acids. The classical regulation of mTOR relies on insulin signalling through the PI3K/Akt pathway, an axis associated with survival and anabolic processes such as protein and glycogen synthesis. This results in GSK3 inhibition, which prevents the catabolic processes that are associated with it (Rayasam et al., 2009a).

Autophagy has been implicated in the pathogenesis of several human metabolic disorders such as type-2 diabetes and cancer (García-Arencibia et al., 2010, Meijer and Codogno, 2009). Furthermore there is growing evidence for its involvement with AD and there is now a growing body of evidence to argue that AD is largely a metabolic disease or even a new type of diabetes, sharing the same dysregulated signalling pathways (de la Monte and Wands, 2008, Rivera et al., 2005). Central to these revolutionary ideas is the protein GSK3, which can be thought as a molecular link between metabolism, cell survival and neurodegeneration.

5.1.3 Autophagosome formation

As outlined in figure 5.1, AV nucleation, expansion and vesicle closure are a complex coordination of cellular events that are largely controlled by the 18 autophagy-related (Atg) gene products, along with some other key kinase mediators that link the formation to sensory cues and signalling pathways. This core set of Atg genes are conserved from yeast to humans, which highlights the importance of this phenomenon to cellular homeostasis (Fleming et al., 2011, Meijer and Codogno, 2009).

Initially, an inducing stimulus negatively regulates mTOR that relieves its negative regulation on the ULK complex, which initiates membrane formation (Hosokawa et al., 2009). This initial step results in the marking and generation of the membrane dynamics from intracellular organelles such as the endoplasmic reticulum (Tooze and Yoshimori, 2010) mediated by the secondary messenger, phosphatidylinositol 3-phosphate (PI3P), which is generated by the PI3K-III activity within the Vps34-complex (Simonsen and Tooze, 2009, Noda et al., 2010). This

complex is largely regulated by Atg-6 or beclin-1, which has been mentioned previously, with its functions distributed between varying complexes linking to apoptosis (see figure 5.1B). This molecular signposting with PI3P results in the recruitment of the effector proteins WIPI2 (WD45-repeat interacting protein-12) and DFCP1 (double FYVE-containing protein-1) that in combination with the Atg5-12-16 complex coordinate the complicated invagination process required for vesicular formation. This complex also is important for the concomitant phosphatidylethanolamine (PE) conjugation of Atg-8 (LC3) to form Atg-8-PE (LC3-II), which is inserted into the outer and inner membrane of the autophagy compartment being formed with its eventual closure to form a vesicle, while the preliminary complexes mentioned dissociate (Kabeya et al., 2004, Kabeya et al., 2000). For this reason, LC3-II is often used as a biomarker for autophagy vesicles in *in vitro* and *in vivo* studies (Klionsky et al., 2008). However, the outer LC3-II is recycled back to the cytosol through its deconjugation by the protease Atg4 and the inner LC3-II is broken down by proteases when the AV fuses with a lysosome to form the mature autophagolysosome (AVL). Therefore, LC3 can only be used to probe early AV formation events (Mizushima and Yoshimori, 2007). The additional Atg proteins are concerned with regulating the conjugations leading (Tanida et al., 2005) to the formation of the various complexes and the post-translational processing of LC3. This generic process has been assembled from multiple studies but may differ slightly between organisms and also the cellular context with reference to the stimulus and the cargo. Furthermore chaperone-mediated autophagy requires a series of ubiquitin-like enzymes that target and link its cargo to this bulk degradation process. One such protein is p62, which forms part of the sequestrome complex that targets protein aggregates that are heavily ubiquinated (Meijer and Codogno, 2009).

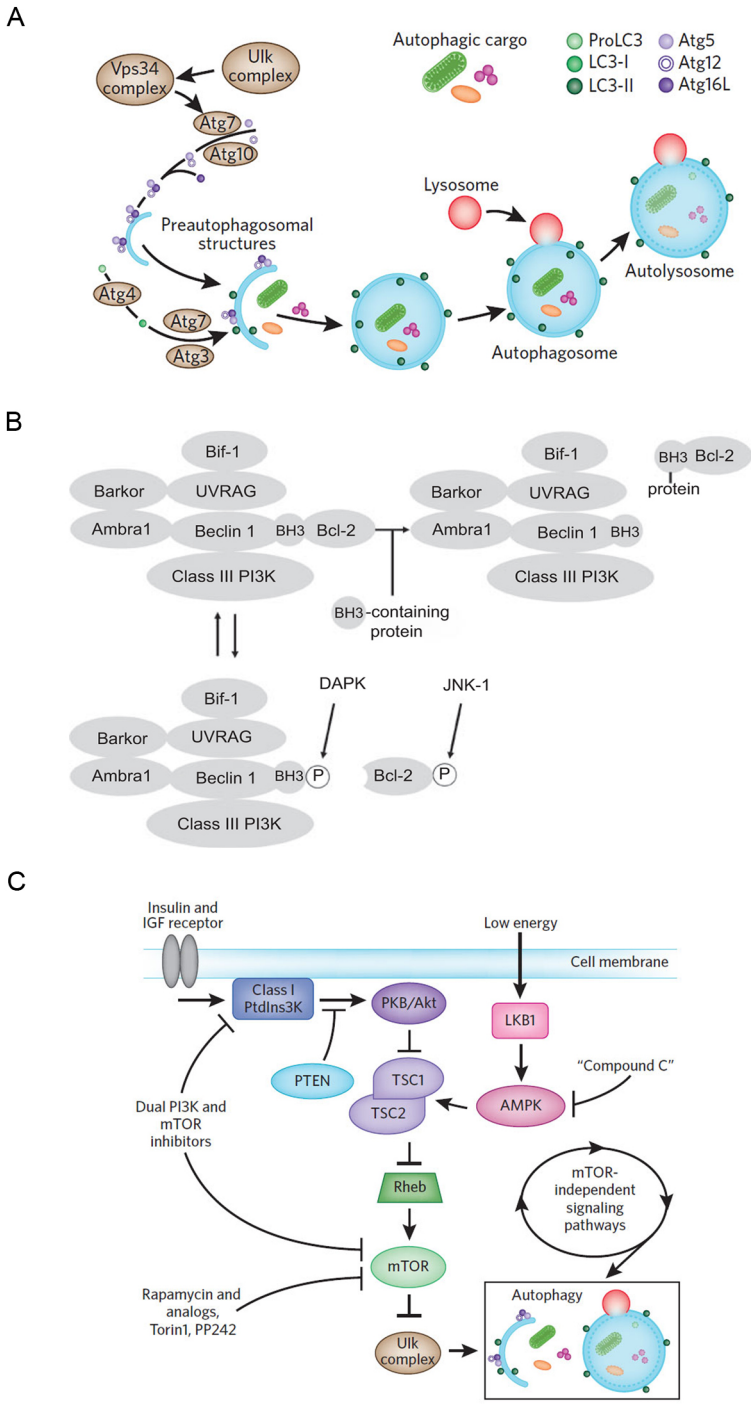


Figure 5.1: Formation and regulation of autophagy.

(A) Formation and maturation of autophagy compartments. (B) Regulation of beclin-1 function by interacting with other binding partners. (C) Multiple signalling pathways converge onto the mTOR complex (mTORC), which ultimately alters its ability to negatively regulate the ULK complex, the initial complex in the autophagy response. Schemes shown in (A) and (B) were taken from Flemming et al, 2001 (C) from Meijer and Codogno, 2009.

It should be noted that while there is controversial data related to the role of GSK3 in inducing autophagy, it does appear that the destabilisation of FL-APP resulting from specific GSK3 inhibition may be mediated through autophagy degradation as shown in figure 4.11. Furthermore, there are numerous examples of autophagy regulators acting at multiple levels and therefore, it is possible that GSK3 may have a myriad of influences on autophagy especially when considering the number of pathways it signals within.

The second aim of the project was to determine whether specific GSK3 inhibition could induce autophagy and account for the increased degradation rate of FL-APP.

5.2 Results

5.2.1 Specific inhibition of GSK3 activity can induce autophagy vesicle formation as shown by LC3-GFP puncta and LC3-II production

Following on from the results from the previous chapter, the hypothesis that specific GSK3 inhibition could favour FL-APP degradation via the autophagy/lysosomal pathway was explored. Therefore, to determine whether specific GSK3 inhibition affected autophagy formation, N2aSw cells (shown in figure 5.2) were transfected with a GFP-tagged version of the LC3 protein and then treated the cells with the GSK3 inhibitor VIII. LC3 is a selective marker for autophagy, which appears diffuse in normal conditions (LC3-I) and becomes punctate when it is lipidated and cleaved to form LC3-II that is associated with the membranes of autophagy compartments (Yoshimori, 2004, Kabeya et al., 2000). As shown in figure 5.2A-F there was a dramatic increase in the GFP-puncta formation (shown by white arrows), which is indicative of AV formation after specific GSK3 inhibition. This was attenuated by combination treatment of 500μM 3-MA. As a positive control, the cells were serum starved overnight to illustrate the punctate pattern shown by the arrows (see figure 5.1G). As excessive overexpression of protein can lead to aggregation and GFP-puncta formation irrespective of AV formation, only 0.25μg of the LC3-GFP construct was transfected into each well of a 6-well plate (9.4cm^2). Figure 5.2C-D shows the transfection efficiency in GFP-positive cells and also that transfected cells display normal cellular morphology with LC3 overexpression and VIII treatment (E-F).

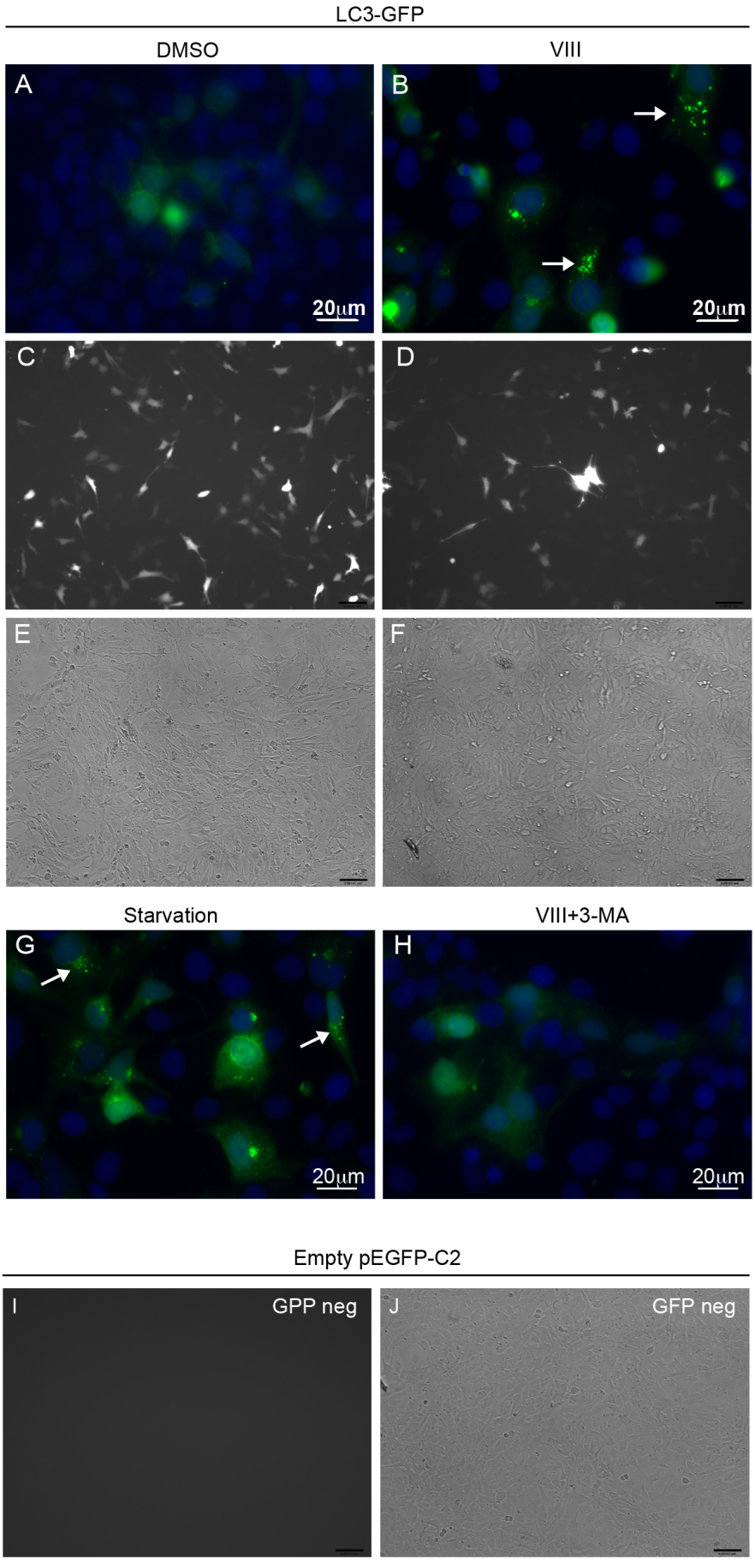

LC3-GFP
DMSO
VIII
A
B
20μm
20μm
C
D
E
F
Starvation
VIII+3-MA
G
H
20μm
20μm
Empty pEGFP-C2
I
GPP neg
J
GFP neg

Figure 5.2: Autophagosome formation as visualised with LC3-GFP formation.

N2aSw cells transiently expressed LC3-GFP (A-H) or transfected with the empty pEGFP-C2 vector (I-J). The cells were either treated with DMSO (A, C, E, G, I and J), 5μM VIII (B, D and F) or 5μM VIII with 500μM 3-MA (H) for up to 24hrs as shown. Fixed cells (A, B, G and H) were captured on a standard epifluorescent microscope at x40 with live fluorescent (C, D and I) and Bright field images (E, F and J) were taken at x20 before fixing to show the transfection efficiency. Scale bars shown on live images (C-F, I-J) are equivalent to 50μm. White arrows indicate GFP-LC3 puncta. The figure is representative of 3 independent experiments.

To circumvent the problem that the puncta seen in figure 5.2 were only the result of aggregation from an artefact associated with transient transfection, the HEK 293 cell line stably expressing LC3-GFP was used. From figure 5.3 it is clear that VIII treatment genuinely increases the number of LC3-GFP puncta formation indicating that specific GSK3 inhibition with VIII leads to autophagy induction.

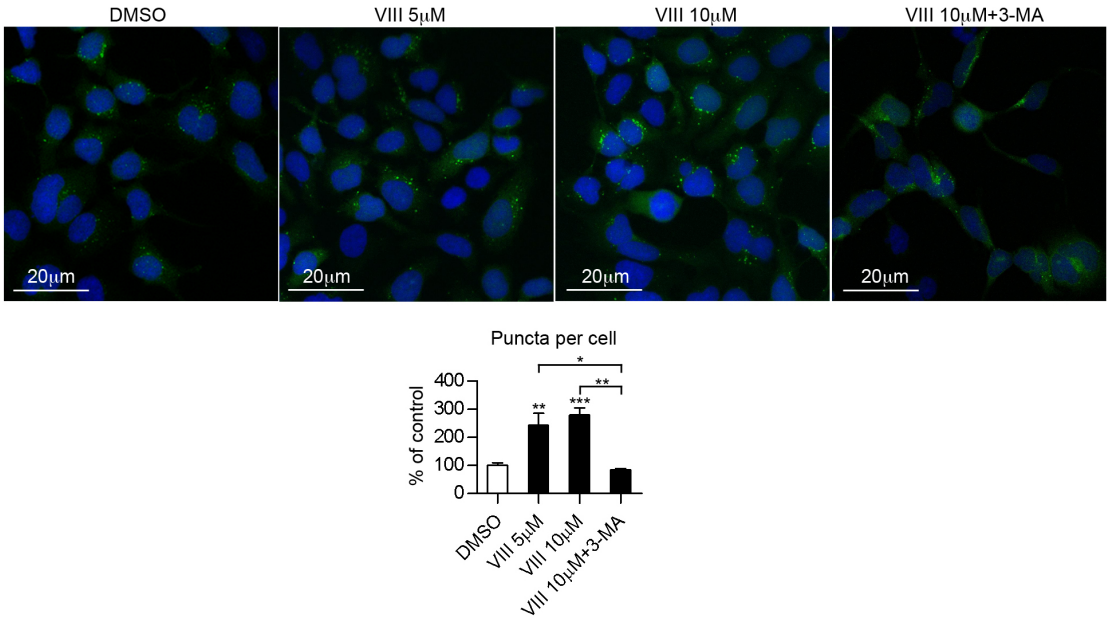


Figure 5.3: VIII treatment in HEK293 LC3-GFP cells leads to GFP puncta formation

Representative fields from HEK293 LC3-GFP cells treated with DMSO, VIII (5μM and 10μM) or VIII in combination with 3-MA (500μM). Quantification of the number of puncta shows a significant increase with both concentrations of VIII and this increase is sensitive to 3-MA treatment, which blocks autophagy induction. Statistics based on three independent experiments each of 10 fields per treatment. Values shown in graph represent the mean value ±SEM and expressed as a percentage of control. Statistical analysis included one-way ANOVA with a post-hoc Tukey's test, *<0.05, **P<0.01 and ***P<0.001.

To further support this point, total-lysates from N2aSw cells were run on a 16% tris-glycine gel to determine the conversion of endogenous LC3 I (18kDa) into LC3-II (16kDa). Specific GSK3 inhibition led to a dose-dependent increase in the specific production of LC3-II, which was abolished by pre-treatment of 3-MA (see figure 5.4A). Rapamycin, a well-known inducer of autophagy, was used as a positive control and also showed an increase in LC3-II production. The specificity of the LC3 antibody is illustrated in figure 5.4B. The faster migrating band (16kDa), which represents LC3-II increased with serum deprivation and decreased when N2aSw cells were treated with 3-MA. Overexpression of LC3 leads to the increase in the intensity of the 16kDa and 18kDa bands. Both properties are characteristic of LC3-II and therefore prove the specificity of the antibody to detect both forms of LC3.

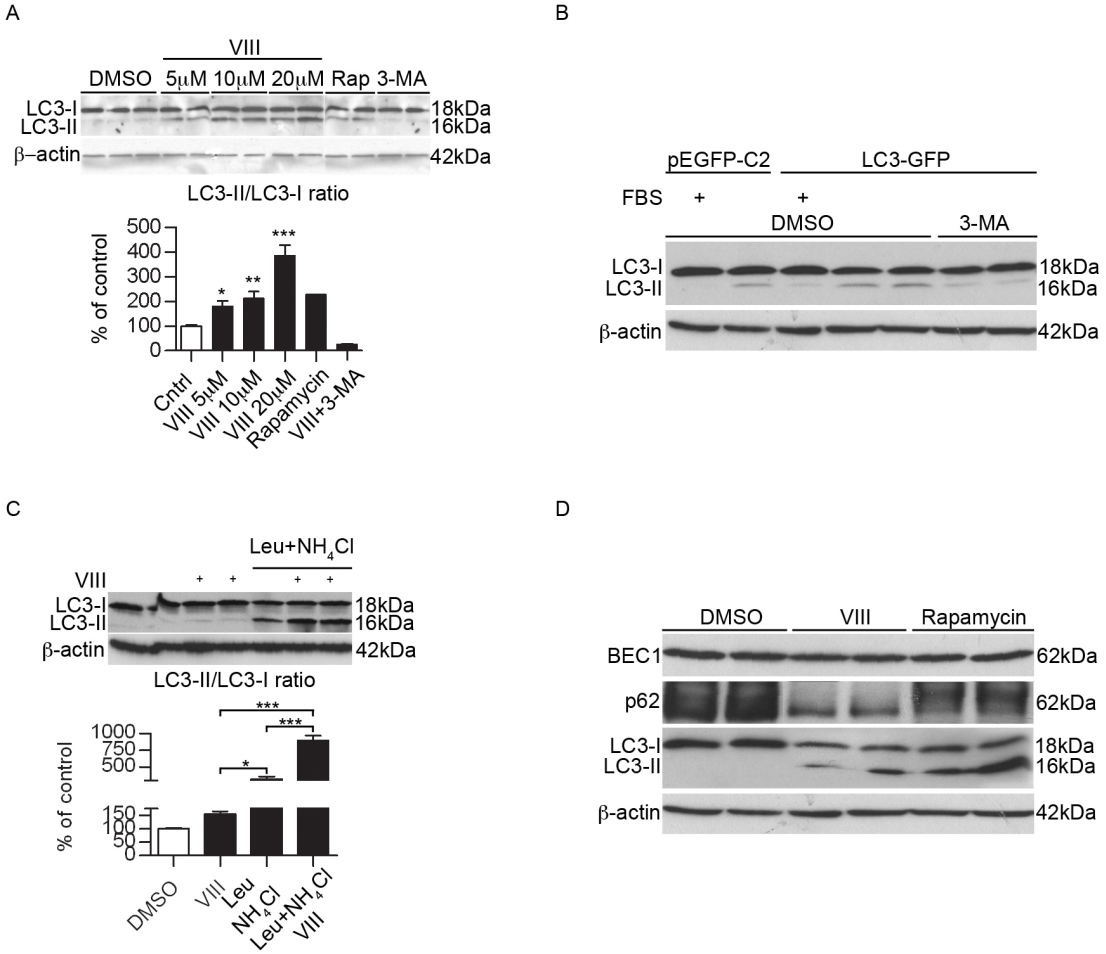


Figure 5.4: Specific GSK3 inhibition increases both endogenous LC3-II production and autophagy flux.

Representative blots and quantification. (A) The levels of LC3-II and LC3-I were measured in N2aSw cells treated with DMSO or 5μM VIII overnight. The dose-response increase in the LC3-II/I ratio was attenuated with 500μM 3-MA autophagy blockade (n=9 per group). (B) The specificity of the LC3 antibody which shows two bands that roughly migrate to 18kDa (LC3-I) and 16kDa (LC3-II). This faster migrating band (16kDa) accumulates when FBS is removed from the medium and decreases when cells were treated with 3-MA, which is characteristic of LC3-II. Additionally when LC3 is overexpressed there was an increase in the intensity of the same 16kDa and 18kDa bands (C) Autophagy flux is increased by VIII when compared to cells treated with both lysosome blockers and VIII (n=9 per group). (D) Both VIII and the positive control, rapamycin, decrease the steady-state level of p62 while increasing LC3-II production concomitantly. Values shown in graphs represent the mean value ±SEM and expressed as a percentage of control. Statistical analysis included one-way ANOVA with a post-hoc Tukey's test (A and C), *P<0.05, **P<0.01 and ***P<0.001.

As both of these assays indicate an induction in autophagy, the next step was to ascertain whether this was accompanied by an increased flux of material through this system. Therefore, autophagy substrates need to be monitored to verify that they have reached this organelle, and, when appropriate, degraded. This is a noteworthy point as LC3-II is usually released from the outer membrane of the AV compartment once it has matured and fused with a lysosome (Kabeya et al., 2004). Thus an increase in LC3-II can just as likely result from the disruption of fusion between an AV compartment and a lysosome to form the proteolytically active autophagolysosome (AVL). Therefore, to determine whether VIII-induced accumulation of LC3-II is caused by enhanced formation of autophagy vacuoles or to blockage of autophagy vacuole degradation, we treated cells with the inhibitor VIII in the absence or presence of the inhibitors of lysosomal proteolysis leupeptin (200μM) and NH_4Cl (20mM) for 4hrs (Mizushima and Yoshimori, 2007). Figure 5.4C shows that LC3-II levels were further accumulated in the presence of lysosome protease inhibitors, indicating an enhancement of the autophagy flux. These results were also supported when following the degradation of p62. p62 is thought to deliver cytoplasmic aggregates to AVL structures in a constitutive manner and upon doing so is itself degraded within them (Kim et al., 2008). As a result, the protein level of p62 has been documented to serve as a robust indicator of autophagy flux (Klionsky et al., 2008, Kim et al., 2008). Figure 5.4D shows that specific GSK3 inhibition results in a

reduced steady-state level of p62, indicating an increased autophagy flux. In addition, the levels of beclin-1 remained unchanged by specific GSK3 inhibition.

Thus, from these initial indirect assays, it appears that indeed specific GSK3 inhibition in N2aSw cells, that are not undergoing apoptotic events, can result in autophagy induction and flux.

5.2.3 Ultrastructure observation reveals no change in the AV formation but a dramatic increase in primary lysosome formation

The maturation of autophagy compartments and lysosomes is a complex process sharing similar structures and proteins and is therefore more of a continuum. To determine whether the results obtained in autophagy induction were truly representative of an increase in the number of AV formation, ultrastructure analysis was carried out on N2aSw cells treated with GSK3 inhibitor VIII. Using transmission electron microscopy (TEM) it is possible to reveal the high-resolution structure of individual vesicles. As such, it is possible to visualise and categorise the varying vesicles by their morphology, which has been standardised through decades of research (Eskelinen, 2008, Meijer and Codogno, 2011, Tanida et al., 2005, Ylä-Anttila et al., 2009).

AVs are often seen as double membrane vesicles with a clear lumen, a size greater than 300nm and often contain mitochondria and/or rough endoplasmic reticulum (Ylä-Anttila et al., 2009). Figure 5.5B-C shows the maturation of AVs as they fuse with a lysosome to form an AVL, which appears multivesicular with fusion with multiple lysosomes in addition to the engulfed organelles seen in the initial AV. Often this late stage formation may revert to a single membrane but a double membrane is possible. Figure 5.5D shows an AVL showing partially digested material but still maintained size and membrane structure (Eskelinen, 2008). Figure 5.5E shows a double membrane vesicle with a translucent lumen that is not counted as being an AV/AVL compartment. The varying forms of AVs and AVLs were grouped as one category. A mature lysosome is shown in figure 5.5G, which appears to be highly layered owing to the multiple membrane fusion events that occur during the lifecycle of a lysosome vesicle, they will also vary in their electron density owing to differing states of degradation of its luminal contents (Saftig et al., 1997, Grunwald). In contrast, a primary lysosome has a singular containing membrane that is irregular shaped and the lumen contains a dense core as shown in figure 5.5F (Schraermeyer

and Heimann, 1999, Schraermeyer et al., 1999, Grunwald). Again these two classes of lysosome were grouped for the analysis.

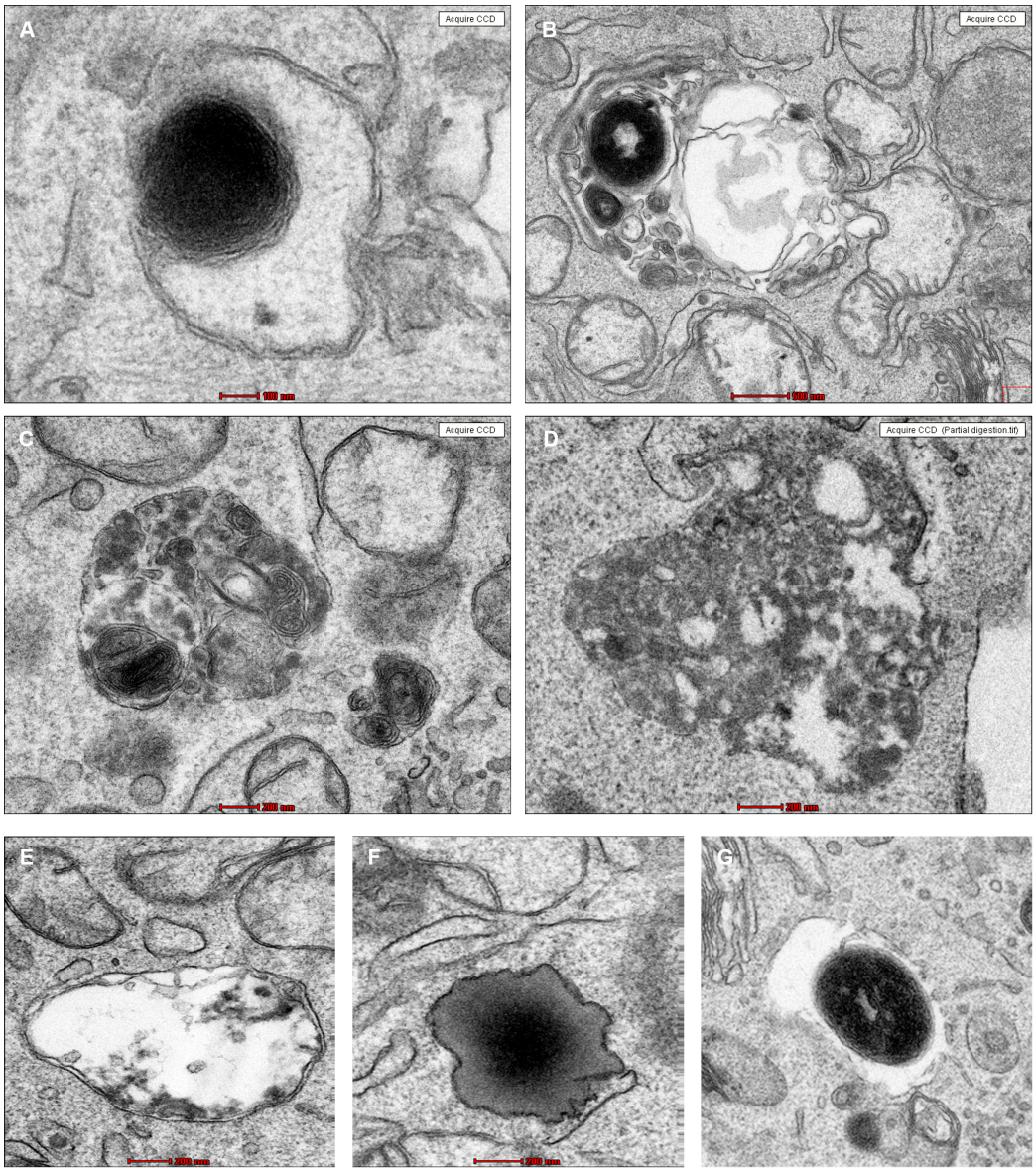
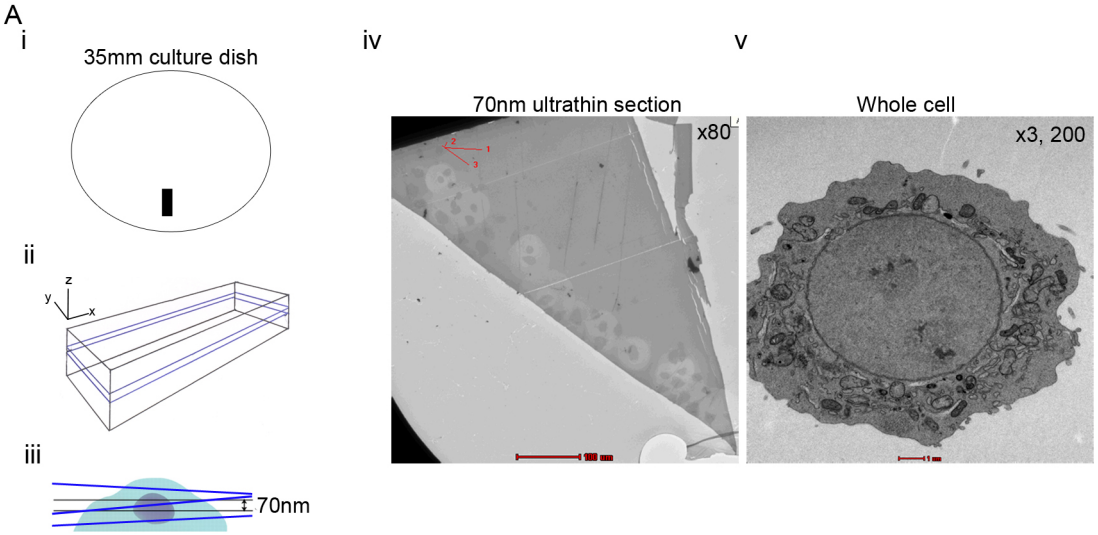
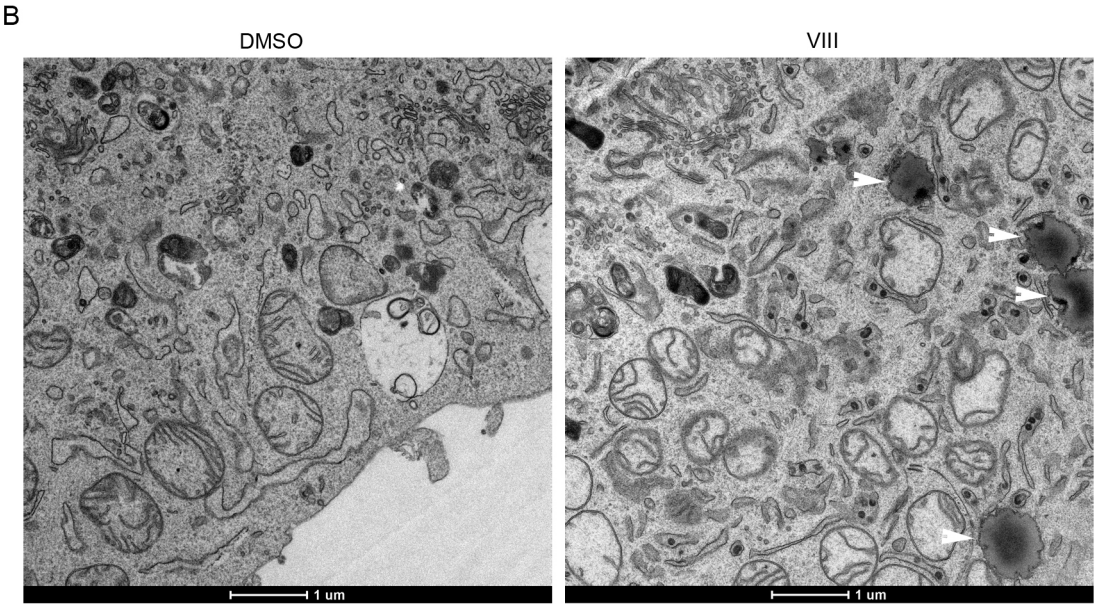


Figure 5.5: Characterisation of intracellular autophagy-lysosomal compartments for cell vesicle counts.

Images of organelles within N2aSw cells in a basal state were captured on a TEM microscope with the help from Dr Raffa Carzaniga. The various stages of autophagy maturation are illustrated (A-D) starting with initial fusion events with lysosomes (A) to the appearance of multivesicular events (B-C) and finally digestion of the intracellular constituents (D). (E) Shows a double membranous vesicle but does not correspond to an autophagy compartment for the lack of any fusion event of an internalised organelle or RER. (F-G) The structures representing lysosomes, both primary (F) and the mature multilamellar form (G) are represented. Scales bars equivalent to 100nm (A), 500nm (B) and 200nm (C-G).


A
i
35mm culture dish
ii
z
y
x
iii
70nm
iv
70nm ultrathin section
x80
v
Whole cell
x3, 200


B
DMSO
VIII
1 um
1 um

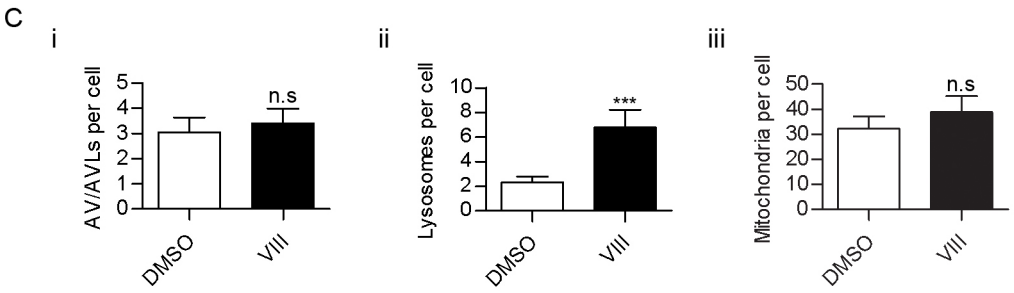

C
i
AV/AVLs per cell
5
4
3
2
1
0
n.s
DMSO
VIII
ii
Lysosomes per cell
10
8
6
4
2
0
***
DMSO
VIII
iii
Mitochondria per cell
50
40
30
20
10
0
n.s
DMSO
VIII

Figure 5.6: Ultrastructure analysis of N2aSw cells incubated with or without GSK3 inhibitor VIII.

(A) N2aSw cells were cultured on 35mm dishes (i) and embedded in resin. Ultrathin (70nm) sections (ii) were cut at random planes through several blocks at several heights to give an unbiased representation through the cells (iii). An example section containing multiple cells is shown (iv) and a whole cell (v). (B) Representative field at x6, 500 showing an increase in lysosomes but not AV/AVL compartments with 5μM VIII treatment. White arrows indicate primary lysosomes. (C) Quantification of lysosomes, AV/AVLs and mitochondria per cell (n=30 per section per group). Values shown in graphs represent the mean value ±SEM and expressed as counts per cell. Statistical analysis included an unpaired t-test (C), ***P<0.001. Scales bars are equivalent to 100nm in (iv) and 1μm in (v) and (B).

Figure 5.6A briefly outlines the methodology used to produce an unbiased representation of the cultured cells. Multiple random cutting planes were taken from various heights through several resin blocks (represented by blue lines in the figure). This enabled the sampling through the Z-plane of the cells. These criteria were used to quantify the numbers of each vesicle type as well as the number of mitochondria. Multiple images were taken at a magnification of x6, 500 to cover the entirety of the cytoplasm of each cell. 30 cells were counted per 70nm ultrathin section and multiple sections from varying heights through the Z-plane of the cells were taken for analysis. Interestingly, despite the increase in LC3-GFP puncta and LC3-II levels, there was no significant or observable increase in the number of AV/AVL structures (see figure 5.6Bi). The varying forms of autophagy compartments (see figure 5.5) were grouped for the analysis but still no significant differences were seen when separated either. Importantly, there were numerous observable fusion events between AVs and lysosomes and there was no evidence of enlarged AVs, which would result from incorrect fusion. This indicates that there is correct maturation required to maintain flux through autophagy degradation. Secondly, specific GSK3 inhibition caused a general increase in mature lysosomes and a massive increase in the formation of primary lysosomes (indicated by the white arrow heads) from 2 per cell with DMSO to 6 per cell (see figure 5.6Bii) (mean value ±SEM. ***<0.001 based on 30 cells per ultrathin section). This increase in number was not associated with an observable defect in the morphology of the primary lysosomes. This result was consistently replicated through the varying Z-planes of the cell. There were no significant differences in the number or the size of mitochondria observed between the treatments (see figure 5.6Biii). Furthermore, several mitochondrial biogenic events

such as fusion and fission were observed which is indicative of the healthy viability of the cells under the culturing conditions stated.

5.2.4 Specific inhibition of GSK3 led to an increase in the biogenesis of lysosomes

To confirm the previous ultrastructure observations, immunofluorescence labelling with Lysotracker®-Red (a molecular probe for lysosomes and other acidic vesicles) was carried out in N2aSw and also in an unrelated COS-7 cell-line to show consistency. In both cell-lines there was a dramatic and significant increase in the Lysotracker®-positive vesicles by 113.90% ±23.09 (mean value ±SEM. ***P<0.001 based on 3 independent repeats) and 63.22% ±17.58 (mean value ±SEM. *P<0.05 based on three independent repeats) respectively when cells were treated with the GSK3 inhibitor VIII. This observation confirms the increase in lysosomes seen in figure 5.6B (see figure 5.7A-B). The specificity of the dye was verified by incubation of the cells with bafilomycin A1, which prevents the acidification of the lysosomes and therefore the retention of the Lysotracker®-Red (see figure 5.7A). The number of vesicles per cell (% of control) was measured by the "Analyse particle" function in Image J having pre-set the size and circularity of the particles to be counted (see 3.11.3 Image capture and analysis).

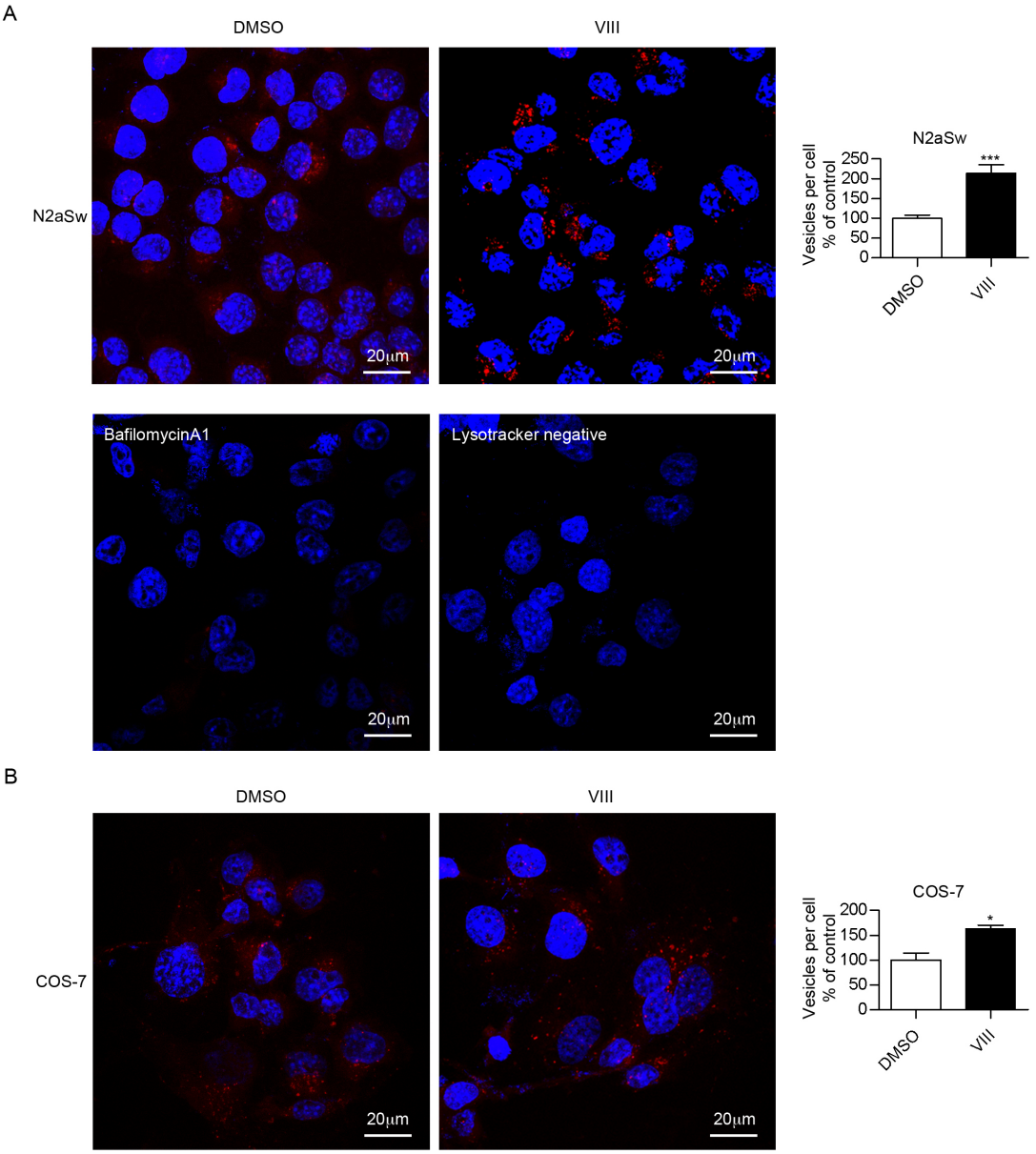


Figure 5.7: Specific GSK3 inhibition increases Lysotracker®-red retention.

Specific GSK3 inhibition by 5μM VIII overnight results in a significant increase in Lysotracker®-positive vesicles by 113.90% ±23.09 in N2aSw cells (A) and 63.22% ±17.58 in COS-7 cells (B) (based on three independent repeats each of 5 fields). Images were taken with an optical magnification of x63 optical zoom and a further 2.5 digital zoom. Values shown in graphs are mean value ±SEM and expressed as percentage of the control (vesicles per cell). An unpaired t-test was used to assess the statistical significance of any difference between the means.

Because Lysotracker®-Red retention within lysosomes is based only on the acidic environment, a mouse anti-LAMP1 antibody was also used to specifically label the lysosomes (see figure 5.8). Again, there was a significant increase in LAMP1 positive vesicles with specific GSK3 inhibition of 154% ±31.74 in N2aSw cells (mean value ±SEM. ***P<0.001 based on three independent repeats each of 5 fields). The number of vesicles was calculated by using the "Analyse particle" measurement in Image J as well.

To determine whether APP localisation in lysosomes was altered after specific GSK3 inhibition, double immunofluorescence labelling with APP and LAMP-1 antibodies in N2aSw cells was performed. After exposure to the GSK3 inhibitor VIII there was an increase in the accumulation of APP in lysosomes, indicated by an increase of 2.79% ±0.77 in the percentage of the field that was colocalised (mean value ±SEM. *P<0.05 based on three independent repeats each of 5 fields) (see inset of figure 5.8A-B). This increase in colocalisation was associated with an increase in the Pearson's correlation coefficient from 0.2549 when cells were treated with DMSO to 0.4176 when cells were treated with VIII.

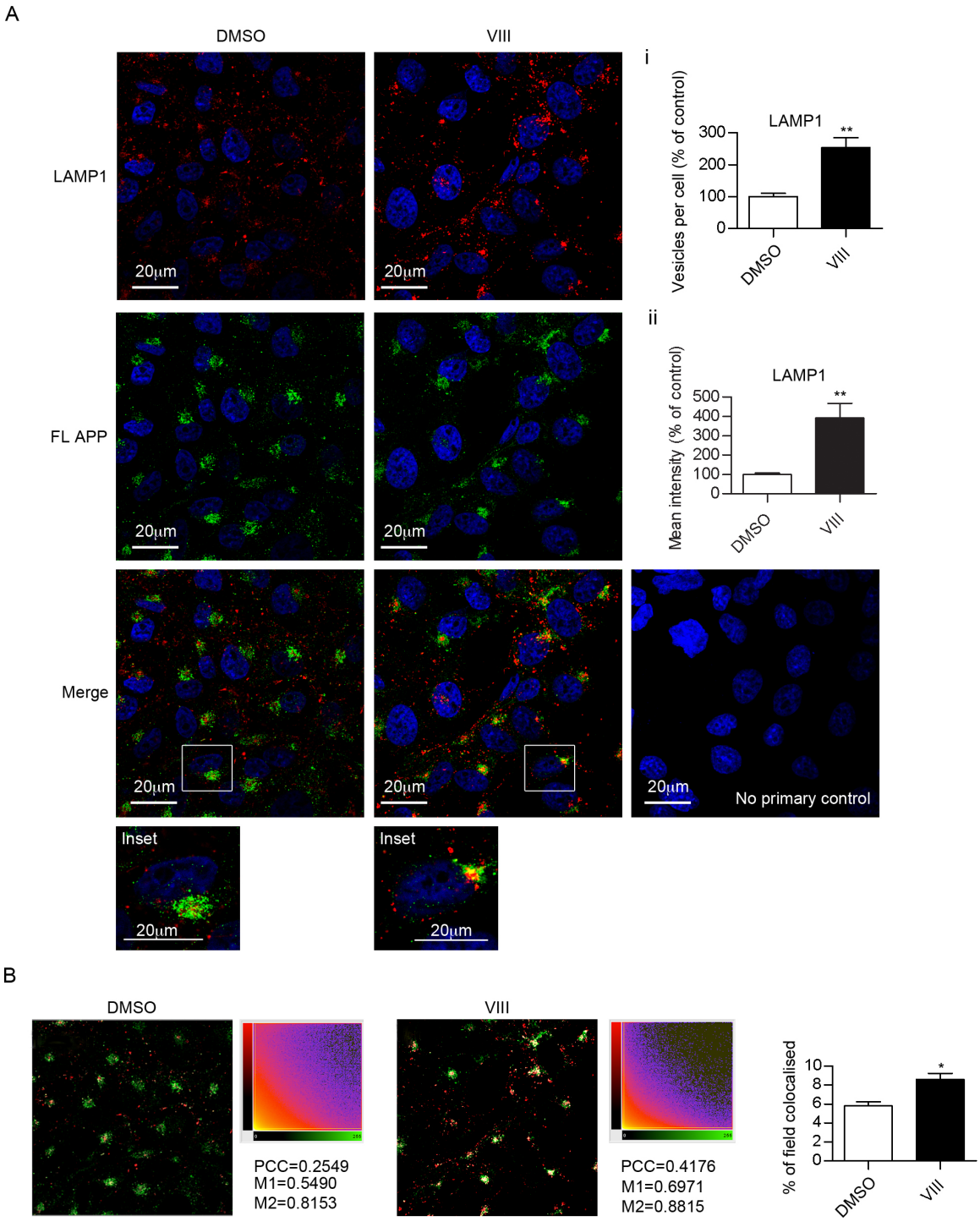

A
DMSO
VIII
LAMP1
FL APP
Merge
20μm
Inset
i
LAMP1
Vesicles per cell (% of control)
300
200
100
0
**
DMSO
VIII
ii
LAMP1
Mean intensity (% of control)
500
400
300
200
100
0
**
DMSO
VIII
No primary control
B
DMSO
VIII
PCC=0.2549
M1=0.5490
M2=0.8153
PCC=0.4176
M1=0.6971
M2=0.8815
% of field colocalised
10
8
6
4
2
0
*
DMSO
VIII

Figure 5.8: Specific GSK3 inhibition increases the number of lysosomes and the subcellular localisation of APP in lysosomes.

This figure shows the representative images of LAMP1 and APP staining in N2aSw cells. (A) An anti-LAMP1 antibody was used to stain lysosomes (i) which were found to increase with specific GSK3 inhibition by 154% ±31.74 and an overall increase in in the mean intensity of the stain by 294% ±62.90 (ii) with a non-significant decrease in the mean intensity of the APP stain (based on 3 independent repeats each of 5 fields). This was accompanied with an increase in localisation of APP with LAMP1 (see insets) with specific GSK3 inhibition. (B) Imaris software was used to assess the colocalisation between the green and red channel with the thresholding shown in the 2-D histograms. There was an increase in the percentage of the ROI of the 2 channels being colocalised. Both the Pearson's correlation coefficient (PCC) and Mander's coefficient (M1 and M2) were used to statistically assess the colocalisation (based on 3 independent repeats and each of 5 fields). Values shown in graphs represent the mean value ±SEM. An unpaired t-test was used to test the statistical significance in the differences between means, *P<0.05 and **P<0.01.

Quantification for each experiment was made from five randomly surveyed fields with a Z-stack covering the entire height of the cell (from the Bright field image) and an optical magnification of x63 and a zoom factor of x2.5. The DAPI counter-stain was used to count the number of cells within each field and to express as counts per cell (% of control).

A recent paper reported that the transcription factor EB (TFEB) is a master regulator of genes associated with biogenesis for lysosomes and autophagy and, therefore, provides a link and concerted action between these two intracellular compartments (Cuervo, 2011, Settembre et al., 2011, Settembre and Ballabio, 2011). Interestingly, GSK3 was identified as a potential kinase for TFEB (Settembre et al, 2011). To investigate the relation between GSK3 signalling and TFEB, N2aSw cells transfected with TFEB-FLAG were treated with the GSK3 inhibitor VIII. FLAG immunostaining of TFEB showed that specific GSK3 inhibition resulted in TFEB nuclear translocation as shown in the representative plane from a Z-stack (figure 5.8A); there was a significant increase of 75.97% ±9.72 in the percentage of cells with nuclear staining for TFEB out of the total cells that were TFEB positive. Figure 5.9 shows a complete translocation of TFEB to the nucleus using the orthogonal views and 3D representations 1 and 2 (see appendix) from the Z-stack.

In addition, specific GSK3 inhibition in N2aSw cells overexpressing TFEB-FLAG cDNA, resulted in an increase of 83.24% ±36.36 in the amount of TFEB in the

nuclear fraction (mean value ±SEM. *P<0.05 and based on n=9 per group). This band migrated to approximately 52kDa, consistent with the predicted size (Carr and Sharp, 1990), was absent in nuclear extracts from pcDNA3 control transfected N2aSw cells (see figure 5.10). In summary, these results show that specific inhibition of GSK3 results in translocation of TFEB to the nucleus, which in turn may regulate genes required for lysosome and autophagy biogenesis.

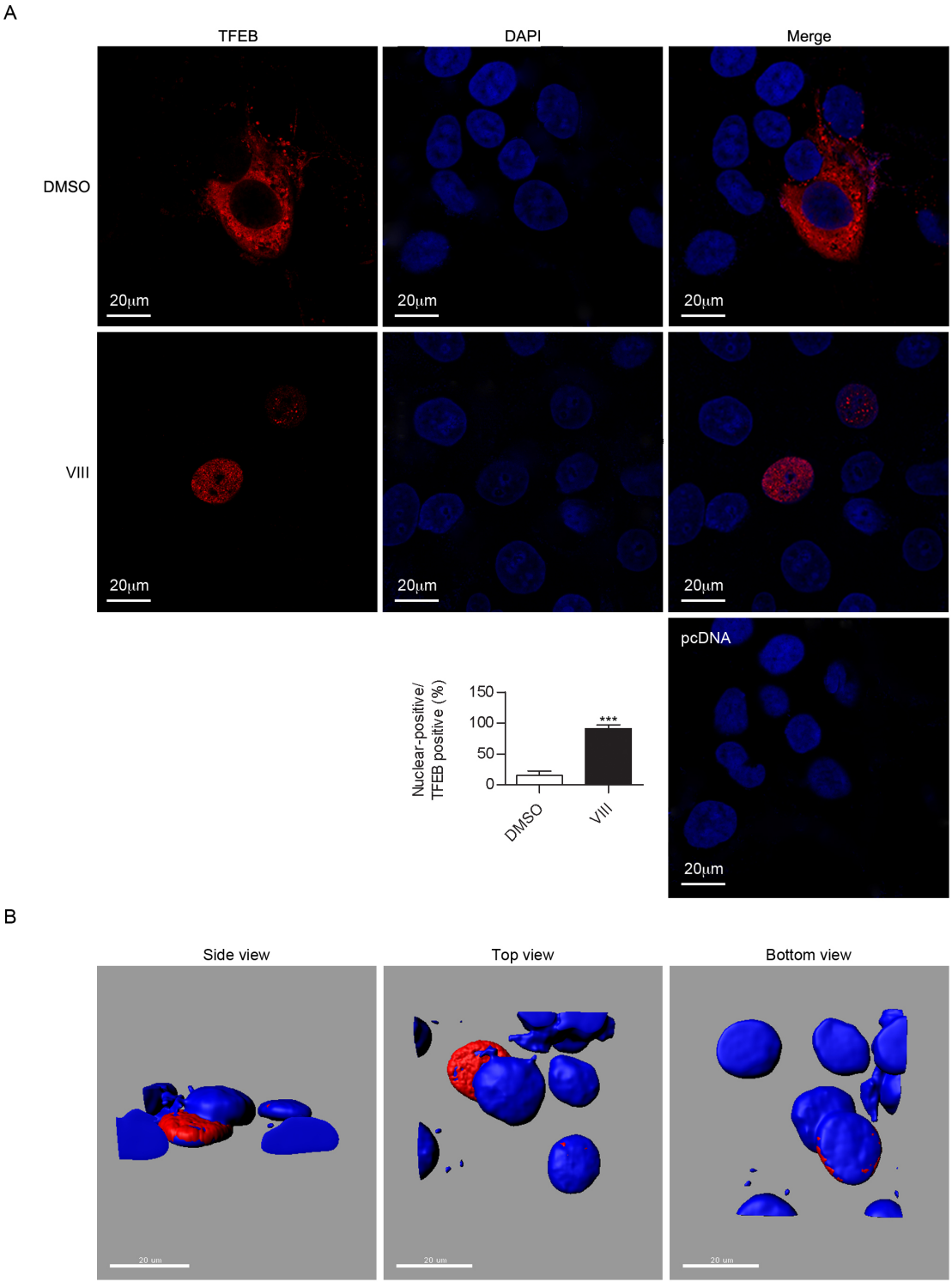

A
TFEB
DAPI
Merge
DMSO
VIII
20μm
pcDNA
Nuclear-positive/
TFEB positive (%)
150
100
50
0
***
DMSO
VIII
B
Side view
Top view
Bottom view

Figure 5.9: Specific GSK3 inhibition promotes the translocation of TFEB in N2aSw cells.

(A) A FLAG-tagged TFEB construct was transiently transfected in N2aSw cells for up to 48hrs. Specific GS3K inhibition with 5μM VIII resulted in a shift in the distribution of TFEB. There was an increase of 75.97% ±9.72 in the percentage of TFEB nuclear-positive cells when treated with the inhibitor VIII (based on 3 independent repeats each of 5 fields). The confocal images were captured with x63 optical magnification and a 2.5 digital zoom. (B) Orthogonal views (side, top and bottom) of surface thresholds show the inclusion of the red channel within the blue (nucleus) channel when GSK3 is inhibited. Values shown in the graph represent the mean value ±SEM and expressed as a percentage of control. A unpaired t-test was used to show statistical significance in the differences between the means, ***P<0.01.

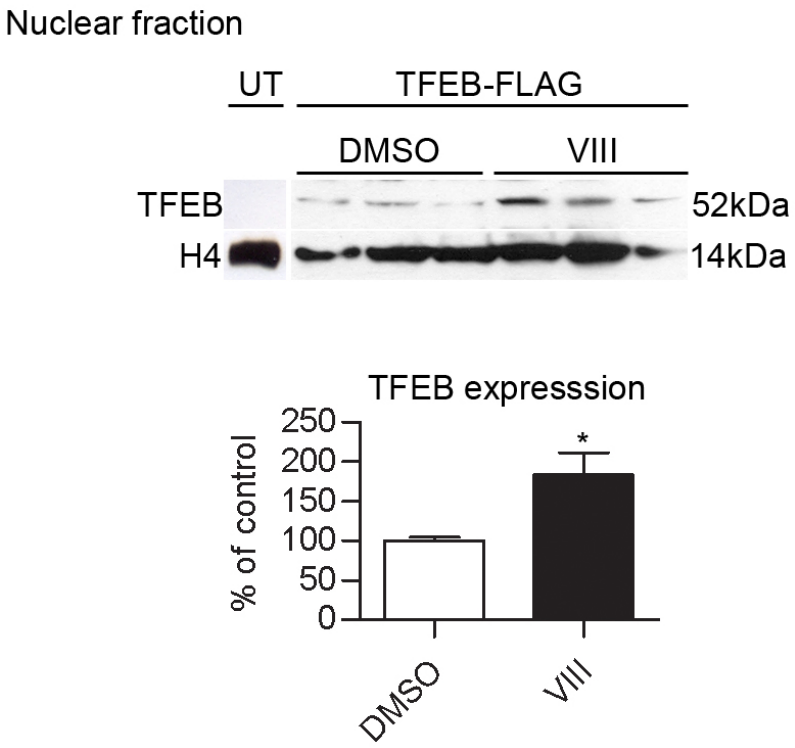


Figure 5.10: Increased nuclear localisation of TFEB by specific GSK3 inhibition.

N2aSw cells were transiently transfected with either empty FLAG-tag vector or a FLAG-tagged TFEB construct (TFEB-FLAG). A specific band appears in cells overexpressing TFEB-FLAG at around 52kDa. This band significantly increases with specific GSK3 inhibition resulting from 5μM VIII treatment overnight (n=9 group). Values shown in graphs represent the mean value ±SEM and expressed as a percentage of control. An unpaired t-test was used to show the statistical significance in the difference between the means, *P<0.05.

5.2.5 Blockade of lysosomal degradation rescues FL-APP protein level reduced by specific GSK3 inhibition

The previous section demonstrated a clear upregulation in lysosomal formation by specific GSK3 inhibition, which in turn increased the localisation of APP species within these vesicles. To establish whether this also resulted in increased degradation of FL-APP, the expression level of FL-APP was measured in the presence of lysosomal inhibitors. Leupeptin (Sigma Aldrich) is a well-established inhibitor of cysteine and serine peptidases and thus inhibits a broad spectrum of proteases in the acidic lysosome. In particular, it inhibits cathepsin-B, which has been shown to act as a non-canonical secretase during incomplete proteolytic processing of APP (Hook et al., 2005, Hook et al., 2007). Treatment with leupeptin (100µM for 7hrs), to inhibit cysteine proteases, significantly increased FL-APP levels (34.75% ±5.95). The combination of leupeptin and VIII resulted in a recovery of the FL-APP protein level and a significant increase of 48.08% ±7.39 compared to VIII alone (mean value ±SEM. ***P<0.001 based on n=9 per group). Similar results were obtained when the acidification of the lysosomes was blocked with 10nM bafilomycin A1 and 20mM NH_4Cl (data not shown), which is required for the optimum pH for protease activity.

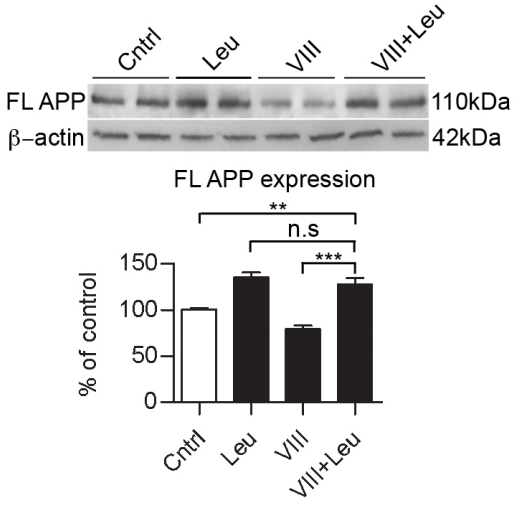


Figure 5.11: FL-APP degradation induced by specific GSK3 inhibition is dependent on lysosomal proteolysis.

There was a complete recovery of the FL-APP protein level when lysosomal proteolysis was blocked with pre-incubation of 100µM leupeptin. When N2aSw cells were treated with both VIII and leupeptin, there was an increase of 48.08% ±7.39 in the protein level of FL-APP (n=9 per group). Values shown in graphs represent the mean value ±SEM and expressed as a percentage of control. An unpaired t-test (A) or a one-way ANOVA with a post-hoc Tukey's test (B) were used to show statistical significance in the differences between the means, **P<0.01 and ***P<0.01.

5.3 Discussion

Results from chapter 4 suggested that the increase in FL-APP degradation in response to specific GSK3 inhibition was dependent on the induction of autophagy and increased autophagy-mediated degradation. However, the role of GSK3 on autophagy induction has raised a lot of speculation and controversy.

LiCl was reported to induce autophagy by an mTOR-independent mechanism, via reduction of IMPase, lowering IP3 (Sarkar et al., 2005, 2007). On the other hand, other groups have demonstrated that LiCl treatment inhibits mTOR (Aguib et al, 2009; Heiseke, 2009). Still, the inhibitory effect of LiCl is likely mediated by a GSK3-independent mechanism (Flemming et al, 2011) because there are indications that GSK3 activation inhibits the mTOR pathway (Sarkar et al., 2008; Inoki et al, 2006; Fu et al., 2009). At the molecular level, GSK3 can directly interact and phosphorylate the TSC1/2 complex, which in turn affects its activation of mTOR itself (Inoki et al., 2006). What is interesting is that this GSK3 activity is largely dependent on a priming event from AMP kinase (AMPK), whose activity is indicative of the energy state of the cell. Therefore in a high glucose and ATP environment where there is minimal or no AMPK activity, GSK3 cannot impair the mTOR pathway. In addition to the role of GSK3 sensing the nutrient environment through the insulin-PI3K/Akt pathway, it also responds to canonical Wnt regulation from the external environment, which provides a ligand mediated paracrine signal from the surrounding cell-niche. The studies from the group of Rubinsztein provide the mechanisms by which GSK3 activity promotes autophagy induction through the mTORC1 dependent pathway (Rubinsztein et al., 2005, Sarkar et al., 2008).

Using more specific inhibitors, other studies have reported that GSK3 inhibition induces autophagy by increasing bif-1 levels (Yang et al., 2010). However, this autophagy response was accompanied by apoptosis of the cell-lines tested. This illustrates the potential role of autophagy leading to autophagy-mediated cell-death. In other circumstances, it seems that GSK3 largely has no effect on autophagy regulation, as GSK3 inhibition led to inconsistent and non-significant activation of mTOR signalling (Liu et al., 2009). Furthermore, while LiCl has consistently been shown to induce autophagy, a recent study showed that LiCl dampened the autophagy response and the cellular apoptosis induced in mice with unilateral hypoxic-ischemia (Li et al., 2010a).

The use of different cell-lines, incubation times, GSK3 inhibitors and culture conditions (with or without serum) could be the reason for all these different outcomes. For example, the study from Liu et al (2009), where GSK3 seemed to have no effect on mTOR signalling, was only in the case when there was nutrient stimulation of mTOR. The induction of autophagy can also lead to completely divergent responses, as illustrated by two papers published this year looking at the direct activation of the ULK complex with AMPK phosphorylation. This report showed that, in addition to the role of AMPK acting as a primer on TSC2 upstream of mTOR to induce autophagy, GSK3 can also act directly downstream of mTOR on the ULK complex (Egan et al., 2011). However, the latter was only resulting from glucose starvation conditions as opposed to amino-acid depletion, which does not appear to reproduce the same outcome, although it did induce autophagy (Meijer and Codogno, 2011, Kim et al., 2011, Egan et al., 2011). In addition, cellular signalling may differ among different cell types. For instance, in highly energetic neurones, the mitochondrial throughput is high, and as a result, the basal level of autophagy is considerably higher comparatively. Indeed, a specialised form of autophagy for mitochondria, namely mitophagy exists. In extending this point, it is known that the insulin signalling and sensitisation differ largely in neuronal cells compared to the peripheral tissues. Therefore, the function of GSK3 concerning regulation of autophagy maybe slightly adapted to suit the individual cell type and its demands.

5.3.1 Specific GSK3 inhibition induces autophagy and increases autophagy flux

In this study, various methods were applied to investigate whether indeed GSK3 plays a role in regulating autophagy: Firstly, the use of LC3-GFP to detect by immunofluorescence its puncta formation has been widely used by numerous groups to illustrate AV formation and autophagy induction (Klionsky et al., 2008, Kimura et al., 2009). In addition to measuring the puncta formation of exogenous LC3, both in N2aSw cells (see figure 5.2) and the stable HEK 293 LC3-GFP cell line (see figure 5.3), the endogenous levels of both LC3 forms were shown in figure 5.4, which shows an increase similar to that of rapamycin that is also sensitive to 3-MA (see figure 5.4). The ratio of LC3-II/LC3-I, in combination with other measurements, as means to ascertain autophagy induction has been debated in several reviews and concluded to be very effective (Kadowaki and Karim, 2009). Therefore, it can be concluded that

specific GSK3 inhibition leads to an increase in the induction in autophagy and increased flux. This is firstly assumed by the fact that there is a concomitant decrease in the half-life of FL-APP but secondly there is also a decrease in the level of p62 (see figure 5.4). This protein operates to deliver protein-aggregates to autophagy compartments to aid their destruction and in doing so is itself degraded. As a result, many leading experts in the autophagy field have promoted its use as an indicator of autophagy flux (Bjørkøy et al., 2009, Kim et al., 2008). The autophagy flux was also shown to be increased by demonstrating a further increase in the LC3-II level in cells treated with GSK3 inhibitor VIII in combination with lysosomal inhibitors, compared with inhibitor VIII alone (Mizushima and Yoshimori, 2007).

It is of interest that the increase in LC3-GFP puncta with specific GSK3 inhibition is not associated with major cell toxicity, as shown from normal morphology, similar cell densities and previous preliminary observations of cell counts as discussed previously (see 4.3.3 Proteasomal and autophagy targeting of APP upon specific GSK3 inhibition).

These results show that the levels of beclin-1 remain largely unchanged when autophagy is induced by specific GSK3 inhibition. Previously, it was shown that beclin-1 is important for activating the PI3K class III in the ULK complex, which ultimately lead to the AV membrane formation. It has been stated that the protein levels of beclin-1 are probably not important for its activity but rather from altering its binding partners. As such, it can also be associated with Bcl-2 where it serves in regulating apoptosis (Codogno and Meijer, 2010, Levine et al., 2008). Thus, from these initial indirect assaying techniques it appears that indeed specific GSK3 inhibition in N2aSw cells, that are not undergoing apoptotic events, can result in autophagy induction and increased autophagy flux.

5.3.2 Specific GSK3 inhibition does not lead to a significant increase in autophagy vesicles

Showing that specific GSK3 inhibition can induce autophagy, it was surprising that further analysis with TEM displayed no difference in the number of autophagy compartments. Inspection of the cytoplasm of the cells showed a strong basal level of autophagy compartments that had a typical morphology and did not appear to be altered by specific GSK3 inhibition, such as enlargement, which can occur from disruption of correct fusion with lysosomes. In this respect, this ultrastructure

analysis is in line with the previous observations of increased autophagy flux. However, immuno-gold labelling of LC3-II should be carried out in order to give absolute confirmation of autophagy structures. Immuno-gold labelling is an extremely technical method with multiple steps requiring expert optimisation. A literature search has found detailed protocols in order to do this in mammalian cell-lines, which would be an initial step for further optimisation for the cell-lines used here and the antibodies (Ylä-Anttila et al., 2009).

However, there is a dichotomy between an increase in LC3-II/I ratio and LC3-GFP puncta formation with GSK3 inhibition, and the lack of a corresponding increase in AV compartments as shown by TEM. There are certainly previous indications that LC3-II can bind to protein aggregates in a process independent of autophagy (Kuma et al., 2007, Shvets and Elazar, 2008) and LC3-GFP can form punctate staining upon certain staining protocols (Ciechomska and Tolkovsky, 2007). This illustrates the point that transient expression of LC3-GFP and formation of puncta do not always represent AV formation. In defence of this argument, it should be reiterated that the amount of overexpression was kept to a minimum, aided by preliminary optimisation of the assay and the LC3-GFP puncta formation behaved characteristically in response to serum starvation and 3-MA treatment (see figure 5.2). Secondly, these results were also repeated in a HEK 293 cell line that stably expresses the LC3-GFP and does not have aggregate artefacts (see figure 5.3). In addition, the endogenous LC3-II levels from N2aSw cells were also found to be sensitive to serum starvation, rapamycin and 3-MA (see figure 5.4). A possible explanation could be that the specific GSK3 inhibition causes protein aggregation for both exogenous and endogenous LC3-II to be incorporated and, therefore, accumulate within the cell. Further still it has been shown that these autophagy-independent aggregates can bind to p62, which is usually involved in the chaperone of aggregates to the autophagosome structures for destruction (Shvets and Elazar, 2008, Shvets et al., 2008). The assessment of p62 activity is a critical issue, as its knockdown is associated with decreased turnover of protein-aggregates and even a neurodegenerative phenotype in mice (Ramesh Babu et al., 2008). The concomitant decrease in p62 protein level shown in figure 5.3, which is indicative of an increased flux of degradation (Bjørkøy et al., 2009), would argue against that the GFP puncta formations observed are aggregates of LC3. However, measurement of the p62 mRNA is required to prove that the decreased p62 protein expression is the result of

increased targeting and degradation by autophagy and not simply reduced transcriptional expression. Further assays of metabolic labelling with tritium could be used to show a general increase in protein degradation (Morales-Corraliza et al., 2009).

5.3.3 Specific GSK3 inhibition led to an increase in lysosome vesicles

In this study it is shown that treatment of N2aSw cells with the specific GSK3 inhibitor VIII results in a dramatic increase in the number of lysosomal compartments. This was first shown from ultrastructure analysis of cultured cells and later confirmed by the molecular probe, Lysotracker®-Red and also LAMP1 staining in cultured cells.

The increase in the lysosomal compartments could also explain the increase in autophagy flux seen with specific GSK3 inhibition, as the associated degradation can only come from the fusion of an AV compartment with a lysosome, which contains the necessary proteases. Therefore, increasing the number of lysosomes may lead to increased fusion with AV compartments and accelerate the rate of degradation normally associated with a basal level of autophagy-mediated processing of FL-APP.

5.3.4 Specific GSK3 inhibition results in an increase of TFEB nuclear localisation

This increase in lysosomal biogenesis is likely the result of the nuclear translocation of TFEB upon specific GSK3 inhibition. This transcription factor was found to be a master regulator for lysosomal biogenesis and also links increased autophagy-mediated degradation with an increase in lysosomal production (Settembre et al., 2011, Settembre and Ballabio, 2011, Cuervo, 2011). This study found that stimulation through the MAPK pathway results in the serine-phosphorylation and sequestration of TFEB to the cytoplasm. However, decreased TFEB phosphorylation results in nuclear-shuttling of TFEB and induction of several key genes required for lysosomal and autophagy biogenesis. As there are links between this MAPK pathway and GSK3, with particular reference to ERK1/2 signalling, it is conceivable that there are crosstalk mechanisms that regulate the sequestration of TFEB (Palmieri et al., 2011). Furthermore, the present study also illustrates the ability for GSK3 to phosphorylate TFEB. At the moment, this preliminary data only implicates GSK3 in transactivation of lysosomal biogenesis and will require further experimentation (see CHAPTER 7: DISCUSSION).

5.3.5 FL-APP degradation induced by specific GSK3 inhibition is dependent on lysosomal degradation

As specific GSK3 inhibition led to a decrease in the protein level of p62, this suggests that GSK3 inhibition can indeed increase autophagy flux. The increased autophagy flux is likely the result of increased lysosomal biogenesis and fusion with autophagosome structures. This could have consequences in protein degradation, such as the effect we observe on FL-APP after specific GSK3 inhibition.

APP is internalised and processed through the endocytic-lysosomal pathway. In the present study, there is an increase in the colocalisation of APP with LAMP1-positive vesicles as shown from confocal microscopy (see figure 5.8). Moreover, co-incubation with leupeptin, a broad inhibitor of lysosomal proteases, blocks the degradation of FL-APP induced by specific GSK3 inhibition (see figure 5.11). Thus specific GSK3 inhibition appears to promote the basal targeting of FL-APP to the lysosomes for degradation. Unknown at this juncture is whether the increased degradation of FL-APP with specific GSK3 inhibition is just by driving the basal level degradation or also by actively targeting APP to be degraded in a chaperone-mediated manner. Interestingly, direct interaction between LC3-I/II and APP/APLP has been reported very recently (Zhou et al., 2011). It would be prudent to demonstrate if the increased degradation of FL-APP seen with specific GSK3 inhibition is mediated through a direct binding of APP to both forms of LC3. Such a mechanism would constitute the basis for chaperone-mediated autophagy (CMA), a more specific autophagy response than the better understood macroautophagy, which is associated with general cytoplasmic and organelle digestion. This scenario coincides with the data of p62, because its targeting of aggregates to autophagosomes function is dependent on a chaperone effect of LC3 (Shvets et al., 2008). This chaperone-mediated response is also described in microautophagy, where there is direct targeting of the protein to the lysosome or engulfment of cytoplasmic material directly involves the lysosome and sidesteps the need for autophagosome formation (Cuervo, 2011). The dramatic increase in lysosomal compartments may argue for a microautophagy process driving the degradation of FL-APP. Microautophagy, to date, is poorly understood and it is unknown as to whether LC3 plays a role in the dynamics of microautophagy as it does with macroautophagy. Therefore, this raises the issue as to why the FL-APP degradation induced by specific GSK3 inhibition is sensitive to 3-MA and beclin-1 silencing. The issue that there are no other specific

autophagy markers make it very complicated to give a definitive answer to the question as whether autophagy vesicle number increases by specific GSK3 inhibition. It can only be concluded firmly at this point that the present results suggest that specific GSK3 inhibition induces degradation of FL-APP by increasing the levels of lysosomal proteases in autophagy.

CHAPTER 6 : THE ROLE OF CANONICAL WNT SIGNALLING IN THE REGULATION OF APP PROCESSING

6.1 Introduction

As outlined earlier (see 2.9 Wnt cascade and AD) there is a strong genetic and mechanistic link between the canonical Wnt cascade and AD. Alterations in the Wnt signalling pathway may play an important role in the pathogenesis of AD because of its effects on axonal growth, synaptogenesis and Aβ toxicity. β-catenin is a key regulator of the canonical Wnt signalling pathway. Very few studies have analysed expression of β-catenin in adult tissues of any model organism. Some reports show strong β-catenin staining of brain subventricular zones and areas with neurogenesis indicative of functions in cell proliferation of pluripotent cell types. Recently, β-catenin was found to play a significant role in memory consolidation *in vivo* (Maguschak and Ressler, 2008). A direct link of the Wnt pathway to a neuroprotective role against Aβ toxicity was shown in rat cortical neurones by Wnt3a attenuation of neurotoxicity through binding to the Frizzled receptor-1 (Chacón et al., 2008). Other studies have shown that Aβ binds to the CRD of the Frizzled receptor (Magdesian et al., 2008). However nothing is known of any regulatory role this pathway has on APP processing.

The conclusions from the previous chapters illustrate that specific inhibition on GSK3 results in reduced Aβ production, BACE1 expression, β-secretase activity and increased degradation of FL-APP resulting from increased lysosomal biogenesis.

Therefore it was hypothesised that at least part of the regulation on APP processing by GSK3 may lay downstream of the canonical Wnt cascade, as it is known that GSK3 is a negative regulator of this signalling pathway. As canonical Wnt stimulation results in inactivation of GSK3, the aim of this chapter was to investigate whether canonical Wnt stimulation would replicate the same effects of specific GSK3 inhibition on APP processing.

In the case that canonical Wnt stimulation affects the processing of APP, it needs to be investigated whether these effects are mediated through the downstream activation of β-catenin and the subsequent transactivation of Wnt target genes. Interestingly, pharmacological GSK3 inhibition affected the transcriptional regulation

of mouse *Bace1* as shown in sections 4.2.3.1 (Specific GSK3 inhibition results in a decrease in β-secretase activity, transcription and expression of BACE1) and 4.2.3.2 (Transient overexpression of GSK3 led to an increase in BACE1 expression). Therefore, it could be possible that *Bace1* is transcriptionally regulated by β-catenin.

The third and final aim of the project was to investigate whether activation of the canonical Wnt signalling cascade can affect APP processing and if so, to determine what mechanism(s) are involved.

As activation of the canonical Wnt pathway results in inhibition of GSK3, some of the outcomes should be similar to those found by GSK3 pharmacological inhibition.

In addition, the specific role of β-catenin transactivation on the processing of APP was evaluated.

6.2 Results

6.2.1 Alterations in the activity of the canonical Wnt cascade affect APP processing

In order to study the activation of the canonical Wnt pathway, Wnt3a and β-catenin S33 (mutated at serine 33, which is resistant to proteasomal degradation) cDNAs were transiently transfected into N2aSw cells. The Wnt3a is a ligand that has been associated with canonical Wnt stimulation (MacDonald et al., 2009). To assess the transfection efficiencies and the ability of the constructs to activate the cascade, the stabilised level of β-catenin was measured from the total-lysate of N2aSw cells by Western blotting (see figure 6.1). In both cases, there was an increase in the protein level of β-catenin. This was taken a step further by measuring the functional significance of increasing the expression of stabilised β-catenin. For this purpose, N2aSw cells were transiently transfected with a luciferase construct that was either downstream of a consensus LEF/TCF promoter (TOPflash) or a mutant promoter (FOPflash). Again, in both cases the luciferase activity from the LEF/TCF consensus promoter was significantly higher in cells expressing Wnt3a and β-catenin S33. The Firefly luciferase activity was normalised to the expression of the *Renilla* luciferase signal, which was expressed constitutively. This allowed for normalisation owing to different transfection efficiencies between groups. Induction was expressed as percentage of control (pcDNA3/ TOPflash) (see figure 6.2). This was comparable to the direct addition of mouse recombinant Wnt3a, which showed significant induction at 10nM and 20nM. N2a cells have previously been shown to be responsive to Wnt3a (Magdesian et al., 2008). The activation of the canonical Wnt cascade by the addition of recombinant Wnt3a was attenuated by knocking down the expression of β-catenin with a specific shRNA transiently expressed in the same N2aSw cells (see figure 6.2C).

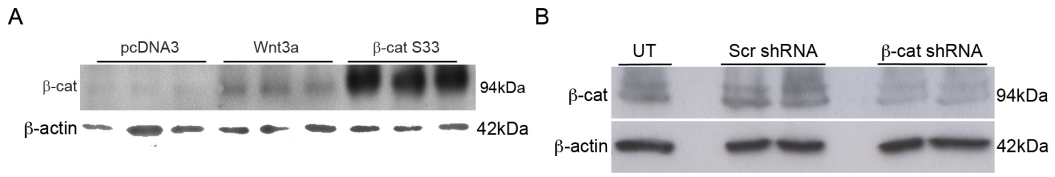


Figure 6.1: Confirmation of transfection with Wnt3a, β-catenin and β-catenin shRNA and the effect on β-catenin levels.

(A) Representative Western blots for β-catenin from total-lysates in N2aSw cells transiently transfected with the following constructs: pcDNA3, Wnt3a and β-catenin S33. (B) Reduced expression of β-catenin from total-lysates in cells transiently transfected with β-catenin shRNA. A scrambled shRNA construct was used as a control.

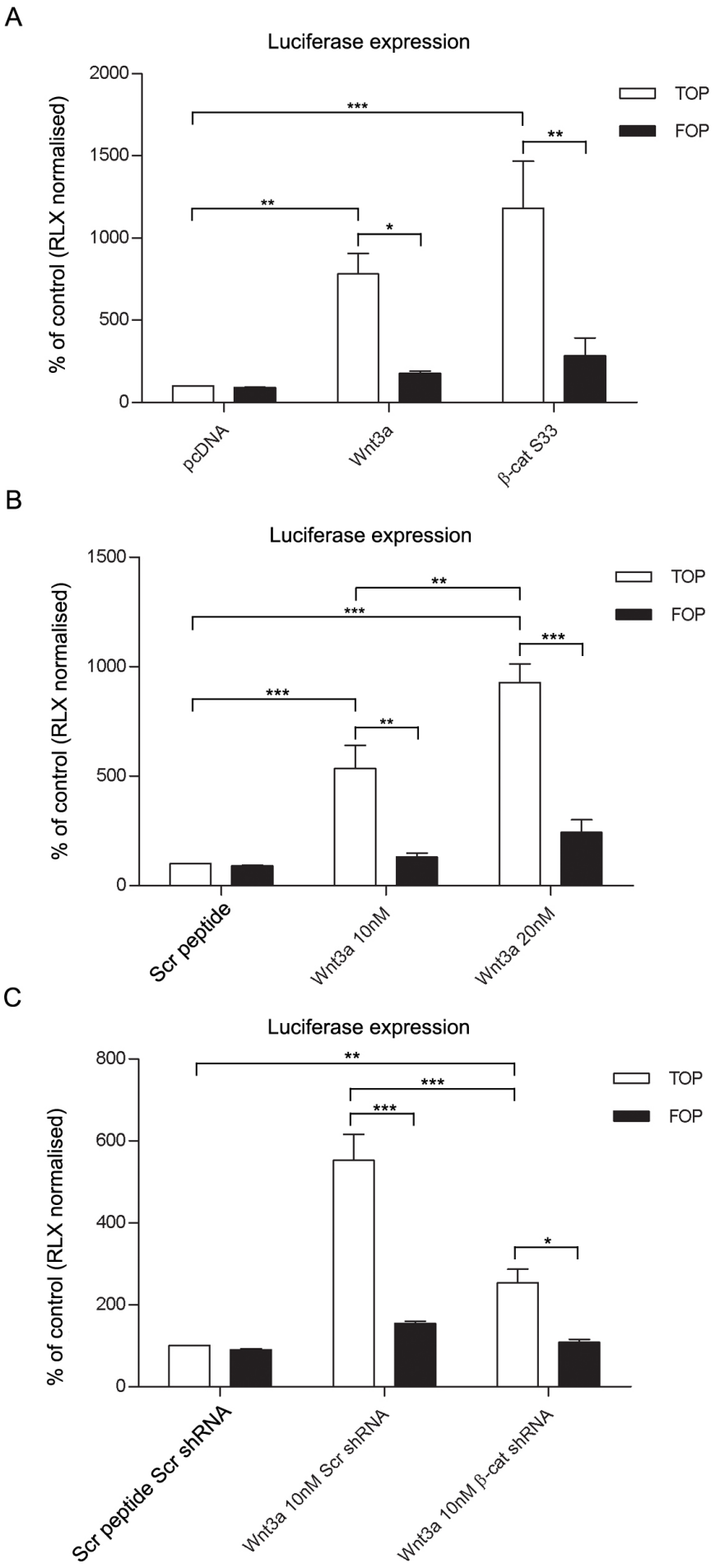

A
Luciferase expression
% of control (RLX normalised)
2000
1500
1000
500
0
TOP
FOP
***
**
**
*
pcDNA
Wnt3a
β-cat S33
B
Luciferase expression
% of control (RLX normalised)
1500
1000
500
0
TOP
FOP
**
***
***
***
**
Scr peptide
Wnt3a 10nM
Wnt3a 20nM
C
Luciferase expression
% of control (RLX normalised)
800
600
400
200
0
TOP
FOP
**
***
***
*
Scr peptide Scr shRNA
Wnt3a 10nM Scr shRNA
Wnt3a 10nM β-cat shRNA

Figure 6.2: Wnt3a and β-catenin overexpression led to induction of the canonical Wnt cascade.

(A) N2aSw cells expressed a Firefly luciferase construct that was either downstream of a consensus LEF/TCF promoter (TOPflash) or a mutant promoter (FOPflash). The canonical Wnt cascade was significantly activated by the overexpression of either Wnt3a or the stabilised β-catenin S33 when compared to cells transfected with just pcDNA3. There was a significant difference between the TOPflash and FOPflash with both Wnt3a and β-catenin S33 overexpression. The Firefly luciferase activity was normalised to the expression of *Renilla* luciferase (RLX), which was expressed constitutively. This allowed for normalisation of different transfection efficiencies between the different treatment groups. Induction was expressed as percentage of control (pcDNA/TOPflash). This activation was comparable to direct addition of mouse recombinant Wnt3a to the culture medium (B). (C) Knockdown of β-catenin attenuates the recombinant mouse Wnt3a induced luciferase expression. One-way ANOVA was used to assess the significance of the differences between the TOPflash and FOPflash independently and a Tukey's post-hoc test assessed differences to control (A) or the pairwise combinations (B-C), *P<0.05, **P<0.01 and ***P<0.001.

To determine whether activation of the canonical Wnt cascade could affect APP processing, the Wnt3a ligand was overexpressed in N2aSw cells. Activation by Wnt3a decreased Aβ generation by 32.25% ±5.00 (mean value ±SEM.***P<0.001) (see figure 6.3A) but did not affect the levels of sAPPα (see figure 6.3D). The addition of recombinant mouse Wnt3a to the medium of N2aSw cells reproduced the same effects as Wnt3a transfection, resulting in reduced levels of secreted Aβ by 41.00% ±6.00 and 52.00% ±5.00 with 10nM and 20nM of recombinant Wnt3a respectively (mean values ±SEM. **P<0.01 and **P<0.001 based on n=9 per group) (see figure 6.3B).

β-catenin S33 transfection also resulted in decreased Aβ secretion by 27.90% ±3.51 (mean value ±SEM.***P<0.001) (see figure 6.3A), without changing the sAPPα production (see figure 6.3D). Interestingly, β-catenin knockdown with shRNA led to a significant increase in the generation of Aβ by 52.04% ±23.25 (mean value ±SEM.*P<0.05 based on n=12 per group) compared to cells treated with scrambled shRNA (see figure 6.3C). There was a trend for a decrease in the production of the sAPPα from cells with reduced levels of β-catenin by shRNA knockdown, but this was not significant.

Because it was shown previously that specific pharmacological inhibition of GSK3 reduced the total level of FL-APP, it was determined whether canonical Wnt activation also altered FL-APP expression. Wnt3a transfection resulted in a decrease in FL-APP expression by 18.39% ±6.91 (mean value ±SEM. *P<0.05 based on n=9

per group). Although there was a trend for a decrease in FL-APP, transfection with β-catenin S33 did not significantly affect the levels of FL-APP (see figure 6.3G). In addition, β-catenin shRNA did not reverse the effect of pharmacological inhibition of GSK3 on the levels of FL-APP (see figure 6.3H), indicating that this destabilisation event is not mediated through downstream effects of β-catenin signalling.

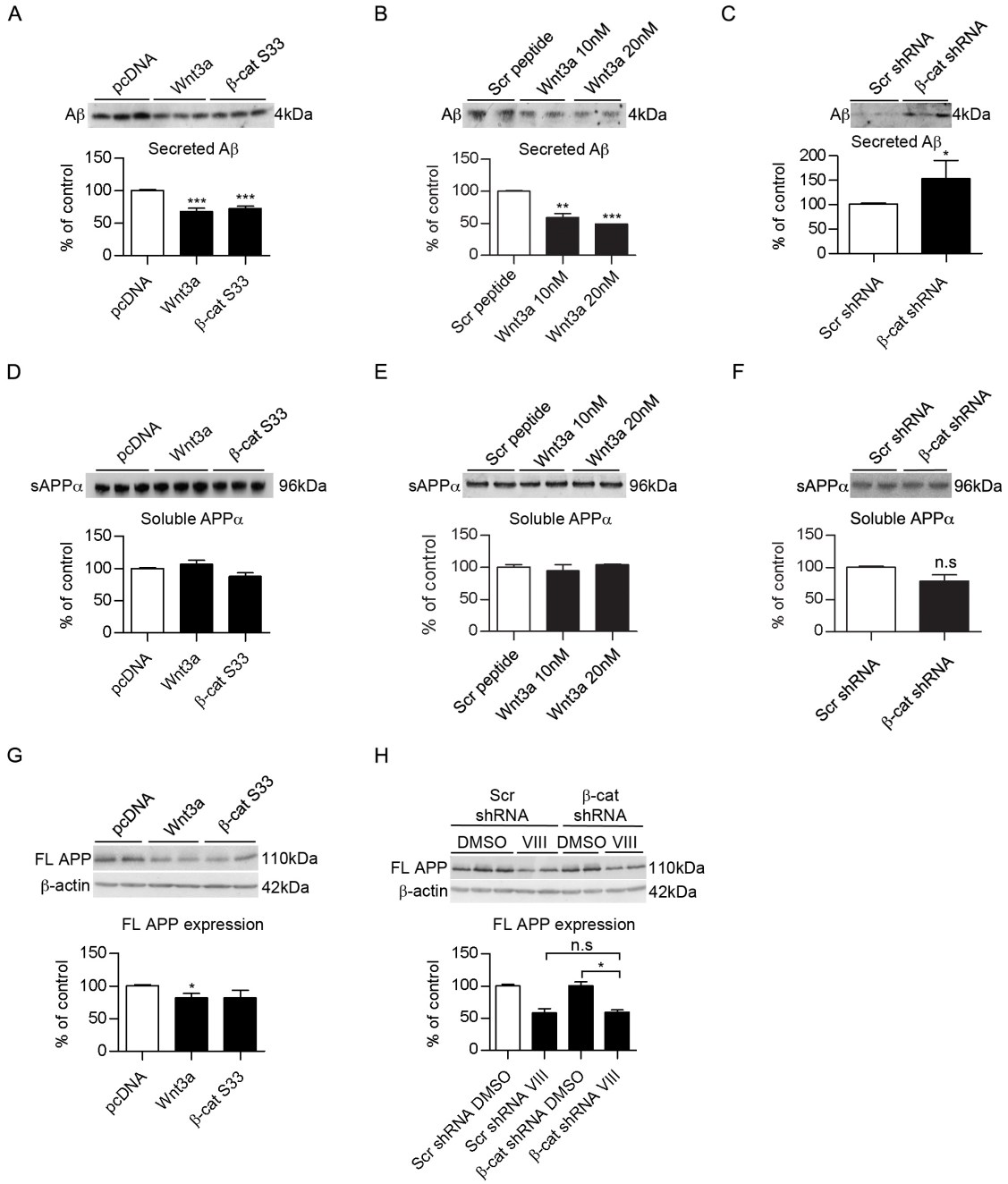


Figure 6.3: Changes in the canonical Wnt cascade activity affect APP processing.

Representative blots and quantification. (A) Transient overexpression of Wnt3a and β-catenin S33 results in a significant decrease of 32.25% ±5.00 and 27.90% ±3.51 in the production of Aβ, respectively (n=12 per group). (B) Similarly there was a significant decrease in Aβ of 41.00% ±6.00 and 52.00% ±5.00 with 10nM and 20nM by treatment with recombinant Wnt3a respectively (n=9 per group). (C) In contrast, β-catenin knockdown resulted in a significant increase in the amount of secreted Aβ by 52.04% ±23.25 (n=12 per group). There was, however, no significant alteration in the amount of secreted sAPPα when the activity of the canonical Wnt cascade was altered (D-F). (G) There was a significant decrease in the protein level of FL-APP of 18.39% ±6.91 with Wnt3a overexpression and a trend for a decrease with β-catenin S33 overexpression. (H) N2aSw cells were either transiently transfected with shRNA specific for β-catenin or a scramble control. These transfected cells were either treated with DMSO or 5μM VIII overnight. The decreased FL-APP protein expression mediated by specific GSK3 inhibition could not be rescued by knocking down β-catenin (n=9 per group). Values shown in graphs represent the mean value ±SEM and expressed as a percentage of control. One-way ANOVA with a post-hoc Tukey's test (B, E and H) and an unpaired t-test (A, C-D and F-G) were used to show statistical significance in the differences between the means, *P<0.05, **P<0.01 and ***P<0.001.

6.2.2 Canonical Wnt stimulation affects mouse *Bace1* transcription

In agreement with the results obtained with pharmacological inhibition of GSK3, stimulation of the canonical Wnt cascade upstream and downstream of GSK3 by transient transfection of Wnt3a and β-catenin S33 resulted in an alteration in the transcription, expression and activity of BACE1 (see figure 6.4). The production of β-CTF was reduced by 36.90% ±9.35 and 47.13% ±5.35 in N2aSw cells overexpressing Wnt3a and β-catenin S33 respectively (mean value ±SEM. *P<0.05 and **P<0.01 based on n=6 per group). The BACE1 protein level was reduced by 37.93% ±9.88 (mean value ±SEM. *P<0.05) and 37.46% ±12.03 (mean value ±SEM. *P<0.05 based on n=12) (see figure 6.4B) by Wnt3a and β-catenin S33 overexpression respectively. This was associated with a decrease in *Bace1* mRNA levels and in the activity of the BACE1 promoter (see figure 6.4C and D). However, this effect was stronger with Wnt3a compared to β-catenin S33 overexpression because β-catenin S33 transfection resulted only in a slight and non-significant reduction in *Bace1* mRNA levels. The effect of pharmacological GSK3 inhibition on BACE1 levels was not completely reversed by β-catenin knockdown (see figure 6.4E).

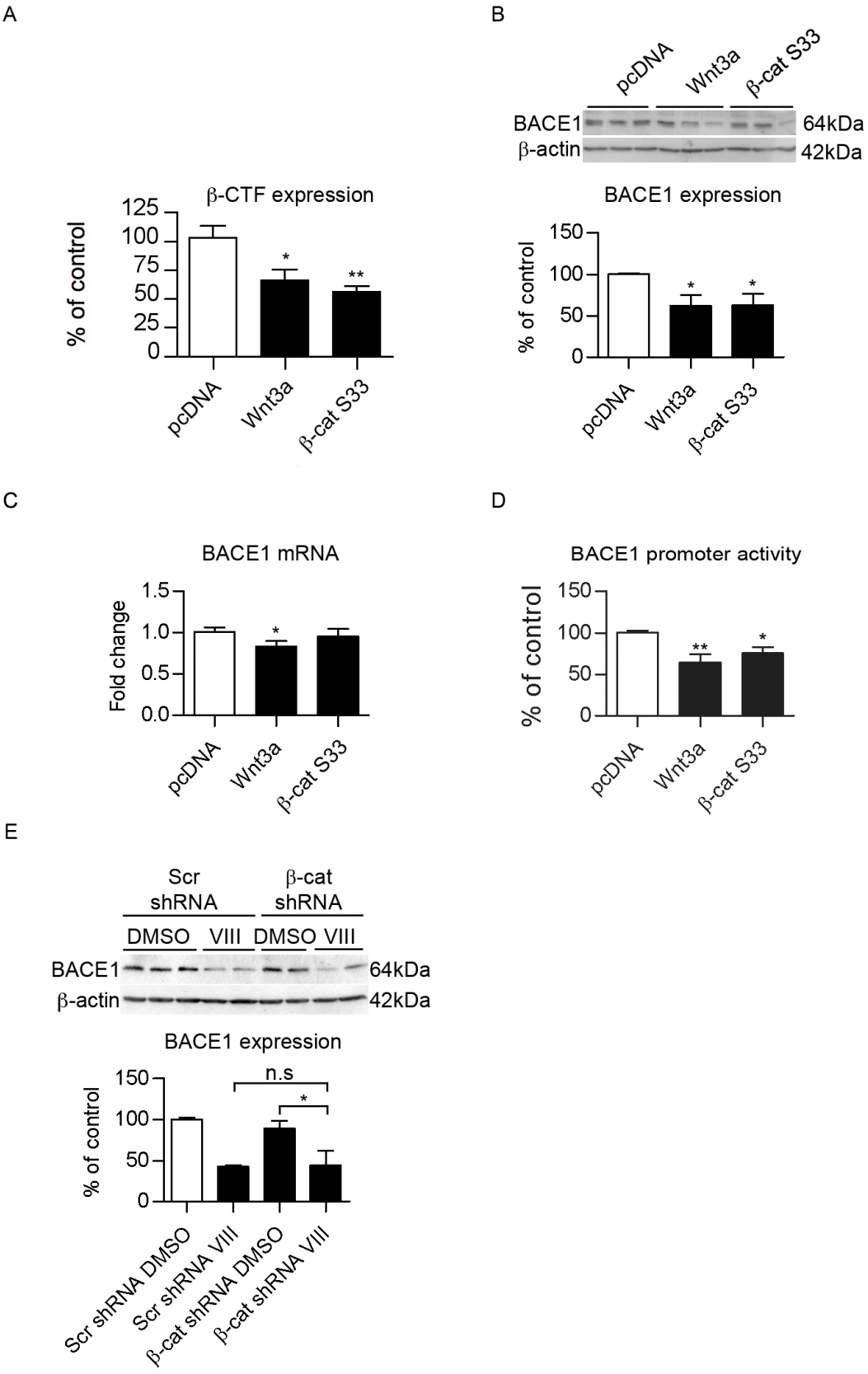

A
β-CTF expression
% of control
125
100
75
50
25
0
*
**
pcDNA
Wnt3a
β-cat S33
B
pcDNA
Wnt3a
β-cat S33
BACE1
β-actin
64kDa
42kDa
BACE1 expression
% of control
150
100
50
0
*
*
pcDNA
Wnt3a
β-cat S33
C
BACE1 mRNA
Fold change
1.5
1.0
0.5
0.0
*
pcDNA
Wnt3a
β-cat S33
D
BACE1 promoter activity
% of control
150
100
50
0
**
*
pcDNA
Wnt3a
β-cat S33
E
Scr shRNA
β-cat shRNA
DMSO
VIII
DMSO
VIII
BACE1
β-actin
64kDa
42kDa
BACE1 expression
% of control
150
100
50
0
n.s
*
Scr shRNA DMSO
Scr shRNA VIII
β-cat shRNA DMSO
β-cat shRNA VIII

Figure 6.4: Altering the activity of the canonical Wnt cascade affects the expression of BACE1.

Quantification and representative blots. (A) Stimulation of the canonical Wnt cascade by Wnt3a and β-catenin S33 overexpression in N2aSw cells results in a reduction in the production of the β-CTF detected from membrane preparations by 36.90% ±9.35 and 47.13% ±5.35 respectively (mean value SEM) (n=6 per group). (B) Wnt3a and β-catenin S33 overexpression in N2aSw cells results in a decrease of 37.93% ±9.88 and 37.46% ±12.03 respectively in the protein level of BACE1 from membrane preparations (n=12 per group). In line with a decrease protein expression, there was both a decrease in the (C) mRNA (n=9 per group) and (D) the BACE1 promoter activity with the same conditions (n=12 per group). (E) N2aSw cells were either transiently transfected with shRNA specific for β-catenin or a scramble control. In combination these transfected cells were either treated with DMSO or 5μM VIII overnight. Values shown in graphs represent the mean value ±SEM and expressed as a percentage of control. One-way ANOVA with a post-hoc Tukey's test (E) or an unpaired t-test (A-D) were used to show statistical significance in the differences between the means, *P<0.05 and **P<0.01.

6.2.3 β-catenin protein levels are reduced in the brains of sporadic AD patients

It was previously reported that familial mutations in *PSEN1* could affect the stabilisation of β-catenin leading to an alteration in its steady state level (see 2.9.2 *PSEN1* mutations and regulation of cytoplasmic β-catenin). This could be explained by the physical interaction of PSEN1 and β-catenin at the cell membrane (Kang et al., 1999). In addition, brains from FAD patients with *PSEN1* polymorphisms have shown a significant decrease in the level of β-catenin. Interestingly, while there is a clear functional interaction between FAD PSEN1 and β-catenin levels, there are no reported changes in β-catenin levels in SAD patients (Zhang et al., 1998a). We therefore explored whether β-catenin levels were altered in sporadic cases of AD by performing subcellular fractionation of frontal-cortex tissue from 6 non-demented (ND) control patients (3M, 3F, 85±8 year old) and 7 SAD patients (3M, 4F, 81±5 years). The expression of β-catenin was studied in these fractions by Western blotting and it was normalised to the loading control of each fraction. Preliminary Western analysis showed the nuclear fraction was absent for β-actin and β3-tubulin but positive for histone 4 (H4) while the cytoplasmic fraction was positive for β-actin and β3-tubulin but very little H4 expression. For each fraction, the densitometry (see 3.7 Western blotting) of β-catenin staining was normalised to its respective marker. There was a significant decrease of 30.73% ±6.73 (mean value ±SEM. **P<0.01 based on n=6 for SAD cases and n=7 for ND cases) in total β-catenin levels within the nuclear

fraction in AD cases compared to healthy controls. However, no significant changes were detected in the other two cell fractions of either phosphorylated or unphosphorylated β-catenin forms (see figure 6.5A-C). The nuclear fraction represents the functional compartment wherein β-catenin operates as a transcription factor for the canonical Wnt pathway.

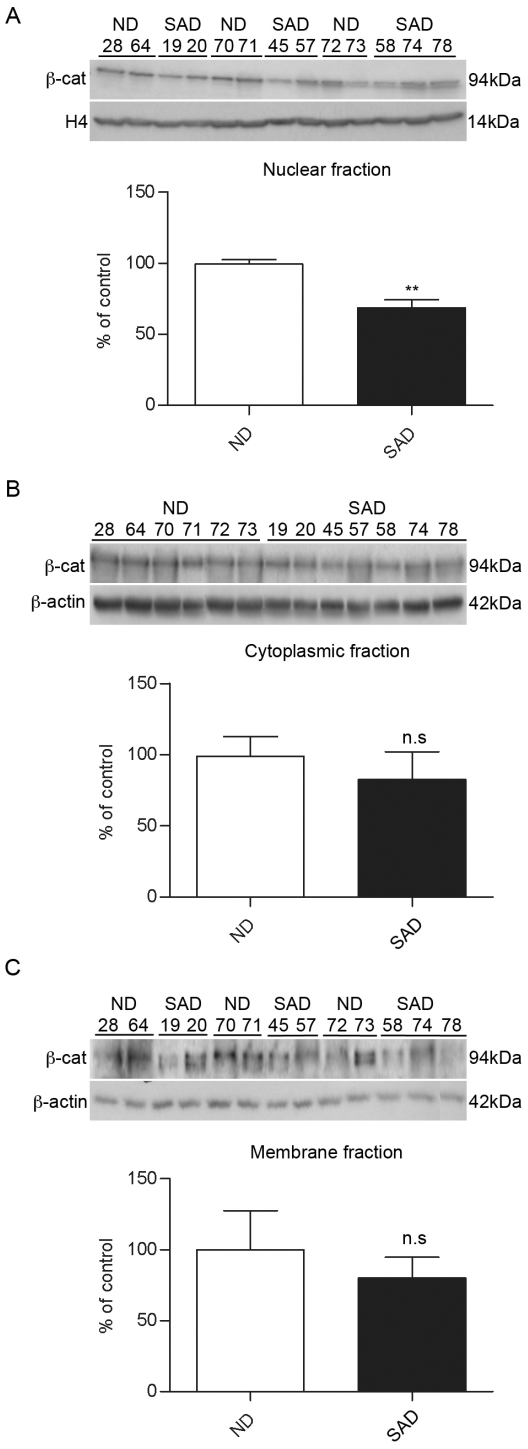


Figure 6.5: Nuclear β-catenin levels are reduced in post-mortem sporadic AD brains.

Western blots and quantification. Frontal-cortex from non-demented (ND) and sporadic AD (SAD) brains were crudely fractionated for nuclear (A), cytoplasmic (B) and membrane (C) fractions. The densitometry was normalised to that of the fraction marker. From each, the total β-catenin protein level was probed by blotting with the mouse monoclonal anti-β-catenin antibody (BD Biosciences) (n=6 for ND brains, 3M, 3F, 85yrs ±8. n=7 for SAD brains, 3M, 4F, 81yrs ±5). Values shown in graphs represent the mean value ±SEM and expressed as a percentage of control. The unpaired t-test was used to show statistical significance in the differences between the means, **P<0.01.

6.3 Discussion

Several studies have linked the canonical Wnt cascade and its dysregulation to the pathogenesis of AD. A recent unbiased systems biology approach identified several AD associated genes as direct targets of canonical Wnt induction, such as *APP*, *BACE1*, *PSEN1* and *DR6* in addition to the fronto-temporal dementia associated *MAPT* and *GRN* (Wexler et al., 2010, Rosen et al., 2011).

It has been reported that Aβ neurotoxicity on cortical neurones can be neutralised by the addition of Wnt3a, blocking its interaction with Frizzled-1 and leading to a reduction in caspase-3 activation and apoptosis (Chacon et al., 2008). Aβ could well have a role in synaptogenesis and plasticity, which are highly regulated by the canonical Wnt cascade because it was shown that indeed Aβ can bind to the extracellular CRD of Frizzled-1 and inhibit Wnt/β-catenin signalling (Magdesian et al., 2008). However, it is known that Aβ is a very sticky protein and could bind the receptor non-specifically and as such further work is required to prove this point. It is of interest that Aβ can promote LTD (Hsieh et al., 2006) while inhibiting LTP (Walsh et al., 2002, Shankar et al., 2008) in a process involving an axis of caspase-3/Akt/GSK3 (Li et al., 2010b).

In addition, neuroprotective Wnt signalling is significantly reduced in most of the genetic risks to AD and in familial AD; such as *PSEN1* linked FAD (Zhang et al., 1998), *APOE4* (Caruso et al., 2006) and FAD associated with *LRP6* polymorphisms (De Ferrari et al., 2007). Here it is shown that there is a reduction in nuclear β-catenin in SAD patients (see figure 6.5). This is in line with a recent paper that shows that glial progenitor cells (GPCs) from AD patients exhibited elevated levels of GSK3β, accompanied by an increase in phosphorylated β-catenin and a decrease in nonphosphorylated β-catenin compared with healthy counterparts (He & Shen, 2009). This provides yet more evidence that in terms of the underlying pathogenesis, FAD may display similar mechanisms as the more common sporadic disease, albeit played in a fast forward speed. Furthermore, this disruption in β-catenin levels in SAD cases may result from the effect of other AD relevant proteins, such as APP, which can alter the stabilisation of β-catenin in mechanism similar to what has been described for PSEN1 in FAD patients (Chen and Bodles, 2007).

6.3.1 Canonical Wnt induction influences APP processing via its negative regulation of GSK3

As direct GSK3 inhibition affects APP processing, and GSK3 is a major regulator of the Wnt pathway, there could be a potential role for canonical Wnt signalling in the control of APP cleavage and degradation (see chapters 4 and 5).

Within nature, GSK3 activity can be negatively regulated by different mechanisms:

1. Via an inhibitory phosphorylation event of the regulatory N-terminal Ser9/21 of GSK3α/β respectively. A typical example of which is Akt signalling in the PI3K/Akt survival cascade (Medina and Wandosell, 2011).

2. An intracellular sequestration model that has largely been characterised from canonical Wnt signalling. Until recently, understanding of this mechanism was far from complete but additional information is now available to produce a clearer picture (Taelman et al., 2010).

In chapters four and five the focus of study has mainly been on pharmacological regulation of GSK3 through drugs that inhibit by outcompeting ATP molecules required for kinase activity or through reduced expression of GSK3. Such mechanisms therefore differ substantially from the two modes of GSK3 regulation highlighted above. It is also important that the downstream effects from GSK3 inhibition can vary dramatically depending on the manner in which it is inhibited. For example, specifically in the canonical Wnt cascade, GSK3 activity is defined within the destruction complex that is made up of several direct binding partners including priming kinases that alter its activity and substrate specificity.

Therefore, it cannot be assumed that negative regulation of GSK3 from upstream would lead to the same effects as direct chemical inhibition of GSK3 as reported in previous chapters. Furthermore, if canonical Wnt induction can regulate APP processing, it could be that this is associated with either Wnt target gene activation mediated by β-catenin stabilisation or through reduced GSK3 activity on its many other targets. Certainly, the latter could well be the case concerning the degradation of FL-APP, which as described in the previous chapter is likely the result of autophagy-lysosomal degradation (see 5.3.4 Specific GSK3 inhibition results in increased TFEB nuclear localisation).

Here it is shown for the first time that indeed the canonical Wnt cascade can regulate APP processing whereby Wnt stimulation reduces the Aβ production. This effect was shown either by overexpression of Wnt3a (upstream of GSK3) or β-catenin (downstream of GSK3). Conversely, when β-catenin was knocked down there was an increase in the amyloidogenic processing of APP. In addition, we observed a reduction in the FL-APP protein level by Wnt3a activation. This effect is similar to that found by pharmacological inhibition of GSK3 with the inhibitor VIII. However, this effect on FL-APP was not significantly reproduced by β-catenin S33 overexpression. This suggests that the reduction of APP levels by specific GSK3 inhibition is independent on the transcriptional function of β-catenin. To further support this point, knockdown of β-catenin did not reverse the effect of specific GSK3 inhibition on the decrease in FL-APP.

6.3.2 Canonical Wnt induction affects BACE1 transcription

Another possible explanation for a reduction in the Aβ load by the canonical Wnt pathway could involve the reduction in the activity of β-secretase, which is seen as the rate-limiting step in the amyloidogenic pathway of APP. As shown there was an observed reduction in the β-secretase activity by detection of the levels of β-CTF. The control of BACE1 transcription by the canonical Wnt pathway could occur through the interactions of β-catenin with nuclear receptors (Mulholland et al., 2005), such as the RAR (retinoic acid receptor), the oestrogen receptor, and the PPARs (PGC1-α peroxisome-activated receptor), which have been reported to affect the expression of BACE1 (Sastre et al., 2006b). However, this is not completely clear, since β-catenin knockdown did not reverse the effects of GSK3 inhibition on BACE1 expression.

Recently β-catenin was shown to have two distinct functions when released after canonical Wnt activation. First, and already well known, is the transactivation of genes targeted by the canonical Wnt cascade. In addition and unexpectedly, it has recently been shown that the sequestration model for GSK3 inhibition is also actually dependent on β-catenin. Overexpression of a similar stabilised β-catenin construct resulted in an increased sequestration of GSK3 in MVB structures, thus limiting its activity in the cytosol (Taelman et al., 2010). In our own paradigm, β-catenin S33 therefore could be an additional inhibitor of GSK3 and mimic Wnt3a and chemical inhibition. However, this would need further investigation in order to confirm that

there was indeed a concurrent sequestration of GSK3. This hypothesis can only be confirmed after further experimentation (see CHAPTER 7: DISCUSSION).

CHAPTER 7 : DISCUSSION

7.1 Introduction

Despite almost twenty-five years of molecular-level research that has made fundamental breakthroughs, the situation regarding AD therapy is seemingly in stasis. This is highlighted by the recent announcement of three failures at phase-3 that were designed to intervene in the production or promote the clearance of Aβ. More often than not, the reported absence of clinical improvement has resulted from the lack of efficacy, low therapeutic-index, intervening at too late a stage or a combination of these factors (Selkoe, 2011). The duration of the treatment is also a critical factor and, since AD is a disease with a long pre-clinical period, trials of short duration in severe cases of AD do not provide reliable information regarding the development of AD (Bennett and Whitmer, 2009). Despite the degree of supporting evidence, there has been an increasing amount of scepticism for the amyloid cascade hypothesis. Thankfully, the differing factions within the AD field have suggested either completely differing alternatives to the amyloid cascade hypothesis (Pimplikar et al., 2010), such as the autophagy hypothesis (Nixon, 2007, Barnett and Brewer, 2011, Ling and Salvaterra, 2009) or a much broader scheme such as the GSK3 hypothesis that connects the separate elements (Hooper et al., 2008). The latter illustrates that the differing views need not be mutually exclusive, for instance the dichotomy of the BAPtist reliance on the amyloid pathology and TAUists dependence on the tau pathology is a false one. Animal modelling has since resolved their exclusivity placing tau downstream of amyloid. In addition there is plenty of evidence that the two can interact with each other (Small and Duff, 2008).

7.2 GSK3 hypothesis of AD

Owing to the almost omnipotence of GSK3 in cellular signalling, dysregulation of its activity has been linked to a wide array of human disease. A natural consequence of this is that GSK3 has been studied from different angles and these can be assimilated to form a more comprehensive knowledge of this important signalling kinase including its rather complex regulation (Medina and Wandosell, 2011) (see 2.8.2 Regulation of GSK3). Activation of GSK3 is found in a number of degenerative diseases including AD, Parkinson's disease, Huntington's disease, in addition to other

syndromes like schizophrenia, and diabetes (Hooper et al., 2008, Frame and Zheleva, 2006). Insulin induces inactivation of GSK3, which can contribute to stimulation of glucose uptake and glycogen synthesis (Jope and Johnson, 2004). There is the hypothesis that failure to inactivate GSK3, as a result of insulin deficiency and impaired insulin signalling (insulin resistance) could lead to increased inflammation and cell death (Hooper et al., 2008). Factors such as excessive caloric diet, hypertension and aging, which have been associated with deficiency in insulin signalling and higher GSK3 activity, could affect the accumulation of aggregated proteins that have been involved in neurodegenerative disorders, such as AD (Jope and Johnson, 2004, Jope et al., 2007). Therefore, GSK3 has become an interesting target, since it links aging, metabolic disease, inflammation, protein-aggregation and cell death.

GSK3 activity was first associated with AD when it was isolated as one of the main culprits for the tau kinase (Ishiguro et al., 1988, Ishiguro et al., 1993). This was particularly pertinent as its activity is increased in AD brains (Blalock et al., 2004). In recent years it has become apparent that GSK3 activity is associated with most of the major factors associated with AD, such as neurotoxicity and inflammation, in addition to providing a bridge between the amyloid and tau pathology (see 2.8.3 GSK3 hypothesis of AD). As its aberrant activity is implicated in multiple aspects of AD pathogenesis, including its effects on LTP and LTD, it is intuitive to target GSK therapeutically (see later).

However, what has been lacking is a clear and descriptive analysis of any effects on APP processing in response to GSK3 activity. This is particularly relevant, since it is widely accepted that Aβ is the main trigger and driver of AD pathogenesis. Thus the field must be sure that any therapy directed at GSK3 does not promote more harm that it alleviates. Conflicting studies provide evidence that GSK3 inhibition can both promote and reduce Aβ production. Such an unresolved issue is naturally a barrier to any further development in a clinical setting. Further to this, most failures in the clinic arise from an absence of knowledge at the molecular level. This is illustrated by the recent failings of GSIs, which in addition to the increased cancer frequencies resulting from a low therapeutic-index, may have toxicity associated with the concomitant accumulation of the β-CTF (Bittner et al., 2009). Hence what may seem, as a simple task of reducing Aβ production may actually be intrinsically far

more complicated. This example is particularly resonant, as GSK3 has been known to influence the activity of PSEN1 through direct structural interaction. Furthermore, despite the promising data obtained with LiCl treatment in animal models of AD, improving many of the behavioural and biochemical symptoms, a recent multi-centre human drug trial with mild-AD patients was completed with unsatisfactory end-points (Hampel et al., 2009). LiCl as an actual GSK3 inhibitor was called into a question because in those patients there was neither amelioration in cognitive decline nor improvement in CSF biochemical markers, such as the level of phosphorylated tau (Hampel et al., 2009) (see 7.3 LiCl versus specific GSK3 inhibition).

Therefore, the overall aim of this project was to provide the much needed clarity and descriptive analysis for possible mechanisms of GSK3 influencing APP processing. The evidence provided here illustrates clearly that GSK3 activity is associated with the stability of the FL-APP protein that feeds into the two processing pathways and also the expression of BACE1, the rate-limiting enzyme in Aβ production. As such, specific GSK3 inhibition resulted in increased lysosomal degradation of FL-APP and decreased mouse *Bace1* expression, which ultimately reduced generation of Aβ. Such benefits would make a strong case for developing potent and specific GSK3 inhibitors that target a specific GSK3 function, to give the maximal therapeutic effect.

7.3 LiCl versus specific GSK3 inhibition

In terms of a mood stabiliser, LiCl is believed to be a relatively beneficial and cheap therapy for neuropsychiatric disorders such as schizophrenia. However, the target responsible for its action is to date not fully understood owing to its promiscuity as an inhibitor (Ghasemi and Dehpour, 2011, Agam et al., 2009).

The question remains as to whether this relative potency can be exploited for an AD therapy. However, as discussed previously, the benefits of LiCl altering amyloidogenic processing are controversial (Feyt et al., 2007, Feyt et al., 2005, Caccamo et al., 2007) and the various *in vitro* and *in vivo* studies that shine a positive light, use concentrations that are well beyond physiological relevance, in which it is likely multiple targets are inhibited (Ryder et al., 2003a, Su et al., 2004, Phiel et al., 2003). Furthermore, it has been documented that dosing regimes for more than two days in animals that has a equivalence to concentrations inhibiting GSK3 *in vitro*, are

highly toxic (Kremer et al., 2011). With the aid of recent developments for inhibitors with potencies within the micromolar range and siRNA technologies, it was observed here that there appears to be a dichotomy in the response when GSK3 is inhibited with LiCl or AR-A014418 (VIII) (Bhat et al., 2003). The results of the present study indicate that LiCl concentrations ranging from 5mM up to 40mM, do not affect APP processing, despite being able to inhibit GSK3, as shown by stabilisation of β-catenin. Simplistically, the additional off-site targets affected by the high dosage of LiCl could lead to numerous alterations in other signalling pathways that could well mask any inhibitory effect on GSK3.

Another possible explanation for the different effect between LiCl and other more potent and specific inhibitors of GSK3 is that it has been noticed that, unlike LiCl, specific inhibitors decrease the level of phosphorylation of GSK3 at position 216 (Y216), despite both reducing its activity (Simón et al., 2008). This residue was originally presumed to be a site of autophosphorylation that increases GSK3 activity and as such should decrease when inhibiting its kinase function (Lochhead et al., 2006). In fact, it is increased in response to various insults such as ischemia (Bhat et al., 2000), the prion protein (Pérez et al., 2003) and Aβ (Muñoz-Montaño et al., 1997), all of which lead to hyperactivity of GSK3. In addition to autophosphorylation, there is also a possibility that the residue is dynamically regulated through unknown tyrosine kinases and phosphatases. The end result is that while LiCl and specific GSK3 inhibitors both reduce GSK3 activity by altering the active site, only the latter decreases the phosphorylation of this regulatory Y216 residue of GSK3 when followed up several hours after administration. The functional significance of this is unknown, but it is likely that the reduced pY216 leads to a deeper inactivity of GSK3. This slight variance might also influence interactions with other proteins such as FRAT, and as such lead to alternative downstream effects. An analogous situation is found with the differential stabilisation of protein targets of GSK3 in response to either direct LiCl inhibition or with dominant negative mutants that disrupt the destruction complex of the canonical Wnt cascade (Kim et al., 2009b).

7.4 GSK3 activity and FL-APP stability

7.4.1 TFEB and lysosomal biogenesis

An important function of GSK3 has been associated with the phosphorylation-mediated degradation of proteins, such as β-catenin. Canonical activation of the Wnt pathway, which inhibits GSK3, has been associated with the stabilisation of a specific subset of proteins that may well alter several signalling cascades independent of the β-catenin-mediated transactivation of downstream target genes (Kim et al., 2009b). Taelman et al, 2010 found that the stability of approximately 20% of the proteasome is mediated through GSK3. This was compounded by a bioinformatics approach that identified several thousand putative targets with three consecutive GSK3 kinase sites that could be subjected to proteasomal targeting made typical by β-catenin. Of the numerous candidates highlighted, transcription factors make up a significant portion.

In the present study, proteasome inhibition just partially reversed the GSK3-mediated degradation of FL-APP, which indicates that other degradative pathways must be involved. Evidence presented here for the first time illustrates that GSK3 is able to regulate the activity of TFEB, which contains 3 consecutive sites for GSK3 phosphorylation and can be primed by p90/Rsk1 (Taelman et al., 2010, Settembre and Ballabio, 2011). Phosphorylation of TFEB by MAPK is believed to underlie the sequestration of TFEB from the nucleus (Settembre et al., 2011). However, it is shown here that specific GSK3 inhibition with the inhibitor VIII leads to a dramatic translocation of TFEB to the nucleus. It could be hypothesised therefore that GSK3 activity could be associated as well with TFEB phosphorylation (see figure 7.1A-B).

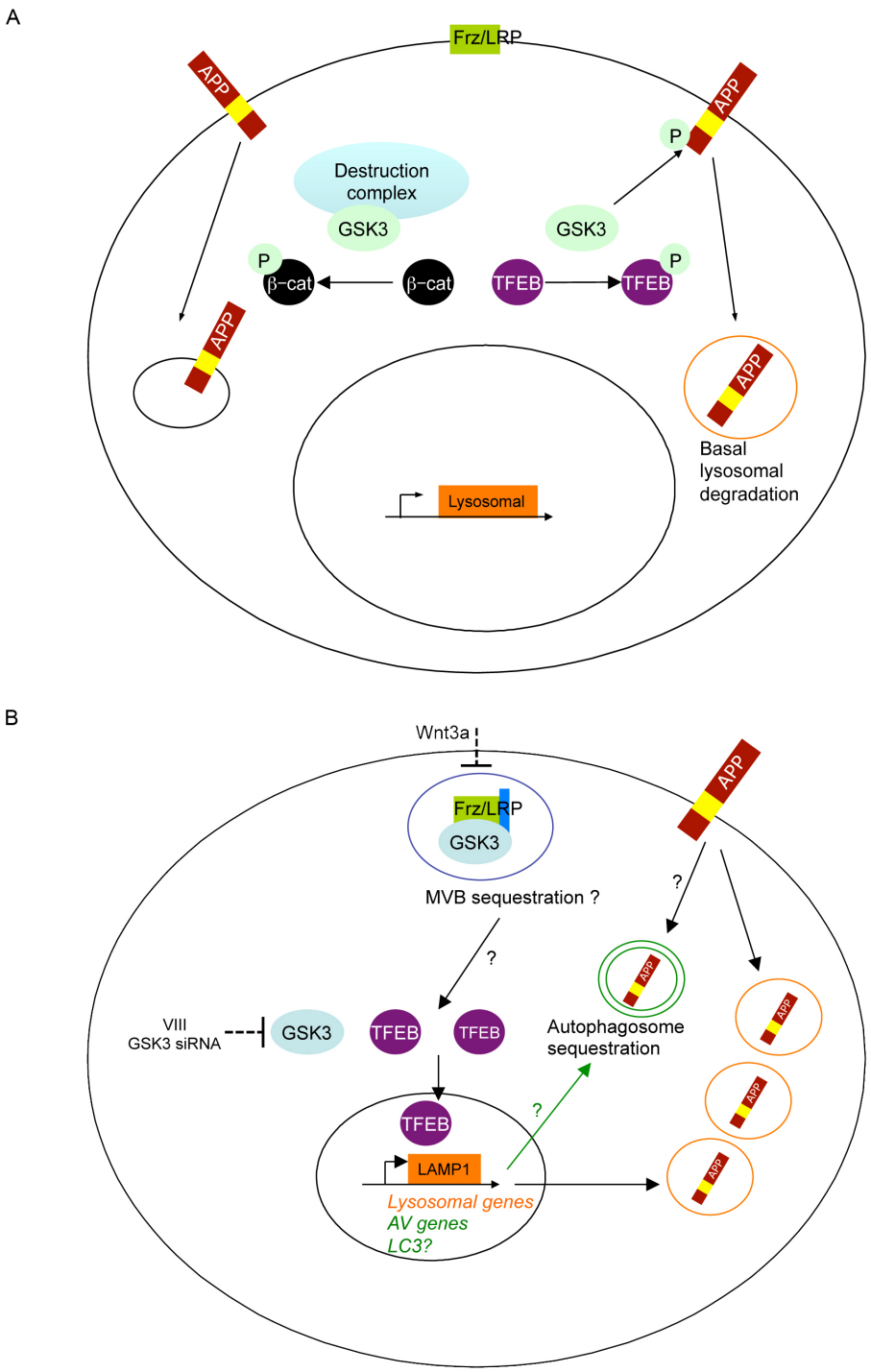


Figure 7.1: Schematics of the hypothetical effects of specific GSK3 inhibition on FL-APP degradation.

(A) Signalling under basal conditions, with normal lysosomal degradation following the secretory pathway of APP. (B) GSK3 activity is reduced by canonical Wnt activation, pharmacological inhibition and siRNA knockdown of GSK3 expression. Reduced GSK3 phosphorylation of TFEB leads to nuclear translocation and upregulation of lysosomal biogenesis genes (Palmieri et al., 2011). This leads to an increase in localisation of APP with LAMP1-positive vesicles and possibly an increase sequestration of APP in autophagosome structures.

7.4.2 Further investigation on TFEB

Further investigation is needed in order to provide *bona fide* evidence of this hypothesis stating GSK3 can regulate the nuclear translocation and therefore activity of TFEB. For instance several routes could be taken to demonstrate that the transient transfection of TFEB-FLAG is specific and indicative of the mechanism. As overexpression of TFEB has been used so far, studying the endogenous TFEB could be possible by knocking down TFEB using siRNA approach, which is commercially available. Secondly, using specific antibodies against TFEB, which have only just been made available commercially, it is possible to monitor the endogenous localisation of TFEB with specific GSK3 inhibition. Once it is proven that endogenous TFEB is sensitive to specific GSK3 inhibition, RT-qPCR analysis could be employed to ascertain which, if any lysosomal biogenesis genes are upregulated. A recent study combining several techniques including chromatin-immunoprecipitation (ChIP) analysis into a high-throughput screen for direct targets of TFEB have shown LAMP1 to be one of these (Palmieri et al., 2011).

Having shown that endogenous TFEB is sensitive to specific GSK3 inhibition and responsible for gene upregulation, it would be of interest to use an *in vitro* kinase assay to demonstrate that GSK3 is actually capable of phosphorylating TFEB as indicated elsewhere (Settembre et al., 2011). Experiments using mutated TFEB at putative positions of GSK3 phosphorylation would allow to determine whether this phosphorylation affects the function of TEFB and its nuclear translocation (Taelman et al., 2010).

Lastly it would be relevant to see if activation of the canonical Wnt cascade leading to GSK3 inactivation can also lead to increased TFEB nuclear localisation and lysosomal biogenesis.

7.5 Decreased GSK3 activity reduces BACE1 transcription

The data presented here establishes a link between GSK3 activity and transcriptional regulation of BACE1. This effect was shown by both pharmacological inhibition of GSK3 and upstream negative regulation on GSK3 via activation of the canonical Wnt pathway. Concomitant with reduced BACE1 mRNA expression, specific GSK3 inhibition also led to a reduction in the BACE1 promoter activity, which indicates that the BACE1 promoter may contain consensus sites for transcription factors regulated by GSK3. Because GSK3 inhibition leads to β-catenin stabilisation in the nucleus, one could speculate that β-catenin in conjunction with other transcription factors could regulate the transcription of BACE1. In contrast, the BACE1 transcription alteration with specific GSK3 inhibition could be independent of any transactivating function of β-catenin. Both contrasting hypotheses are discussed below.

7.5.1 Decreased GSK3 activity reduces BACE1 transcription through β-catenin regulation

In support of the β-catenin-transactivation dependent hypothesis, it was observed that overexpression of β-catenin S33 led to a reduction in the BACE1 promoter activity. However β-catenin is normally associated with transactivation and not repression of canonical Wnt target genes. As a paradigm, direct canonical Wnt target genes are usually driven by activity at LEF/TCF binding sites but are usually repressed in the basal case through interaction with Groucho (Nusse, 2008). This interaction leads to chromatin remodelling, closing off the promoter. An increased β-catenin level leads to the displacement of Groucho and consequently the opening of the promoter for transactivation. However it cannot be ruled out that the increased β-catenin signalling may lead to repression at LEF/TCF binding sites through some other alternative mechanism (see figure 7.2). A preliminary bioinformatics approach revealed several putative LEF/TCF binding sites within the minimal rat promoter, which is shown in figure 7.3A with site details in table 7.1. The initial 601bp of the BACE1 promoter sequence is highly conserved between rat, mouse and human and multiple binding sites where also found in these promoters (Lange-Dohna et al., 2003).

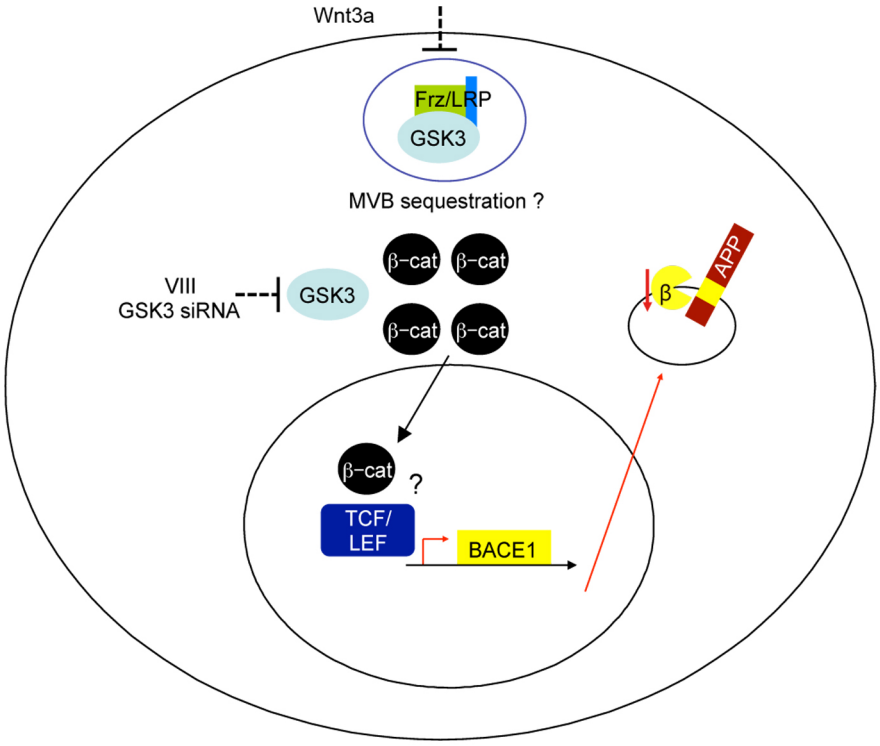


Figure 7.2: Hypothetical mechanism for BACE1 transcriptional regulation 1.

A hypothetical mechanism leading to repressed BACE1 transcription resulting from reduced GSK3 activity, that is β-catenin-transactivation dependent and relies on direct action on the BACE1 promoter. In addition β-catenin may function to inhibit GSK3 by increasing its sequestration.

Table 7.1: Putative binding sites for LEF/TCF family of transcription factors in the rat BACE1 promoter.

Accession no.	Matrix	Opt. *	Start position	End position	Anchor position	Strand	Core sim. **	Matrix sim. ***	Sequence
GXP_1419160	V$LEF1.04	0.84	172	188	180	-	1	0.919	tcctaaTCAAtaaatgg
GXP_1750874	V$LEF1.02	0.94	573	589	581	+	1	0.949	gtggggtCAAAggcaga
GXP_3427733	V$LEF1.01	0.86	340	356	348	+	1	0.88	aagccaaCAAAgtaaga
GXP_3427734	V$TCF7.01	0.85	450	466	458	-	1	0.867	gcgtcatCAAAtaaatt
GXP_3427735	V$LEF1.04	0.84	67	83	75	+	1	0.841	caatttTCAAttagtga
GXP_3427735	V$TCF7L1.01	0.86	486	502	494	-	1	0.882	aacaaatCAAAaggctg
GXP_3427735	V$LEF1.02	0.94	514	530	522	-	1	0.949	cctacctCAAAggttat

Table 7.1: Several submitted promoter sequences (Accession no. column) for the *Rattus Norvegicus Bace1* gene (Gene ID: 29392) were scrutinised for all submitted matrices for transcription factor binding sites using the MatInspector software tool from Genomatix (Cartharius et al., 2005, Quandt et al., 1995). Numerous putative consensus-binding sites for the LEF/TCF family of transcription factors were found and described by the Matrix column and the corresponding matching sequence in the promoter. Each match was annotated by which strand it was located and its start, finish and anchor point. *Optimised matrix similarity threshold sets a stringency tailored to each independent matrix to allow for maximum power without finding false positives. **Core similarity is set to 1.0, where by each of the highest conserved bases in the matrix (core sequence) must match exactly in the found sequence (shown in upper case). ***Matrix similarity describes how similar the identified sequence is to the full matrix sequence with a maximum score of 1.0.

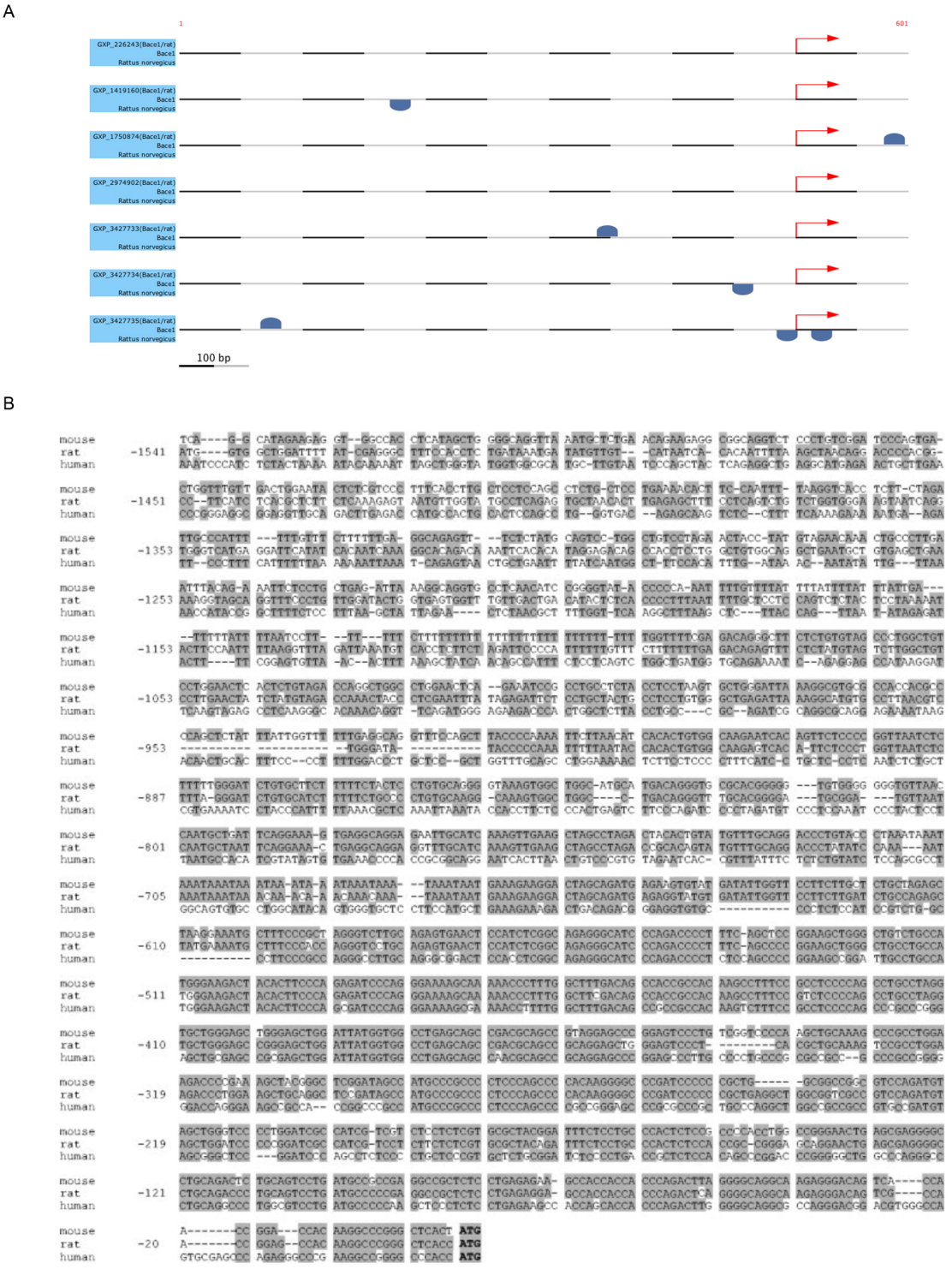


Figure 7.3: Putative consensus LEF/TCF binding sites within the rat BACE1 promoter.

Genomatix's MatInspector was used to search several submitted rat BACE1 promoter sequences for putative consensus binding sites for the LEF/TCF transcription factors (A). These binding sites are shown with the blue tabs shown at their position along the promoter sequence. Full details are given in Table 3.1. The red arrow indicates the transcription start sites. The submitted sequences consist of 601bp immediately upstream of the ATG transcription start codon, which shares high sequence homology to mouse (92%) and human (81%) BACE1 (B) (Lange-Dohna et al., 2003).

A comprehensive analysis of genes regulated by Wnt1, another canonical Wnt cascade activator, revealed that BACE1 transcription might be a target of this cascade. In addition, there was evidence that this regulation was from a first wave of transcriptional alterations in a times series (Wexler et al., 2010). Alternatively, this would imply that the reduced BACE1 transcription observed here is not an immediate effect, but resulting from changes in the transcriptional expression of an intermediary gene target (see figure 7.4).

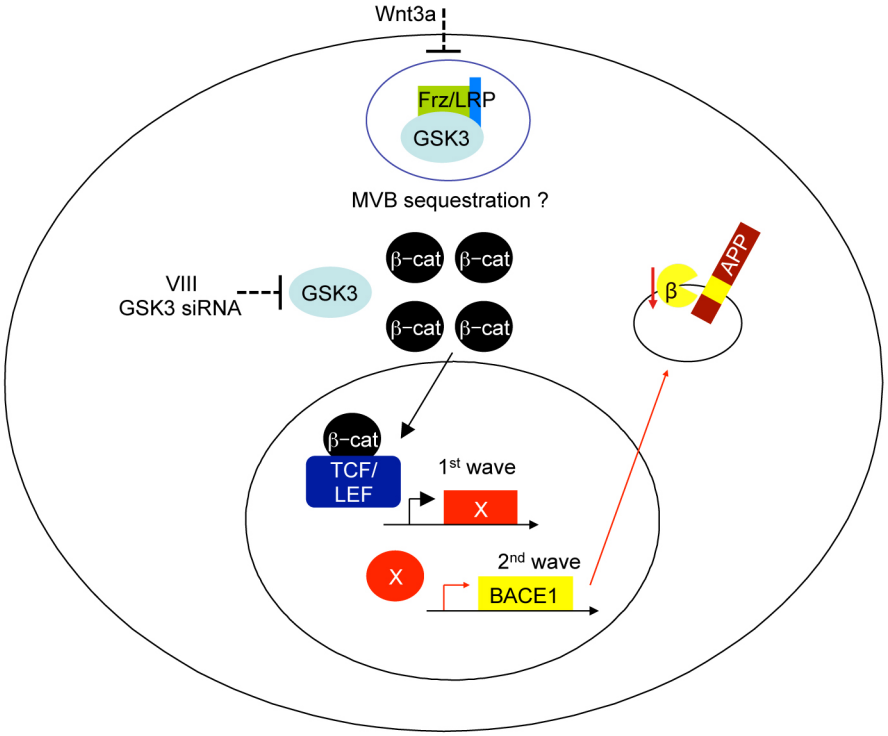


Figure 7.4: Hypothetical mechanism for BACE1 transcriptional regulation 2.

Illustrated above is a hypothetical two-wave and β-catenin-transactivation dependent mechanism. With reduced GSK3 activity, β-catenin alters the expression of an intermediary gene, which in turn alters the transcriptional expression of BACE1.

A possible mechanism could be that β-catenin could affect the activity of other transcription factors, such as PPARγ or NFκB (Mulholland et al., 2005, Shitashige et al., 2008). In this regard, it was reported that activation of the Wnt/β-catenin pathway, increases PPARγ levels by decreasing its degradation (Jansson et al., 2005). PPARγ has been shown to reduce BACE1 transcription through binding to a PPARγ-repression-element (PPRE) present on the BACE1 promoter (Sastre et al., 2006a). Interestingly, it was shown that PPARγ and β-catenin contain an interaction domain that allows a direct physical interaction between each other (Liu et al., 2006) (see figure 7.5).

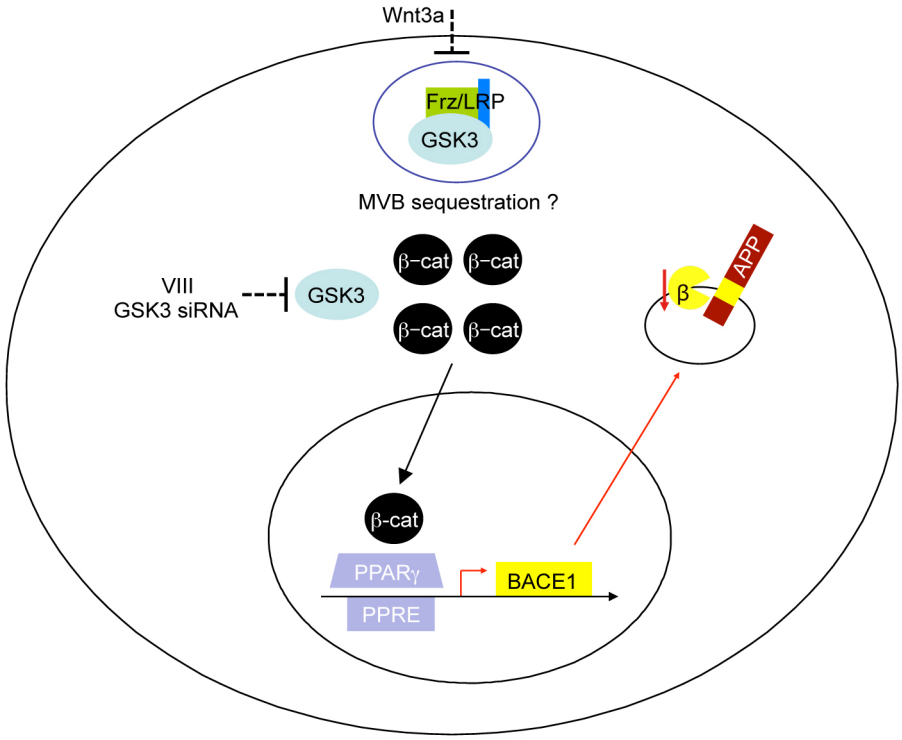


Figure 7.5: Hypothetical mechanism for BACE1 transcriptional regulation 3.

Final β-catenin-transactivation dependent mechanism for altered BACE1 transcriptional regulation with decreased GSK3 activity. β-catenin influences the already characterised PPARγ action at the PPRE site in the BACE1 promoter sequence.

7.5.2 Decreased GSK3 activity reduces BACE1 transcription through β-catenin-transactivation independent mechanisms

Another possible explanation is that the reduction of the BACE1 promoter activity with β-catenin S33 overexpression may result from the increase in subcellular sequestration of GSK3, and not through its nuclear functions. In addition to this other factors influenced by GSK3 inactivation could modulate BACE1 repression (see figure 7.6A).

The alteration of BACE1 transcription may be mediated through other factors directly affected by GSK3 inhibition as opposed to being dependent on β-catenin-transactivation. Several confirmed regulation sites within the upstream promoter region of BACE1 have been documented for NFκB (Bourne et al., 2007), YY1 (Nowak et al., 2006) and Spa1 (Christensen et al., 2004), with a mixture of repression and activation (Rossner et al., 2006). This is of interest as a bioinformatics approach identified of the many transcription regulators, that contain three or more consecutive GSK3 consensus phosphorylation sites and as such maybe stabilised upon canonical Wnt induction, include NFκB, YY1 and PPARγ (see figure 7.6A-B and table 7.2). This table, which was adapted from a supplementary table from Taelman et al (2010), lists a selection of relevant transcription factors and additional regulating factors that are putative GSK3 targets and therefore may alter BACE1 expression in response to an alteration in GSK3 activity.

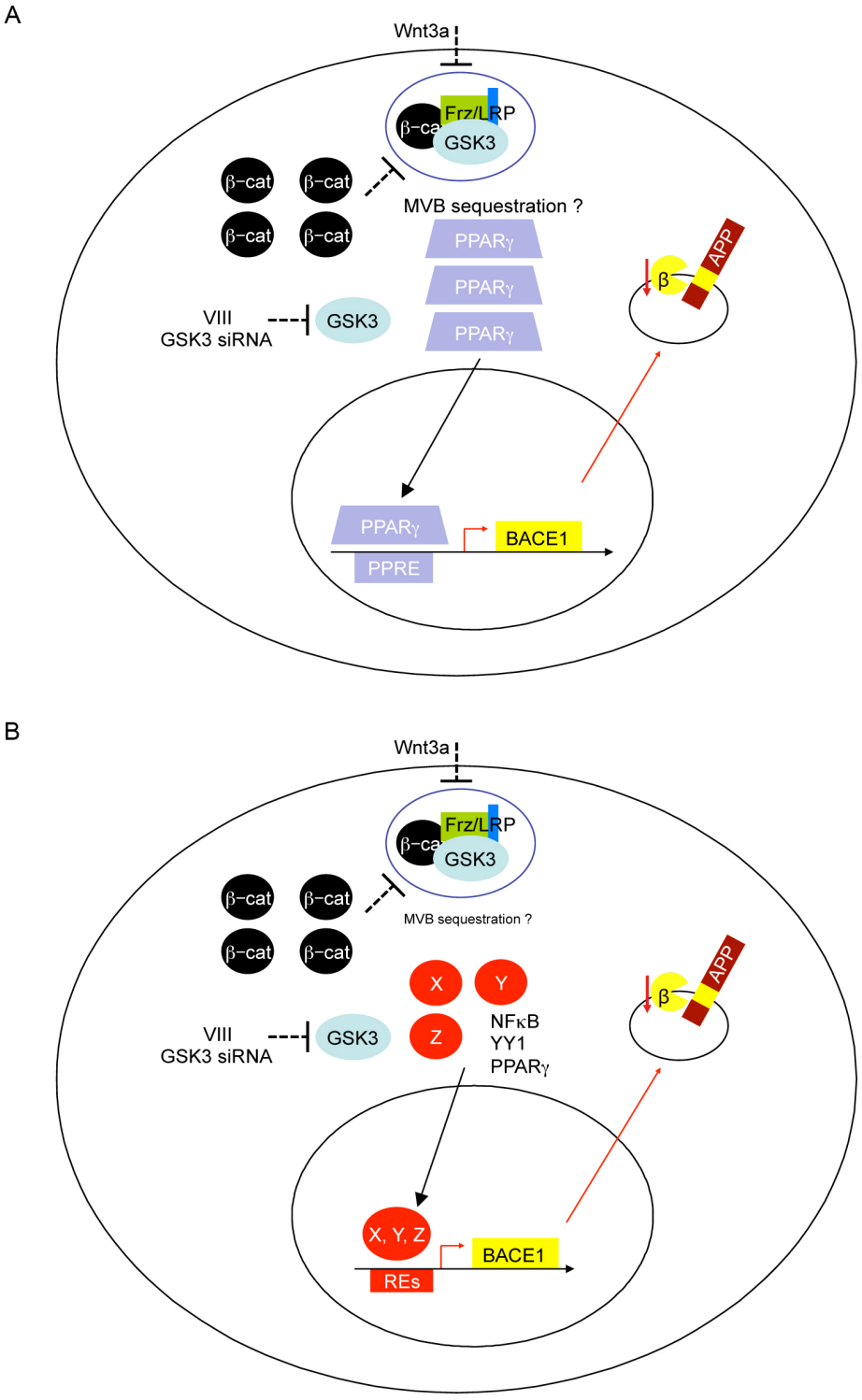


Figure 7.6: Hypothetical mechanism for BACE1 transcription regulation 4 and 5.

BACE1 transcriptional regulation is altered with reduced GSK3 activity by β-catenin-transactivation independent mechanisms. Increased β-catenin levels act to increase GSK3 activity by increasing its sequestration. (A) With the increased inactivity of GSK3, PPARγ is stabilised and can signal more strongly in the nucleus at the PPRE of the BACE1 promoter. (B) Molecules X, Y and Z represent unknown transcription factors that directly alter the transcription of BACE1 by interacting with repression elements (RE) or antagonising positive regulators.

Table 7.2: List of selected putative GSK3 kinase targets.

Ensebl Family ID	Gene name	Description	Consecutive GSK3 sites*	Conservation index**	BACE1 association	Reference
ENSFM00250000000692	TFEB	Transcription factor EB	3	32	N/A	
ENSFM00250000006958	PPARGC1A (PGC1a)	Co-activator of PPARγ	3	6	Unaltered	Parr et al., 2011
ENSFM00250000003534	PPARBP	PPARγ binding protein	6	7	Unknown	
ENSFM00250000000390	PPARG	PPARγ	5	8	Down	Sastre et., 2006
ENSFM00500000274652	RYBP	Ring1 and YY1 binding protein	4	6	Unknown	
ENSFM00250000003042	YY1	Ying Yang 1	6	13	Up	Nowak et al., 2006
ENSFM00250000000565	NFKB2-RELA/NFKB1-REL	NFκB	3	5	Down	Bourne et al., 2007
ENSFM00250000006650	NKRF	NFκB repressing factor	3	7	Unknown	
ENSFM00250000007050	NFKBIE	NFκB inhibitor epsilon	3	5	Unknown	

Table 7.2: A selection of the 4, 802 putative GSK3 kinase targets identified from containing three or more consecutive consensus sites for GSK3-mediated phosphorylation upstream of serine/threonine priming event. *The maximum number of these consecutive consensus kinase sites. **Compares phosphorylation sites found in human protein families to several other organism's proteomes including *Mus Murulus*. The higher the number the more conserved this site is. Up, down, unaltered and unknown define the putative affect on BACE1 transcription established from data already published and referenced within the table.

The signalling for each regulator alone is complex and so the combinatorial effects of multiple factors within the nucleus is far beyond reasonable speculation and thus warrants further investigation.

7.5.3 Further investigation

To ascertain the mechanisms by which β-catenin regulates BACE1 transcription by changes in GSK3 activity, further experimentation should be carried out.

Despite the rat, mouse and human promoter being highly homologous, the first step should be confirming the effect of GSK3 inactivation on BACE1 transcription with mouse and human BACE1 promoter constructs. In order to confirm if the effects of specific GSK3 inhibition on BACE1 transcription are mediated through β-catenin transcriptional regulation, a β-catenin clone mutated at positions K312E and K435E could be used. These mutations are located in an interaction domain needed for LEF/TCF interaction, and therefore β-catenin would not be capable of transactivation, as shown by the TOPflash assay (Liu et al., 2006). Alternatively the Inhibitor of β-catenin And TCF (ICAT) (Daniels and Weis, 2002) could be overexpressed to block any nuclear function of β-catenin, in combination with specific GSK3 inhibition, and measure if there are differences in the promoter activity of BACE1. As shown above there are several putative binding sites for the family of LEF/TCF transcription factors but these would need to be confirmed. Site-specific mutagenesis of the potential sites in the rat BACE1 promoter-luciferase construct can be used to ascertain which or if any are sensitive to GSK3 inactivation. Fragmentation of the BACE1 promoter can be combined with gel-shift analysis to identify which regions of the promoter are involved in the binding of the LEF/TCF transcription factors with BACE1 promoter.

In order to determine whether the effects of β-catenin are mediated through changes in GSK3 localisation rather than transactivation, experiments using confocal analysis of GSK3 in Rab7-positive multivesicular bodies (MVBs) could be carried out, altering the expression of β-catenin in the cell (Taelman et al., 2010). Increased sequestration would infer less GSK3 activity and therefore would mimic Wnt3a or pharmacological inhibition in terms of their effects on BACE1 expression.

To differentiate between canonical and non-canonical Wnt signalling, a couple of approaches could be taken. In addition to Wnt3a, which is classically a canonical Wnt cascade activator, other non-canonical Wnt activators like Wnt5a and Wnt7a could be used to understand the regulation on APP processing. Conversely, Wnt antagonist like sFRP-1 and DKK1 could be used as well. In the case of non-canonical regulation, Wnt target genes are regulated through β-catenin-independent mechanisms

and therefore could elucidate further mechanisms still that influence APP processing, in particular BACE1.

To explore the involvement of PPARγ in the GSK3-mediated regulation of BACE1 transcription, experiments with specific GSK3 inhibitors can be carried out in wild-type mouse embryonic fibroblasts (MEFs) and knockout PPARγ$^{-/-}$ MEF cells. Access to these cell-lines will come through collaboration with Evan Rosen (Beth Israel Deaconess Medical Centre, Boston). These cells could be transfected with PPARγ, to determine whether the effect is rescued (Sastre et al., 2006a). To corroborate these effects in N2aSw cells, PPARγ could be silenced by siRNA (Sastre et al., 2006a).

To understand whether β-catenin can influence PPARγ repression of BACE1 transcription, the β-catenin K312E/K435E mutant could be used, which prevents the interaction between β-catenin and PPARγ. Again by using the same wild-type MEF cells and PPARγ$^{-/-}$ MEF cells, overexpression of β-catenin and its effect on BACE1 transcription could be studied. The complex interactions of nuclear factors mentioned above could be studied using ChIP analysis on the BACE1 promoter following specific GSK3 inhibition, in similar approach recently used to identify LAMP1 as a direct transcription target of TFEB (Palmieri et al., 2011).

In the case that BACE1 transcription is independent of β-catenin transcriptional regulation, the involvement of further transcription factors would also be of interest, using similar methods of overexpression, BACE1 promoter activity and ChIP analysis.

7.5 Canonical Wnt cascade and sporadic AD

Evidence presented in chapter 5 demonstrates the ability of the canonical Wnt cascade to regulate APP processing. Therefore, any aberrant canonical Wnt signalling may result in altered APP processing, including dysregulation of BACE1 transcription. The study of AD patients with familiar *PSEN1* mutations, where the pathogenesis is strongly linked to increased Aβ production, has revealed strong links to the canonical Wnt cascade. Mutations in the *PSEN* genes can alter β-catenin stabilisation and presumably canonical Wnt signalling (Boonen et al., 2009). To further understand the role of the canonical Wnt cascade in the pathogenesis of SAD, the level of β-catenin from brain homogenates was investigated. If altered this would be in part an

indication of aberrant canonical Wnt signalling in SAD. Indeed it was evident that the level of β-catenin from the nuclear fraction of homogenised brains of SAD patients was reduced when compared to age-matched, non-demented controls. This only bolsters the consensus from the literature that AD, both familial and sporadic, is associated with a decreased induction of the canonical Wnt cascade, which has profound effects for synaptogenesis, LTP and synaptic plasticity. As a result, any method of restoring the homeostatic levels of Wnt activity would prove beneficial. It would seem that a therapy already approved as an AChE inhibitor could even promote a beneficial effect by activating Wnt/β-catenin signalling (Wang et al., 2011). However, aberrantly activating the canonical Wnt pathway could result in secondary side effects such as increased cancer incidence.

7.6 General limitations and future directions

While best efforts were made to corroborate some of the major findings in multiple cell-lines, this data would need to be verified in both primary neuronal cultures and ultimately in animal models, something which is underway. The collaboration with Professor Fred Van Leuven is a great benefit in providing the necessary animal models for investigating GSK3 regulation on APP processing. This is particularly pertinent to ascertain *in vivo* which GSK3 isoform or if both are responsible for the effect on APP processing. More recent publications have shown that *Gsk3α* conditional knockout crossed with *APP.V717I* mice showed no alteration in APP processing (Jaworski et al., 2009). In contrast, data regarding the contribution of the GSK3β isoform has been more difficult to obtain owing to the lethality of a complete knockout (Kremer et al., 2011). To avoid this, Professor Van Leuven's group has generated *Gsk3* conditional knockouts and shown that, GSK3α and GSK3β do not have a major effect on APP processing, that was published only very recently (Jaworski et al., 2011). In contrast, in a limited number of mice shown here (see the addendum), there is a trend for a decrease in FL-APP levels and an increase in LC3-II production in *Gsk3β* conditional knockout mice.

One could argue that knocking down the protein to reduce activity could be dramatically different to pharmacological inhibition of GSK3 because in the latter, GSK3 can still interact with its binding partners. Further to biochemical analysis of Aβ generation *in vitro*, it would be necessary to investigate the effects of the treatment

with a specific GSK3 inhibitor such as AR-A014418 (VIII) in AD transgenic models. Specific GSK3 inhibition with a novel inhibitor, NP12, was found to reduce the amyloid plaque load, hyperphosphorylated tau and neuronal loss in a double transgenic model that was specific to the Swedish variant of APP (Serenó et al., 2009). However, no mechanism was proposed. While evidence presented here and from other studies establishes that the effects of GSK3 inhibition do not seem to be specific to any particular familial form of APP, it would be beneficial to check different types of AD transgenic models, with different mutations and treated with a specific inhibitor such as AR-A014418. In a limited number of *APP/tau* transgenic mice, specific GSK3 inhibition resulted in a trend for reduced FL-APP protein expression (data not shown).

This preliminary investigation into the regulation of APP processing by the canonical Wnt cascade is a stepping-stone into understanding much broader themes. For instance, overexpression of APP has been shown to increase β-catenin degradation (Chen and Bodles, 2007) and therefore could explain the cognitive deficits in patients with increased gene-dosage of APP, such as in DS patients. Several key players such as PSEN1, GSK3, and β-catenin can physically interact with each other to alter their activities. Therefore, it would be relevant to investigate whether APP and β-catenin could also interact directly to influence each other. Preliminary data from our laboratory not included in this study show that APP and β-catenin can bind to one another by co-immunoprecipitation studies. We hope to confirm this with more robust methods such as fluorescent-resonance energy transfer (FRET), which can also tell something of the dynamics between the interactions. Both PSEN1 and β-catenin have close interactions with cadherin complexes, which in turn are thought to indirectly maintain synaptic connections. APP itself is also thought to, in some way, promote synaptic integrity from knockout mice and it could be interesting to prove that APP could be associated with tight junction complexes (Wang et al., 2005, Guo et al., 2011, Yang et al., 2005). These studies could also shed more light on the native functions of APP.

7.7 Developments of current AD therapies and GSK3 as a promising therapeutic target

Currently, only the symptoms of AD can be treated, with therapies that bolster cholinergic signalling by inhibiting the acetylcholinesterase and those that dampen the NMDAR excitotoxicity. As a result, and based on the amyloid cascade hypothesis, several disease-modifying therapies are currently in the clinical stages of development that generally either inhibit the amyloidogenic secretases or promote the α-secretase (Carter et al., 2010). The latter has proved more promising. There are several classes of approved drugs such as statins (Bettermann et al., 2011, Jick et al., 2000, Fassbender et al., 2001) and muscarinic G-protein coupled receptor agonists (Müller et al., 1997, Davis et al., 2010), which may promote non-amyloidogenic processing. The major barrier to developing inhibitors to reduce amyloidogenic production of Aβ is that both BACE1 (Vassar et al., 2009, Hu et al., 2006, Willem et al., 2006) and PSEN1/2 (Cummings, 2010, Bittner et al., 2009) have several other targets independent of their secretase function, and therefore lead to a low therapeutic-index with major side effects. As a result, there has been a recent barrage of clinical-phase failures that has called in to question the amyloid cascade hypothesis as the central process in AD pathogenesis (Selkoe, 2011, Karran et al., 2011). However, efforts are still being maintained to develop novel therapeutic strategies (Rajendran et al., 2008) and there are also several other proteins that modulate the secretase function that could be targeted instead of direct inhibition (Yasojima et al., 2000, Hu et al., 2007, Schwab et al., 2000, Tesco et al., 2007). Even better still, a revolution has brought about a shift to trialling therapies in recruited patients in the milder stages of the disease, which has been aided by better diagnosis and prognosis for full conversion to AD (Zhang et al., 2011). Better still, is the ability to trial these disease-modifying therapies in individuals who are currently asymptomatic but have a familial history of FAD and therefore pre-empt the amyloid trigger, central to the amyloid cascade hypothesis. This will be the ultimate test of the hypothesis.

There has been a concerted effort from both industry and academia to develop immunotherapies that can prevent and clear the formation of these amyloid plaques. Indeed, the initial studies from Elan and Wyeth pharmaceuticals showed efficacy in clearing amyloid deposits shown with imaging studies (Schnabel, 2011). Unfortunately, the study was cut short owing to deaths resulting from isolated incidents of menigoencephalitis. This however has not stopped other drug companies

picking up the baton and developing these vaccination therapies further using alternative antibodies and dosing regimes. Ultimately, advocates of the amyloid vaccination proposal would argue for a preventative treatment as opposed to clearing amyloid in already demented individuals. This is a worthy consideration as amyloid plaques levels correlate very badly with cognition and is seen more as a trigger of events, that once started are irreversible.

GSK3 activity is strongly associated with tau hyper-phosphorylation, Aβ-mediated toxicity, NFκB induced inflammation, LTP and finally APP processing as shown through *in vitro* modelling presented here. Furthermore, specific GSK3 inhibition in diabetic patients normalises insulin sensitisation and glucose synthesis, this is promising when considering the strong association between type-II diabetes and AD (Rayasam et al., 2009b). Therefore, it provides a crucial therapeutic target beyond the more disappointing studies with LiCl. While more recent literature with specific GSK3 inhibitors is promising, more research is required in order to manipulate GSK3 in a more controlled fashion without disrupting the many signalling pathways they maybe be influenced. GSK3 signalling can vary greatly depending on the upstream stimulus. This will be based on the downstream targets and altering the specificity of GSK3 depending on the context. For the reason that subcellular pooling of different isoforms can regulate GSK3, its activity can affect specific targets by forming complexes with additional proteins. Archetypal of this is the destruction complex within the canonical Wnt cascade. However, additional adaptor proteins have been discovered including the GSK3-binding proteins (GBP/ FRAT) (Yost et al., 1998) and the GSK3-interaction protein (GSKIP) (Chou et al., 2006) that act as natural modulators of activity as opposed to straight inhibitors/activators. This new research will be beneficial in order to develop novel disease-modifying therapies centred on GSK3 without detrimental side effects. Like other disease-modifying therapies being developed for AD, the greatest success will come from early or even preventive regimes and therefore patients might have to be maintained on this therapy for decades. It is of up-most importance that research should air on the side of caution as GSK3 activity dampens common pathways such as the canonical Wnt cascade that are hyper-activated in many cancers (Luo et al., 2007). Some confidence can be taken from case histories of patients being administered with LiCl for neuropsychiatric conditions for years, even decades without an increase of cancer incidence (Cohen et al., 1998). This is however may result from LiCl being at best a

very poor inhibitor of GSK3 and therefore allowing for a modest level of GSK3 activity.

Of great interest was the finding that specific GSK3 inhibition is involved with increased lysosome biogenesis and autophagy flux through the autophagy-lysosome degradation pathway. In addition to the many lysosomal storage diseases which show a similar neurodegenerative phenotype (Tamboli et al., 2011), autopsy analysis of human SAD brains (Cataldo et al., 1997) and certain AD transgenic models (Yang et al., 2008), have reported the presence of altered endosomal, lysosomal and autophagy compartments (Rubinsztein et al., 2005, Boland et al., 2008). This may also arise from the *PSEN1* familial mutations, which have shown to disrupt these processes (Qiang et al., 2011, Lee et al., 2010). Furthermore, inhibition of effective lysosomal proteolysis was enough to directly induce Alzheimer's-like axonal dystrophy in primary neuronal cultures (Lee et al., 2011). With age it seems that homeostatic processes such as autophagy become inefficient, which ultimately may arise from the increase expression and activity of GSK3 associated with aging shown *in vivo* and in humans. Therefore, there could be a call for therapies to target GSK3 to improve the homeostasis of these important degradative and processing compartments.

CONCLUSION

The main aim of this project was to clarify and extend the current knowledge of the role that GSK3 plays in the processing of APP. This is of importance, as it would plug a significant gap in the provocative GSK3 hypothesis of AD pathogenesis. Firstly, the early studies have heavily relied on the assumption that LiCl is a potent GSK3 inhibitor, an assumption, which many now doubt. Secondly, the lack of the specific mechanism by which GSK3 affects Aβ generation. Lastly the previous consensus was shaped from a mishmash of data generated in divergent paradigms.

Provided here is a comprehensive elucidation of the effects that occur from altering GSK3 activity. The focus has mainly been by lowering GSK3 activity owing to the fact that the basal activity for GSK3 is already high in cells. In addition to using specific GSK3 inhibitors not used before, it was taken further by incorporating the activation of the canonical Wnt cascade, which also leads to GSK3 inactivation and found to reduce the production of Aβ. A reduction in nuclear β-catenin in SAD patients could be indicative of collapsed Wnt signalling in these brains that ultimately may drive pathogenesis, firstly by promoting Aβ generation but also by losing synaptic integrity.

The increased lysosomal biogenesis promoted by specific GSK3 inhibition was an unexpected outcome that may prove beneficial for therapy. Focusing on protein turnover and homeostasis, it would be of interest to see if similar treatments would benefit this aspect of pathogenesis in the many AD transgenic models. The implication of disrupted Wnt signalling in AD and the evidence provided here, would argue that activating this cascade would be beneficial by promoting neurogenesis and negatively regulating GSK3 and its detrimental functions in AD.

The expanded investigation *in vitro* was required to establish consistency and allow for complex mechanistic detail to be studied. Therefore, while much can be gained from this study, it is important to take this initial step and confirm major findings or signposts *in vivo* with AD transgenic models and human tissue.

ABERLE, H., BAUER, A., STAPPERT, J., KISPERT, A. & KEMLER, R. 1997. beta-catenin is a target for the ubiquitin-proteasome pathway. *EMBO J,* 16**,** 3797-804.

ABRAMOV, E., DOLEV, I., FOGEL, H., CICCOTOSTO, G. D., RUFF, E. & SLUTSKY, I. 2009. Amyloid-beta as a positive endogenous regulator of release probability at hippocampal synapses. *Nat Neurosci,* 12**,** 1567-76.

ADACHI, K., MIRZADEH, Z., SAKAGUCHI, M., YAMASHITA, T., NIKOLCHEVA, T., GOTOH, Y., PELTZ, G., GONG, L., KAWASE, T., ALVAREZ-BUYLLA, A., OKANO, H. & SAWAMOTO, K. 2007. Beta-catenin signaling promotes proliferation of progenitor cells in the adult mouse subventricular zone. *Stem Cells,* 25**,** 2827-36.

AGAM, G., BERSUDSKY, Y., BERRY, G. T., MOECHARS, D., LAVI-AVNON, Y. & BELMAKER, R. H. 2009. Knockout mice in understanding the mechanism of action of lithium. *Biochem Soc Trans,* 37**,** 1121-5.

ALAFUZOFF, I., ARZBERGER, T., AL-SARRAJ, S., BODI, I., BOGDANOVIC, N., BRAAK, H., BUGIANI, O., DEL-TREDICI, K., FERRER, I., GELPI, E., GIACCONE, G., GRAEBER, M. B., INCE, P., KAMPHORST, W., KING, A., KORKOLOPOULOU, P., KOVÁCS, G. G., LARIONOV, S., MEYRONET, D., MONORANU, C., PARCHI, P., PATSOURIS, E., ROGGENDORF, W., SEILHEAN, D., TAGLIAVINI, F., STADELMANN, C., STREICHENBERGER, N., THAL, D. R., WHARTON, S. B. & KRETZSCHMAR, H. 2008. Staging of neurofibrillary pathology in Alzheimer's disease: a study of the BrainNet Europe Consortium. *Brain Pathol,* 18**,** 484-96.

ALAFUZOFF, I., THAL, D. R., ARZBERGER, T., BOGDANOVIC, N., AL-SARRAJ, S., BODI, I., BOLUDA, S., BUGIANI, O., DUYCKAERTS, C., GELPI, E., GENTLEMAN, S., GIACCONE, G., GRAEBER, M., HORTOBAGYI, T., HÖFTBERGER, R., INCE, P., IRONSIDE, J. W., KAVANTZAS, N., KING, A., KORKOLOPOULOU, P., KOVÁCS, G. G., MEYRONET, D., MONORANU, C., NILSSON, T., PARCHI, P., PATSOURIS, E., PIKKARAINEN, M., REVESZ, T., ROZEMULLER, A., SEILHEAN, D., SCHULZ-SCHAEFFER, W., STREICHENBERGER, N., WHARTON, S. B. & KRETZSCHMAR, H. 2009. Assessment of beta-amyloid deposits in human brain: a study of the BrainNet Europe Consortium. *Acta Neuropathol,* 117**,** 309-20.

ALLSOP, D., WONG, C. W., IKEDA, S., LANDON, M., KIDD, M. & GLENNER, G. G. 1988. Immunohistochemical evidence for the derivation of a peptide ligand from the amyloid beta-protein precursor of Alzheimer disease. *Proc Natl Acad Sci U S A,* 85**,** 2790-4.

ALVAREZ, G., MUÑOZ-MONTAÑO, J. R., SATRÚSTEGUI, J., AVILA, J., BOGÓNEZ, E. & DÍAZ-NIDO, J. 1999. Lithium protects cultured neurons against beta-amyloid-induced neurodegeneration. *FEBS Lett,* 453**,** 260-4.

ALZHEIMER, A. 1907. Uber eine eigenartige Erkrankung der Hirnrinde. *Allg Z. Psychiat* 64**,** 146-148.

AMBASUDHAN, R., TALANTOVA, M., COLEMAN, R., YUAN, X., ZHU, S., LIPTON, S. A. & DING, S. 2011. Direct reprogramming of adult human fibroblasts to functional neurons under defined conditions. *Cell Stem Cell,* 9**,** 113-8.

AMIT, S., HATZUBAI, A., BIRMAN, Y., ANDERSEN, J. S., BEN-SHUSHAN, E., MANN, M., BEN-NERIAH, Y. & ALKALAY, I. 2002. Axin-mediated CKI phosphorylation of beta-catenin at Ser 45: a molecular switch for the Wnt pathway. *Genes Dev,* 16**,** 1066-76.

ANDERSON, J. P., REFOLO, L. M., WALLACE, W., MEHTA, P., KRISHNAMURTHI, M., GOTLIB, J., BIERER, L., HAROUTUNIAN, V., PERL, D. & ROBAKIS, N. K. 1989. Differential brain expression of the Alzheimer's amyloid precursor protein. *EMBO J,* 8**,** 3627-32.

APLIN, A. E., JACOBSEN, J. S., ANDERTON, B. H. & GALLO, J. M. 1997. Effect of increased glycogen synthase kinase-3 activity upon the maturation of the amyloid precursor protein in transfected cells. *Neuroreport,* 8**,** 639-43.

APODACA, J., KIM, I. & RAO, H. 2006. Cellular tolerance of prion protein PrP in yeast involves proteolysis and the unfolded protein response. *Biochem Biophys Res Commun,* 347**,** 319-26.

BAKI, L., SHIOI, J., WEN, P., SHAO, Z., SCHWARZMAN, A., GAMA-SOSA, M., NEVE, R. & ROBAKIS, N. K. 2004. PS1 activates PI3K thus inhibiting GSK-3 activity and tau overphosphorylation: effects of FAD mutations. *EMBO J,* 23**,** 2586-96.

BALLARD, C., GAUTHIER, S., CORBETT, A., BRAYNE, C., AARSLAND, D. & JONES, E. 2011. Alzheimer's disease. *Lancet,* 377**,** 1019-31.

BAMMENS, L., CHÁVEZ-GUTIÉRREZ, L., TOLIA, A., ZWIJSEN, A. & DE STROOPER, B. 2011. Functional and topological analysis of Pen-2, the fourth subunit of the gamma-secretase complex. *J Biol Chem,* 286**,** 12271-82.

BARBER, R. C. 2010. Biomarkers for early detection of Alzheimer disease. *J Am Osteopath Assoc,* 110**,** S10-5.

BARKER, W. W., LUIS, C. A., KASHUBA, A., LUIS, M., HARWOOD, D. G., LOEWENSTEIN, D., WATERS, C., JIMISON, P., SHEPHERD, E., SEVUSH, S., GRAFF-RADFORD, N., NEWLAND, D., TODD, M., MILLER, B., GOLD, M., HEILMAN, K., DOTY, L., GOODMAN, I., ROBINSON, B., PEARL, G., DICKSON, D. & DUARA, R. 2002. Relative frequencies of Alzheimer disease, Lewy body, vascular and frontotemporal dementia, and hippocampal sclerosis in the State of Florida Brain Bank. *Alzheimer Dis Assoc Disord,* 16**,** 203-12.

BARNETT, A. & BREWER, G. J. 2011. Autophagy in aging and Alzheimer's disease: pathologic or protective? *J Alzheimers Dis,* 25**,** 385-94.

BECKETT, C., NALIVAEVA, N. N., BELYAEV, N. D. & TURNER, A. J. 2011. Nuclear signalling by membrane protein intracellular domains: The AICD enigma. *Cell Signal*.

BEHRENS, J., VON KRIES, J. P., KÜHL, M., BRUHN, L., WEDLICH, D., GROSSCHEDL, R. & BIRCHMEIER, W. 1996. Functional interaction of beta-catenin with the transcription factor LEF-1. *Nature,* 382**,** 638-42.

BELL, K. F., ZHENG, L., FAHRENHOLZ, F. & CUELLO, A. C. 2008. ADAM-10 over-expression increases cortical synaptogenesis. *Neurobiol Aging,* 29**,** 554-65.

BELYAEV, N. D., KELLETT, K. A., BECKETT, C., MAKOVA, N. Z., REVETT, T. J., NALIVAEVA, N. N., HOOPER, N. M. & TURNER, A. J. 2010. The transcriptionally active amyloid precursor protein (APP) intracellular domain is preferentially produced from the 695 isoform of APP in a {beta}-secretase-dependent pathway. *J Biol Chem,* 285**,** 41443-54.

BENNETT, B. D., DENIS, P., HANIU, M., TEPLOW, D. B., KAHN, S., LOUIS, J. C., CITRON, M. & VASSAR, R. 2000. A furin-like convertase mediates propeptide cleavage of BACE, the Alzheimer's beta -secretase. *J Biol Chem,* 275**,** 37712-7.

BENNETT, D. A. & WHITMER, R. A. 2009. NSAID exposure and risk of Alzheimer disease: is timing everything? *Neurology,* 72**,** 1884-5.

BERTRAM, L. 2011. Alzheimer's genetics in the GWAS era: a continuing story of 'replications and refutations'. *Curr Neurol Neurosci Rep,* 11**,** 246-53.

BETTERMANN, K., ARNOLD, A. M., WILLIAMSON, J., RAPP, S., SINK, K., TOOLE, J. F., CARLSON, M. C., YASAR, S., DEKOSKY, S. & BURKE, G. L. 2011. Statins, Risk of Dementia, and Cognitive Function: Secondary Analysis of the Ginkgo Evaluation of Memory Study. *J Stroke Cerebrovasc Dis*.

BHAT, R., XUE, Y., BERG, S., HELLBERG, S., ORMO, M., NILSSON, Y., RADESATER, A. C., JERNING, E., MARKGREN, P. O., BORGEGARD, T., NYLOF, M., GIMENEZ-CASSINA, A., HERNANDEZ, F., LUCAS, J. J., DIAZ-NIDO, J. & AVILA, J. 2003. Structural insights and

biological effects of glycogen synthase kinase 3-specific inhibitor AR-A014418. *J Biol Chem.* United States.

BHAT, R. V., BUDD HAEBERLEIN, S. L. & AVILA, J. 2004. Glycogen synthase kinase 3: a drug target for CNS therapies. *J Neurochem,* 89**,** 1313-7.

BHAT, R. V., SHANLEY, J., CORRELL, M. P., FIELES, W. E., KEITH, R. A., SCOTT, C. W. & LEE, C. M. 2000. Regulation and localization of tyrosine216 phosphorylation of glycogen synthase kinase-3beta in cellular and animal models of neuronal degeneration. *Proc Natl Acad Sci U S A,* 97**,** 11074-9.

BIJUR, G. N. & JOPE, R. S. 2003. Glycogen synthase kinase-3 beta is highly activated in nuclei and mitochondria. *Neuroreport,* 14**,** 2415-9.

BILIC, J., HUANG, Y. L., DAVIDSON, G., ZIMMERMANN, T., CRUCIAT, C. M., BIENZ, M. & NIEHRS, C. 2007. Wnt induces LRP6 signalosomes and promotes dishevelled-dependent LRP6 phosphorylation. *Science,* 316**,** 1619-22.

BIRKS, J., GRIMLEY EVANS, J., IAKOVIDOU, V., TSOLAKI, M. & HOLT, F. E. 2009. Rivastigmine for Alzheimer's disease. *Cochrane Database Syst Rev***,** CD001191.

BITTNER, T., FUHRMANN, M., BURGOLD, S., JUNG, C. K., VOLBRACHT, C., STEINER, H., MITTEREGGER, G., KRETZSCHMAR, H. A., HAASS, C. & HERMS, J. 2009. Gamma-secretase inhibition reduces spine density in vivo via an amyloid precursor protein-dependent pathway. *J Neurosci,* 29**,** 10405-9.

BJØRKØY, G., LAMARK, T., PANKIV, S., ØVERVATN, A., BRECH, A. & JOHANSEN, T. 2009. Monitoring autophagic degradation of p62/SQSTM1. *Methods Enzymol,* 452**,** 181-97.

BLALOCK, E. M., GEDDES, J. W., CHEN, K. C., PORTER, N. M., MARKESBERY, W. R. & LANDFIELD, P. W. 2004. Incipient Alzheimer's disease: microarray correlation analyses reveal major transcriptional and tumor suppressor responses. *Proc Natl Acad Sci U S A,* 101**,** 2173-8.

BLASKO, I., BEER, R., BIGL, M., APELT, J., FRANZ, G., RUDZKI, D., RANSMAYR, G., KAMPFL, A. & SCHLIEBS, R. 2004. Experimental traumatic brain injury in rats stimulates the expression, production and activity of Alzheimer's disease beta-secretase (BACE-1). *J Neural Transm,* 111**,** 523-36.

BLITZER, J. T. & NUSSE, R. 2006. A critical role for endocytosis in Wnt signaling. *BMC Cell Biol,* 7**,** 28.

BOLAND, B., KUMAR, A., LEE, S., PLATT, F. M., WEGIEL, J., YU, W. H. & NIXON, R. A. 2008. Autophagy induction and autophagosome clearance in neurons: relationship to autophagic pathology in Alzheimer's disease. *J Neurosci,* 28**,** 6926-37.

BOLAND, B., SMITH, D. A., MOONEY, D., JUNG, S. S., WALSH, D. M. & PLATT, F. M. 2010. Macroautophagy is not directly involved in the metabolism of amyloid precursor protein. *J Biol Chem,* 285**,** 37415-26.

BOONEN, R. A., VAN TIJN, P. & ZIVKOVIC, D. 2009. Wnt signaling in Alzheimer's disease: up or down, that is the question. *Ageing Res Rev,* 8**,** 71-82.

BORCHELT, D. R., RATOVITSKI, T., VAN LARE, J., LEE, M. K., GONZALES, V., JENKINS, N. A., COPELAND, N. G., PRICE, D. L. & SISODIA, S. S. 1997. Accelerated amyloid deposition in the brains of transgenic mice coexpressing mutant presenilin 1 and amyloid precursor proteins. *Neuron,* 19**,** 939-45.

BORDJI, K., BECERRIL-ORTEGA, J., NICOLE, O. & BUISSON, A. 2010. Activation of extrasynaptic, but not synaptic, NMDA receptors modifies amyloid precursor protein expression pattern and increases amyloid-ß production. *J Neurosci,* 30**,** 15927-42.

BOSSY-WETZEL, E., SCHWARZENBACHER, R. & LIPTON, S. A. 2004. Molecular pathways to neurodegeneration. *Nat Med,* 10 Suppl**,** S2-9.

BOURNE, K. Z., FERRARI, D. C., LANGE-DOHNA, C., ROSSNER, S., WOOD, T. G. & PEREZ-POLO, J. R. 2007. Differential regulation of BACE1 promoter activity by nuclear factor-kappaB in neurons and glia upon exposure to beta-amyloid peptides. *J Neurosci Res,* 85**,** 1194-204.

BRAAK, H. & BRAAK, E. 1991. Neuropathological stageing of Alzheimer-related changes. *Acta Neuropathol,* 82**,** 239-59.

BROWNLEES, J., IRVING, N. G., BRION, J. P., GIBB, B. J., WAGNER, U., WOODGETT, J. & MILLER, C. C. 1997. Tau phosphorylation in transgenic mice expressing glycogen synthase kinase-3beta transgenes. *Neuroreport,* 8**,** 3251-5.

BUSCIGLIO, J., LORENZO, A., YEH, J. & YANKNER, B. A. 1995. beta-amyloid fibrils induce tau phosphorylation and loss of microtubule binding. *Neuron,* 14**,** 879-88.

BUXBAUM, J. D., LIU, K. N., LUO, Y., SLACK, J. L., STOCKING, K. L., PESCHON, J. J., JOHNSON, R. S., CASTNER, B. J., CERRETTI, D. P. & BLACK, R. A. 1998. Evidence that tumor necrosis factor alpha converting enzyme is involved in regulated alpha-secretase cleavage of the Alzheimer amyloid protein precursor. *J Biol Chem,* 273**,** 27765-7.

CACCAMO, A., ODDO, S., TRAN, L. X. & LAFERLA, F. M. 2007. Lithium reduces tau phosphorylation but not A beta or working memory deficits in a transgenic model with both plaques and tangles. *Am J Pathol,* 170**,** 1669-75.

CAPORASO, G. L., TAKEI, K., GANDY, S. E., MATTEOLI, M., MUNDIGL, O., GREENGARD, P. & DE CAMILLI, P. 1994. Morphologic and biochemical analysis of the intracellular trafficking of the Alzheimer beta/A4 amyloid precursor protein. *J Neurosci,* 14**,** 3122-38.

CARICASOLE, A., COPANI, A., CARACI, F., ARONICA, E., ROZEMULLER, A. J., CARUSO, A., STORTO, M., GAVIRAGHI, G., TERSTAPPEN, G. C. & NICOLETTI, F. 2004. Induction of Dickkopf-1, a negative modulator of the Wnt pathway, is associated with neuronal degeneration in Alzheimer's brain. *J Neurosci,* 24**,** 6021-7.

CARR, C. S. & SHARP, P. A. 1990. A helix-loop-helix protein related to the immunoglobulin E box-binding proteins. *Mol Cell Biol,* 10**,** 4384-8.

CARTER, M. D., SIMMS, G. A. & WEAVER, D. F. 2010. The development of new therapeutics for Alzheimer's disease. *Clin Pharmacol Ther,* 88**,** 475-86.

CARTHARIUS, K., FRECH, K., GROTE, K., KLOCKE, B., HALTMEIER, M., KLINGENHOFF, A., FRISCH, M., BAYERLEIN, M. & WERNER, T. 2005. MatInspector and beyond: promoter analysis based on transcription factor binding sites. *Bioinformatics,* 21**,** 2933-42.

CARUSO, A., MOTOLESE, M., IACOVELLI, L., CARACI, F., COPANI, A., NICOLETTI, F., TERSTAPPEN, G. C., GAVIRAGHI, G. & CARICASOLE, A. 2006. Inhibition of the canonical Wnt signaling pathway by apolipoprotein E4 in PC12 cells. *J Neurochem,* 98**,** 364-71.

CASTELLANO, J. M., KIM, J., STEWART, F. R., JIANG, H., DEMATTOS, R. B., PATTERSON, B. W., FAGAN, A. M., MORRIS, J. C., MAWUENYEGA, K. G., CRUCHAGA, C., GOATE, A. M., BALES, K. R., PAUL, S. M., BATEMAN, R. J. & HOLTZMAN, D. M. 2011a. Human apoE Isoforms Differentially Regulate Brain Amyloid-{beta} Peptide Clearance. *Sci Transl Med,* 3**,** 89ra57.

CASTELLANO, J. M., KIM, J., STEWART, F. R., JIANG, H., DEMATTOS, R. B., PATTERSON, B. W., FAGAN, A. M., MORRIS, J. C., MAWUENYEGA, K. G., CRUCHAGA, C., GOATE, A. M., BALES, K. R., PAUL, S. M., BATEMAN, R. J. & HOLTZMAN, D. M. 2011b. Human apoE isoforms differentially regulate brain amyloid-β peptide clearance. *Sci Transl Med,* 3**,** 89ra57.

CATALDO, A. M., BARNETT, J. L., PIERONI, C. & NIXON, R. A. 1997. Increased neuronal endocytosis and protease delivery to early endosomes in sporadic Alzheimer's disease: neuropathologic evidence for a mechanism of increased beta-amyloidogenesis. *J Neurosci,* 17**,** 6142-51.

CHACON, M. A., VARELA-NALLAR, L. & INESTROSA, N. C. 2008. Frizzled-1 is involved in the neuroprotective effect of Wnt3a against Abeta oligomers. *J Cell Physiol,* 217**,** 215-27.

CHACÓN, M. A., VARELA-NALLAR, L. & INESTROSA, N. C. 2008. Frizzled-1 is involved in the neuroprotective effect of Wnt3a against Abeta oligomers. *J Cell Physiol,* 217**,** 215-27.

CHANG, Y., TESCO, G., JEONG, W. J., LINDSLEY, L., ECKMAN, E. A., ECKMAN, C. B., TANZI, R. E. & GUÉNETTE, S. Y. 2003. Generation of the beta-amyloid peptide and the amyloid precursor protein C-terminal fragment gamma are potentiated by FE65L1. *J Biol Chem,* 278**,** 51100-7.

CHEN, F., GU, Y., HASEGAWA, H., RUAN, X., ARAWAKA, S., FRASER, P., WESTAWAY, D., MOUNT, H. & ST GEORGE-HYSLOP, P. 2002. Presenilin 1 mutations activate gamma 42-secretase but reciprocally inhibit epsilon-secretase cleavage of amyloid precursor protein (APP) and S3-cleavage of notch. *J Biol Chem,* 277**,** 36521-6.

CHEN, Y. & BODLES, A. M. 2007. Amyloid precursor protein modulates beta-catenin degradation. *J Neuroinflammation,* 4**,** 29.

CHEVALLIER, N. L., SORIANO, S., KANG, D. E., MASLIAH, E., HU, G. & KOO, E. H. 2005. Perturbed neurogenesis in the adult hippocampus associated with presenilin-1 A246E mutation. *Am J Pathol,* 167**,** 151-9.

CHOU, H. Y., HOWNG, S. L., CHENG, T. S., HSIAO, Y. L., LIEU, A. S., LOH, J. K., HWANG, S. L., LIN, C. C., HSU, C. M., WANG, C., LEE, C. I., LU, P. J., CHOU, C. K., HUANG, C. Y. & HONG, Y. R. 2006. GSKIP is homologous to the Axin GSK3beta interaction domain and functions as a negative regulator of GSK3beta. *Biochemistry,* 45**,** 11379-89.

CHRISTENSEN, M. A., ZHOU, W., QING, H., LEHMAN, A., PHILIPSEN, S. & SONG, W. 2004. Transcriptional regulation of BACE1, the beta-amyloid precursor protein beta-secretase, by Sp1. *Mol Cell Biol,* 24**,** 865-74.

CHRISTIE, R. H., FREEMAN, M. & HYMAN, B. T. 1996. Expression of the macrophage scavenger receptor, a multifunctional lipoprotein receptor, in microglia associated with senile plaques in Alzheimer's disease. *Am J Pathol,* 148**,** 399-403.

CHUBB, J. E., BRADSHAW, N. J., SOARES, D. C., PORTEOUS, D. J. & MILLAR, J. K. 2008. The DISC locus in psychiatric illness. *Mol Psychiatry,* 13**,** 36-64.

CHYUNG, J. H., RAPER, D. M. & SELKOE, D. J. 2005. Gamma-secretase exists on the plasma membrane as an intact complex that accepts substrates and effects intramembrane cleavage. *J Biol Chem,* 280**,** 4383-92.

CIECHOMSKA, I. A. & TOLKOVSKY, A. M. 2007. Non-autophagic GFP-LC3 puncta induced by saponin and other detergents. *Autophagy,* 3**,** 586-90.

CITRON, M., OLTERSDORF, T., HAASS, C., MCCONLOGUE, L., HUNG, A. Y., SEUBERT, P., VIGO-PELFREY, C., LIEBERBURG, I. & SELKOE, D. J. 1992. Mutation of the beta-amyloid precursor protein in familial Alzheimer's disease increases beta-protein production. *Nature,* 360**,** 672-4.

CLEMENT, A. B., HANSTEIN, R., SCHRÖDER, A., NAGEL, H., ENDRES, K., FAHRENHOLZ, F. & BEHL, C. 2008. Effects of neuron-specific ADAM10 modulation in an in vivo model of acute excitotoxic stress. *Neuroscience,* 152**,** 459-68.

CODOGNO, P. & MEIJER, A. J. 2010. Autophagy: a potential link between obesity and insulin resistance. *Cell Metab,* 11**,** 449-51.

COHEN, Y., CHETRIT, A., SIROTA, P. & MODAN, B. 1998. Cancer morbidity in psychiatric patients: influence of lithium carbonate treatment. *Med Oncol,* 15**,** 32-6.

COPANI, A., HOOZEMANS, J. J., CARACI, F., CALAFIORE, M., VAN HAASTERT, E. S., VEERHUIS, R., ROZEMULLER, A. J., ARONICA, E., SORTINO, M. A. & NICOLETTI, F. 2006. DNA polymerase-beta is expressed early in neurons of Alzheimer's disease brain and is loaded into DNA replication forks in neurons challenged with beta-amyloid. *J Neurosci,* 26**,** 10949-57.

COPANI, A., SORTINO, M. A., CARICASOLE, A., CHIECHIO, S., CHISARI, M., BATTAGLIA, G., GIUFFRIDA-STELLA, A. M., VANCHERI, C. & NICOLETTI, F. 2002. Erratic expression of DNA polymerases by beta-amyloid causes neuronal death. *FASEB J,* 16**,** 2006-8.

CREEMERS, J. W., INES DOMINGUEZ, D., PLETS, E., SERNEELS, L., TAYLOR, N. A., MULTHAUP, G., CRAESSAERTS, K., ANNAERT, W. & DE STROOPER, B. 2001. Processing of beta-secretase by furin and other members of the proprotein convertase family. *J Biol Chem,* 276**,** 4211-7.

CUERVO, A. M. 2011. Cell biology. Autophagy's top chef. *Science,* 332**,** 1392-3.

CUMMINGS, J. 2010. What can be inferred from the interruption of the semagacestat trial for treatment of Alzheimer's disease? *Biol Psychiatry,* 68**,** 876-8.

D'ABRAMO, C., MASSONE, S., ZINGG, J. M., PIZZUTI, A., MARAMBAUD, P., DALLA PICCOLA, B., AZZI, A., MARINARI, U. M., PRONZATO, M. A. & RICCIARELLI, R. 2005. Role of peroxisome proliferator-activated receptor gamma in amyloid precursor protein processing and amyloid beta-mediated cell death. *Biochem J,* 391**,** 693-8.

D'AMELIO, M., CAVALLUCCI, V., MIDDEI, S., MARCHETTI, C., PACIONI, S., FERRI, A., DIAMANTINI, A., DE ZIO, D., CARRARA, P., BATTISTINI, L., MORENO, S., BACCI, A., AMMASSARI-TEULE, M., MARIE, H. & CECCONI, F. 2011. Caspase-3 triggers early synaptic dysfunction in a mouse model of Alzheimer's disease. *Nat Neurosci,* 14**,** 69-76.

DANIELS, D. L. & WEIS, W. I. 2002. ICAT inhibits beta-catenin binding to Tcf/Lef-family transcription factors and the general coactivator p300 using independent structural modules. *Mol Cell,* 10**,** 573-84.

DAVIES, P. & MALONEY, A. J. 1976. Selective loss of central cholinergic neurons in Alzheimer's disease. *Lancet,* 2**,** 1403.

DAVIS, A. A., FRITZ, J. J., WESS, J., LAH, J. J. & LEVEY, A. I. 2010. Deletion of M1 muscarinic acetylcholine receptors increases amyloid pathology in vitro and in vivo. *J Neurosci,* 30**,** 4190-6.

DE FERRARI, G. V., PAPASSOTIROPOULOS, A., BIECHELE, T., WAVRANT DE-VRIEZE, F., AVILA, M. E., MAJOR, M. B., MYERS, A., SÁEZ, K., HENRÍQUEZ, J. P., ZHAO, A., WOLLMER, M. A., NITSCH, R. M., HOCK, C., MORRIS, C. M., HARDY, J. & MOON, R. T. 2007. Common genetic variation within the low-density lipoprotein receptor-related protein 6 and late-onset Alzheimer's disease. *Proc Natl Acad Sci U S A,* 104**,** 9434-9.

DE LA MONTE, S. M. & WANDS, J. R. 2008. Alzheimer's disease is type 3 diabetes-evidence reviewed. *J Diabetes Sci Technol,* 2**,** 1101-13.

DE STROOPER, B. & ANNAERT, W. 2010. Novel research horizons for presenilins and γ-secretases in cell biology and disease. *Annu Rev Cell Dev Biol,* 26**,** 235-60.

DE STROOPER, B., ANNAERT, W., CUPERS, P., SAFTIG, P., CRAESSAERTS, K., MUMM, J. S., SCHROETER, E. H., SCHRIJVERS, V., WOLFE, M. S., RAY, W. J., GOATE, A. & KOPAN, R. 1999. A presenilin-1-dependent gamma-secretase-like protease mediates release of Notch intracellular domain. *Nature,* 398**,** 518-22.

DE STROOPER, B., UMANS, L., VAN LEUVEN, F. & VAN DEN BERGHE, H. 1993. Study of the synthesis and secretion of normal and artificial mutants of murine amyloid precursor protein (APP): cleavage of APP occurs in a late compartment of the default secretion pathway. *J Cell Biol,* 121**,** 295-304.

DEANE, R., BELL, R. D., SAGARE, A. & ZLOKOVIC, B. V. 2009. Clearance of amyloid-beta peptide across the blood-brain barrier: implication for therapies in Alzheimer's disease. *CNS Neurol Disord Drug Targets,* 8**,** 16-30.

DIEHL, J. A., CHENG, M., ROUSSEL, M. F. & SHERR, C. J. 1998. Glycogen synthase kinase-3beta regulates cyclin D1 proteolysis and subcellular localization. *Genes Dev,* 12**,** 3499-511.

DODART, J. C., BALES, K. R., GANNON, K. S., GREENE, S. J., DEMATTOS, R. B., MATHIS, C., DELONG, C. A., WU, S., WU, X., HOLTZMAN, D. M. & PAUL, S. M. 2002. Immunization reverses memory deficits without reducing brain Abeta burden in Alzheimer's disease model. *Nat Neurosci,* 5**,** 452-7.

DOMINGUEZ, D., TOURNOY, J., HARTMANN, D., HUTH, T., CRYNS, K., DEFORCE, S., SERNEELS, L., CAMACHO, I. E., MARJAUX, E., CRAESSAERTS, K., ROEBROEK, A. J., SCHWAKE, M., D'HOOGE, R., BACH, P., KALINKE, U., MOECHARS, D., ALZHEIMER, C., REISS, K., SAFTIG, P. & DE STROOPER, B. 2005. Phenotypic and biochemical analyses of BACE1- and BACE2-deficient mice. *J Biol Chem,* 280**,** 30797-806.

EDBAUER, D., WINKLER, E., REGULA, J. T., PESOLD, B., STEINER, H. & HAASS, C. 2003. Reconstitution of gamma-secretase activity. *Nat Cell Biol,* 5**,** 486-8.

EGAN, D. F., SHACKELFORD, D. B., MIHAYLOVA, M. M., GELINO, S., KOHNZ, R. A., MAIR, W., VASQUEZ, D. S., JOSHI, A., GWINN, D. M., TAYLOR, R., ASARA, J. M., FITZPATRICK, J., DILLIN, A., VIOLLET, B., KUNDU, M., HANSEN, M. & SHAW, R. J. 2011. Phosphorylation of ULK1 (hATG1) by AMP-activated protein kinase connects energy sensing to mitophagy. *Science,* 331**,** 456-61.

EGGERT, S., PALIGA, K., SOBA, P., EVIN, G., MASTERS, C. L., WEIDEMANN, A. & BEYREUTHER, K. 2004. The proteolytic processing of the amyloid precursor protein gene family members APLP-1 and APLP-2 involves alpha-, beta-, gamma-, and epsilon-like cleavages: modulation of APLP-1 processing by n-glycosylation. *J Biol Chem,* 279**,** 18146-56.

EMBI, N., RYLATT, D. B. & COHEN, P. 1980. Glycogen synthase kinase-3 from rabbit skeletal muscle. Separation from cyclic-AMP-dependent protein kinase and phosphorylase kinase. *Eur J Biochem,* 107**,** 519-27.

ENGEL, T., GOÑI-OLIVER, P., LUCAS, J. J., AVILA, J. & HERNÁNDEZ, F. 2006a. Chronic lithium administration to FTDP-17 tau and GSK-3beta overexpressing mice prevents tau hyperphosphorylation and neurofibrillary tangle formation, but pre-formed neurofibrillary tangles do not revert. *J Neurochem,* 99**,** 1445-55.

ENGEL, T., HERNÁNDEZ, F., AVILA, J. & LUCAS, J. J. 2006b. Full reversal of Alzheimer's disease-like phenotype in a mouse model with conditional overexpression of glycogen synthase kinase-3. *J Neurosci,* 26**,** 5083-90.

ERIKSEN, J. L., SAGI, S. A., SMITH, T. E., WEGGEN, S., DAS, P., MCLENDON, D. C., OZOLS, V. V., JESSING, K. W., ZAVITZ, K. H., KOO, E. H. & GOLDE, T. E. 2003. NSAIDs and enantiomers of flurbiprofen target gamma-secretase and lower Abeta 42 in vivo. *J Clin Invest,* 112**,** 440-9.

ESKELINEN, E. L. 2008. To be or not to be? Examples of incorrect identification of autophagic compartments in conventional transmission electron microscopy of mammalian cells. *Autophagy,* 4**,** 257-60.

ESTUS, S., GOLDE, T. E. & YOUNKIN, S. G. 1992. Normal processing of the Alzheimer's disease amyloid beta protein precursor generates potentially amyloidogenic carboxyl-terminal derivatives. *Ann N Y Acad Sci,* 674**,** 138-48.

FAGHIHI, M. A., MODARRESI, F., KHALIL, A. M., WOOD, D. E., SAHAGAN, B. G., MORGAN, T. E., FINCH, C. E., ST LAURENT, G., KENNY, P. J. & WAHLESTEDT, C. 2008. Expression of a noncoding RNA is elevated in Alzheimer's disease and drives rapid feed-forward regulation of beta-secretase. *Nat Med,* 14**,** 723-30.

FASSBENDER, K., SIMONS, M., BERGMANN, C., STROICK, M., LUTJOHANN, D., KELLER, P., RUNZ, H., KUHL, S., BERTSCH, T., VON BERGMANN, K., HENNERICI, M., BEYREUTHER, K. & HARTMANN, T. 2001. Simvastatin strongly reduces levels of Alzheimer's disease beta -amyloid peptides Abeta 42 and Abeta 40 in vitro and in vivo. *Proc Natl Acad Sci U S A,* 98**,** 5856-61.

FERRI, C. P., PRINCE, M., BRAYNE, C., BRODATY, H., FRATIGLIONI, L., GANGULI, M., HALL, K., HASEGAWA, K., HENDRIE, H., HUANG, Y., JORM, A., MATHERS, C., MENEZES, P. R., RIMMER, E., SCAZUFCA, M. & INTERNATIONAL, A. S. D. 2005. Global prevalence of dementia: a Delphi consensus study. *Lancet,* 366**,** 2112-7.

FEYT, C., KIENLEN-CAMPARD, P., LEROY, K., N'KULI, F., COURTOY, P. J., BRION, J. P. & OCTAVE, J. N. 2005. Lithium chloride increases the production of amyloid-beta peptide independently from its inhibition of glycogen synthase kinase 3. *J Biol Chem,* 280**,** 33220-7.

FEYT, C., PIERROT, N., TASIAUX, B., VAN HEES, J., KIENLEN-CAMPARD, P., COURTOY, P. J. & OCTAVE, J. N. 2007. Phosphorylation of APP695 at Thr668 decreases gamma-cleavage and extracellular Abeta. *Biochem Biophys Res Commun,* 357**,** 1004-10.

FIOL, C. J., MAHRENHOLZ, A. M., WANG, Y., ROESKE, R. W. & ROACH, P. J. 1987. Formation of protein kinase recognition sites by covalent modification of the substrate. Molecular mechanism for the synergistic action of casein kinase II and glycogen synthase kinase 3. *J Biol Chem,* 262**,** 14042-8.

FJELL, A. M., WALHOVD, K. B., FENNEMA-NOTESTINE, C., MCEVOY, L. K., HAGLER, D. J., HOLLAND, D., BREWER, J. B., DALE, A. M. & INITIATIVE, A. S. D. N. 2010. CSF biomarkers in prediction of cerebral and clinical change in mild cognitive impairment and Alzheimer's disease. *J Neurosci,* 30**,** 2088-101.

FLEMING, A., NODA, T., YOSHIMORI, T. & RUBINSZTEIN, D. C. 2011. Chemical modulators of autophagy as biological probes and potential therapeutics. *Nat Chem Biol,* 7**,** 9-17.

FLOREZ-MCCLURE, M. L., HOHSFIELD, L. A., FONTE, G., BEALOR, M. T. & LINK, C. D. 2007. Decreased insulin-receptor signaling promotes the autophagic degradation of beta-amyloid peptide in C. elegans. *Autophagy,* 3**,** 569-80.

FOWLER, K. S., SALING, M. M., CONWAY, E. L., SEMPLE, J. M. & LOUIS, W. J. 1997. Computerized neuropsychological tests in the early detection of dementia: prospective findings. *J Int Neuropsychol Soc,* 3**,** 139-46.

FRAME, S. & COHEN, P. 2001. GSK3 takes centre stage more than 20 years after its discovery. *Biochem J,* 359**,** 1-16.

FRAME, S. & ZHELEVA, D. 2006. Targeting glycogen synthase kinase-3 in insulin signalling. *Expert Opin Ther Targets,* 10**,** 429-44.

FROLICH, L. 2002. The cholinergic pathology in Alzheimer's disease--discrepancies between clinical experience and pathophysiological findings. *J Neural Transm,* 109**,** 1003-13.

FUENTEALBA, R. A., FARIAS, G., SCHEU, J., BRONFMAN, M., MARZOLO, M. P. & INESTROSA, N. C. 2004. Signal transduction during amyloid-beta-peptide neurotoxicity: role in Alzheimer disease. *Brain Res Brain Res Rev,* 47**,** 275-89.

FUKUMOTO, H., CHEUNG, B. S., HYMAN, B. T. & IRIZARRY, M. C. 2002. Beta-secretase protein and activity are increased in the neocortex in Alzheimer disease. *Arch Neurol,* 59**,** 1381-9.

FUKUMOTO, H., ROSENE, D. L., MOSS, M. B., RAJU, S., HYMAN, B. T. & IRIZARRY, M. C. 2004. Beta-secretase activity increases with aging in human, monkey, and mouse brain. *Am J Pathol,* 164**,** 719-25.

GALVAN, V., GOROSTIZA, O. F., BANWAIT, S., ATAIE, M., LOGVINOVA, A. V., SITARAMAN, S., CARLSON, E., SAGI, S. A., CHEVALLIER, N., JIN, K., GREENBERG, D. A. & BREDESEN, D. E. 2006. Reversal of Alzheimer's-like pathology and behavior in human APP transgenic mice by mutation of Asp664. *Proc Natl Acad Sci U S A,* 103**,** 7130-5.

GAO, Y. & PIMPLIKAR, S. W. 2001. The gamma -secretase-cleaved C-terminal fragment of amyloid precursor protein mediates signaling to the nucleus. *Proc Natl Acad Sci U S A,* 98**,** 14979-84.

GARCÍA-ARENCIBIA, M., HOCHFELD, W. E., TOH, P. P. & RUBINSZTEIN, D. C. 2010. Autophagy, a guardian against neurodegeneration. *Semin Cell Dev Biol,* 21**,** 691-8.

GENTLEMAN, S. M., GREENBERG, B. D., SAVAGE, M. J., NOORI, M., NEWMAN, S. J., ROBERTS, G. W., GRIFFIN, W. S. & GRAHAM, D. I. 1997. A beta 42 is the predominant form of amyloid beta-protein in the brains of short-term survivors of head injury. *Neuroreport,* 8**,** 1519-22.

GERTZ, H. J., CERVOS-NAVARRO, J., FRYDL, V. & SCHULTZ, F. 1985. Glycogen accumulation of the aging human brain. *Mech Ageing Dev,* 31**,** 25-35.

GERVAIS, F. G., XU, D., ROBERTSON, G. S., VAILLANCOURT, J. P., ZHU, Y., HUANG, J., LEBLANC, A., SMITH, D., RIGBY, M., SHEARMAN, M. S., CLARKE, E. E., ZHENG, H., VAN DER PLOEG, L. H., RUFFOLO, S. C., THORNBERRY, N. A., XANTHOUDAKIS, S., ZAMBONI, R. J., ROY, S. & NICHOLSON, D. W. 1999. Involvement of caspases in proteolytic cleavage of Alzheimer's amyloid-beta precursor protein and amyloidogenic A beta peptide formation. *Cell,* 97**,** 395-406.

GHASEMI, M. & DEHPOUR, A. R. 2011. The NMDA receptor/nitric oxide pathway: a target for the therapeutic and toxic effects of lithium. *Trends Pharmacol Sci,* 32**,** 420-34.

GOATE, A., CHARTIER-HARLIN, M. C., MULLAN, M., BROWN, J., CRAWFORD, F., FIDANI, L., GIUFFRA, L., HAYNES, A., IRVING, N., JAMES, L. & ET AL. 1991. Segregation of a missense mutation in the amyloid precursor protein gene with familial Alzheimer's disease. *Nature,* 349**,** 704-6.

GOEDERT, M. 2009. Oskar Fischer and the study of dementia. *Brain,* 132**,** 1102-11.

GOLDE, T. E., ECKMAN, C. B. & YOUNKIN, S. G. 2000. Biochemical detection of Abeta isoforms: implications for pathogenesis, diagnosis, and treatment of Alzheimer's disease. *Biochim Biophys Acta,* 1502**,** 172-87.

GOLDE, T. E., ESTUS, S., YOUNKIN, L. H., SELKOE, D. J. & YOUNKIN, S. G. 1992. Processing of the amyloid protein precursor to potentially amyloidogenic derivatives. *Science,* 255**,** 728-30.

GOLDGABER, D., LERMAN, M. I., MCBRIDE, O. W., SAFFIOTTI, U. & GAJDUSEK, D. C. 1987. Characterization and chromosomal localization of a cDNA encoding brain amyloid of Alzheimer's disease. *Science,* 235**,** 877-80.

GONG, B., CHEN, F., PAN, Y., ARRIETA-CRUZ, I., YOSHIDA, Y., HAROUTUNIAN, V. & PASINETTI, G. M. 2010. SCFFbx2-E3-ligase-mediated degradation of BACE1 attenuates Alzheimer's disease amyloidosis and improves synaptic function. *Aging Cell,* 9**,** 1018-31.

GRIFFIN, W. S., STANLEY, L. C., LING, C., WHITE, L., MACLEOD, V., PERROT, L. J., WHITE, C. L. & ARAOZ, C. 1989. Brain interleukin 1 and S-100 immunoreactivity are elevated in Down syndrome and Alzheimer disease. *Proc Natl Acad Sci U S A,* 86**,** 7611-5.

GRIFFITHS, H. H., WHITEHOUSE, I. J., BAYBUTT, H., BROWN, D., KELLETT, K. A., JACKSON, C. D., TURNER, A. J., PICCARDO, P., MANSON, J. C. & HOOPER, N. M. 2011a. Prion protein interacts with bace1 and differentially regulates its activity towards wild type and swedish mutant amyloid precursor protein. *J Biol Chem*.

GRIFFITHS, H. H., WHITEHOUSE, I. J., BAYBUTT, H., BROWN, D., KELLETT, K. A., JACKSON, C. D., TURNER, A. J., PICCARDO, P., MANSON, J. C. & HOOPER, N. M. 2011b. Prion protein interacts with BACE1 protein and differentially regulates its activity toward wild type and Swedish mutant amyloid precursor protein. *J Biol Chem,* 286**,** 33489-500.

GRUNWALD, G. Duane's Clinical Ophthalmology. *Chapter 21: Structure and Function of the Retinal Pigment Epithelium.*

GUO, Q., WANG, Z., LI, H., WIESE, M. & ZHENG, H. 2011. APP physiological and pathophysiological functions: insights from animal models. *Cell Res*.

HAASS, C., LEMERE, C. A., CAPELL, A., CITRON, M., SEUBERT, P., SCHENK, D., LANNFELT, L. & SELKOE, D. J. 1995. The Swedish mutation causes early-onset Alzheimer's disease by beta-secretase cleavage within the secretory pathway. *Nat Med,* 1**,** 1291-6.

HAASS, C. & SELKOE, D. J. 2007. Soluble protein oligomers in neurodegeneration: lessons from the Alzheimer's amyloid beta-peptide. *Nat Rev Mol Cell Biol,* 8**,** 101-12.

HAMPEL, H., EWERS, M., BÜRGER, K., ANNAS, P., MÖRTBERG, A., BOGSTEDT, A., FRÖLICH, L., SCHRÖDER, J., SCHÖNKNECHT, P., RIEPE, M. W., KRAFT, I., GASSER, T., LEYHE, T., MÖLLER, H. J., KURZ, A. & BASUN, H. 2009. Lithium trial in Alzheimer's disease: a randomized, single-blind, placebo-controlled, multicenter 10-week study. *J Clin Psychiatry,* 70**,** 922-31.

HANGER, D. P., HUGHES, K., WOODGETT, J. R., BRION, J. P. & ANDERTON, B. H. 1992. Glycogen synthase kinase-3 induces Alzheimer's disease-like phosphorylation of tau: generation of paired helical filament epitopes and neuronal localisation of the kinase. *Neurosci Lett,* 147**,** 58-62.

HARDY, J. & ALLSOP, D. 1991. Amyloid deposition as the central event in the aetiology of Alzheimer's disease. *Trends Pharmacol Sci,* 12**,** 383-8.

HARDY, J. & SELKOE, D. J. 2002. The amyloid hypothesis of Alzheimer's disease: progress and problems on the road to therapeutics. *Science,* 297**,** 353-6.

HARDY, J. A. & HIGGINS, G. A. 1992. Alzheimer's disease: the amyloid cascade hypothesis. *Science,* 256**,** 184-5.

HAROLD, D., ABRAHAM, R., HOLLINGWORTH, P., SIMS, R., GERRISH, A., HAMSHERE, M. L., PAHWA, J. S., MOSKVINA, V., DOWZELL, K., WILLIAMS, A., JONES, N., THOMAS, C., STRETTON, A., MORGAN, A. R., LOVESTONE, S., POWELL, J., PROITSI, P., LUPTON, M. K., BRAYNE, C., RUBINSZTEIN, D. C., GILL, M., LAWLOR, B., LYNCH, A., MORGAN, K., BROWN, K. S., PASSMORE, P. A., CRAIG, D., MCGUINNESS, B., TODD, S., HOLMES, C., MANN, D., SMITH, A. D., LOVE, S., KEHOE, P. G., HARDY, J., MEAD, S., FOX, N., ROSSOR, M., COLLINGE, J., MAIER, W., JESSEN, F., SCHÜRMANN, B., VAN DEN BUSSCHE, H., HEUSER, I., KORNHUBER, J., WILTFANG, J., DICHGANS, M., FRÖLICH, L., HAMPEL, H., HÜLL, M., RUJESCU, D., GOATE, A. M., KAUWE, J. S., CRUCHAGA, C., NOWOTNY, P., MORRIS, J. C., MAYO, K., SLEEGERS, K., BETTENS, K., ENGELBORGHS, S., DE DEYN, P. P., VAN BROECKHOVEN, C., LIVINGSTON, G., BASS, N. J., GURLING, H., MCQUILLIN, A., GWILLIAM, R., DELOUKAS, P., AL-CHALABI, A., SHAW, C. E., TSOLAKI, M., SINGLETON, A. B., GUERREIRO, R., MÜHLEISEN, T. W., NÖTHEN, M. M., MOEBUS, S., JÖCKEL, K. H., KLOPP, N., WICHMANN, H. E., CARRASQUILLO, M. M., PANKRATZ, V. S., YOUNKIN, S. G., HOLMANS, P. A., O'DONOVAN, M., OWEN, M. J. & WILLIAMS, J. 2009. Genome-wide association study identifies variants at CLU and PICALM associated with Alzheimer's disease. *Nat Genet,* 41**,** 1088-93.

HE, G., LUO, W., LI, P., REMMERS, C., NETZER, W. J., HENDRICK, J., BETTAYEB, K., FLAJOLET, M., GORELICK, F., WENNOGLE, L. P. & GREENGARD, P. 2010. Gamma-secretase activating protein is a therapeutic target for Alzheimer's disease. *Nature,* 467**,** 95-8.

HE, P. & SHEN, Y. 2009. Interruption of beta-catenin signaling reduces neurogenesis in Alzheimer's disease. *J Neurosci,* 29**,** 6545-57.

HE, W., LU, Y., QAHWASH, I., HU, X. Y., CHANG, A. & YAN, R. 2004. Reticulon family members modulate BACE1 activity and amyloid-beta peptide generation. *Nat Med,* 10**,** 959-65.

HE, X., COOLEY, K., CHUNG, C. H., DASHTI, N. & TANG, J. 2007. Apolipoprotein receptor 2 and X11 alpha/beta mediate apolipoprotein E-induced endocytosis of amyloid-beta precursor protein and beta-secretase, leading to amyloid-beta production. *J Neurosci,* 27**,** 4052-60.

HEBER, S., HERMS, J., GAJIC, V., HAINFELLNER, J., AGUZZI, A., RÜLICKE, T., VON KRETZSCHMAR, H., VON KOCH, C., SISODIA, S., TREMML, P., LIPP, H. P., WOLFER, D. P. & MÜLLER, U. 2000. Mice with combined gene knock-outs reveal essential and partially redundant functions of amyloid precursor protein family members. *J Neurosci,* 20**,** 7951-63.

HEBERT, L. E., SCHERR, P. A., BIENIAS, J. L., BENNETT, D. A. & EVANS, D. A. 2003. Alzheimer disease in the US population: prevalence estimates using the 2000 census. *Arch Neurol,* 60**,** 1119-22.

HENEKA, M. T., SASTRE, M., DUMITRESCU-OZIMEK, L., DEWACHTER, I., WALTER, J., KLOCKGETHER, T. & VAN LEUVEN, F. 2005. Focal glial activation coincides with increased BACE1 activation and precedes amyloid plaque deposition in APP[V717I] transgenic mice. *J Neuroinflammation,* 2**,** 22.

HERMS, J., ANLIKER, B., HEBER, S., RING, S., FUHRMANN, M., KRETZSCHMAR, H., SISODIA, S. & MÜLLER, U. 2004. Cortical dysplasia resembling human type 2 lissencephaly in mice lacking all three APP family members. *EMBO J,* 23**,** 4106-15.

HERNÁNDEZ, F., BORRELL, J., GUAZA, C., AVILA, J. & LUCAS, J. J. 2002. Spatial learning deficit in transgenic mice that conditionally over-express GSK-3beta in the brain but do not form tau filaments. *J Neurochem,* 83**,** 1529-33.

HERNÁNDEZ, F., DE BARREDA, E. G., FUSTER-MATANZO, A., GOÑI-OLIVER, P., LUCAS, J. J. & AVILA, J. 2009. The role of GSK3 in Alzheimer disease. *Brain Res Bull,* 80**,** 248-50.

HERRUP, K., NEVE, R., ACKERMAN, S. L. & COPANI, A. 2004. Divide and die: cell cycle events as triggers of nerve cell death. *J Neurosci,* 24**,** 9232-9.

HOEFLICH, K. P., LUO, J., RUBIE, E. A., TSAO, M. S., JIN, O. & WOODGETT, J. R. 2000. Requirement for glycogen synthase kinase-3beta in cell survival and NF-kappaB activation. *Nature,* 406**,** 86-90.

HOLCOMB, L., GORDON, M. N., MCGOWAN, E., YU, X., BENKOVIC, S., JANTZEN, P., WRIGHT, K., SAAD, I., MUELLER, R., MORGAN, D., SANDERS, S., ZEHR, C., O'CAMPO, K., HARDY, J., PRADA, C. M., ECKMAN, C., YOUNKIN, S., HSIAO, K. & DUFF, K. 1998. Accelerated Alzheimer-type phenotype in transgenic mice carrying both mutant amyloid precursor protein and presenilin 1 transgenes. *Nat Med,* 4**,** 97-100.

HOLTZMAN, D. M., MORRIS, J. C. & GOATE, A. M. 2011. Alzheimer's disease: the challenge of the second century. *Sci Transl Med,* 3**,** 77sr1.

HOOK, V., KINDY, M. & HOOK, G. 2007. Cysteine protease inhibitors effectively reduce in vivo levels of brain beta-amyloid related to Alzheimer's disease. *Biol Chem,* 388**,** 247-52.

HOOK, V., TONEFF, T., BOGYO, M., GREENBAUM, D., MEDZIHRADSZKY, K. F., NEVEU, J., LANE, W., HOOK, G. & REISINE, T. 2005. Inhibition of cathepsin B reduces beta-amyloid

production in regulated secretory vesicles of neuronal chromaffin cells: evidence for cathepsin B as a candidate beta-secretase of Alzheimer's disease. *Biol Chem,* 386**,** 931-40.

HOOPER, C., KILLICK, R. & LOVESTONE, S. 2008. The GSK3 hypothesis of Alzheimer's disease. *J Neurochem,* 104**,** 1433-9.

HOSHI, M., TAKASHIMA, A., NOGUCHI, K., MURAYAMA, M., SATO, M., KONDO, S., SAITOH, Y., ISHIGURO, K., HOSHINO, T. & IMAHORI, K. 1996. Regulation of mitochondrial pyruvate dehydrogenase activity by tau protein kinase I/glycogen synthase kinase 3beta in brain. *Proc Natl Acad Sci U S A,* 93**,** 2719-23.

HOSOKAWA, N., HARA, T., KAIZUKA, T., KISHI, C., TAKAMURA, A., MIURA, Y., IEMURA, S., NATSUME, T., TAKEHANA, K., YAMADA, N., GUAN, J. L., OSHIRO, N. & MIZUSHIMA, N. 2009. Nutrient-dependent mTORC1 association with the ULK1-Atg13-FIP200 complex required for autophagy. *Mol Biol Cell,* 20**,** 1981-91.

HSIEH, H., BOEHM, J., SATO, C., IWATSUBO, T., TOMITA, T., SISODIA, S. & MALINOW, R. 2006. AMPAR removal underlies Abeta-induced synaptic depression and dendritic spine loss. *Neuron,* 52**,** 831-43.

HU, X., HICKS, C. W., HE, W., WONG, P., MACKLIN, W. B., TRAPP, B. D. & YAN, R. 2006. Bace1 modulates myelination in the central and peripheral nervous system. *Nat Neurosci,* 9**,** 1520-5.

HU, X., SHI, Q., ZHOU, X., HE, W., YI, H., YIN, X., GEARING, M., LEVEY, A. & YAN, R. 2007. Transgenic mice overexpressing reticulon 3 develop neuritic abnormalities. *EMBO J,* 26**,** 2755-67.

HUSSAIN, I., POWELL, D. J., HOWLETT, D. R., CHAPMAN, G. A., GILMOUR, L., MURDOCK, P. R., TEW, D. G., MEEK, T. D., CHAPMAN, C., SCHNEIDER, K., RATCLIFFE, S. J., TATTERSALL, D., TESTA, T. T., SOUTHAN, C., RYAN, D. M., SIMMONS, D. L., WALSH, F. S., DINGWALL, C. & CHRISTIE, G. 2000. ASP1 (BACE2) cleaves the amyloid precursor protein at the beta-secretase site. *Mol Cell Neurosci,* 16**,** 609-19.

HYMAN, B. T. 2011. Caspase activation without apoptosis: insight into Aβ initiation of neurodegeneration. *Nat Neurosci,* 14**,** 5-6.

HYMAN, B. T. & GOMEZ-ISLA, T. 1997. The natural history of Alzheimer neurofibrillary tangles and amyloid deposits. *Neurobiol Aging,* 18**,** 386-7; discussion 389-92.

HÉBERT, S. S., HORRÉ, K., NICOLAÏ, L., PAPADOPOULOU, A. S., MANDEMAKERS, W., SILAHTAROGLU, A. N., KAUPPINEN, S., DELACOURTE, A. & DE STROOPER, B. 2008. Loss of microRNA cluster miR-29a/b-1 in sporadic Alzheimer's disease correlates with increased BACE1/beta-secretase expression. *Proc Natl Acad Sci U S A,* 105**,** 6415-20.

INOKI, K., OUYANG, H., ZHU, T., LINDVALL, C., WANG, Y., ZHANG, X., YANG, Q., BENNETT, C., HARADA, Y., STANKUNAS, K., WANG, C. Y., HE, X., MACDOUGALD, O. A., YOU, M., WILLIAMS, B. O. & GUAN, K. L. 2006. TSC2 integrates Wnt and energy signals via a coordinated phosphorylation by AMPK and GSK3 to regulate cell growth. *Cell,* 126**,** 955-68.

IRVINE, G. B., EL-AGNAF, O. M., SHANKAR, G. M. & WALSH, D. M. 2008. Protein aggregation in the brain: the molecular basis for Alzheimer's and Parkinson's diseases. *Mol Med,* 14**,** 451-64.

ISHIGURO, K., IHARA, Y., UCHIDA, T. & IMAHORI, K. 1988. A novel tubulin-dependent protein kinase forming a paired helical filament epitope on tau. *J Biochem,* 104**,** 319-21.

ISHIGURO, K., SHIRATSUCHI, A., SATO, S., OMORI, A., ARIOKA, M., KOBAYASHI, S., UCHIDA, T. & IMAHORI, K. 1993. Glycogen synthase kinase 3 beta is identical to tau protein kinase I generating several epitopes of paired helical filaments. *FEBS Lett,* 325**,** 167-72.

ITTNER, L. M. & GÖTZ, J. 2011. Amyloid-β and tau--a toxic pas de deux in Alzheimer's disease. *Nat Rev Neurosci,* 12**,** 65-72.

ITTNER, L. M., KE, Y. D., DELERUE, F., BI, M., GLADBACH, A., VAN EERSEL, J., WÖLFING, H., CHIENG, B. C., CHRISTIE, M. J., NAPIER, I. A., ECKERT, A., STAUFENBIEL, M., HARDEMAN, E. & GÖTZ, J. 2010. Dendritic function of tau mediates amyloid-beta toxicity in Alzheimer's disease mouse models. *Cell,* 142**,** 387-97.

IWATA, N., TSUBUKI, S., TAKAKI, Y., SHIROTANI, K., LU, B., GERARD, N. P., GERARD, C., HAMA, E., LEE, H. J. & SAIDO, T. C. 2001. Metabolic regulation of brain Abeta by neprilysin. *Science,* 292**,** 1550-2.

IWATA, N., TSUBUKI, S., TAKAKI, Y., WATANABE, K., SEKIGUCHI, M., HOSOKI, E., KAWASHIMA-MORISHIMA, M., LEE, H. J., HAMA, E., SEKINE-AIZAWA, Y. & SAIDO, T. C. 2000. Identification of the major Abeta1-42-degrading catabolic pathway in brain parenchyma: suppression leads to biochemical and pathological deposition. *Nat Med,* 6**,** 143-50.

IWATSUBO, T. 2004. The gamma-secretase complex: machinery for intramembrane proteolysis. *Curr Opin Neurobiol,* 14**,** 379-83.

JACK, C. R., KNOPMAN, D. S., JAGUST, W. J., SHAW, L. M., AISEN, P. S., WEINER, M. W., PETERSEN, R. C. & TROJANOWSKI, J. Q. 2010. Hypothetical model of dynamic biomarkers of the Alzheimer's pathological cascade. *Lancet Neurol,* 9**,** 119-28.

JACK, C. R., PETERSEN, R. C., XU, Y., O'BRIEN, P. C., SMITH, G. E., IVNIK, R. J., TANGALOS, E. G. & KOKMEN, E. 1998. Rate of medial temporal lobe atrophy in typical aging and Alzheimer's disease. *Neurology,* 51**,** 993-9.

JAEGER, P. A., PICKFORD, F., SUN, C. H., LUCIN, K. M., MASLIAH, E. & WYSS-CORAY, T. 2010. Regulation of amyloid precursor protein processing by the Beclin 1 complex. *PLoS One,* 5**,** e11102.

JANSSON, E. A., ARE, A., GREICIUS, G., KUO, I. C., KELLY, D., ARULAMPALAM, V. & PETTERSSON, S. 2005. The Wnt/beta-catenin signaling pathway targets PPARgamma activity in colon cancer cells. *Proc Natl Acad Sci U S A,* 102**,** 1460-5.

JAWHAR, S., WIRTHS, O. & BAYER, T. A. 2011. Pyroglutamate Abeta -- a hatchet man in Alzheimer disease. *J Biol Chem*.

JAWORSKI, T., DEWACHTER, I., LECHAT, B., CROES, S., TERMONT, A., DEMEDTS, D., BORGHGRAEF, P., DEVIJVER, H., FILIPKOWSKI, R. K., KACZMAREK, L., KÜGLER, S. & VAN LEUVEN, F. 2009. AAV-tau mediates pyramidal neurodegeneration by cell-cycle re-entry without neurofibrillary tangle formation in wild-type mice. *PLoS One,* 4**,** e7280.

JAWORSKI, T., DEWACHTER, I., LECHAT, B., GEES, M., KREMER, A., DEMEDTS, D., BORGHGRAEF, P., DEVIJVER, H., KÜGLER, S., PATEL, S., WOODGETT, J. R. & VAN LEUVEN, F. 2011. GSK-3α/β kinases and amyloid production in vivo. *Nature,* 480**,** E4-5; discussion E6.

JICK, H., ZORNBERG, G. L., JICK, S. S., SESHADRI, S. & DRACHMAN, D. A. 2000. Statins and the risk of dementia. *Lancet,* 356**,** 1627-31.

JOPE, R. S. & JOHNSON, G. V. 2004. The glamour and gloom of glycogen synthase kinase-3. *Trends Biochem Sci,* 29**,** 95-102.

JOPE, R. S., YUSKAITIS, C. J. & BEUREL, E. 2007. Glycogen synthase kinase-3 (GSK3): inflammation, diseases, and therapeutics. *Neurochem Res,* 32**,** 577-95.

KABEYA, Y., MIZUSHIMA, N., UENO, T., YAMAMOTO, A., KIRISAKO, T., NODA, T., KOMINAMI, E., OHSUMI, Y. & YOSHIMORI, T. 2000. LC3, a mammalian homologue of yeast Apg8p, is localized in autophagosome membranes after processing. *EMBO J,* 19**,** 5720-8.

KABEYA, Y., MIZUSHIMA, N., YAMAMOTO, A., OSHITANI-OKAMOTO, S., OHSUMI, Y. & YOSHIMORI, T. 2004. LC3, GABARAP and GATE16 localize to autophagosomal membrane depending on form-II formation. *J Cell Sci,* 117**,** 2805-12.

KADOWAKI, M. & KARIM, M. R. 2009. Cytosolic LC3 ratio as a quantitative index of macroautophagy. *Methods Enzymol,* 452**,** 199-213.

KALARIA, R. N., MAESTRE, G. E., ARIZAGA, R., FRIEDLAND, R. P., GALASKO, D., HALL, K., LUCHSINGER, J. A., OGUNNIYI, A., PERRY, E. K., POTOCNIK, F., PRINCE, M., STEWART, R., WIMO, A., ZHANG, Z. X. & ANTUONO, P. 2008. Alzheimer's disease and vascular dementia in developing countries: prevalence, management, and risk factors. *Lancet Neurol,* 7**,** 812-26.

KANEKO, M., KOIKE, H., SAITO, R., KITAMURA, Y., OKUMA, Y. & NOMURA, Y. 2010. Loss of HRD1-mediated protein degradation causes amyloid precursor protein accumulation and amyloid-beta generation. *J Neurosci,* 30**,** 3924-32.

KANG, D. E., SORIANO, S., FROSCH, M. P., COLLINS, T., NARUSE, S., SISODIA, S. S., LEIBOWITZ, G., LEVINE, F. & KOO, E. H. 1999. Presenilin 1 facilitates the constitutive turnover of beta-catenin: differential activity of Alzheimer's disease-linked PS1 mutants in the beta-catenin-signaling pathway. *J Neurosci,* 19**,** 4229-37.

KANG, D. E., SORIANO, S., XIA, X., EBERHART, C. G., DE STROOPER, B., ZHENG, H. & KOO, E. H. 2002. Presenilin couples the paired phosphorylation of beta-catenin independent of axin: implications for beta-catenin activation in tumorigenesis. *Cell,* 110**,** 751-62.

KANG, J., LEMAIRE, H. G., UNTERBECK, A., SALBAUM, J. M., MASTERS, C. L., GRZESCHIK, K. H., MULTHAUP, G., BEYREUTHER, K. & MULLER-HILL, B. 1987. The precursor of Alzheimer's disease amyloid A4 protein resembles a cell-surface receptor. *Nature,* 325**,** 733-6.

KANG, J. & MÜLLER-HILL, B. 1990. Differential splicing of Alzheimer's disease amyloid A4 precursor RNA in rat tissues: PreA4(695) mRNA is predominantly produced in rat and human brain. *Biochem Biophys Res Commun,* 166**,** 1192-200.

KARRAN, E., MERCKEN, M. & DE STROOPER, B. 2011. The amyloid cascade hypothesis for Alzheimer's disease: an appraisal for the development of therapeutics. *Nat Rev Drug Discov,* 10**,** 698-712.

KATSOURI, L., PARR, C., BOGDANOVIC, N., WILLEM, M. & SASTRE, M. 2011. PPARγ Co-Activator-1α (PGC-1α) Reduces Amyloid-β Generation Through a PPARγ-Dependent Mechanism. *J Alzheimers Dis,* 25**,** 151-62.

KIDD, P. M. 2008. Alzheimer's disease, amnestic mild cognitive impairment, and age-associated memory impairment: current understanding and progress toward integrative prevention. *Altern Med Rev,* 13**,** 85-115.

KIM, H. S., KIM, E. M., LEE, J. P., PARK, C. H., KIM, S., SEO, J. H., CHANG, K. A., YU, E., JEONG, S. J., CHONG, Y. H. & SUH, Y. H. 2003. C-terminal fragments of amyloid precursor protein exert neurotoxicity by inducing glycogen synthase kinase-3beta expression. *FASEB J,* 17**,** 1951-3.

KIM, J., BASAK, J. M. & HOLTZMAN, D. M. 2009a. The role of apolipoprotein E in Alzheimer's disease. *Neuron,* 63**,** 287-303.

KIM, J., KUNDU, M., VIOLLET, B. & GUAN, K. L. 2011. AMPK and mTOR regulate autophagy through direct phosphorylation of Ulk1. *Nat Cell Biol,* 13**,** 132-41.

KIM, N. G., XU, C. & GUMBINER, B. M. 2009b. Identification of targets of the Wnt pathway destruction complex in addition to beta-catenin. *Proc Natl Acad Sci U S A,* 106**,** 5165-70.

KIM, P. K., HAILEY, D. W., MULLEN, R. T. & LIPPINCOTT-SCHWARTZ, J. 2008. Ubiquitin signals autophagic degradation of cytosolic proteins and peroxisomes. *Proc Natl Acad Sci U S A,* 105**,** 20567-74.

KIMBERLY, W. T., LAVOIE, M. J., OSTASZEWSKI, B. L., YE, W., WOLFE, M. S. & SELKOE, D. J. 2003. Gamma-secretase is a membrane protein complex comprised of presenilin, nicastrin, Aph-1, and Pen-2. *Proc Natl Acad Sci U S A,* 100**,** 6382-7.

KIMURA, S., FUJITA, N., NODA, T. & YOSHIMORI, T. 2009. Monitoring autophagy in mammalian cultured cells through the dynamics of LC3. *Methods Enzymol,* 452**,** 1-12.

KING, G. D. & SCOTT TURNER, R. 2004. Adaptor protein interactions: modulators of amyloid precursor protein metabolism and Alzheimer's disease risk? *Exp Neurol,* 185**,** 208-19.

KINGSTON, R. E., CHEN, C. A. & OKAYAMA, H. 2001. Calcium phosphate transfection. *Curr Protoc Immunol,* Chapter 10**,** Unit 10 13.

KISHIDA, S., YAMAMOTO, H., IKEDA, S., KISHIDA, M., SAKAMOTO, I., KOYAMA, S. & KIKUCHI, A. 1998. Axin, a negative regulator of the wnt signaling pathway, directly interacts with adenomatous polyposis coli and regulates the stabilization of beta-catenin. *J Biol Chem,* 273**,** 10823-6.

KLAFKI, H. W., WILTFANG, J. & STAUFENBIEL, M. 1996. Electrophoretic separation of betaA4 peptides (1-40) and (1-42). *Anal Biochem.* United States.

KLIONSKY, D. J., ABELIOVICH, H., AGOSTINIS, P., AGRAWAL, D. K., ALIEV, G., ASKEW, D. S., BABA, M., BAEHRECKE, E. H., BAHR, B. A., BALLABIO, A., BAMBER, B. A., BASSHAM, D. C., BERGAMINI, E., BI, X., BIARD-PIECHACZYK, M., BLUM, J. S., BREDESEN, D. E., BRODSKY, J. L., BRUMELL, J. H., BRUNK, U. T., BURSCH, W., CAMOUGRAND, N., CEBOLLERO, E., CECCONI, F., CHEN, Y., CHIN, L. S., CHOI, A., CHU, C. T., CHUNG, J., CLARKE, P. G., CLARK, R. S., CLARKE, S. G., CLAVE, C., CLEVELAND, J. L., CODOGNO, P., COLOMBO, M. I., COTO-MONTES, A., CREGG, J. M., CUERVO, A. M., DEBNATH, J., DEMARCHI, F., DENNIS, P. B., DENNIS, P. A., DERETIC, V., DEVENISH, R. J., DI SANO, F., DICE, J. F., DIFIGLIA, M., DINESH-KUMAR, S., DISTELHORST, C. W., DJAVAHERI-MERGNY, M., DORSEY, F. C., DROGE, W., DRON, M., DUNN, W. A., JR., DUSZENKO, M., EISSA, N. T., ELAZAR, Z., ESCLATINE, A., ESKELINEN, E. L., FESUS, L., FINLEY, K. D., FUENTES, J. M., FUEYO, J., FUJISAKI, K., GALLIOT, B., GAO, F. B., GEWIRTZ, D. A., GIBSON, S. B., GOHLA, A., GOLDBERG, A. L., GONZALEZ, R., GONZALEZ-ESTEVEZ, C., GORSKI, S., GOTTLIEB, R. A., HAUSSINGER, D., HE, Y. W., HEIDENREICH, K., HILL, J. A., HOYER-HANSEN, M., HU, X., HUANG, W. P., IWASAKI, A., JAATTELA, M., JACKSON, W. T., JIANG, X., JIN, S., JOHANSEN, T., JUNG, J. U., KADOWAKI, M., KANG, C., KELEKAR, A., KESSEL, D. H., KIEL, J. A., KIM, H. P., KIMCHI, A., KINSELLA, T. J., KISELYOV, K., KITAMOTO, K., KNECHT, E., et al. 2008. Guidelines for the use and interpretation of assays for monitoring autophagy in higher eukaryotes. *Autophagy.* United States.

KOIKE, H., TOMIOKA, S., SORIMACHI, H., SAIDO, T. C., MARUYAMA, K., OKUYAMA, A., FUJISAWA-SEHARA, A., OHNO, S., SUZUKI, K. & ISHIURA, S. 1999. Membrane-anchored metalloprotease MDC9 has an alpha-secretase activity responsible for processing the amyloid precursor protein. *Biochem J,* 343 Pt 2**,** 371-5.

KOISTINAHO, J., MALM, T. & GOLDSTEINS, G. 2011. Glycogen synthase kinase-3β: a mediator of inflammation in Alzheimer's disease? *Int J Alzheimers Dis,* 2011**,** 129753.

KOO, E. H. & SQUAZZO, S. L. 1994. Evidence that production and release of amyloid beta-protein involves the endocytic pathway. *J Biol Chem,* 269**,** 17386-9.

KORCZYN, A. D. & VAKHAPOVA, V. 2007. The prevention of the dementia epidemic. *J Neurol Sci,* 257**,** 2-4.

KOREN, J., JINWAL, U. K., LEE, D. C., JONES, J. R., SHULTS, C. L., JOHNSON, A. G., ANDERSON, L. J. & DICKEY, C. A. 2009. Chaperone signalling complexes in Alzheimer's disease. *J Cell Mol Med,* 13**,** 619-30.

KOVACS, D. M., FAUSETT, H. J., PAGE, K. J., KIM, T. W., MOIR, R. D., MERRIAM, D. E., HOLLISTER, R. D., HALLMARK, O. G., MANCINI, R., FELSENSTEIN, K. M., HYMAN, B. T., TANZI, R. E. & WASCO, W. 1996. Alzheimer-associated presenilins 1 and 2: neuronal expression in brain and localization to intracellular membranes in mammalian cells. *Nat Med,* 2**,** 224-9.

KREMER, A., LOUIS, J. V., JAWORSKI, T. & VAN LEUVEN, F. 2011. GSK3 and Alzheimer's Disease: Facts and Fiction…. *Front Mol Neurosci,* 4**,** 17.

KUENTZEL, S. L., ALI, S. M., ALTMAN, R. A., GREENBERG, B. D. & RAUB, T. J. 1993. The Alzheimer beta-amyloid protein precursor/protease nexin-II is cleaved by secretase in a trans-Golgi secretory compartment in human neuroglioma cells. *Biochem J,* 295 (Pt 2)**,** 367-78.

KUHN, P. H., WANG, H., DISLICH, B., COLOMBO, A., ZEITSCHEL, U., ELLWART, J. W., KREMMER, E., ROSSNER, S. & LICHTENTHALER, S. F. 2010. ADAM10 is the physiologically relevant, constitutive alpha-secretase of the amyloid precursor protein in primary neurons. *EMBO J,* 29**,** 3020-32.

KUMA, A., MATSUI, M. & MIZUSHIMA, N. 2007. LC3, an autophagosome marker, can be incorporated into protein aggregates independent of autophagy: caution in the interpretation of LC3 localization. *Autophagy,* 3**,** 323-8.

KUMAR, S., REZAEI-GHALEH, N., TERWEL, D., THAL, D. R., RICHARD, M., HOCH, M., MC DONALD, J. M., WÜLLNER, U., GLEBOV, K., HENEKA, M. T., WALSH, D. M., ZWECKSTETTER, M. & WALTER, J. 2011. Extracellular phosphorylation of the amyloid β-peptide promotes formation of toxic aggregates during the pathogenesis of Alzheimer's disease. *EMBO J,* 30**,** 2255-65.

KUMMER, M. P., HERMES, M., DELEKARTE, A., HAMMERSCHMIDT, T., KUMAR, S., TERWEL, D., WALTER, J., PAPE, H. C., KÖNIG, S., ROEBER, S., JESSEN, F., KLOCKGETHER, T., KORTE, M. & HENEKA, M. T. 2011. Nitration of tyrosine 10 critically enhances amyloid β aggregation and plaque formation. *Neuron,* 71**,** 833-44.

KUO, Y. M., WEBSTER, S., EMMERLING, M. R., DE LIMA N & ROHER, A. E. 1998. Irreversible dimerization/tetramerization and post-translational modifications inhibit proteolytic degradation of A beta peptides of Alzheimer's disease. *Biochim Biophys Acta,* 1406**,** 291-8.

KUROKAWA, T., OZAKI, N., SATO, E. & ISHIBASHI, S. 1997. Rapid decrease of glycogen concentration in the hearts of senescence-accelerated mice during aging. *Mech Ageing Dev,* 97**,** 227-36.

LADIKA, D. J. & GUREVITZ, S. L. 2011. Identifying the most common causes of reversible dementias: a review. *JAAPA,* 24**,** 28-31, 57.

LAMMICH, S., SCHÖBEL, S., ZIMMER, A. K., LICHTENTHALER, S. F. & HAASS, C. 2004. Expression of the Alzheimer protease BACE1 is suppressed via its 5'-untranslated region. *EMBO Rep,* 5**,** 620-5.

LANGE-DOHNA, C., ZEITSCHEL, U., GAUNITZ, F., PEREZ-POLO, J. R., BIGL, V. & ROSSNER, S. 2003. Cloning and expression of the rat BACE1 promoter. *J Neurosci Res,* 73**,** 73-80.

LEE, C. Y. & LANDRETH, G. E. 2010. The role of microglia in amyloid clearance from the AD brain. *J Neural Transm,* 117**,** 949-60.

LEE, H. J., JUNG, K. M., HUANG, Y. Z., BENNETT, L. B., LEE, J. S., MEI, L. & KIM, T. W. 2002. Presenilin-dependent gamma-secretase-like intramembrane cleavage of ErbB4. *J Biol Chem,* 277**,** 6318-23.

LEE, J. H., YU, W. H., KUMAR, A., LEE, S., MOHAN, P. S., PETERHOFF, C. M., WOLFE, D. M., MARTINEZ-VICENTE, M., MASSEY, A. C., SOVAK, G., UCHIYAMA, Y., WESTAWAY, D., CUERVO, A. M. & NIXON, R. A. 2010. Lysosomal proteolysis and autophagy require presenilin 1 and are disrupted by Alzheimer-related PS1 mutations. *Cell,* 141**,** 1146-58.

LEE, M. S., KAO, S. C., LEMERE, C. A., XIA, W., TSENG, H. C., ZHOU, Y., NEVE, R., AHLIJANIAN, M. K. & TSAI, L. H. 2003. APP processing is regulated by cytoplasmic phosphorylation. *J Cell Biol,* 163**,** 83-95.

LEE, S., SATO, Y. & NIXON, R. A. 2011. Lysosomal proteolysis inhibition selectively disrupts axonal transport of degradative organelles and causes an Alzheimer's-like axonal dystrophy. *J Neurosci,* 31**,** 7817-30.

LEROY, K., YILMAZ, Z. & BRION, J. P. 2007. Increased level of active GSK-3beta in Alzheimer's disease and accumulation in argyrophilic grains and in neurones at different stages of neurofibrillary degeneration. *Neuropathol Appl Neurobiol,* 33**,** 43-55.

LEVINE, B., SINHA, S. & KROEMER, G. 2008. Bcl-2 family members: dual regulators of apoptosis and autophagy. *Autophagy,* 4**,** 600-6.

LEVY-LAHAD, E., WASCO, W., POORKAJ, P., ROMANO, D. M., OSHIMA, J., PETTINGELL, W. H., YU, C. E., JONDRO, P. D., SCHMIDT, S. D. & WANG, K. 1995. Candidate gene for the chromosome 1 familial Alzheimer's disease locus. *Science,* 269**,** 973-7.

LI, Q., LI, H., ROUGHTON, K., WANG, X., KROEMER, G., BLOMGREN, K. & ZHU, C. 2010a. Lithium reduces apoptosis and autophagy after neonatal hypoxia-ischemia. *Cell Death Dis,* 1**,** e56.

LI, Z., JO, J., JIA, J. M., LO, S. C., WHITCOMB, D. J., JIAO, S., CHO, K. & SHENG, M. 2010b. Caspase-3 activation via mitochondria is required for long-term depression and AMPA receptor internalization. *Cell,* 141**,** 859-71.

LICINIO, J. & WONG, M. L. 1999. The role of inflammatory mediators in the biology of major depression: central nervous system cytokines modulate the biological substrate of depressive symptoms, regulate stress-responsive systems, and contribute to neurotoxicity and neuroprotection. *Mol Psychiatry,* 4**,** 317-27.

LING, D. & SALVATERRA, P. M. 2009. A central role for autophagy in Alzheimer-type neurodegeneration. *Autophagy,* 5**,** 738-40.

LIPINA, T. V., KAIDANOVICH-BEILIN, O., PATEL, S., WANG, M., CLAPCOTE, S. J., LIU, F., WOODGETT, J. R. & RODER, J. C. 2011. Genetic and pharmacological evidence for schizophrenia-related Disc1 interaction with GSK-3. *Synapse,* 65**,** 234-48.

LIU, C., KATO, Y., ZHANG, Z., DO, V. M., YANKNER, B. A. & HE, X. 1999. beta-Trcp couples beta-catenin phosphorylation-degradation and regulates Xenopus axis formation. *Proc Natl Acad Sci U S A,* 96**,** 6273-8.

LIU, C., LI, Y., SEMENOV, M., HAN, C., BAEG, G. H., TAN, Y., ZHANG, Z., LIN, X. & HE, X. 2002. Control of beta-catenin phosphorylation/degradation by a dual-kinase mechanism. *Cell,* 108**,** 837-47.

LIU, H., REMEDI, M. S., PAPPAN, K. L., KWON, G., ROHATGI, N., MARSHALL, C. A. & MCDANIEL, M. L. 2009. Glycogen synthase kinase-3 and mammalian target of rapamycin pathways contribute to DNA synthesis, cell cycle progression, and proliferation in human islets. *Diabetes.* United States.

LIU, J., WANG, H., ZUO, Y. & FARMER, S. R. 2006. Functional interaction between peroxisome proliferator-activated receptor gamma and beta-catenin. *Mol Cell Biol,* 26**,** 5827-37.

LIU, Z., TANABE, K., BERNAL-MIZRACHI, E. & PERMUTT, M. A. 2008. Mice with beta cell overexpression of glycogen synthase kinase-3beta have reduced beta cell mass and proliferation. *Diabetologia,* 51**,** 623-31.

LO, A. C., HAASS, C., WAGNER, S. L., TEPLOW, D. B. & SISODIA, S. S. 1994. Metabolism of the "Swedish" amyloid precursor protein variant in Madin-Darby canine kidney cells. *J Biol Chem,* 269**,** 30966-73.

LOCHHEAD, P. A., KINSTRIE, R., SIBBET, G., RAWJEE, T., MORRICE, N. & CLEGHON, V. 2006. A chaperone-dependent GSK3beta transitional intermediate mediates activation-loop autophosphorylation. *Mol Cell,* 24**,** 627-33.

LOGAN, C. Y. & NUSSE, R. 2004. The Wnt signaling pathway in development and disease. *Annu Rev Cell Dev Biol,* 20**,** 781-810.

LOO, D. T., COPANI, A., PIKE, C. J., WHITTEMORE, E. R., WALENCEWICZ, A. J. & COTMAN, C. W. 1993. Apoptosis is induced by beta-amyloid in cultured central nervous system neurons. *Proc Natl Acad Sci U S A,* 90**,** 7951-5.

LORENZEN, A., SAMOSH, J., VANDEWARK, K., ANBORGH, P. H., SEAH, C., MAGALHAES, A. C., CREGAN, S. P., FERGUSON, S. S. & PASTERNAK, S. H. 2010. Rapid and direct transport of cell surface APP to the lysosome defines a novel selective pathway. *Mol Brain,* 3**,** 11.

LOVESTONE, S., REYNOLDS, C. H., LATIMER, D., DAVIS, D. R., ANDERTON, B. H., GALLO, J. M., HANGER, D., MULOT, S., MARQUARDT, B. & STABEL, S. 1994. Alzheimer's disease-like phosphorylation of the microtubule-associated protein tau by glycogen synthase kinase-3 in transfected mammalian cells. *Curr Biol,* 4**,** 1077-86.

LUCAS, J. J., HERNÁNDEZ, F., GÓMEZ-RAMOS, P., MORÁN, M. A., HEN, R. & AVILA, J. 2001. Decreased nuclear beta-catenin, tau hyperphosphorylation and neurodegeneration in GSK-3beta conditional transgenic mice. *EMBO J,* 20**,** 27-39.

LUCIN, K. M. & WYSS-CORAY, T. 2009. Immune activation in brain aging and neurodegeneration: too much or too little? *Neuron,* 64**,** 110-22.

LUO, J., CHEN, J., DENG, Z. L., LUO, X., SONG, W. X., SHARFF, K. A., TANG, N., HAYDON, R. C., LUU, H. H. & HE, T. C. 2007. Wnt signaling and human diseases: what are the therapeutic implications? *Lab Invest,* 87**,** 97-103.

LUO, W. J., WANG, H., LI, H., KIM, B. S., SHAH, S., LEE, H. J., THINAKARAN, G., KIM, T. W., YU, G. & XU, H. 2003. PEN-2 and APH-1 coordinately regulate proteolytic processing of presenilin 1. *J Biol Chem,* 278**,** 7850-4.

LUO, Y., BOLON, B., KAHN, S., BENNETT, B. D., BABU-KHAN, S., DENIS, P., FAN, W., KHA, H., ZHANG, J., GONG, Y., MARTIN, L., LOUIS, J. C., YAN, Q., RICHARDS, W. G., CITRON, M. & VASSAR, R. 2001. Mice deficient in BACE1, the Alzheimer's beta-secretase, have normal phenotype and abolished beta-amyloid generation. *Nat Neurosci,* 4**,** 231-2.

MA, G., LI, T., PRICE, D. L. & WONG, P. C. 2005. APH-1a is the principal mammalian APH-1 isoform present in gamma-secretase complexes during embryonic development. *J Neurosci,* 25**,** 192-8.

MACAULAY, K., DOBLE, B. W., PATEL, S., HANSOTIA, T., SINCLAIR, E. M., DRUCKER, D. J., NAGY, A. & WOODGETT, J. R. 2007. Glycogen synthase kinase 3alpha-specific regulation of murine hepatic glycogen metabolism. *Cell Metab,* 6**,** 329-37.

MACDONALD, B. T., TAMAI, K. & HE, X. 2009. Wnt/beta-catenin signaling: components, mechanisms, and diseases. *Dev Cell,* 17**,** 9-26.

MAGDESIAN, M. H., CARVALHO, M. M., MENDES, F. A., SARAIVA, L. M., JULIANO, M. A., JULIANO, L., GARCIA-ABREU, J. & FERREIRA, S. T. 2008. Amyloid-beta binds to the

extracellular cysteine-rich domain of Frizzled and inhibits Wnt/beta-catenin signaling. *J Biol Chem,* 283**,** 9359-68.

MAGUSCHAK, K. A. & RESSLER, K. J. 2008. Beta-catenin is required for memory consolidation. *Nat Neurosci,* 11**,** 1319-26.

MAJUMDAR, A., CRUZ, D., ASAMOAH, N., BUXBAUM, A., SOHAR, I., LOBEL, P. & MAXFIELD, F. R. 2007. Activation of microglia acidifies lysosomes and leads to degradation of Alzheimer amyloid fibrils. *Mol Biol Cell,* 18**,** 1490-6.

MAO, B., WU, W., LI, Y., HOPPE, D., STANNEK, P., GLINKA, A. & NIEHRS, C. 2001. LDL-receptor-related protein 6 is a receptor for Dickkopf proteins. *Nature,* 411**,** 321-5.

MARTINEZ, A., ALONSO, M., CASTRO, A., PÉREZ, C. & MORENO, F. J. 2002. First non-ATP competitive glycogen synthase kinase 3 beta (GSK-3beta) inhibitors: thiadiazolidinones (TDZD) as potential drugs for the treatment of Alzheimer's disease. *J Med Chem,* 45**,** 1292-9.

MASTERS, C. L., SIMMS, G., WEINMAN, N. A., MULTHAUP, G., MCDONALD, B. L. & BEYREUTHER, K. 1985. Amyloid plaque core protein in Alzheimer disease and Down syndrome. *Proc Natl Acad Sci U S A,* 82**,** 4245-9.

MATEO, I., INFANTE, J., LLORCA, J., RODRÍGUEZ, E., BERCIANO, J. & COMBARROS, O. 2006. Association between glycogen synthase kinase-3beta genetic polymorphism and late-onset Alzheimer's disease. *Dement Geriatr Cogn Disord,* 21**,** 228-32.

MATTHEWS, F., BRAYNE, C. & INVESTIGATORS, M. R. C. C. F. A. A. S. 2005. The incidence of dementia in England and Wales: findings from the five identical sites of the MRC CFA Study. *PLoS Med,* 2**,** e193.

MATTSON, M. P. 1997. Cellular actions of beta-amyloid precursor protein and its soluble and fibrillogenic derivatives. *Physiol Rev,* 77**,** 1081-132.

MATTSON, M. P., CHENG, B., CULWELL, A. R., ESCH, F. S., LIEBERBURG, I. & RYDEL, R. E. 1993. Evidence for excitoprotective and intraneuronal calcium-regulating roles for secreted forms of the beta-amyloid precursor protein. *Neuron,* 10**,** 243-54.

MATTSON, M. P., GUO, Z. H. & GEIGER, J. D. 1999. Secreted form of amyloid precursor protein enhances basal glucose and glutamate transport and protects against oxidative impairment of glucose and glutamate transport in synaptosomes by a cyclic GMP-mediated mechanism. *J Neurochem,* 73**,** 532-7.

MC DONALD, J. M., SAVVA, G. M., BRAYNE, C., WELZEL, A. T., FORSTER, G., SHANKAR, G. M., SELKOE, D. J., INCE, P. G., WALSH, D. M. & STUDY, M. R. C. C. F. A. A. 2010. The presence of sodium dodecyl sulphate-stable Abeta dimers is strongly associated with Alzheimer-type dementia. *Brain,* 133**,** 1328-41.

MCGEER, P. L. & MCGEER, E. G. 1996. Anti-inflammatory drugs in the fight against Alzheimer's disease. *Ann N Y Acad Sci,* 777**,** 213-20.

MCKHANN, G., DRACHMAN, D., FOLSTEIN, M., KATZMAN, R., PRICE, D. & STADLAN, E. M. 1984. Clinical diagnosis of Alzheimer's disease: report of the NINCDS-ADRDA Work Group under the auspices of Department of Health and Human Services Task Force on Alzheimer's Disease. *Neurology,* 34**,** 939-44.

MEDINA, M. & WANDOSELL, F. 2011. Deconstructing GSK-3: The Fine Regulation of Its Activity. *Int J Alzheimers Dis,* 2011**,** 479249.

MEIJER, A. J. & CODOGNO, P. 2009. Autophagy: regulation and role in disease. *Crit Rev Clin Lab Sci,* 46**,** 210-40.

MEIJER, A. J. & CODOGNO, P. 2011. Autophagy: regulation by energy sensing. *Curr Biol,* 21**,** R227-9.

MENÉNDEZ-GONZÁLEZ, M., PÉREZ-PINERA, P., MARTÍNEZ-RIVERA, M., CALATAYUD, M. T. & BLÁZQUEZ MENES, B. 2005. APP processing and the APP-KPI domain involvement in the amyloid cascade. *Neurodegener Dis,* 2**,** 277-83.

MERLOS-SUÁREZ, A., RUIZ-PAZ, S., BASELGA, J. & ARRIBAS, J. 2001. Metalloprotease-dependent protransforming growth factor-alpha ectodomain shedding in the absence of tumor necrosis factor-alpha-converting enzyme. *J Biol Chem,* 276**,** 48510-7.

MILLER, J. R. & MOON, R. T. 1996. Signal transduction through beta-catenin and specification of cell fate during embryogenesis. *Genes Dev,* 10**,** 2527-39.

MILLER, J. R. & MOON, R. T. 1997. Analysis of the signaling activities of localization mutants of beta-catenin during axis specification in Xenopus. *J Cell Biol,* 139**,** 229-43.

MING, G. L. & SONG, H. 2009. DISC1 partners with GSK3beta in neurogenesis. *Cell,* 136**,** 990-2.

MIZUSHIMA, N. & YOSHIMORI, T. 2007. How to interpret LC3 immunoblotting. *Autophagy,* 3**,** 542-5.

MORALES-CORRALIZA, J., MAZZELLA, M. J., BERGER, J. D., DIAZ, N. S., CHOI, J. H., LEVY, E., MATSUOKA, Y., PLANEL, E. & MATHEWS, P. M. 2009. In vivo turnover of tau and APP metabolites in the brains of wild-type and Tg2576 mice: greater stability of sAPP in the beta-amyloid depositing mice. *PLoS One,* 4**,** e7134.

MORGAN, D. 2011. Immunotherapy for Alzheimer's disease. *J Intern Med,* 269**,** 54-63.

MORI, H., ISHII, K., TOMIYAMA, T., FURIYA, Y., SAHARA, N., ASANO, S., ENDO, N., SHIRASAWA, T. & TAKIO, K. 1994. Racemization: its biological significance on neuropathogenesis of Alzheimer's disease. *Tohoku J Exp Med,* 174**,** 251-62.

MORRIS, J. C. 1993. The Clinical Dementia Rating (CDR): current version and scoring rules. *Neurology,* 43**,** 2412-4.

MOSCONI, L., RINNE, J. O., TSUI, W. H., BERTI, V., LI, Y., WANG, H., MURRAY, J., SCHEININ, N., NÅGREN, K., WILLIAMS, S., GLODZIK, L., DE SANTI, S., VALLABHAJOSULA, S. & DE LEON, M. J. 2010. Increased fibrillar amyloid-{beta} burden in normal individuals with a family history of late-onset Alzheimer's. *Proc Natl Acad Sci U S A,* 107**,** 5949-54.

MUKAI, F., ISHIGURO, K., SANO, Y. & FUJITA, S. C. 2002. Alternative splicing isoform of tau protein kinase I/glycogen synthase kinase 3beta. *J Neurochem,* 81**,** 1073-83.

MULHOLLAND, D. J., DEDHAR, S., COETZEE, G. A. & NELSON, C. C. 2005. Interaction of nuclear receptors with the Wnt/beta-catenin/Tcf signaling axis: Wnt you like to know? *Endocr Rev,* 26**,** 898-915.

MULLAN, M., CRAWFORD, F., AXELMAN, K., HOULDEN, H., LILIUS, L., WINBLAD, B. & LANNFELT, L. 1992. A pathogenic mutation for probable Alzheimer's disease in the APP gene at the N-terminus of beta-amyloid. *Nat Genet,* 1**,** 345-7.

MURAYAMA, K. S., KAMETANI, F., SAITO, S., KUME, H., AKIYAMA, H. & ARAKI, W. 2006. Reticulons RTN3 and RTN4-B/C interact with BACE1 and inhibit its ability to produce amyloid beta-protein. *Eur J Neurosci,* 24**,** 1237-44.

MUÑOZ-MONTAÑO, J. R., MORENO, F. J., AVILA, J. & DIAZ-NIDO, J. 1997. Lithium inhibits Alzheimer's disease-like tau protein phosphorylation in neurons. *FEBS Lett,* 411**,** 183-8.

MÜLLER, D. M., MENDLA, K., FARBER, S. A. & NITSCH, R. M. 1997. Muscarinic M1 receptor agonists increase the secretion of the amyloid precursor protein ectodomain. *Life Sci,* 60**,** 985-91.

NARUSE, S., THINAKARAN, G., LUO, J. J., KUSIAK, J. W., TOMITA, T., IWATSUBO, T., QIAN, X., GINTY, D. D., PRICE, D. L., BORCHELT, D. R., WONG, P. C. & SISODIA, S. S. 1998. Effects of PS1 deficiency on membrane protein trafficking in neurons. *Neuron,* 21**,** 1213-21.

NELSON, P. T., BRAAK, H. & MARKESBERY, W. R. 2009. Neuropathology and cognitive impairment in Alzheimer disease: a complex but coherent relationship. *J Neuropathol Exp Neurol,* 68**,** 1-14.

NETZER, W. J., DOU, F., CAI, D., VEACH, D., JEAN, S., LI, Y., BORNMANN, W. G., CLARKSON, B., XU, H. & GREENGARD, P. 2003. Gleevec inhibits beta-amyloid production but not Notch cleavage. *Proc Natl Acad Sci U S A,* 100**,** 12444-9.

NIKOLAEV, A., MCLAUGHLIN, T., O'LEARY, D. D. & TESSIER-LAVIGNE, M. 2009. APP binds DR6 to trigger axon pruning and neuron death via distinct caspases. *Nature,* 457**,** 981-9.

NISHIMURA, M., YU, G., LEVESQUE, G., ZHANG, D. M., RUEL, L., CHEN, F., MILMAN, P., HOLMES, E., LIANG, Y., KAWARAI, T., JO, E., SUPALA, A., ROGAEVA, E., XU, D. M., JANUS, C., LEVESQUE, L., BI, Q., DUTHIE, M., ROZMAHEL, R., MATTILA, K., LANNFELT, L., WESTAWAY, D., MOUNT, H. T., WOODGETT, J. & ST GEORGE-HYSLOP, P. 1999. Presenilin mutations associated with Alzheimer disease cause defective intracellular trafficking of beta-catenin, a component of the presenilin protein complex. *Nat Med,* 5**,** 164-9.

NIXON, R. A. 2007. Autophagy, amyloidogenesis and Alzheimer disease. *J Cell Sci,* 120**,** 4081-91.

NODA, T., MATSUNAGA, K., TAGUCHI-ATARASHI, N. & YOSHIMORI, T. 2010. Regulation of membrane biogenesis in autophagy via PI3P dynamics. *Semin Cell Dev Biol,* 21**,** 671-6.

NOWAK, K., LANGE-DOHNA, C., ZEITSCHEL, U., GÜNTHER, A., LÜSCHER, B., ROBITZKI, A., PEREZ-POLO, R. & ROSSNER, S. 2006. The transcription factor Yin Yang 1 is an activator of BACE1 expression. *J Neurochem,* 96**,** 1696-707.

NUSSE, R. 2008. Wnt signaling and stem cell control. *Cell Res,* 18**,** 523-7.

O'BRIEN, R. J. & WONG, P. C. 2011. Amyloid precursor protein processing and Alzheimer's disease. *Annu Rev Neurosci,* 34**,** 185-204.

ODDO, S., CACCAMO, A., SHEPHERD, J. D., MURPHY, M. P., GOLDE, T. E., KAYED, R., METHERATE, R., MATTSON, M. P., AKBARI, Y. & LAFERLA, F. M. 2003. Triple-transgenic model of Alzheimer's disease with plaques and tangles: intracellular Abeta and synaptic dysfunction. *Neuron,* 39**,** 409-21.

OHNO, M., SAMETSKY, E. A., YOUNKIN, L. H., OAKLEY, H., YOUNKIN, S. G., CITRON, M., VASSAR, R. & DISTERHOFT, J. F. 2004. BACE1 deficiency rescues memory deficits and cholinergic dysfunction in a mouse model of Alzheimer's disease. *Neuron,* 41**,** 27-33.

OMURA, T., KANEKO, M., OKUMA, Y., ORBA, Y., NAGASHIMA, K., TAKAHASHI, R., FUJITANI, N., MATSUMURA, S., HATA, A., KUBOTA, K., MURAHASHI, K., UEHARA, T. & NOMURA, Y. 2006. A ubiquitin ligase HRD1 promotes the degradation of Pael receptor, a substrate of Parkin. *J Neurochem,* 99**,** 1456-69.

ORIAN, A., GONEN, H., BERCOVICH, B., FAJERMAN, I., EYTAN, E., ISRAËL, A., MERCURIO, F., IWAI, K., SCHWARTZ, A. L. & CIECHANOVER, A. 2000. SCF(beta)(-TrCP) ubiquitin ligase-mediated processing of NF-kappaB p105 requires phosphorylation of its C-terminus by IkappaB kinase. *EMBO J,* 19**,** 2580-91.

OSBORN, G. G. & SAUNDERS, A. V. 2010. Current treatments for patients with Alzheimer disease. *J Am Osteopath Assoc,* 110**,** S16-26.

PALMIERI, M., IMPEY, S., KANG, H., DI RONZA, A., PELZ, C., SARDIELLO, M. & BALLABIO, A. 2011. Characterization of the CLEAR network reveals an integrated control of cellular clearance pathways. *Hum Mol Genet,* 20**,** 3852-66.

PARDOSSI-PIQUARD, R., PETIT, A., KAWARAI, T., SUNYACH, C., ALVES DA COSTA, C., VINCENT, B., RING, S., D'ADAMIO, L., SHEN, J., MÜLLER, U., ST GEORGE HYSLOP, P. & CHECLER, F. 2005. Presenilin-dependent transcriptional control of the Abeta-degrading enzyme neprilysin by intracellular domains of betaAPP and APLP. *Neuron,* 46**,** 541-54.

PARK, S. A., SHAKED, G. M., BREDESEN, D. E. & KOO, E. H. 2009. Mechanism of cytotoxicity mediated by the C31 fragment of the amyloid precursor protein. *Biochem Biophys Res Commun,* 388**,** 450-5.

PARKIN, E. T., WATT, N. T., HUSSAIN, I., ECKMAN, E. A., ECKMAN, C. B., MANSON, J. C., BAYBUTT, H. N., TURNER, A. J. & HOOPER, N. M. 2007. Cellular prion protein regulates beta-secretase cleavage of the Alzheimer's amyloid precursor protein. *Proc Natl Acad Sci U S A,* 104**,** 11062-7.

PARKS, A. L. & CURTIS, D. 2007. Presenilin diversifies its portfolio. *Trends Genet,* 23**,** 140-50.

PASTERNAK, S. H., BAGSHAW, R. D., GUIRAL, M., ZHANG, S., ACKERLEY, C. A., PAK, B. J., CALLAHAN, J. W. & MAHURAN, D. J. 2003. Presenilin-1, nicastrin, amyloid precursor protein, and gamma-secretase activity are co-localized in the lysosomal membrane. *J Biol Chem,* 278**,** 26687-94.

PATWARDHAN, M. B., MCCRORY, D. C., MATCHAR, D. B., SAMSA, G. P. & RUTSCHMANN, O. T. 2004. Alzheimer disease: operating characteristics of PET--a meta-analysis. *Radiology,* 231**,** 73-80.

PEI, J. J., TANAKA, T., TUNG, Y. C., BRAAK, E., IQBAL, K. & GRUNDKE-IQBAL, I. 1997. Distribution, levels, and activity of glycogen synthase kinase-3 in the Alzheimer disease brain. *J Neuropathol Exp Neurol,* 56**,** 70-8.

PERRIN, R. J., FAGAN, A. M. & HOLTZMAN, D. M. 2009. Multimodal techniques for diagnosis and prognosis of Alzheimer's disease. *Nature,* 461**,** 916-22.

PHIEL, C. J., WILSON, C. A., LEE, V. M. & KLEIN, P. S. 2003. GSK-3alpha regulates production of Alzheimer's disease amyloid-beta peptides. *Nature,* 423**,** 435-9.

PIERROT, N., SANTOS, S. F., FEYT, C., MOREL, M., BRION, J. P. & OCTAVE, J. N. 2006. Calcium-mediated transient phosphorylation of tau and amyloid precursor protein followed by intraneuronal amyloid-beta accumulation. *J Biol Chem,* 281**,** 39907-14.

PIKE, C. J., WALENCEWICZ, A. J., GLABE, C. G. & COTMAN, C. W. 1991. In vitro aging of beta-amyloid protein causes peptide aggregation and neurotoxicity. *Brain Res,* 563**,** 311-4.

PIMPLIKAR, S. W., NIXON, R. A., ROBAKIS, N. K., SHEN, J. & TSAI, L. H. 2010. Amyloid-independent mechanisms in Alzheimer's disease pathogenesis. *J Neurosci,* 30**,** 14946-54.

PINNIX, I., MUSUNURU, U., TUN, H., SRIDHARAN, A., GOLDE, T., ECKMAN, C., ZIANI-CHERIF, C., ONSTEAD, L. & SAMBAMURTI, K. 2001. A novel gamma -secretase assay based on detection of the putative C-terminal fragment-gamma of amyloid beta protein precursor. *J Biol Chem,* 276**,** 481-7.

PLASSMAN, B. L., LANGA, K. M., FISHER, G. G., HEERINGA, S. G., WEIR, D. R., OFSTEDAL, M. B., BURKE, J. R., HURD, M. D., POTTER, G. G., RODGERS, W. L., STEFFENS, D. C., WILLIS, R. J. & WALLACE, R. B. 2007. Prevalence of dementia in the United States: the aging, demographics, and memory study. *Neuroepidemiology,* 29**,** 125-32.

PODLISNY, M. B., CITRON, M., AMARANTE, P., SHERRINGTON, R., XIA, W., ZHANG, J., DIEHL, T., LEVESQUE, G., FRASER, P., HAASS, C., KOO, E. H., SEUBERT, P., ST GEORGE-

HYSLOP, P., TEPLOW, D. B. & SELKOE, D. J. 1997. Presenilin proteins undergo heterogeneous endoproteolysis between Thr291 and Ala299 and occur as stable N- and C-terminal fragments in normal and Alzheimer brain tissue. *Neurobiol Dis,* 3**,** 325-37.

POSTINA, R., SCHROEDER, A., DEWACHTER, I., BOHL, J., SCHMITT, U., KOJRO, E., PRINZEN, C., ENDRES, K., HIEMKE, C., BLESSING, M., FLAMEZ, P., DEQUENNE, A., GODAUX, E., VAN LEUVEN, F. & FAHRENHOLZ, F. 2004. A disintegrin-metalloproteinase prevents amyloid plaque formation and hippocampal defects in an Alzheimer disease mouse model. *J Clin Invest,* 113**,** 1456-64.

PÉREZ, M., RIBE, E., RUBIO, A., LIM, F., MORÁN, M. A., RAMOS, P. G., FERRER, I., ISLA, M. T. & AVILA, J. 2005. Characterization of a double (amyloid precursor protein-tau) transgenic: tau phosphorylation and aggregation. *Neuroscience,* 130**,** 339-47.

PÉREZ, M., ROJO, A. I., WANDOSELL, F., DÍAZ-NIDO, J. & AVILA, J. 2003. Prion peptide induces neuronal cell death through a pathway involving glycogen synthase kinase 3. *Biochem J,* 372**,** 129-36.

QIANG, L., FUJITA, R., YAMASHITA, T., ANGULO, S., RHINN, H., RHEE, D., DOEGE, C., CHAU, L., AUBRY, L., VANTI, W. B., MORENO, H. & ABELIOVICH, A. 2011. Directed conversion of Alzheimer's disease patient skin fibroblasts into functional neurons. *Cell,* 146**,** 359-71.

QUANDT, K., FRECH, K., KARAS, H., WINGENDER, E. & WERNER, T. 1995. MatInd and MatInspector: new fast and versatile tools for detection of consensus matches in nucleotide sequence data. *Nucleic Acids Res,* 23**,** 4878-84.

RAJENDRAN, L., SCHNEIDER, A., SCHLECHTINGEN, G., WEIDLICH, S., RIES, J., BRAXMEIER, T., SCHWILLE, P., SCHULZ, J. B., SCHROEDER, C., SIMONS, M., JENNINGS, G., KNOLKER, H. J. & SIMONS, K. 2008. Efficient inhibition of the Alzheimer's disease beta-secretase by membrane targeting. *Science,* 320**,** 520-3.

RAMESH BABU, J., LAMAR SEIBENHENER, M., PENG, J., STROM, A. L., KEMPPAINEN, R., COX, N., ZHU, H., WOOTEN, M. C., DIAZ-MECO, M. T., MOSCAT, J. & WOOTEN, M. W. 2008. Genetic inactivation of p62 leads to accumulation of hyperphosphorylated tau and neurodegeneration. *J Neurochem,* 106**,** 107-20.

RATOVITSKI, T., SLUNT, H. H., THINAKARAN, G., PRICE, D. L., SISODIA, S. S. & BORCHELT, D. R. 1997. Endoproteolytic processing and stabilization of wild-type and mutant presenilin. *J Biol Chem,* 272**,** 24536-41.

RAYASAM, G. V., TULASI, V. K., SODHI, R., DAVIS, J. A. & RAY, A. 2009a. Glycogen synthase kinase 3: more than a namesake. *Br J Pharmacol.* England.

RAYASAM, G. V., TULASI, V. K., SODHI, R., DAVIS, J. A. & RAY, A. 2009b. Glycogen synthase kinase 3: more than a namesake. *Br J Pharmacol,* 156**,** 885-98.

REISS, K. & SAFTIG, P. 2009. The "a disintegrin and metalloprotease" (ADAM) family of sheddases: physiological and cellular functions. *Semin Cell Dev Biol,* 20**,** 126-37.

RING, S., WEYER, S. W., KILIAN, S. B., WALDRON, E., PIETRZIK, C. U., FILIPPOV, M. A., HERMS, J., BUCHHOLZ, C., ECKMAN, C. B., KORTE, M., WOLFER, D. P. & MÜLLER, U. C. 2007. The secreted beta-amyloid precursor protein ectodomain APPs alpha is sufficient to rescue the anatomical, behavioral, and electrophysiological abnormalities of APP-deficient mice. *J Neurosci,* 27**,** 7817-26.

RINGMAN, J. M., MEDINA, L. D., RODRIGUEZ-AGUDELO, Y., CHAVEZ, M., LU, P. & CUMMINGS, J. L. 2009. Current concepts of mild cognitive impairment and their applicability to persons at-risk for familial Alzheimer's disease. *Curr Alzheimer Res,* 6**,** 341-6.

RIVERA, E. J., GOLDIN, A., FULMER, N., TAVARES, R., WANDS, J. R. & DE LA MONTE, S. M. 2005. Insulin and insulin-like growth factor expression and function deteriorate with progression of Alzheimer's disease: link to brain reductions in acetylcholine. *J Alzheimers Dis,* 8**,** 247-68.

ROBERTS, S. B., RIPELLINO, J. A., INGALLS, K. M., ROBAKIS, N. K. & FELSENSTEIN, K. M. 1994. Non-amyloidogenic cleavage of the beta-amyloid precursor protein by an integral membrane metalloendopeptidase. *J Biol Chem,* 269**,** 3111-6.

ROCKENSTEIN, E., TORRANCE, M., ADAME, A., MANTE, M., BAR-ON, P., ROSE, J. B., CREWS, L. & MASLIAH, E. 2007. Neuroprotective effects of regulators of the glycogen synthase kinase-3beta signaling pathway in a transgenic model of Alzheimer's disease are associated with reduced amyloid precursor protein phosphorylation. *J Neurosci,* 27**,** 1981-91.

RODIONOVA, E., CONZELMANN, M., MARASKOVSKY, E., HESS, M., KIRSCH, M., GIESE, T., HO, A. D., ZÖLLER, M., DREGER, P. & LUFT, T. 2007. GSK-3 mediates differentiation and activation of proinflammatory dendritic cells. *Blood,* 109**,** 1584-92.

RODRÍGUEZ, J. J., JONES, V. C., TABUCHI, M., ALLAN, S. M., KNIGHT, E. M., LAFERLA, F. M., ODDO, S. & VERKHRATSKY, A. 2008. Impaired adult neurogenesis in the dentate gyrus of a triple transgenic mouse model of Alzheimer's disease. *PLoS One,* 3**,** e2935.

ROSEN, E. Y., WEXLER, E. M., VERSANO, R., COPPOLA, G., GAO, F., WINDEN, K. D., OLDHAM, M. C., MARTENS, L. H., ZHOU, P., FARESE, R. V. & GESCHWIND, D. H. 2011. Functional genomic analyses identify pathways dysregulated by progranulin deficiency, implicating Wnt signaling. *Neuron,* 71**,** 1030-42.

ROSES, A. D. 1996. Apolipoprotein E alleles as risk factors in Alzheimer's disease. *Annu Rev Med,* 47**,** 387-400.

ROSI, M. C., LUCCARINI, I., GROSSI, C., FIORENTINI, A., SPILLANTINI, M. G., PRISCO, A., SCALI, C., GIANFRIDDO, M., CARICASOLE, A., TERSTAPPEN, G. C. & CASAMENTI, F. 2010. Increased Dickkopf-1 expression in transgenic mouse models of neurodegenerative disease. *J Neurochem,* 112**,** 1539-51.

ROSSNER, S., SASTRE, M., BOURNE, K. & LICHTENTHALER, S. F. 2006. Transcriptional and translational regulation of BACE1 expression--implications for Alzheimer's disease. *Prog Neurobiol,* 79**,** 95-111.

ROSSOR, M. N., NEWMAN, S., FRACKOWIAK, R. S., LANTOS, P. & KENNEDY, A. M. 1993. Alzheimer's disease families with amyloid precursor protein mutations. *Ann N Y Acad Sci,* 695**,** 198-202.

RUBINSZTEIN, D. C., DIFIGLIA, M., HEINTZ, N., NIXON, R. A., QIN, Z. H., RAVIKUMAR, B., STEFANIS, L. & TOLKOVSKY, A. 2005. Autophagy and its possible roles in nervous system diseases, damage and repair. *Autophagy,* 1**,** 11-22.

RYAN, K. A. & PIMPLIKAR, S. W. 2005. Activation of GSK-3 and phosphorylation of CRMP2 in transgenic mice expressing APP intracellular domain. *J Cell Biol.* United States.

RYDER, J., SU, Y., LIU, F., LI, B., ZHOU, Y. & NI, B. 2003a. Divergent roles of GSK3 and CDK5 in APP processing. *Biochem Biophys Res Commun,* 312**,** 922-9.

RYDER, J., SU, Y., LIU, F., LI, B., ZHOU, Y. & NI, B. 2003b. Divergent roles of GSK3 and CDK5 in APP processing. *Biochem Biophys Res Commun,* 312**,** 922-9.

SAFTIG, P., HARTMANN, D., LÜLLMANN-RAUCH, R., WOLFF, J., EVERS, M., KÖSTER, A., HETMAN, M., VON FIGURA, K. & PETERS, C. 1997. Mice deficient in lysosomal acid phosphatase develop lysosomal storage in the kidney and central nervous system. *J Biol Chem,* 272**,** 18628-35.

SAITO, T., SUEMOTO, T., BROUWERS, N., SLEEGERS, K., FUNAMOTO, S., MIHIRA, N., MATSUBA, Y., YAMADA, K., NILSSON, P., TAKANO, J., NISHIMURA, M., IWATA, N., VAN BROECKHOVEN, C., IHARA, Y. & SAIDO, T. C. 2011. Potent amyloidogenicity and pathogenicity of Aβ43. *Nat Neurosci,* 14**,** 1023-32.

SANO, Y., NAKAYA, T., PEDRINI, S., TAKEDA, S., IIJIMA-ANDO, K., IIJIMA, K., MATHEWS, P. M., ITOHARA, S., GANDY, S. & SUZUKI, T. 2006. Physiological mouse brain Abeta levels are not related to the phosphorylation state of threonine-668 of Alzheimer's APP. *PLoS One,* 1**,** e51.

SARKAR, S., KRISHNA, G., IMARISIO, S., SAIKI, S., O'KANE, C. J. & RUBINSZTEIN, D. C. 2008. A rational mechanism for combination treatment of Huntington's disease using lithium and rapamycin. *Hum Mol Genet,* 17**,** 170-8.

SASTRE, M. 2010. Troubleshooting methods for APP processing in vitro. *J Pharmacol Toxicol Methods.* United States: 2010 Elsevier Inc.

SASTRE, M., DEWACHTER, I., ROSSNER, S., BOGDANOVIC, N., ROSEN, E., BORGHGRAEF, P., EVERT, B. O., DUMITRESCU-OZIMEK, L., THAL, D. R., LANDRETH, G., WALTER, J., KLOCKGETHER, T., VAN LEUVEN, F. & HENEKA, M. T. 2006a. Nonsteroidal anti-inflammatory drugs repress beta-secretase gene promoter activity by the activation of PPARgamma. *Proc Natl Acad Sci U S A,* 103**,** 443-8.

SASTRE, M. & GENTLEMAN, S. M. 2010. NSAIDs: How they Work and their Prospects as Therapeutics in Alzheimer's Disease. *Front Aging Neurosci,* 2**,** 20.

SASTRE, M., KLOCKGETHER, T. & HENEKA, M. T. 2006b. Contribution of inflammatory processes to Alzheimer's disease: molecular mechanisms. *Int J Dev Neurosci,* 24**,** 167-76.

SASTRE, M., RICHARDSON, J. C., GENTLEMAN, S. M. & BROOKS, D. J. 2011. Inflammatory risk factors and pathologies associated with Alzheimer's disease. *Curr Alzheimer Res,* 8**,** 132-41.

SASTRE, M., STEINER, H., FUCHS, K., CAPELL, A., MULTHAUP, G., CONDRON, M. M., TEPLOW, D. B. & HAASS, C. 2001a. Presenilin-dependent gamma-secretase processing of beta-amyloid precursor protein at a site corresponding to the S3 cleavage of Notch. *EMBO Rep,* 2**,** 835-41.

SASTRE, M., STEINER, H., FUCHS, K., CAPELL, A., MULTHAUP, G., CONDRON, M. M., TEPLOW, D. B. & HAASS, C. 2001b. Presenilin-dependent gamma-secretase processing of beta-amyloid precursor protein at a site corresponding to the S3 cleavage of Notch. *EMBO Rep,* 2**,** 835-41.

SASTRE, M., WALTER, J. & GENTLEMAN, S. M. 2008. Interactions between APP secretases and inflammatory mediators. *J Neuroinflammation,* 5**,** 25.

SAVONENKO, A. V., MELNIKOVA, T., LAIRD, F. M., STEWART, K. A., PRICE, D. L. & WONG, P. C. 2008. Alteration of BACE1-dependent NRG1/ErbB4 signaling and schizophrenia-like phenotypes in BACE1-null mice. *Proc Natl Acad Sci U S A,* 105**,** 5585-90.

SCALI, C., CARACI, F., GIANFRIDDO, M., DIODATO, E., RONCARATI, R., POLLIO, G., GAVIRAGHI, G., COPANI, A., NICOLETTI, F., TERSTAPPEN, G. C. & CARICASOLE, A. 2006. Inhibition of Wnt signaling, modulation of Tau phosphorylation and induction of neuronal cell death by DKK1. *Neurobiol Dis,* 24**,** 254-65.

SCHELTENS, P., FOX, N., BARKHOF, F. & DE CARLI, C. 2002. Structural magnetic resonance imaging in the practical assessment of dementia: beyond exclusion. *Lancet Neurol,* 1**,** 13-21.

SCHEUNER, D., ECKMAN, C., JENSEN, M., SONG, X., CITRON, M., SUZUKI, N., BIRD, T. D., HARDY, J., HUTTON, M., KUKULL, W., LARSON, E., LEVY-LAHAD, E., VIITANEN, M., PESKIND, E., POORKAJ, P., SCHELLENBERG, G., TANZI, R., WASCO, W., LANNFELT, L., SELKOE, D. & YOUNKIN, S. 1996. Secreted amyloid beta-protein similar to that in the senile plaques of Alzheimer's disease is increased in vivo by the presenilin 1 and 2 and APP mutations linked to familial Alzheimer's disease. *Nat Med,* 2**,** 864-70.

SCHIEPERS, O. J., WICHERS, M. C. & MAES, M. 2005. Cytokines and major depression. *Prog Neuropsychopharmacol Biol Psychiatry,* 29**,** 201-17.

SCHNABEL, J. 2011. Vaccines: chasing the dream. *Nature,* 475**,** S18-9.

SCHRAERMEYER, U. & HEIMANN, K. 1999. Current understanding on the role of retinal pigment epithelium and its pigmentation. *Pigment Cell Res,* 12**,** 219-36.

SCHRAERMEYER, U., PETERS, S., THUMANN, G., KOCIOK, N. & HEIMANN, K. 1999. Melanin granules of retinal pigment epithelium are connected with the lysosomal degradation pathway. *Exp Eye Res,* 68**,** 237-45.

SCHROETER, E. H., KISSLINGER, J. A. & KOPAN, R. 1998. Notch-1 signalling requires ligand-induced proteolytic release of intracellular domain. *Nature,* 393**,** 382-6.

SCHWAB, C., DEMAGGIO, A. J., GHOSHAL, N., BINDER, L. I., KURET, J. & MCGEER, P. L. 2000. Casein kinase 1 delta is associated with pathological accumulation of tau in several neurodegenerative diseases. *Neurobiol Aging,* 21**,** 503-10.

SELKOE, D. J. 2011. Resolving controversies on the path to Alzheimer's therapeutics. *Nat Med,* 17**,** 1060-5.

SELKOE, D. J. & SCHENK, D. 2003. Alzheimer's disease: molecular understanding predicts amyloid-based therapeutics. *Annu Rev Pharmacol Toxicol,* 43**,** 545-84.

SEO, Y. H., JUNG, H. J., SHIN, H. T., KIM, Y. M., YIM, H., CHUNG, H. Y., LIM, I. K. & YOON, G. 2008. Enhanced glycogenesis is involved in cellular senescence via GSK3/GS modulation. *Aging Cell,* 7**,** 894-907.

SERENÓ, L., COMA, M., RODRÍGUEZ, M., SÁNCHEZ-FERRER, P., SÁNCHEZ, M. B., GICH, I., AGULLÓ, J. M., PÉREZ, M., AVILA, J., GUARDIA-LAGUARTA, C., CLARIMÓN, J., LLEÓ, A. & GÓMEZ-ISLA, T. 2009. A novel GSK-3beta inhibitor reduces Alzheimer's pathology and rescues neuronal loss in vivo. *Neurobiol Dis,* 35**,** 359-67.

SETTEMBRE, C. & BALLABIO, A. 2011. TFEB regulates autophagy: An integrated coordination of cellular degradation and recycling processes. *Autophagy,* 7.

SETTEMBRE, C., DI MALTA, C., POLITO, V. A., GARCIA ARENCIBIA, M., VETRINI, F., ERDIN, S., ERDIN, S. U., HUYNH, T., MEDINA, D., COLELLA, P., SARDIELLO, M., RUBINSZTEIN, D. C. & BALLABIO, A. 2011. TFEB links autophagy to lysosomal biogenesis. *Science,* 332**,** 1429-33.

SHANKAR, G. M., LI, S., MEHTA, T. H., GARCIA-MUNOZ, A., SHEPARDSON, N. E., SMITH, I., BRETT, F. M., FARRELL, M. A., ROWAN, M. J., LEMERE, C. A., REGAN, C. M., WALSH, D. M., SABATINI, B. L. & SELKOE, D. J. 2008. Amyloid-beta protein dimers isolated directly from Alzheimer's brains impair synaptic plasticity and memory. *Nat Med,* 14**,** 837-42.

SHERRINGTON, R., ROGAEV, E. I., LIANG, Y., ROGAEVA, E. A., LEVESQUE, G., IKEDA, M., CHI, H., LIN, C., LI, G., HOLMAN, K., TSUDA, T., MAR, L., FONCIN, J. F., BRUNI, A. C., MONTESI, M. P., SORBI, S., RAINERO, I., PINESSI, L., NEE, L., CHUMAKOV, I., POLLEN, D., BROOKES, A., SANSEAU, P., POLINSKY, R. J., WASCO, W., DA SILVA, H. A., HAINES, J. L., PERKICAK-VANCE, M. A., TANZI, R. E., ROSES, A. D., FRASER, P. E., ROMMENS, J. M. & ST GEORGE-HYSLOP, P. H. 1995. Cloning of a gene bearing missense mutations in early-onset familial Alzheimer's disease. *Nature,* 375**,** 754-60.

SHIROTANI, K., EDBAUER, D., PROKOP, S., HAASS, C. & STEINER, H. 2004. Identification of distinct gamma-secretase complexes with different APH-1 variants. *J Biol Chem,* 279**,** 41340-5.

SHITASHIGE, M., HIROHASHI, S. & YAMADA, T. 2008. Wnt signaling inside the nucleus. *Cancer Sci,* 99**,** 631-7.

SHVETS, E. & ELAZAR, Z. 2008. Autophagy-independent incorporation of GFP-LC3 into protein aggregates is dependent on its interaction with p62/SQSTM1. *Autophagy,* 4**,** 1054-6.

SHVETS, E., FASS, E., SCHERZ-SHOUVAL, R. & ELAZAR, Z. 2008. The N-terminus and Phe52 residue of LC3 recruit p62/SQSTM1 into autophagosomes. *J Cell Sci,* 121**,** 2685-95.

SIEGFRIED, E., CHOU, T. B. & PERRIMON, N. 1992. wingless signaling acts through zeste-white 3, the Drosophila homolog of glycogen synthase kinase-3, to regulate engrailed and establish cell fate. *Cell,* 71**,** 1167-79.

SIMONSEN, A. & TOOZE, S. A. 2009. Coordination of membrane events during autophagy by multiple class III PI3-kinase complexes. *J Cell Biol,* 186**,** 773-82.

SIMÓN, D., BENITEZ, M. J., GIMENEZ-CASSINA, A., GARRIDO, J. J., BHAT, R. V., DÍAZ-NIDO, J. & WANDOSELL, F. 2008. Pharmacological inhibition of GSK-3 is not strictly correlated with a decrease in tyrosine phosphorylation of residues 216/279. *J Neurosci Res,* 86**,** 668-74.

SINHA, S., ANDERSON, J. P., BARBOUR, R., BASI, G. S., CACCAVELLO, R., DAVIS, D., DOAN, M., DOVEY, H. F., FRIGON, N., HONG, J., JACOBSON-CROAK, K., JEWETT, N., KEIM, P., KNOPS, J., LIEBERBURG, I., POWER, M., TAN, H., TATSUNO, G., TUNG, J., SCHENK, D., SEUBERT, P., SUOMENSAARI, S. M., WANG, S., WALKER, D., ZHAO, J., MCCONLOGUE, L. & JOHN, V. 1999. Purification and cloning of amyloid precursor protein beta-secretase from human brain. *Nature,* 402**,** 537-40.

SIREROL-PIQUER, M., GOMEZ-RAMOS, P., HERNÁNDEZ, F., PEREZ, M., MORÁN, M. A., FUSTER-MATANZO, A., LUCAS, J. J., AVILA, J. & GARCÍA-VERDUGO, J. M. 2010. GSK3β overexpression induces neuronal death and a depletion of the neurogenic niches in the dentate gyrus. *Hippocampus*.

SISODIA, S. S. 1992. Beta-amyloid precursor protein cleavage by a membrane-bound protease. *Proc Natl Acad Sci U S A,* 89**,** 6075-9.

SLOANE, J. A., PIETROPAOLO, M. F., ROSENE, D. L., MOSS, M. B., PETERS, A., KEMPER, T. & ABRAHAM, C. R. 1997. Lack of correlation between plaque burden and cognition in the aged monkey. *Acta Neuropathol,* 94**,** 471-8.

SMALL, S. A. & DUFF, K. 2008. Linking Abeta and tau in late-onset Alzheimer's disease: a dual pathway hypothesis. *Neuron,* 60**,** 534-42.

SOLANS, A., ESTIVILL, X. & DE LA LUNA, S. 2000. A new aspartyl protease on 21q22.3, BACE2, is highly similar to Alzheimer's amyloid precursor protein beta-secretase. *Cytogenet Cell Genet,* 89**,** 177-84.

SOONTORNNIYOMKIJ, V., LYNCH, M. D., MERMASH, S., POMAKIAN, J., BADKOOBEHI, H., CLARE, R. & VINTERS, H. V. 2010. Cerebral microinfarcts associated with severe cerebral beta-amyloid angiopathy. *Brain Pathol,* 20**,** 459-67.

SOUTAR, M. P., KIM, W. Y., WILLIAMSON, R., PEGGIE, M., HASTIE, C. J., MCLAUCHLAN, H., SNIDER, W. D., GORDON-WEEKS, P. R. & SUTHERLAND, C. 2010. Evidence that glycogen synthase kinase-3 isoforms have distinct substrate preference in the brain. *J Neurochem,* 115**,** 974-83.

SPEESE, S. D. & BUDNIK, V. 2007. Wnts: up-and-coming at the synapse. *Trends Neurosci,* 30**,** 268-75.

SPITTAELS, K., VAN DEN HAUTE, C., VAN DORPE, J., GEERTS, H., MERCKEN, M., BRUYNSEELS, K., LASRADO, R., VANDEZANDE, K., LAENEN, I., BOON, T., VAN LINT, J., VANDENHEEDE, J., MOECHARS, D., LOOS, R. & VAN LEUVEN, F. 2000. Glycogen synthase kinase-3beta phosphorylates protein tau and rescues the axonopathy in the central nervous system of human four-repeat tau transgenic mice. *J Biol Chem,* 275**,** 41340-9.

SQUIRE, L. R. 2008. *Fundamental Neuroscience,* London, Elsevier Academic Press.

STAAL, F. J., NOORT MV, M., STROUS, G. J. & CLEVERS, H. C. 2002. Wnt signals are transmitted through N-terminally dephosphorylated beta-catenin. *EMBO Rep,* 3**,** 63-8.

STALDER, M., PHINNEY, A., PROBST, A., SOMMER, B., STAUFENBIEL, M. & JUCKER, M. 1999. Association of microglia with amyloid plaques in brains of APP23 transgenic mice. *Am J Pathol,* 154**,** 1673-84.

SU, Y., RYDER, J., LI, B., WU, X., FOX, N., SOLENBERG, P., BRUNE, K., PAUL, S., ZHOU, Y., LIU, F. & NI, B. 2004. Lithium, a common drug for bipolar disorder treatment, regulates amyloid-beta precursor protein processing. *Biochemistry,* 43**,** 6899-908.

SUN, X., SATO, S., MURAYAMA, O., MURAYAMA, M., PARK, J. M., YAMAGUCHI, H. & TAKASHIMA, A. 2002. Lithium inhibits amyloid secretion in COS7 cells transfected with amyloid precursor protein C100. *Neurosci Lett,* 321**,** 61-4.

SUTHERLAND, C., LEIGHTON, I. A. & COHEN, P. 1993. Inactivation of glycogen synthase kinase-3 beta by phosphorylation: new kinase connections in insulin and growth-factor signalling. *Biochem J,* 296 (Pt 1)**,** 15-9.

SUZUKI, T. & NAKAYA, T. 2008. Regulation of amyloid beta-protein precursor by phosphorylation and protein interactions. *J Biol Chem,* 283**,** 29633-7.

SWERDLOW, R. H. 2007. Is aging part of Alzheimer's disease, or is Alzheimer's disease part of aging? *Neurobiol Aging,* 28**,** 1465-80.

TAELMAN, V. F., DOBROWOLSKI, R., PLOUHINEC, J. L., FUENTEALBA, L. C., VORWALD, P. P., GUMPER, I., SABATINI, D. D. & DE ROBERTIS, E. M. 2010. Wnt signaling requires sequestration of glycogen synthase kinase 3 inside multivesicular endosomes. *Cell,* 143**,** 1136-48.

TAKAMI, M., NAGASHIMA, Y., SANO, Y., ISHIHARA, S., MORISHIMA-KAWASHIMA, M., FUNAMOTO, S. & IHARA, Y. 2009. gamma-Secretase: successive tripeptide and tetrapeptide release from the transmembrane domain of beta-carboxyl terminal fragment. *J Neurosci,* 29**,** 13042-52.

TAKASHIMA, A. 2010. [Drug development for tauopathy and Alzheimer's disease]. *Nihon Shinkei Seishin Yakurigaku Zasshi,* 30**,** 177-80.

TAKASHIMA, A., MURAYAMA, M., MURAYAMA, O., KOHNO, T., HONDA, T., YASUTAKE, K., NIHONMATSU, N., MERCKEN, M., YAMAGUCHI, H., SUGIHARA, S. & WOLOZIN, B. 1998. Presenilin 1 associates with glycogen synthase kinase-3beta and its substrate tau. *Proc Natl Acad Sci U S A,* 95**,** 9637-41.

TAKASHIMA, A., NOGUCHI, K., MICHEL, G., MERCKEN, M., HOSHI, M., ISHIGURO, K. & IMAHORI, K. 1996. Exposure of rat hippocampal neurons to amyloid beta peptide (25-35) induces the inactivation of phosphatidyl inositol-3 kinase and the activation of tau protein kinase I/glycogen synthase kinase-3 beta. *Neurosci Lett,* 203**,** 33-6.

TAKASHIMA, A., NOGUCHI, K., SATO, K., HOSHINO, T. & IMAHORI, K. 1993. Tau protein kinase I is essential for amyloid beta-protein-induced neurotoxicity. *Proc Natl Acad Sci U S A,* 90**,** 7789-93.

TAKASHIMA, A., YAMAGUCHI, H., NOGUCHI, K., MICHEL, G., ISHIGURO, K., SATO, K., HOSHINO, T., HOSHI, M. & IMAHORI, K. 1995. Amyloid beta peptide induces cytoplasmic accumulation of amyloid protein precursor via tau protein kinase I/glycogen synthase kinase-3 beta in rat hippocampal neurons. *Neurosci Lett,* 198**,** 83-6.

TAKASUGI, N., TOMITA, T., HAYASHI, I., TSURUOKA, M., NIIMURA, M., TAKAHASHI, Y., THINAKARAN, G. & IWATSUBO, T. 2003. The role of presenilin cofactors in the gamma-secretase complex. *Nature,* 422**,** 438-41.

TAMBOLI, I. Y., HAMPEL, H., TIEN, N. T., TOLKSDORF, K., BREIDEN, B., MATHEWS, P. M., SAFTIG, P., SANDHOFF, K. & WALTER, J. 2011. Sphingolipid storage affects autophagic metabolism of the amyloid precursor protein and promotes Abeta generation. *J Neurosci,* 31**,** 1837-49.

TANIDA, I., MINEMATSU-IKEGUCHI, N., UENO, T. & KOMINAMI, E. 2005. Lysosomal turnover, but not a cellular level, of endogenous LC3 is a marker for autophagy. *Autophagy,* 1**,** 84-91.

TANZI, R. E., GUSELLA, J. F., WATKINS, P. C., BRUNS, G. A., ST GEORGE-HYSLOP, P., VAN KEUREN, M. L., PATTERSON, D., PAGAN, S., KURNIT, D. M. & NEVE, R. L. 1987. Amyloid beta protein gene: cDNA, mRNA distribution, and genetic linkage near the Alzheimer locus. *Science,* 235**,** 880-4.

TARASSISHIN, L., YIN, Y. I., BASSIT, B. & LI, Y. M. 2004. Processing of Notch and amyloid precursor protein by gamma-secretase is spatially distinct. *Proc Natl Acad Sci U S A,* 101**,** 17050-5.

TERWEL, D., MUYLLAERT, D., DEWACHTER, I., BORGHGRAEF, P., CROES, S., DEVIJVER, H. & VAN LEUVEN, F. 2008. Amyloid activates GSK-3beta to aggravate neuronal tauopathy in bigenic mice. *Am J Pathol,* 172**,** 786-98.

TESCO, G., KOH, Y. H., KANG, E. L., CAMERON, A. N., DAS, S., SENA-ESTEVES, M., HILTUNEN, M., YANG, S. H., ZHONG, Z., SHEN, Y., SIMPKINS, J. W. & TANZI, R. E. 2007. Depletion of GGA3 stabilizes BACE and enhances beta-secretase activity. *Neuron,* 54**,** 721-37.

THINAKARAN, G., BORCHELT, D. R., LEE, M. K., SLUNT, H. H., SPITZER, L., KIM, G., RATOVITSKY, T., DAVENPORT, F., NORDSTEDT, C., SEEGER, M., HARDY, J., LEVEY, A. I., GANDY, S. E., JENKINS, N. A., COPELAND, N. G., PRICE, D. L. & SISODIA, S. S. 1996a. Endoproteolysis of presenilin 1 and accumulation of processed derivatives in vivo. *Neuron,* 17**,** 181-90.

THINAKARAN, G., TEPLOW, D. B., SIMAN, R., GREENBERG, B. & SISODIA, S. S. 1996b. Metabolism of the "Swedish" amyloid precursor protein variant in neuro2a (N2a) cells. Evidence that cleavage at the "beta-secretase" site occurs in the golgi apparatus. *J Biol Chem,* 271**,** 9390-7.

THORNTON, T. M., PEDRAZA-ALVA, G., DENG, B., WOOD, C. D., ARONSHTAM, A., CLEMENTS, J. L., SABIO, G., DAVIS, R. J., MATTHEWS, D. E., DOBLE, B. & RINCON, M. 2008. Phosphorylation by p38 MAPK as an alternative pathway for GSK3beta inactivation. *Science,* 320**,** 667-70.

TIERNEY, M. C., SZALAI, J. P., SNOW, W. G., FISHER, R. H., NORES, A., NADON, G., DUNN, E. & ST GEORGE-HYSLOP, P. H. 1996. Prediction of probable Alzheimer's disease in memory-impaired patients: A prospective longitudinal study. *Neurology,* 46**,** 661-5.

TOMITA, S., KIRINO, Y. & SUZUKI, T. 1998. Cleavage of Alzheimer's amyloid precursor protein (APP) by secretases occurs after O-glycosylation of APP in the protein secretory pathway. Identification of intracellular compartments in which APP cleavage occurs without using toxic agents that interfere with protein metabolism. *J Biol Chem,* 273**,** 6277-84.

TOOZE, S. A. & YOSHIMORI, T. 2010. The origin of the autophagosomal membrane. *Nat Cell Biol,* 12**,** 831-5.

TRINCHESE, F., LIU, S., BATTAGLIA, F., WALTER, S., MATHEWS, P. M. & ARANCIO, O. 2004. Progressive age-related development of Alzheimer-like pathology in APP/PS1 mice. *Ann Neurol,* 55**,** 801-14.

TURNER, P. R., O'CONNOR, K., TATE, W. P. & ABRAHAM, W. C. 2003. Roles of amyloid precursor protein and its fragments in regulating neural activity, plasticity and memory. *Prog Neurobiol,* 70**,** 1-32.

VAN DE WETERING, M., CAVALLO, R., DOOIJES, D., VAN BEEST, M., VAN ES, J., LOUREIRO, J., YPMA, A., HURSH, D., JONES, T., BEJSOVEC, A., PEIFER, M., MORTIN, M. &

CLEVERS, H. 1997. Armadillo coactivates transcription driven by the product of the Drosophila segment polarity gene dTCF. *Cell,* 88**,** 789-99.

VASSAR, R., BENNETT, B. D., BABU-KHAN, S., KAHN, S., MENDIAZ, E. A., DENIS, P., TEPLOW, D. B., ROSS, S., AMARANTE, P., LOELOFF, R., LUO, Y., FISHER, S., FULLER, J., EDENSON, S., LILE, J., JAROSINSKI, M. A., BIERE, A. L., CURRAN, E., BURGESS, T., LOUIS, J. C., COLLINS, F., TREANOR, J., ROGERS, G. & CITRON, M. 1999. Beta-secretase cleavage of Alzheimer's amyloid precursor protein by the transmembrane aspartic protease BACE. *Science,* 286**,** 735-41.

VASSAR, R., KOVACS, D. M., YAN, R. & WONG, P. C. 2009. The beta-secretase enzyme BACE in health and Alzheimer's disease: regulation, cell biology, function, and therapeutic potential. *J Neurosci,* 29**,** 12787-94.

VETRIVEL, K. S., CHENG, H., LIN, W., SAKURAI, T., LI, T., NUKINA, N., WONG, P. C., XU, H. & THINAKARAN, G. 2004. Association of gamma-secretase with lipid rafts in post-Golgi and endosome membranes. *J Biol Chem,* 279**,** 44945-54.

VETRIVEL, K. S., ZHANG, Y. W., XU, H. & THINAKARAN, G. 2006. Pathological and physiological functions of presenilins. *Mol Neurodegener,* 1**,** 4.

VILLEMAGNE, V. L., PEREZ, K. A., PIKE, K. E., KOK, W. M., ROWE, C. C., WHITE, A. R., BOURGEAT, P., SALVADO, O., BEDO, J., HUTTON, C. A., FAUX, N. G., MASTERS, C. L. & BARNHAM, K. J. 2010. Blood-borne amyloid-beta dimer correlates with clinical markers of Alzheimer's disease. *J Neurosci,* 30**,** 6315-22.

VINGTDEUX, V., GILIBERTO, L., ZHAO, H., CHANDAKKAR, P., WU, Q., SIMON, J. E., JANLE, E. M., LOBO, J., FERRUZZI, M. G., DAVIES, P. & MARAMBAUD, P. 2010. AMP-activated protein kinase signaling activation by resveratrol modulates amyloid-beta peptide metabolism. *J Biol Chem,* 285**,** 9100-13.

VLAD, S. C., MILLER, D. R., KOWALL, N. W. & FELSON, D. T. 2008. Protective effects of NSAIDs on the development of Alzheimer disease. *Neurology,* 70**,** 1672-7.

VON ROTZ, R. C., KOHLI, B. M., BOSSET, J., MEIER, M., SUZUKI, T., NITSCH, R. M. & KONIETZKO, U. 2004. The APP intracellular domain forms nuclear multiprotein complexes and regulates the transcription of its own precursor. *J Cell Sci,* 117**,** 4435-48.

VU, H. L., TROUBETZKOY, S., NGUYEN, H. H., RUSSELL, M. W. & MESTECKY, J. 2000. A method for quantification of absolute amounts of nucleic acids by (RT)-PCR and a new mathematical model for data analysis. *Nucleic Acids Res.* England.

WAHLE, T., PRAGER, K., RAFFLER, N., HAASS, C., FAMULOK, M. & WALTER, J. 2005. GGA proteins regulate retrograde transport of BACE1 from endosomes to the trans-Golgi network. *Mol Cell Neurosci,* 29**,** 453-61.

WAHLE, T., THAL, D. R., SASTRE, M., RENTMEISTER, A., BOGDANOVIC, N., FAMULOK, M., HENEKA, M. T. & WALTER, J. 2006. GGA1 is expressed in the human brain and affects the generation of amyloid beta-peptide. *J Neurosci.* United States.

WAHLUND, L. O., JULIN, P., JOHANSSON, S. E. & SCHELTENS, P. 2000. Visual rating and volumetry of the medial temporal lobe on magnetic resonance imaging in dementia: a comparative study. *J Neurol Neurosurg Psychiatry,* 69**,** 630-5.

WAKABAYASHI, T., CRAESSAERTS, K., BAMMENS, L., BENTAHIR, M., BORGIONS, F., HERDEWIJN, P., STAES, A., TIMMERMAN, E., VANDEKERCKHOVE, J., RUBINSTEIN, E., BOUCHEIX, C., GEVAERT, K. & DE STROOPER, B. 2009. Analysis of the gamma-secretase interactome and validation of its association with tetraspanin-enriched microdomains. *Nat Cell Biol,* 11**,** 1340-6.

WALDEMAR, G., GAUTHIER, S., JONES, R., WILKINSON, D., CUMMINGS, J., LOPEZ, O., ZHANG, R., XU, Y., SUN, Y., KNOX, S., RICHARDSON, S. & MACKELL, J. 2011. Effect of donepezil on emergence of apathy in mild to moderate Alzheimer's disease. *Int J Geriatr Psychiatry,* 26**,** 150-7.

WALSH, D. M., KLYUBIN, I., FADEEVA, J. V., CULLEN, W. K., ANWYL, R., WOLFE, M. S., ROWAN, M. J. & SELKOE, D. J. 2002. Naturally secreted oligomers of amyloid beta protein potently inhibit hippocampal long-term potentiation in vivo. *Nature,* 416**,** 535-9.

WALTER, J., FLUHRER, R., HARTUNG, B., WILLEM, M., KAETHER, C., CAPELL, A., LAMMICH, S., MULTHAUP, G. & HAASS, C. 2001. Phosphorylation regulates intracellular trafficking of beta-secretase. *J Biol Chem,* 276**,** 14634-41.

WANG, C. Y., ZHENG, W., WANG, T., XIE, J. W., WANG, S. L., ZHAO, B. L., TENG, W. P. & WANG, Z. Y. 2011. Huperzine A activates Wnt/β-catenin signaling and enhances the nonamyloidogenic pathway in an Alzheimer transgenic mouse model. *Neuropsychopharmacology,* 36**,** 1073-89.

WANG, P., YANG, G., MOSIER, D. R., CHANG, P., ZAIDI, T., GONG, Y. D., ZHAO, N. M., DOMINGUEZ, B., LEE, K. F., GAN, W. B. & ZHENG, H. 2005. Defective neuromuscular synapses in mice lacking amyloid precursor protein (APP) and APP-Like protein 2. *J Neurosci,* 25**,** 1219-25.

WANG, X. P. & DING, H. L. 2008. Alzheimer's disease: epidemiology, genetics, and beyond. *Neurosci Bull,* 24**,** 105-9.

WEGGEN, S., ERIKSEN, J. L., DAS, P., SAGI, S. A., WANG, R., PIETRZIK, C. U., FINDLAY, K. A., SMITH, T. E., MURPHY, M. P., BULTER, T., KANG, D. E., MARQUEZ-STERLING, N., GOLDE, T. E. & KOO, E. H. 2001. A subset of NSAIDs lower amyloidogenic Abeta42 independently of cyclooxygenase activity. *Nature,* 414**,** 212-6.

WEIHL, C. C., GHADGE, G. D., KENNEDY, S. G., HAY, N., MILLER, R. J. & ROOS, R. P. 1999. Mutant presenilin-1 induces apoptosis and downregulates Akt/PKB. *J Neurosci,* 19**,** 5360-9.

WEXLER, E. M., ROSEN, E. & GESCHWIN, D. H. 2010. Altered canonical Wnt signalling implicated in progranulin-mediated frontotemporal dementia. *Neuroscience 2010: 40th annual meeting.* San Diego, CA: Society for Neuroscience.

WHITEHOUSE, I. J., JACKSON, C., TURNER, A. J. & HOOPER, N. M. 2010. Prion protein is reduced in aging and in sporadic but not in familial Alzheimer's disease. *J Alzheimers Dis,* 22**,** 1023-31.

WILLEM, M., GARRATT, A. N., NOVAK, B., CITRON, M., KAUFMANN, S., RITTGER, A., DESTROOPER, B., SAFTIG, P., BIRCHMEIER, C. & HAASS, C. 2006. Control of peripheral nerve myelination by the beta-secretase BACE1. *Science,* 314**,** 664-6.

WILLEM, M., LAMMICH, S. & HAASS, C. 2009. Function, regulation and therapeutic properties of beta-secretase (BACE1). *Semin Cell Dev Biol,* 20**,** 175-82.

WILLIAMSON, J., GOLDMAN, J. & MARDER, K. S. 2009. Genetic aspects of Alzheimer disease. *Neurologist,* 15**,** 80-6.

WILSON, C. A., MURPHY, D. D., GIASSON, B. I., ZHANG, B., TROJANOWSKI, J. Q. & LEE, V. M. 2004. Degradative organelles containing mislocalized alpha-and beta-synuclein proliferate in presenilin-1 null neurons. *J Cell Biol,* 165**,** 335-46.

WISCHIK, C. M., NOVAK, M., EDWARDS, P. C., KLUG, A., TICHELAAR, W. & CROWTHER, R. A. 1988. Structural characterization of the core of the paired helical filament of Alzheimer disease. *Proc Natl Acad Sci U S A,* 85**,** 4884-8.

WISNIEWSKI, K. E., WISNIEWSKI, H. M. & WEN, G. Y. 1985. Occurrence of neuropathological changes and dementia of Alzheimer's disease in Down's syndrome. *Ann Neurol,* 17**,** 278-82.

WOLFE, M. S., XIA, W., OSTASZEWSKI, B. L., DIEHL, T. S., KIMBERLY, W. T. & SELKOE, D. J. 1999. Two transmembrane aspartates in presenilin-1 required for presenilin endoproteolysis and gamma-secretase activity. *Nature,* 398**,** 513-7.

WOODGETT, J. R. 1990. Molecular cloning and expression of glycogen synthase kinase-3/factor A. *EMBO J,* 9**,** 2431-8.

WOODGETT, J. R. 1991. cDNA cloning and properties of glycogen synthase kinase-3. *Methods Enzymol,* 200**,** 564-77.

WU, D. & PAN, W. 2010. GSK3: a multifaceted kinase in Wnt signaling. *Trends Biochem Sci,* 35**,** 161-8.

YAMADA, K., CIRRITO, J. R., STEWART, F. R., JIANG, H., FINN, M. B., HOLMES, B. B., BINDER, L. I., MANDELKOW, E. M., DIAMOND, M. I., LEE, V. M. & HOLTZMAN, D. M. 2011. In vivo microdialysis reveals age-dependent decrease of brain interstitial fluid tau levels in P301S human tau transgenic mice. *J Neurosci,* 31**,** 13110-7.

YAMAMOTO, H., KOMEKADO, H. & KIKUCHI, A. 2006. Caveolin is necessary for Wnt-3a-dependent internalization of LRP6 and accumulation of beta-catenin. *Dev Cell,* 11**,** 213-23.

YAN, R., BIENKOWSKI, M. J., SHUCK, M. E., MIAO, H., TORY, M. C., PAULEY, A. M., BRASHIER, J. R., STRATMAN, N. C., MATHEWS, W. R., BUHL, A. E., CARTER, D. B., TOMASSELLI, A. G., PARODI, L. A., HEINRIKSON, R. L. & GURNEY, M. E. 1999. Membrane-anchored aspartyl protease with Alzheimer's disease beta-secretase activity. *Nature,* 402**,** 533-7.

YAN, R., MUNZNER, J. B., SHUCK, M. E. & BIENKOWSKI, M. J. 2001. BACE2 functions as an alternative alpha-secretase in cells. *J Biol Chem,* 276**,** 34019-27.

YANG, D. S., KUMAR, A., STAVRIDES, P., PETERSON, J., PETERHOFF, C. M., PAWLIK, M., LEVY, E., CATALDO, A. M. & NIXON, R. A. 2008. Neuronal apoptosis and autophagy cross talk in aging PS/APP mice, a model of Alzheimer's disease. *Am J Pathol,* 173**,** 665-81.

YANG, G., GONG, Y. D., GONG, K., JIANG, W. L., KWON, E., WANG, P., ZHENG, H., ZHANG, X. F., GAN, W. B. & ZHAO, N. M. 2005. Reduced synaptic vesicle density and active zone size in mice lacking amyloid precursor protein (APP) and APP-like protein 2. *Neurosci Lett,* 384**,** 66-71.

YANG, H., ZHONG, X., BALLAR, P., LUO, S., SHEN, Y., RUBINSZTEIN, D. C., MONTEIRO, M. J. & FANG, S. 2007. Ubiquitin ligase Hrd1 enhances the degradation and suppresses the toxicity of polyglutamine-expanded huntingtin. *Exp Cell Res,* 313**,** 538-50.

YANG, J., TAKAHASHI, Y., CHENG, E., LIU, J., TERRANOVA, P. F., ZHAO, B., THRASHER, J. B., WANG, H. G. & LI, B. 2010. GSK-3beta promotes cell survival by modulating Bif-1-dependent autophagy and cell death. *J Cell Sci,* 123**,** 861-70.

YANG, L. B., LINDHOLM, K., YAN, R., CITRON, M., XIA, W., YANG, X. L., BEACH, T., SUE, L., WONG, P., PRICE, D., LI, R. & SHEN, Y. 2003. Elevated beta-secretase expression and enzymatic activity detected in sporadic Alzheimer disease. *Nat Med,* 9**,** 3-4.

YANG, Y., GELDMACHER, D. S. & HERRUP, K. 2001. DNA replication precedes neuronal cell death in Alzheimer's disease. *J Neurosci,* 21**,** 2661-8.

YASOJIMA, K., KURET, J., DEMAGGIO, A. J., MCGEER, E. & MCGEER, P. L. 2000. Casein kinase 1 delta mRNA is upregulated in Alzheimer disease brain. *Brain Res,* 865**,** 116-20.

YLÄ-ANTTILA, P., VIHINEN, H., JOKITALO, E. & ESKELINEN, E. L. 2009. Monitoring autophagy by electron microscopy in Mammalian cells. *Methods Enzymol,* 452**,** 143-64.

YOST, C., FARR, G. H., PIERCE, S. B., FERKEY, D. M., CHEN, M. M. & KIMELMAN, D. 1998. GBP, an inhibitor of GSK-3, is implicated in Xenopus development and oncogenesis. *Cell,* 93**,** 1031-41.

YU, W. H., KUMAR, A., PETERHOFF, C., SHAPIRO KULNANE, L., UCHIYAMA, Y., LAMB, B. T., CUERVO, A. M. & NIXON, R. A. 2004. Autophagic vacuoles are enriched in amyloid precursor protein-secretase activities: implications for beta-amyloid peptide over-production and localization in Alzheimer's disease. *Int J Biochem Cell Biol,* 36**,** 2531-40.

YUSKAITIS, C. J. & JOPE, R. S. 2009. Glycogen synthase kinase-3 regulates microglial migration, inflammation, and inflammation-induced neurotoxicity. *Cell Signal,* 21**,** 264-73.

ZENG, X., HUANG, H., TAMAI, K., ZHANG, X., HARADA, Y., YOKOTA, C., ALMEIDA, K., WANG, J., DOBLE, B., WOODGETT, J., WYNSHAW-BORIS, A., HSIEH, J. C. & HE, X. 2008. Initiation of Wnt signaling: control of Wnt coreceptor Lrp6 phosphorylation/activation via frizzled, dishevelled and axin functions. *Development,* 135**,** 367-75.

ZHANG, X., ZHOU, K., WANG, R., CUI, J., LIPTON, S. A., LIAO, F. F., XU, H. & ZHANG, Y. W. 2007. Hypoxia-inducible factor 1alpha (HIF-1alpha)-mediated hypoxia increases BACE1 expression and beta-amyloid generation. *J Biol Chem,* 282**,** 10873-80.

ZHANG, Y. W., THOMPSON, R., ZHANG, H. & XU, H. 2011. APP processing in Alzheimer's disease. *Mol Brain,* 4**,** 3.

ZHANG, Z., HARTMANN, H., DO, V. M., ABRAMOWSKI, D., STURCHLER-PIERRAT, C., STAUFENBIEL, M., SOMMER, B., VAN DE WETERING, M., CLEVERS, H., SAFTIG, P., DE STROOPER, B., HE, X. & YANKNER, B. A. 1998a. Destabilization of beta-catenin by mutations in presenilin-1 potentiates neuronal apoptosis. *Nature,* 395**,** 698-702.

ZHANG, Z., HARTMANN, H., DO, V. M., ABRAMOWSKI, D., STURCHLER-PIERRAT, C., STAUFENBIEL, M., SOMMER, B., VAN DE WETERING, M., CLEVERS, H., SAFTIG, P., DE STROOPER, B., HE, X. & YANKNER, B. A. 1998b. Destabilization of beta-catenin by mutations in presenilin-1 potentiates neuronal apoptosis. *Nature,* 395**,** 698-702.

ZHAO, C., DENG, W. & GAGE, F. H. 2008. Mechanisms and functional implications of adult neurogenesis. *Cell,* 132**,** 645-60.

ZHAO, G., MAO, G., TAN, J., DONG, Y., CUI, M. Z., KIM, S. H. & XU, X. 2004. Identification of a new presenilin-dependent zeta-cleavage site within the transmembrane domain of amyloid precursor protein. *J Biol Chem,* 279**,** 50647-50.

ZHAO, G., TAN, J., MAO, G., CUI, M. Z. & XU, X. 2007. The same gamma-secretase accounts for the multiple intramembrane cleavages of APP. *J Neurochem,* 100**,** 1234-46.

ZHIYOU, C., YONG, Y., SHANQUAN, S., JUN, Z., LIANGGUO, H., LING, Y. & JIEYING, L. 2009. Upregulation of BACE1 and beta-Amyloid Protein Mediated by Chronic Cerebral Hypoperfusion Contributes to Cognitive Impairment and Pathogenesis of Alzheimer's Disease. *Neurochem Res*.

ZHOU, F., VAN LAAR, T., HUANG, H. & ZHANG, L. 2011. APP and APLP1 are degraded through autophagy in response to proteasome inhibition in neuronal cells. *Protein Cell,* 2**,** 377-83.

ZONG, Y., WANG, H., DONG, W., QUAN, X., ZHU, H., XU, Y., HUANG, L., MA, C. & QIN, C. 2011. miR-29c regulates BACE1 protein expression. *Brain Res,* 1395**,** 108-15.